Annexe - Biosourced Coating Systems for Metallic Substrates

Chapter 1

I. Aluminium coil coating materials

Aluminium coils vary depending on the way they are cast, i.e. through hot and cold rolling or through continuous casting, and depending on the type of alloy, which can be identified from a four digit code. For example, a code starting with 1 indicates aluminium of higher than 99% purity. The alloys used for coil coating are classified by 3 and 5, which means aluminium – manganese and aluminium – magnesium alloys respectively. Finally, the treatment to harden the metal and the tensile strength vary and can be matched for different purposes.

Recycling aluminium is widely done as it requires only 5% of the energy needed to source new aluminium from bauxite, and is therefore profitable. An extra step to remove the paint is necessary in order to recycle coated aluminium.

II. Catalysts used in polyester synthesis

Transesterification reactions are often catalysed by $Ti(OBu)_4$, alone or in combination with catalysts such as $La(acac)_3$, $Hf(acac)_3$ and NaH_2PO_4.[1-4] Bi_2O_3 and bismuth(III)acetate can also be used to minimise the formation of cyclic byproducts and the toxicity.

Condensation is catalysed by titanium, tin, germanium and antimony in this order of activity.[5-8] While manganese and zinc can catalyse the transesterification, they are not desirable for esterifications as they often cause side reactions. Condensation of aliphatic monomers such as lactic acid, succinic acid and butanediol was found to be catalysed by 1,3-disubstituted tetraalkyldistannoxane.[10-12] $HfCl_4$, $Hf(O^tBu)_4$ and $ZrCl_4$ are powerful esterification catalysts, but do not catalyse transesterification at all.[13] $Sc(OTf)_3$ and $Sc(NTf_2)_3$ have been used at room temperature to catalyse polyesterification of aliphatic monomers. [14]

Catalysts can also be used to achieve chemoselectivity. For example, $Sc(OTf)_3$ was found to catalyse polymerisation only at primary hydroxyl groups, as in the case of malic acid and tartaric acid in a reaction with a linear diol or in the case of the polyols glycerol and sorbitol.[15]

III. Factors governing the viscosity

The viscosity of a polymer is also closely linked to its chain length, and thus the molecular weight. It can be expressed either as the number average: $M_n=\sum n_iM_i/\sum n_i$ or the weight average: $M_w=\sum n_iM_i^2/\sum n_iM_i$, where n_i is the number of molecules of weight i and M_i is their molecular mass. The viscosity in turn can be related to the viscosity average molecular weight M_v, which is a little lower than the weight average molecular weight. They can be related by the Mark-Houwink equation $\eta = K*(M_v)^a$, where K and a are constants that have to be determined for each polymer by careful calibration. An approximation for a is however possible: At low molecular weight, it can be found between 0,5 and 0,8, while at high molecular weight, due to an entanglement contribution, it will be around 3,4.

The dependence of the viscosity on the concentration is also exponential. It can be described by the formula $\log \mu = [\text{dry content}] * K * \sqrt{M_n}$, where K is a constant accounting for the temperature, and

specific to the solvent and polymer type. The ratio of carboxyl to hydroxyl groups r_0 can also be used to determine the viscosity using the relation $\log(\eta) = b+c*r_0$, where b and c are material dependent constants. Both equations are limited to certain cases, and have to be used carefully where generalisation is required. The former holds best for low concentrations, while the latter is most appropriate for low molecular weight linear polyesters. In general, it is important to compare the viscosity of two resins only at the same concentration.

Furthermore, the viscosity is highly dependent on the temperature and the concentration of the solution. Both the absolute temperature and the distance to the glass transition temperature of the resin are important. The dependence can be described by the below equation, where A is a thermal expansion coefficient and B is a constant accounting for the distance of the glass transition temperature from the temperature at which the viscosity would approach infinity.

$$\ln \mu = \ln \mu_{Tg} - \frac{A\,(T-Tg)}{B+(T-Tg)}$$

Lastly, the resin structure also has an important influence on the viscosity, but the effect can sometimes be hard to separate from the factors described above. Both symmetrical monomers and bushy branches have been observed to decrease the viscosity. On the other hand, it is increased as interactions between the chains increase. For example, the amount of hydroxyl, acid and ester groups is proportional to the viscosity as they can act as hydrogen bond donors and acceptors. However, a large increase of groups is needed to achieve a significant change. Obviously, chemical bonds between the chains through branching or crosslinking in the resin also have an increasing effect. Similarly, double bonds which make the chain more rigid, and therefore the attraction between chain elements harder, have a negative impact.

In the final paint, the type of pigment can also have significant impact, especially at low viscosities.

Chapter 2

IV. Polyethylene terephthalate recycling

As new PET is relatively cheap, cost effectiveness is imperative for all recycling efforts.

In general, two methods of recycling can be differentiated. Mechanical recycling involves the melting and reforming of PET, which is possible due to its thermoplastic nature. It requires a relatively low investment, but the main challenge is to remove impurities from other polymers, labels and consumer use to prevent degradation and quality loss during the melt process. While thus recycled PET has been used in structural parts of vehicles, automotive textiles and food containers, it also often ends up in low value applications such as fibrefill for pillows or polyester foam.

One possibility for high end use of recycled PET is the incorporation in composite materials. It is for example reported by Evstatiev *et al.*, who tested recycled PET as a microfibrillar reinforcement for low density polyethylene (LDPE), and observed an increase in both impact and tensile strength of the material.[16]

The second method is chemical recycling, which involves the complete or partial breakdown of chains to give lower molecular weight polyester, oligomers or the original monomers. The lower the molecular weight of the products, the more diverse are its applications. While it is possible to reform

the original monomers, ethylene glycol and terephthalic acid or dimethyl terephthalate, a large cost is often associated with their purification.

There are a variety of chemical recycling methods, reviewed for example by Paszun *et al.*, and which involves either pyrolysis or more commonly, solvent treatment.[17] The PET ester bonds can be broken either by water or by hydroxy functionalised organic molecules. Hydrolysis can take place in basic, acidic or neutral conditions, and yields ethylene glycol and terephthalic acid. The process temperature, pressure and efficiency can be modified by adding different solvents and catalyst, while also decreasing its environmental impact from non-benign additives.

Alternatives to hydrolysis are aminolysis, and the use of ammonia, both of which yield amide structures, or methanolysis, which yields dimethyl terephthalate.[17] Depending on the process, the production of terephthalic acid and dimethyl terephthalate can be advantageous as the recycling unit can be connected to the PET production plant and the products can be fed directly into the starting material stream.

The most popular recycling method is glycolysis, in which glycols are used to break up the ester bonds.[17] While this can lead to a variety of products, including new condensation products between the glycols and the PET chains, it also produces functionalised material which can easily be adapted for new applications. Different methods have been used to improve the sustainability and efficiency of the glycolysis process, including supercritical temperatures, microwave heating and metal or ionic liquid catalysts.[18] The process conditions can also be modified to tune the functionality, distribution and molecular weight of the final product.

In order to use the glycolysis products in coating applications, several properties have to be modified.[19] An appropriately low molecular weight for processing has to be achieved; sufficient functionalisation for crosslinking, such as hydroxy groups, has to be introduced and the crystallinity has to be lowered. This can be achieved by the incorporation of polyether or long chain aliphatic diols and isophthalic acid respectively.

The main types of polymers synthesised from recycled PET oligomers obtained are polyester polyols, unsaturated polyester resins and polyester urethanes.[20] For example, Lu *et al.* used maleic anhydride to create an unsaturated polyester, which was subsequently crosslinked with styrene.[21] Ristic *et al.* oligomerised the recycled PET with polyethylene glycol and triethylene glycol, and reacted it with 2,2-bis-hydroxymethylpropionic acid.[22] The product was then crosslinked with isophorone diisocyanate to make a polyurethane dispersion. Spliman *et al.* reported a variety of coating products, including a hexamethoxymelamine crosslinked polyester polyol thermoset film.[19] Lastly, Nikles *et al.* methacrylated or acrylated the hydroxyfunctionalised oligomers to give a UV-curable resin.[23]

An alternative to chemical degradation is enzymatic degradation. While PET is generally not very labile to biodegradation due to its limited chain mobility, some examples of lipases that are capable of converting even PET bottles have been reported.[24]

Overall, the incorporation of recycled material into coatings has been proven possible.

V. Examples of biopolymer composites

There are numerous examples of different applications for biopolymer composites reported in the literature. Since each plant is different, the effect of the biopolymer on the material properties are

both hard to predict and hard to transfer from one example to the other. Therefore, a small selection of recent publications is used to illustrate the possibilities in the following paragraphs.

Tran *et al.* reported the combination of polymethylmethacrylate film (PMMA) with cellulose to give a hybrid clear film for use in packaging application.[25] The composite was synthesised by dissolving both materials in trifluoroacetic acid and a transparent film with improved thermal, mechanical and solvent resistance properties was obtained.

Chauhan *et al.* also used cellulose, extracted from pine needles, but grafted 4-vinylpyridine onto it. The product was used to make antimicrobial, softening and emulsifying agents for the water and textile industry.[26]

Kengkhetkit *et al.* used pineapple leaf, which is normally waste, as a filler for polypropylene products, to promote utilisation of the entire pineapple plant. Addition of different pinapple leaf extracts achieved improved tensile, flexibility and impact properties.[27]

Lastly, Audo *et al.* transformed microalgae biomass via hydrothermal liquefaction to give a product similar to bitumen, which can be used as a binder in asphalt concrete and literally pave the road to a more sustainable future.[28]

VI. Valorisation of Kraft lignin by a biorefinery concept proposed by Borges da Silva *et al.*[9]

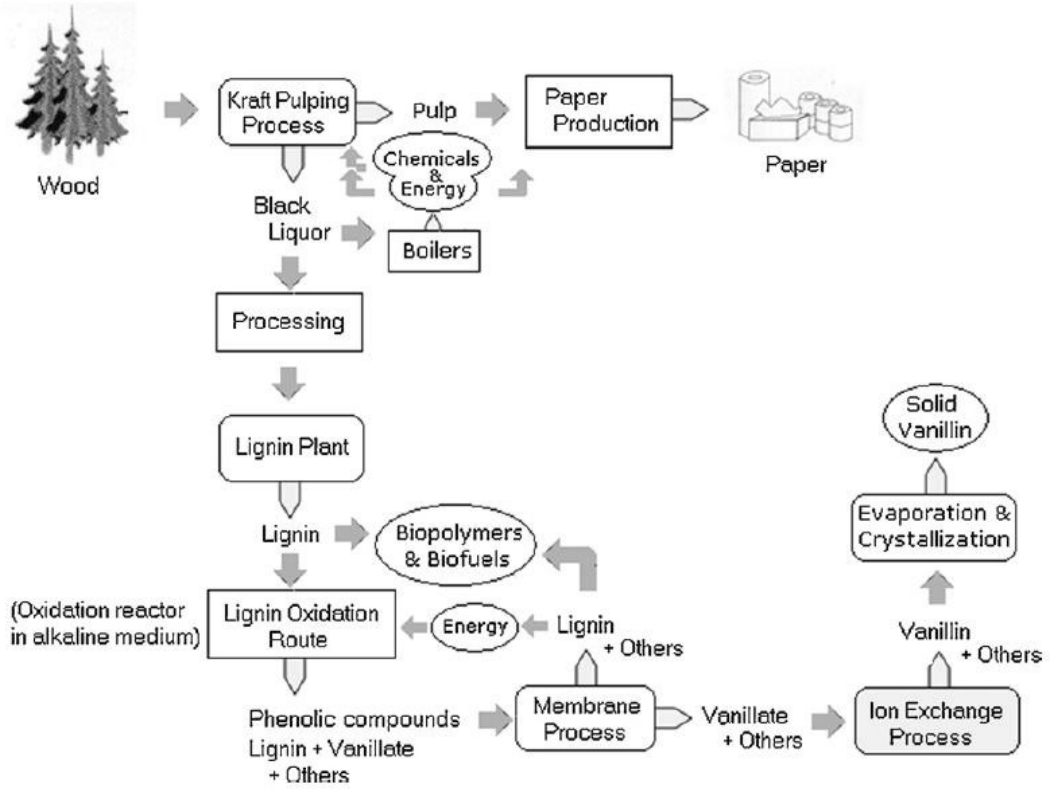

Scheme 1: Valorisation of Kraft lignin by biorefinery concept: The proposed integrated process for producing vanilla and biopolymers (Borges da Silva 2009)[9]

VII. Furfural platform

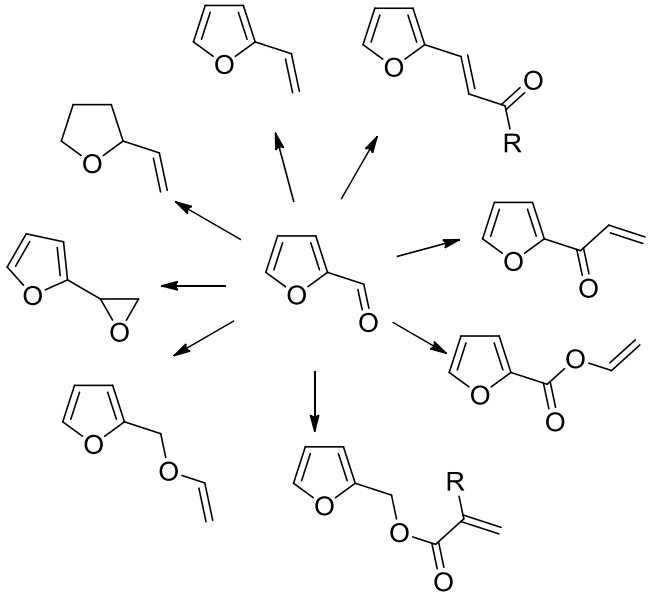

Scheme 2: Furfural platform

VIII. Fatty acid contents of important vegetable oils

Table 1: Fatty acid contents of important vegetable oils

	fatty acids					unsaturation*
Oils	**palmitic**	**stearic**	**oleic**	**linoleic**	**linolenic**	
Canola	4,1	1,8	60,9	21,0	8,8	3,9
Corn	10,9	2,0	25,4	59,6	1,2	4,5
Cottonseed	21,6	2,6	18,6	54,4	0,7	3,9
Linseed	5,5	3,5	19,1	15,3	56,6	6,6
Olive	13,7	2,5	71,1	10,0	0,6	2,8
Soybean	11,0	4,0	23,4	53,3	7,8	4,6
Tung	-	4,0	8,0	4,0	-	7,5
Fish	-	-	18,2	1,1	1,0	3,6
Castor	1,5	0,5	5,0	4,0	0,5	3,0
Palm	39,0	5,0	45,0	9,0	-	-
Oiticica	6,0	4,0	8,0	8,0	-	-
Rapeseed	4,0	2,0	56,0	26,0	10,0	-
Refined tall	4,0	3,0	46,0	35,0	12,0	-
Sunflower	6,0	4,0	42,0	47,0	1,0	-

* average number of double bonds per triglyceride

IX. Examples of dimerisation of fatty acids to make monomers for polycondensations

Bao *et al.*, for example, used a click addition to link a diol group to castor oil methyl undecenoate with a thioether linkage.[29]

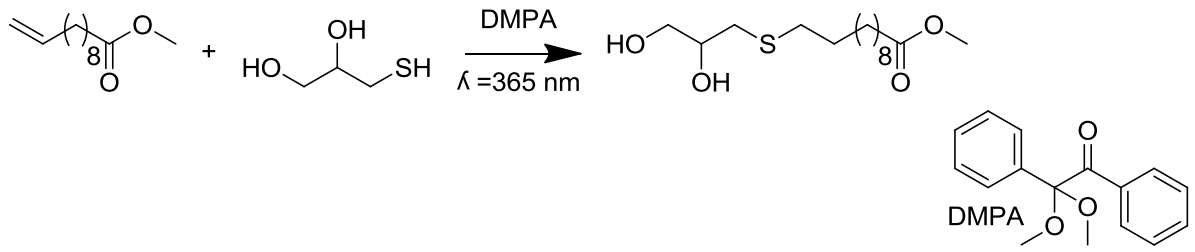

Scheme 3: Click addition of a 1,2-propanediol unit to methyl undecenoate (Bao 2013)

The same chemistry was used by Türünc *et al.*, to create a platform of hydroxy esters and diester monomers based on castor oil.[30]

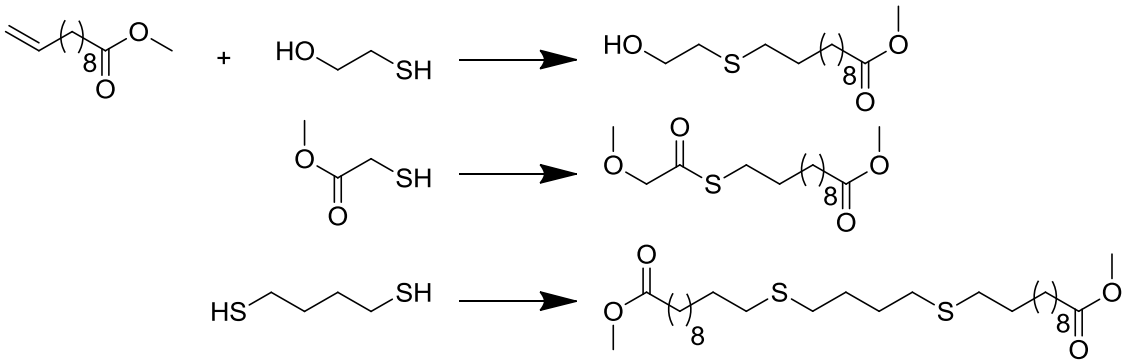

Scheme 4: Castor oil based monomer platform (Türünc 2010)

A different strategy was used by Vilela *et al.* and Quinzler *et al.*, who dimerised fatty acid using self-metathesis of the double bonds.[31, 32] The diacid was then hydrogenated to give a diol, and the two different compounds were used in a polycondensation.

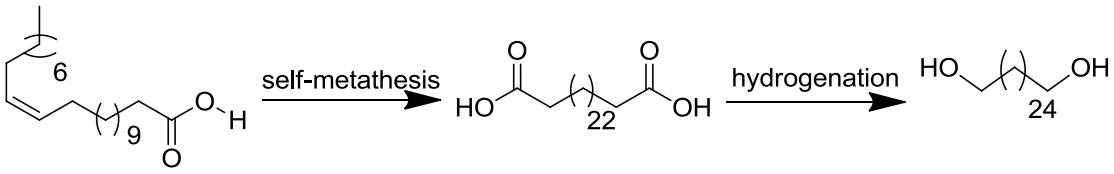

Scheme 5: Fatty acid based diacid and diol (Vilela 2012, Quinzler 2010)

Condensation of fatty acid based dimers with non-vegetable oil based diols such as 1,4-butanediol and ethylene glycol were also reported.[33, 34]

X. Glucose oxidation platform[35]

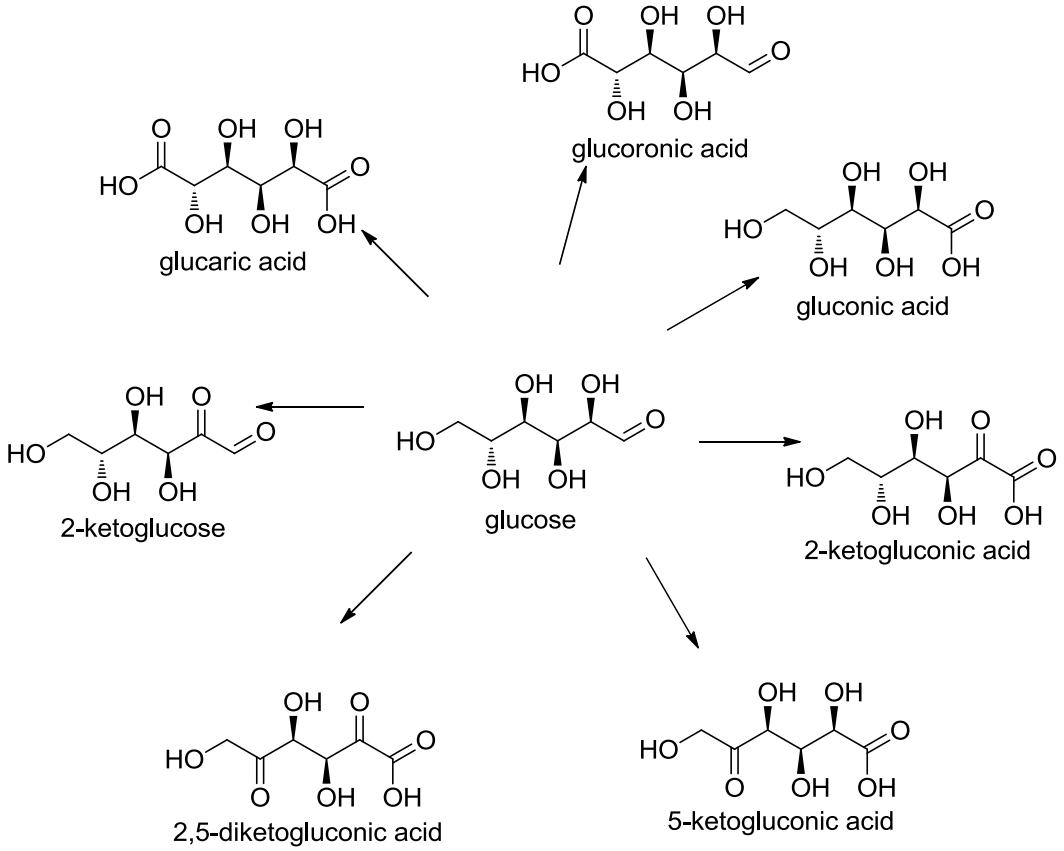

Scheme 6: Glucose oxidation platform

XI. Tartaric acid derivatives in polycondensation reactions

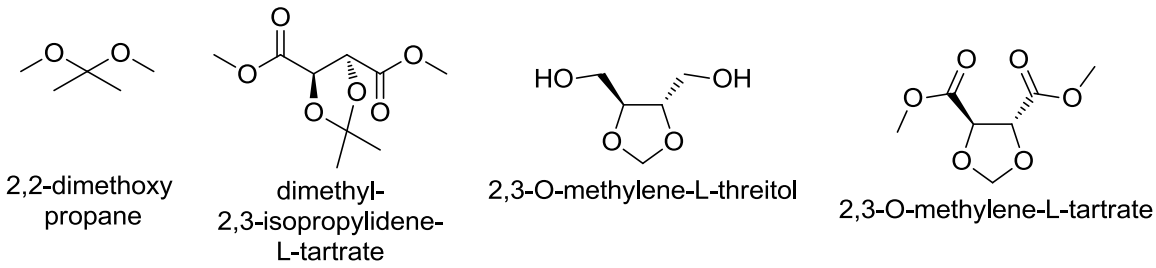

Scheme 7: Tartaric acid derivatives

The secondary hydroxy groups on tartaric acid are more reactive than the tertiary group on citric acid, and use of tartaric acid derivatives as monomers has therefore been preferred. One example is the protection of the hydroxy groups with 2,2-dimethoxypropane, as reported by Dhamaniya *et al.*, which leads to a diester compound.[36] After the polycondensation reaction, the protection could be reversed to give a hydroxy functionalised chain.

A different approach was used by Japu *et al.*, who converted tartaric acid to cyclic acetal compounds 2,3-O-methylene-L-threitol and dimethyl 2,3-O-methylene-L-tartrate.[37] These could then be used as rigid diol and diester monomers respectively, to partially replace terephthalic acid and ethylene glycol in PET.

XII. Polymers for biomedical applications based on citric acid

The biobased monomer citric acid has been used in a variety of polyester products, mostly destined for biomedical applications due to its biocompatibility and its ability to yield highly branched networks.

One example was reported by Dworakowska *et al.*, who used a citric acid containing polyester to make tissue scaffold material with promising properties.[38] A highly crosslinked network was obtained in a two step process. First, polycondensation of citric acid with 1,6-hexanediol yielded a highly acid functionalised network. This was then further crosslinked with a polyol obtained by epoxidation followed by ring opening of rapeseed oil.

Barruso-Bujans *et al.* also synthesised a material for drug release based on citric acid and ethylene glycol.[39] In this case, the excess hydroxy groups were reacted with long chain aliphatic alcohols such as decanol, dodecanol and octadecanol, and the obtained polymers were characterised using NMR spectroscopy.

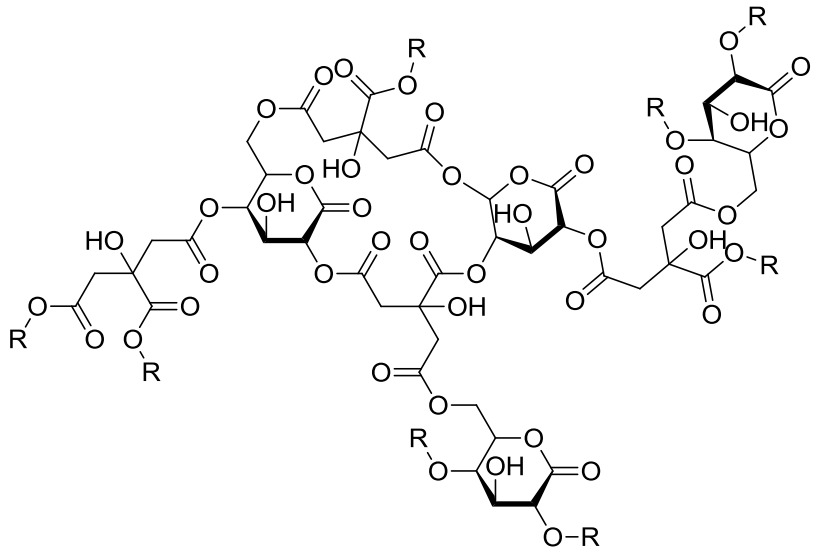

Scheme 8: Citric acid gluconolactone network (Tsutsumi 2004)

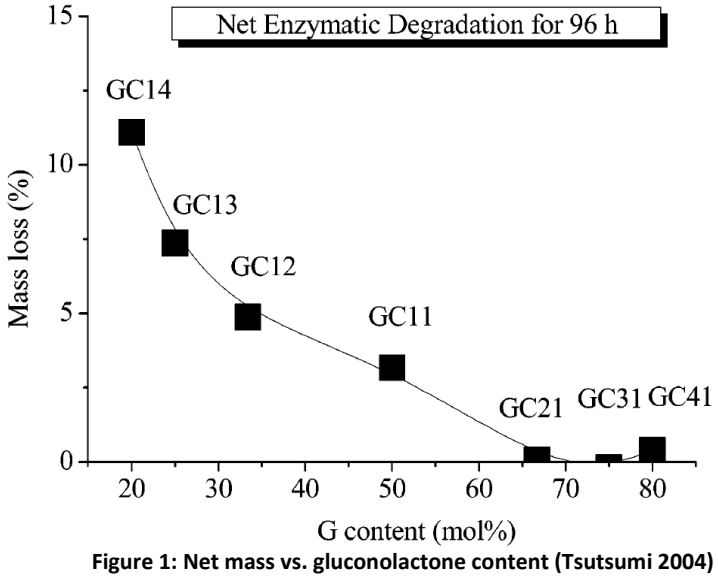

Figure 1: Net mass vs. gluconolactone content (Tsutsumi 2004)

Another biodegradable hyperbranched polymer network, shown above, was synthesised by Tsutsumi *et al.* from citric acid and gluconolactone.[40] The degradability was found to be proportional to the amount of citric acid incorporated in the network, as demonstrated in the graph on the left.

A highly crosslinked network was also synthesised by Doll *et al.* from citric acid and sorbitol.[41] The solubility of the product could be

controlled by impeding the crosslinking process either through the use of a large excess of citric acid, or by using sodium or disodium citrate salts. The esterification reaction proceeds via anhydride formation between two citric acid groups and can therefore be slowed down by the presence of sodium ions.

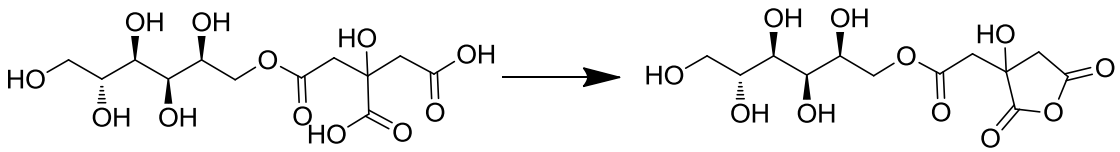

Scheme 9: Anhydride formation in a sorbitol citrate unit

Some examples of less highly crosslinked networks with free acid groups also exist. For example, Ding *et al.* condensed citric acid with polyethylene glycol to obtain a material for controlled drug delivery and biomedical applications.[42] The reaction proceeded uncatalysed, and control of degradation rate and mechanical properties was possible by adjusting the ratio of citric acid and PEG as well as the reaction time.

In a similar approach, Djordjevic *et al.* created a biocompatible polyester with free carboxylic and hydroxy end groups from citric acid, 1,8 octanediol and sebacic acid.[43] Again, no catalyst was used, and the presence of free functional groups can be used to attach biomolecules such as proteins. The properties such as biodegradability and mechanical strength of polyoctanediol citrate have also been investigated by Yang *et al.* in several papers.[44, 45]

Polyester systems both with excess of acid and with excess of hydroxy groups were obtained by Sathiskumar *et al.*, who used sebacic acid, citric acid, D-mannitol and castor oil in different relative quantities to synthesise prepolymers, which were then crosslinked under vacuum in an oven.[46] Glass transition temperatures between -29 °C and -19 °C were observed, as well as a hydrophilic surface leading to good biodegradability.

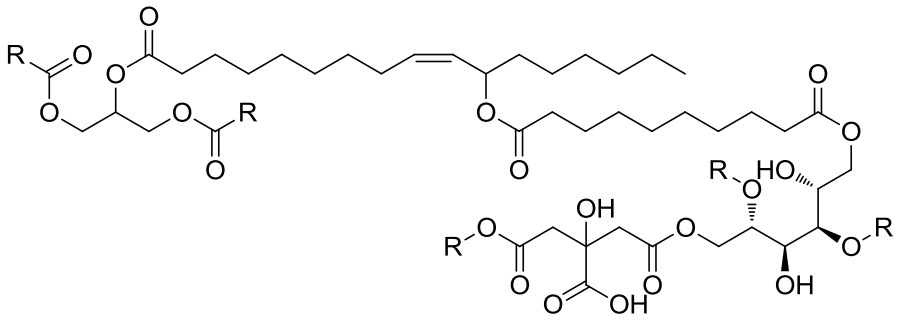

Scheme 10: Polyester from castor oil, sebacic acid, D-mannitol and citric acid (Sathiskumar 2011)

XIII. T-bend test

see chapter 7*, 7.5.1.*

XIV. Polyurethane coatings based on biomass

Gubbels *et al.* prepared a polyester resin from dimethylfurandicarboxylate and 2,3-butanediol and introduced hydroxy functionality with glycerol, pentaerythritol or trimethylol propane.[47] The quantities of the monomers were varied to make resins with OH values from 56 to 130 mg KOH/g

and glass transition temperatures between 35 °C and 83 °C. The resins were then crosslinked using a hexamethylene diisocyanate trimer to obtain transparent coatings of 30 – 55 µm thickness which displayed good solvent resistance but poor performance in impact tests.

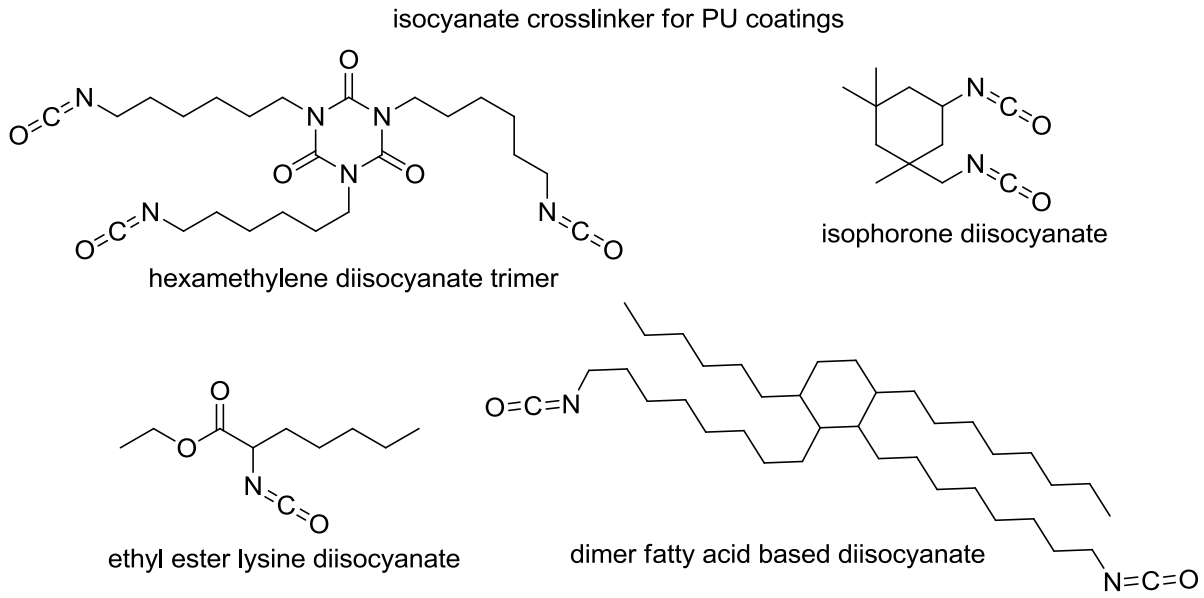

Scheme 11: Isocyanate crosslinker for PU coatings

From the same group, Gustini *et al.* used lipase catalysed synthesis to obtain fully biobased polyurethane coatings.[48] The hydroxy functional polyester resins were synthesised from 1,8-octanediol or 1,10-decanediol, and diacid length was varied from succinic acid to tetradecanedioc acid. Sorbitol was used to introduce branching and free hydroxy groups.

The biobased isocyanates dimer fatty acid based diisocyanate and ethyl ester lysine diisocyanate were used as well as the petroleum based hexamethylene diisocyanate trimer and isophorone diisocyanate to crosslink the resin. While some semicrystallinity was observed in the resins prior to crosslinking, which cause appearance problems in the final coatings, overall, good solvent and impact resistance was found.

Anand *et al.* also used sorbitol to introduce hydroxy functionality in a polyester polyol.[49] However the biosourced content was much lower since tetrahydro phthalic anhydride and adipic acid were used for the resin synthesis, as well as petroleum based isocyanate crosslinkers.

Kong *et al.* used transformed canola oil into a polyol which was then crosslinked with petroleum based isocyanate to obtain a coating with 60% biobased content.[50] As shown below, canola oil was first epoxidised and then hydroxylated with 1,2-propanediol or 1,3-propanediol. The coatings were examined for thermomechanical and mechanical properties, and correlations with the composition of the oils were established.

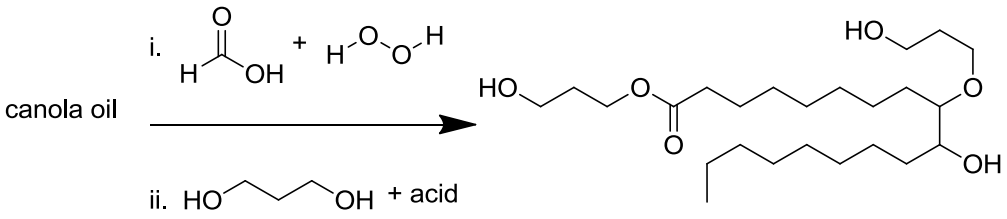

Scheme 12: Transformation of canola oil to trifunctional monomer (Kong 2013)

Similarly, Gaikwad *et al.* used karanja and cotton seed oil to produce a biobased polyurethane coating.[51] As shown below, the oils were epoxidised and then reacted with polyethylene glycol to obtain a polyester polyol that could be used in crosslinking.

The green solvent limonene, or dipentene, was also used to replace xylene in order to decrease the environmental impact of the coating. The final product showed good thermal stability as well as gloss, pencil hardness, adhesion, impact resistance and chemical resistance.

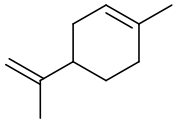

Scheme 13: Limonene

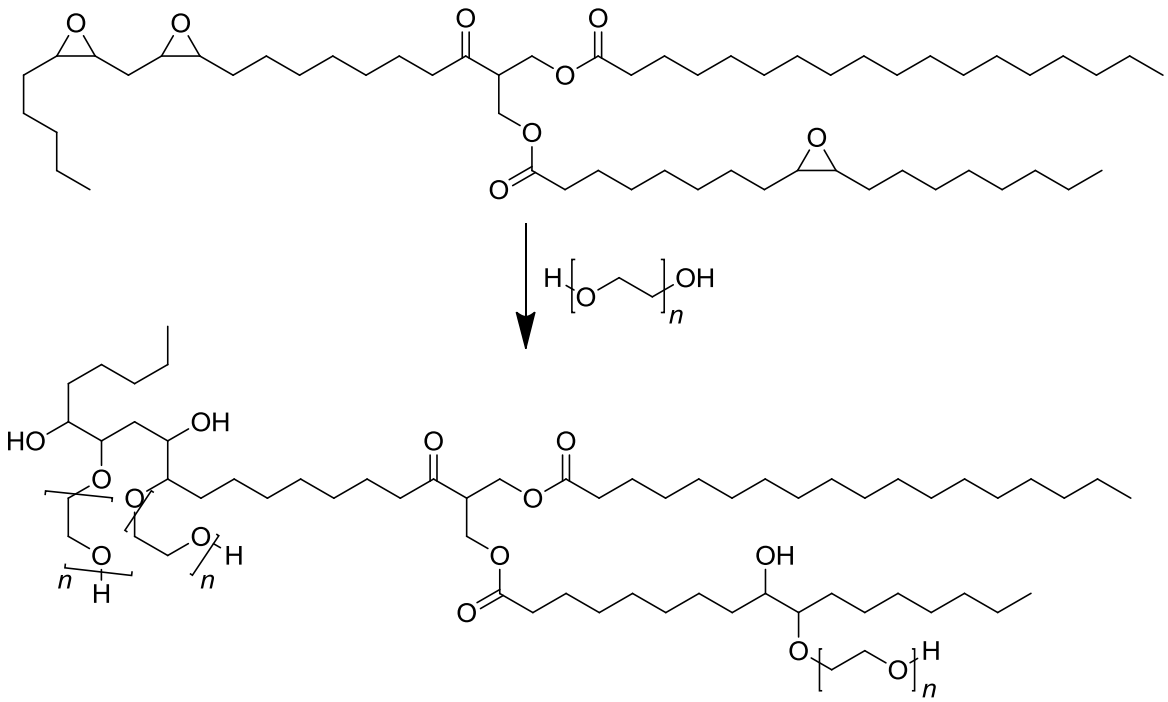

Scheme 14: Preparation of polyols from epoxidised oils (Gaikwad 2015)

XV. Furan containing polymers

While the majority of furan containing polyester compounds has been aimed at the replacement of polyethylene terephthalate, some coating applications were also reported. For example, Gubbels *et al.* produced a polyester by polycondensation of 2,3-butanediol and furandicarboxylic acid.[52] A large excess of diol was used in the reaction to obtain low molecular weight polymers suitable for powder coating applications. Products with glass transition temperatures from 50 °C to 120 °C were obtained.

Hussain *et al.* also aimed for a coating application and incorporated a copolymer made from radical polymerisation of furan or furyl acetate and maleic anhydride into a latex paint.[53] The presence of

furan moieties was found to increase hardness and water resistance, but also lead to low sheen and a slightly darker colour.

The colour problem was also observed by early studies testing the use of furandicarboxylic acid in condensation reactions. Moore *et al.* studied the properties of polymers based on FDCA and THF-dicarboxylic acid and various diols such as 1,6-hexanediol and ethylene glycol.[54] The authors found that polymerisation could be problematic due to sensitivity to aerobic oxidation at high temperatures. Furthermore, only a small dependence of the glass transition temperature on the relative configuration of the monomers was detected.

This was confirmed more recently by de Jong *et al.*, who found that the colour of a furandicarboxylic acid containing polyester increased linearly with increasing amounts of FDCA incorporated, but were able to circumvent this problem by using furan dicarboxylic esters instead of acids in the reaction.[55]

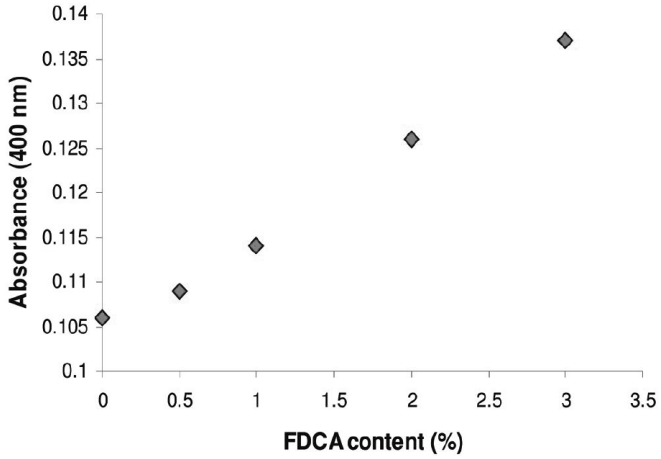

Figure 2: Colour change depending on FDCA content (de Jong 2012)

Gandini *et al.* studied the use of furandicarboxylic acid as a terephthalic acid replacement in PET, and concluded that it can both be readily synthesised and that the properties of the final material are comparable, so that replacement is possible.[56] Similarly, Ma *et al.* synthesised polybutylene furanoate (PBF) as an analogue to polybutylene terephthalate (PBT). They found that the two polyesters had similar crystallinity structures, and concluded that PBF is a promising candidate for PBT replacement.[57]

The company Avantium Chemicals BV actually made some plastic bottles from polyethylene furanoate (PEF) to examine their properties.[55] They found that PEF had higher tensile strength and much lower elongation at break than PET, but also better barrier properties toward water, carbon dioxide and oxygen.

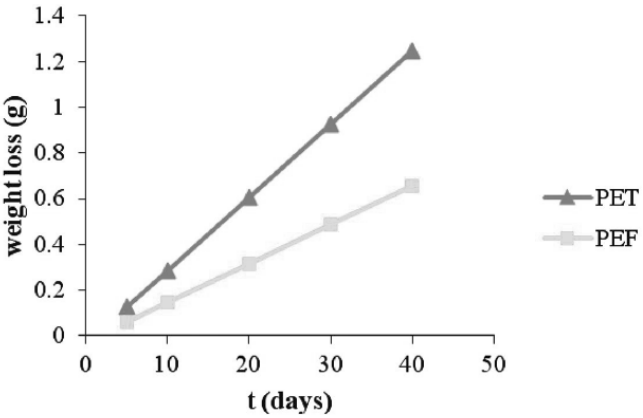

Figure 3: Water loss compared for PET and PEF (de Jong 2012)

The environmental performance of PEF was also evaluated, and it was found that it was possible to recycle it chemically and mechanically in the same procedures as PET. Furthermore, the mixing of PEF in a recycled PET stream was found to have no negative impact up to quantities of 5%. Consumption of non renewable energy and green house gas emissions were found to be 40 – 50% and 45 - 55% lower, respectively.

In a slightly different approach, Sousa *et al.* replaced terephthalic acid with FDCA in a condensation using bis-hydroxyethyl esters of both compounds.[58] Ratios from 4:1 to 1:9 terepthalic

acid to furandicarboxylic acid were examined, and it was found that at 20% replacement, properties are closest to those of pure PET.

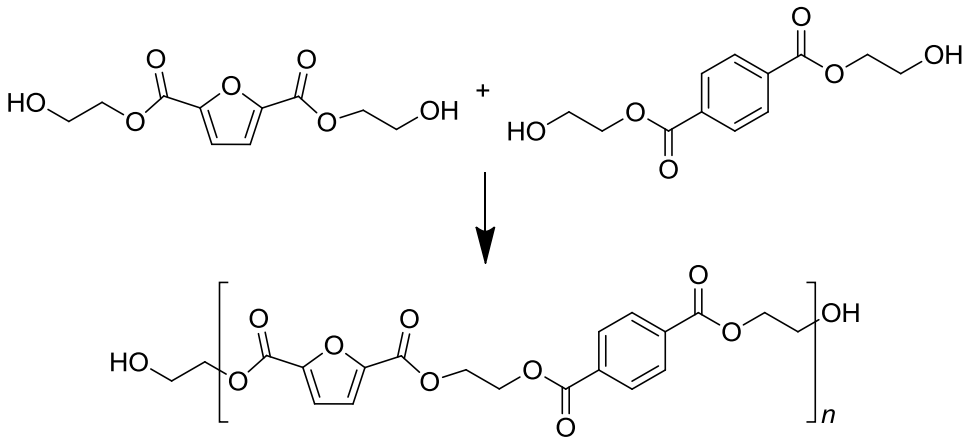

Scheme 15: Copolycondensation of bi-hydroxyethyl esters of FDCA and terephthalic acid

Lasseuguette *et al.* used a furan monomer, 2-hydroxymethyl-5-furanacrylic acid, as a chromophore.[59] The 2-hydroxymethyl-5-furanacrylic acid was obtained from biosourced HMF by a Wittig-Horner reaction with triethylphosphonoacetate. It was incorporated at 3 – 10% in an ethyl-6-hydroxyhexanoate polyester, which could then be crosslinked by UV radiation and thus serve as a photoresist in offset printing plates.

Scheme 16: 2-hydroxymethyl-5-furanacrylic acid (left) and ethyl-6-hydroxyhexanoate (right)

In order to evaluate their potential, Jiang *et al.* synthesised FDCA polyesters based on ethylene glycol, 1,3-propaneidol, 1,4-butanediol, 1,6-hexanediol and 1,8-octaneidol.[60] Diols were used in excess of 1,2 to 2,0 equivalents to FDCA. The products were crystalline, displayed thermoplastic properties, and also showed hydrophilicity. The authors concluded that they were promising replacements for benzene based products as well as suitable for biopolymer materials.

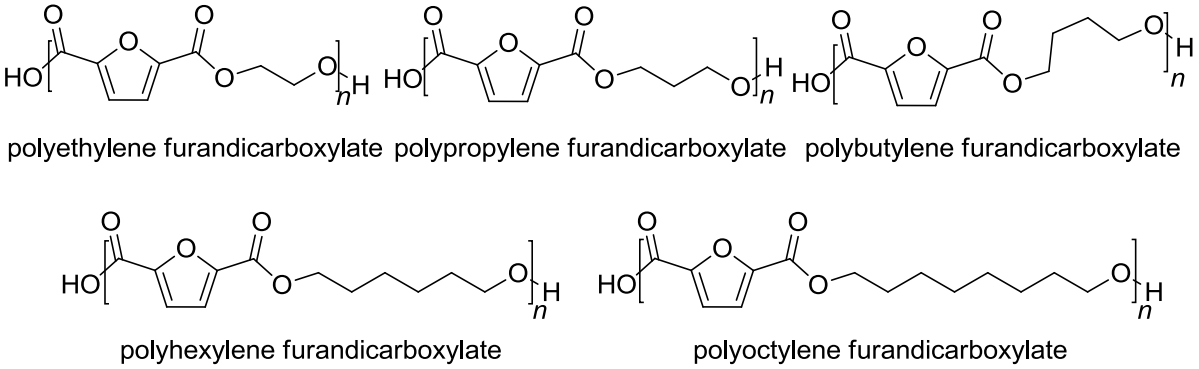

Scheme 17: FDCA polyester

The various aspects of linear polyester products made from furan dimers, shown below, were studied by Khrouf *et al.* in several publications.[61-63] The reaction with ethylene glycol, 1,3-propanediol

and 1,4-butanediol was investigated, as well as several catalysts and the kinetics of the transesterification reaction.

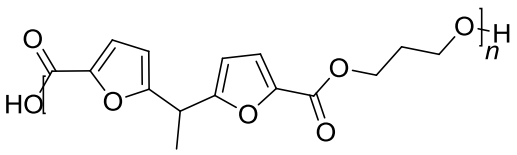

Scheme 18: Polyester from difurandiester and 1,3-propanediol

Papageorgiu *et al.* synthesised polyoctylene furanoate, and studied its thermomechanical characteristics.[64] They found high thermal stability, with a maximum decomposition rate that was reached only at 400 °C, as well as fast crystallisation. The glass transition temperature was found to be -5°C.

In an example of fully biobased polyester compounds, Wu *et al.* examined copolymers from succinic acid, furandicarboxylic acid and butanediol, and examined the effect of changing the succinic acid to furandicarboxylic acid ratio.[65] While the glass transition temperature showed a consistent increase with increasing FDCA content, the melting and crystallisation temperatures were found to decrease up to a content of about 40% FDCA, after which the increased again.

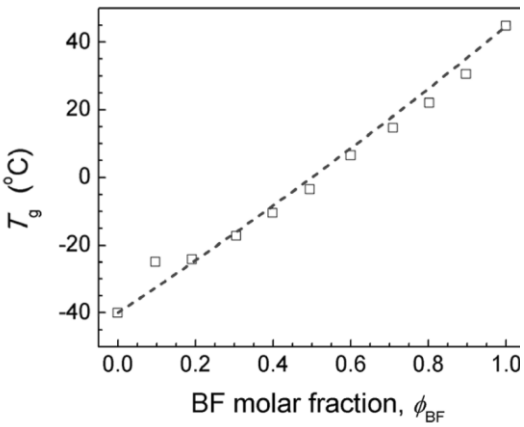

Figure 4: Behavior of T_g with FDCA content (Wu 2012)

In conclusion, it can be said that the versatility of furan monomers has been proven. FDCA polyester properties can be tuned through comonomers and reaction conditions, and a variety of reaction methods has been used to overcome reactivity and coloration problems. While it is a very promising candidate for the partial or full replacement of terephthalic acid in polyethylene terephthalate, detailed investigations into thermoset applications are, to our knowledge, still scarce.

XVI. Polyurethane and polycarbonate structure containing isosorbide

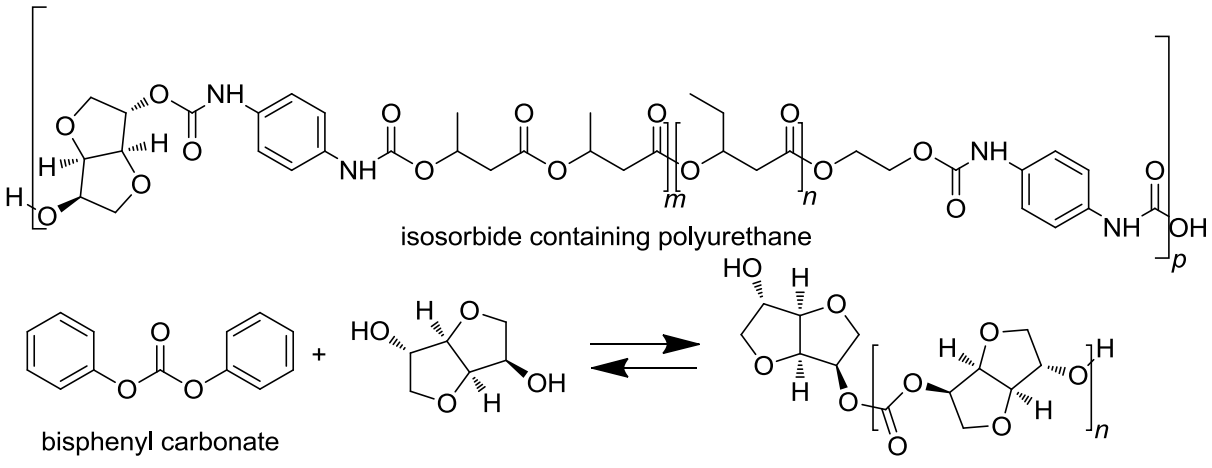

Scheme 19: Other isosorbide containing polymers

XVII. Unsaturated polyester resins containing isosorbide

One example of an unsaturated polyester resin was published by Goerz *et al.*, who made a polymer with shape memory properties from isosorbide, succinic acid and itaconic acid.[66] The resin was crosslinked with dimethyl itaconate, and the ratios of 1:0 to 9:1 of itaconic to succinic acid were investigated.

Fonseca *et al.* synthesised unsaturated polyester resins from sebacic acid and mixtures of isosorbide, diethylene glycol, 1,2-propanediol and 1,3-propanediol.[67] Itaconic or fumaric acid were used to introduce double bonds, and the resins were crosslinked with different amounts of 2-hydroxyethyl methacrylate instead of the less environmentally compatible styrene.

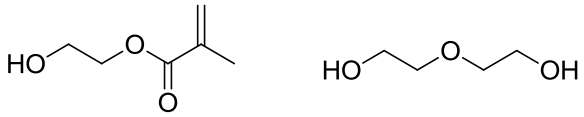

Scheme 20: 2-hydroxyethyl methacrylate (left) and diethylene glycol (right)

Thermomechanical properties were tested both before and after crosslinking. Before crosslinking, the rather low molecular weight compounds showed some differences in the temperature at which 5% of weight loss was observed, but only small difference in glass transition temperatures, as shown below. After crosslinking, the degradation temperature was not found to be dependent on the chemical composition.

Table 2: Properties of isosorbide containing unsaturated polyester resins

		UP1	**UP2**	**UP4**	**UP5**
isosorbide		0,20	0,20	0,10	0,10
1,3-propanediol		0,34	-	-	-
diethylene glycol		-	0,34	0,44	0,44
sebacic acid		0,22	0,22	0,22	0,22
itaconic acid		0,22	0,22	0,22	-
fumaric acid		-	-	-	0,22
T_g	**°C**	-28,0	-30,0	-37,4 and -13,0	-21,7
M_n	**g/mol**	626	920	600	3933
T_{decomp}	**°C**	249,1	279,0	250,8	344,5

An unsaturated and water soluble polyester resin was synthesised by Jasinska *et al.* from isosorbide, maleic anhydride and polyethylene glycol.[68] Most of the maleic anhydride was transformed to fumaric ester units, but some of the double bonds were lost in the condensation process. An increase of glass transition temperature was again observed with increasing isosorbide content, while an increase in polyethylene glycol had the opposite effect. The product was amorphous and deemed suitable to be used in radical crosslinking by the authors.

In a separate study, similar compounds synthesised from isosorbide, maleic anhydride and succinic acid were actually crosslinked with different unsaturated monomers such as 2-hydroxyethyl methacrylate.[69] The polyester structure was examined by NMR, and the existence of isosorbide bonds both to succinic acid, as well as its addition to maleic anhydride double bonds was confirmed.

Finally, another unsatured polyester resin based on isosorbide was made by Sadler *et al.* using ethylene glycol, maleic anhydride and adipic, suberic or sebacic acid.[70] The resins were characterised and cured with 35% styrene. Resins with similar molecular weights showed increased viscosity and less Newtonian flow with higher isosorbide content, but were all in the same range as a commercial unsaturated polyester resin, as shown on the left. After curing, the storage modulus showed a 74% increase for a 24 – 33% increase in isosorbide content. However, high isosorbide contents also led to insolubility in styrene, which made it difficult to obtain thermosets with sufficient rigidity for high demand applications.

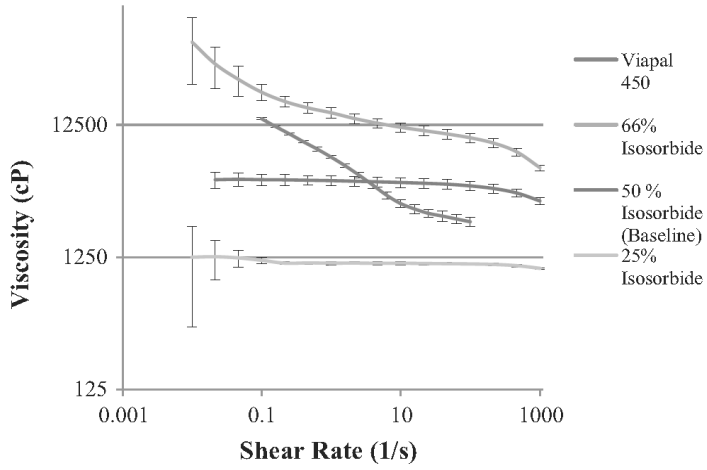

Figure 5: Isosorbide effect on the viscosity of an unsaturated polyester resin (Sadler 2014)

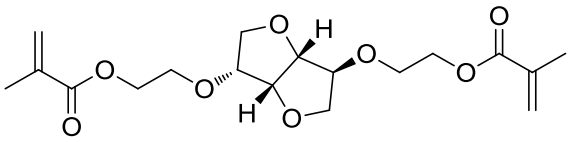

Scheme 21: Ethoxylated isosorbide dimethacrylic resin

Additionally, Lukaszczyk *et al.* made a dimethacrylate resin for dental restorative systems incorporating isosorbide, as shown above, and Raytchev *et al.* obtained a thermoset using azide-alkyne cycloadditions. [71, 72]

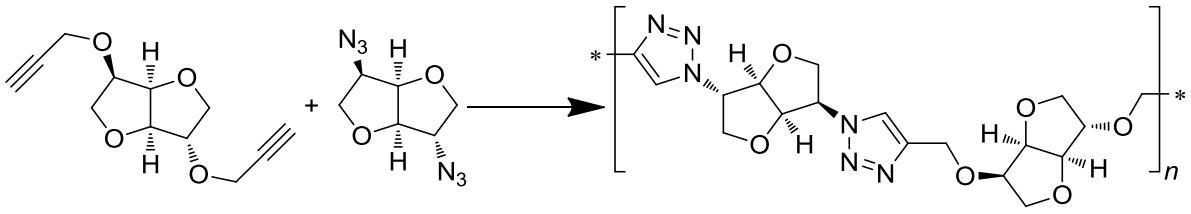

Scheme 22: Isosorbide thermoset from azide-alkyne cycloaddition (Raytchev 2013)

XVIII. Step growth and addition polymers based on vanillin

An alternative use for the monomers described by Pion *et al.* was reported by Oulame *et al*., who reacted the diphenols with isocyanates to make linear polyurethanes.[73, 74] Furthermore, Pemba *et al.* created cyclic and spirocyclic polyacetyl ethers from dialdehydes obtained from the reaction of vanillin with dibromoethane, as shown below.[75]

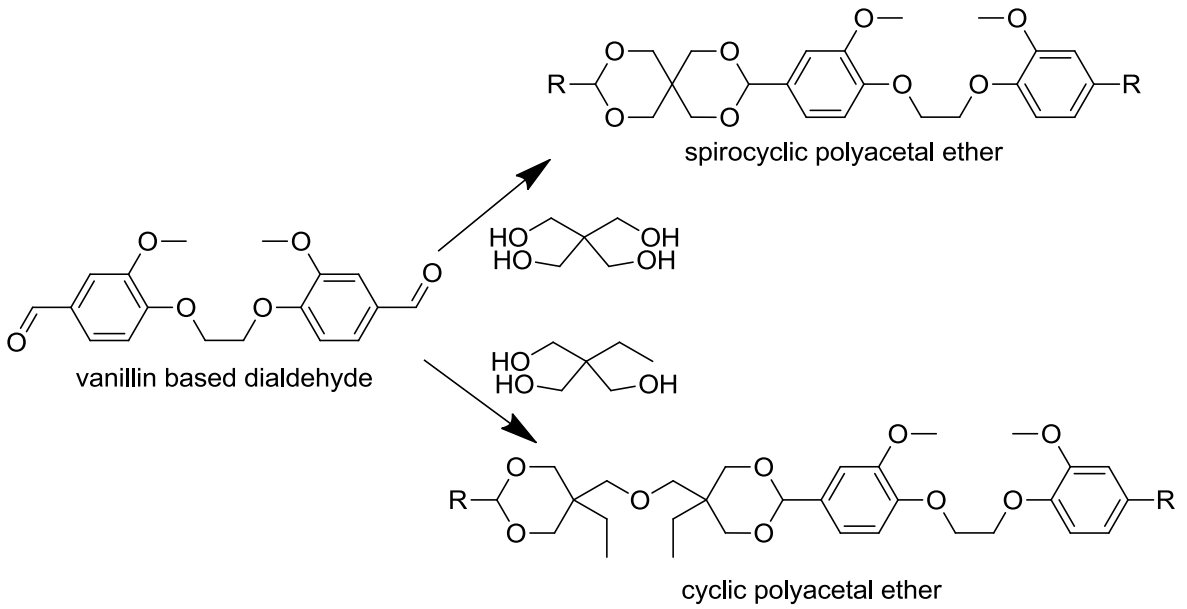

Scheme 23: (Spiro)cyclic polyacetal ethers obtained from vanillin based dialdehyde (Pemba 2014)

Chauhan *et al.* transformed vanillin into vanillin oxime using hydroxylamine hydrochloride, and created a terpolymer with a molecular weight of 5400 g/mol from vanillin oxime, *p*-hydroxy acetophenone and formaldehyde.[76]

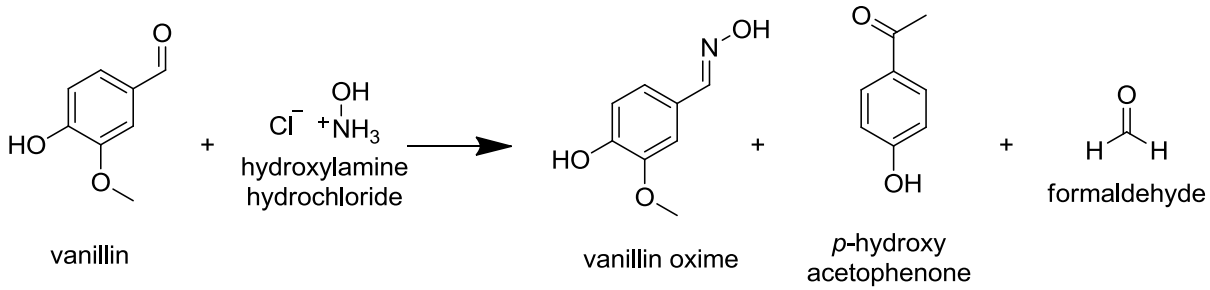

Scheme 24: Monomers for vanillin oxime resin (Chauhan 2014)

An oxidative polymerisation was reported by Beristain *et al.* who reacted ferulic acid with 3-bromo propyne to create a bisacetylene.[77] It was then converted to a polyester-ether, which can further be photo crosslinked using the triple unsaturation.

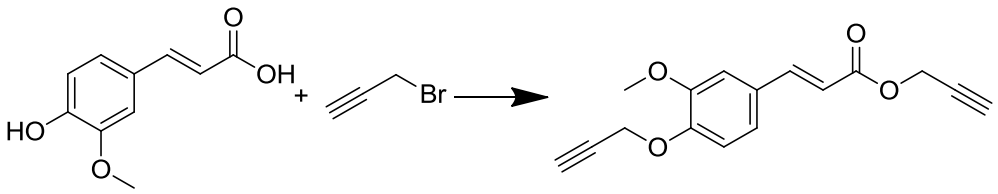

Scheme 25: Ferulic acid reaction with 3-bromo propyne (Beristain 2009)

An example of acyclic diene metathesis was presented by Barbara *et al.*, using an α,ω diene based on ferulic acid and isosorbide.[78]

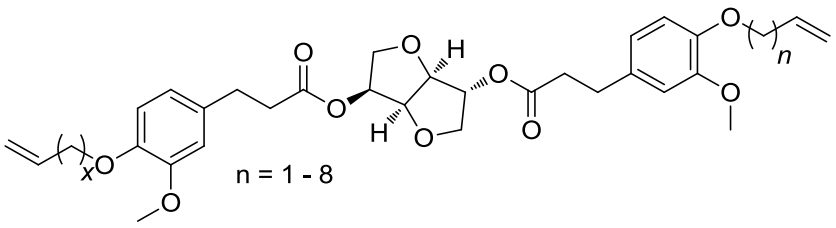

Scheme 26: Ferulic acid – isosorbide α,ω diene monomer

A variety of acrylate polymers have also been reported. Methacrylic anhydride was used for example by Stanzione *et al.* and Zhang *et al.* to create vanillin and vanillin alcohol methacrylates with a DMAP catalyst.[79, 80] Iemma *et al.* and Parisi *et al.* on the other hand used methacrylic acid and ethylene glycol dimethacrylate as comonomers in the polymerisation of ferulic acid.[81, 82]

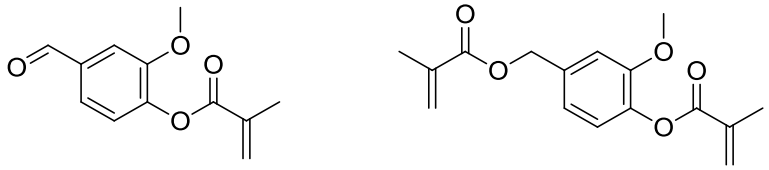

Scheme 27: Methacrylated vanillin (left) and vanillyl alcohol (right)

Zhang *et al.* used methacryloyl chloride in suspension polymerisation to produce polymeric microspheres for waste water treatment.[83] After polymerisation, the free aldehyde groups were reacted with glycine to improve their chelating ability.

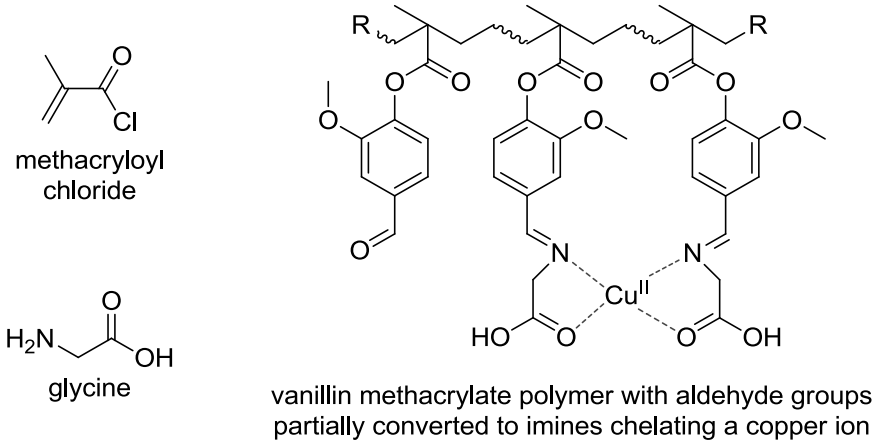

Scheme 28: Vanillin methycrylate polymer for waste water treatment (Zhang 2015)

Lastly, Amarasekara *et al.* reported an electrochemical polymerisation of vanillin.[84] After it was converted to a divanillin derivative using horseradish peroxidase, electrolysis in 1M NaOH was used to reductively crosslink the monomers at the aldehyde group.

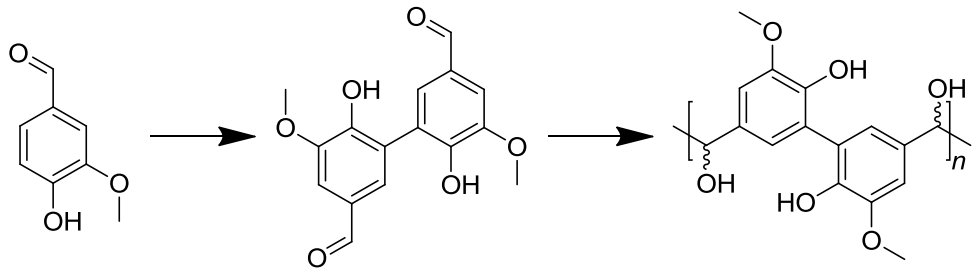

Scheme 29: Electrochemical polymerisation of vanillin (Amarasekara 2012)

Chapter 3

XIX. Hindered amine light stabilisers mechanism of action

The exact mechanism has recently been elucidated by Gryn'ova *et al.* with the help of molecular orbital theory calculations.[85] As shown below, three mechanisms referred to as β-abstraction, γ-abstraction and JKZG cycle, after the proposing authors Jensen, Korcek, Zinbo and Gerlock, are possible.[86] β-abstraction has been identified by the authors and confirmed by Paine *et al.* to be the most probable pathway.[87] Where no β-hydrogens are available, γ-abstraction may also take place.

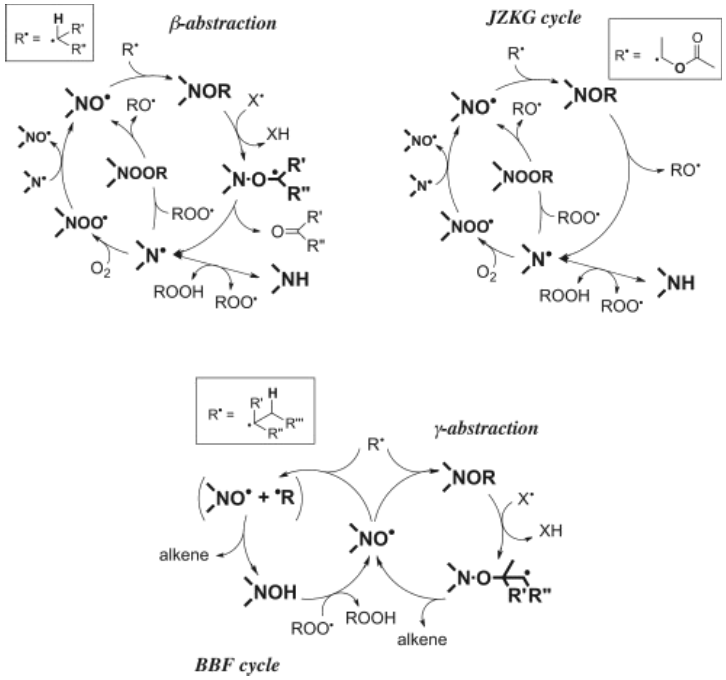

Scheme 30: Possible action mechanisms of HALS (Paine 2014)

XX. Outdoors accelerated weathering

Since it is not possible to expose the material to be tested in all possible use conditions, specific sites which are known to provide harsh conditions of one or several types of exposure are usually selected. However, since the weather is never exactly the same, it is important to measure the exact conditions encountered during the exposure.

The most important variables to be measured corresponding to the different degradation pathways elaborated above are the sunlight, the temperature and moisture. Atmospheric pollutants also need to be taken into accounts where they cause adverse conditions, which is the case for example with acid rain.

Sunlight

Important parameters for the characterisation of sunlight are the distribution of the wavelength and their intensity. A pyranometer, which measures light from 285 – 3000 nm, or a total ultraviolet radiometer, which measures light from 300 – 385 nm can be used to investigate the sunlight at a certain location, depending on which degree of precision is required for the ultraviolet region. The result is reported in $MJ*m^{-2}nm^{-1}$ or in Langleys, which are cal/cm^2.

The angle at which panels are exposed to sunlight is also important, and needs to be considered relative to the angle of the sunlight at the specific time of the year. In order to accelerate the effect of the sunlight, a Fresnel reflector device or Emmaqua device, which concentrates the ultraviolet part of sunlight spectrum to 500% of its natural level and follows the direction of the sunlight throughout the day, can be used.

Temperature

In order to predict the effects of temperature on a substrate, it is important to measure both the ambient temperature, keeping in mind that it can undergo sudden changes for example when it snows, and the actual surface temperature of the sample. The surface temperature is much more important to the actual weathering process, and depends on the type of radiation, and the specific absorbance and thermal conductivity of the sample. A black panel is often used to estimate the surface temperature in a given location.

Humidity

Humidity can affect coatings in the form of relative humidity in the air, rain and condensation. Therefore, it is important to define not only the humidity, but also the hours of wetness, which combine the three factors. They are also dependent on the sample temperature, as high temperatures will cause quicker drying.

In particularly dry areas such as the desert, water can sometimes be added artificially to the exposed panels by regular spraying.

Atmospheric pollution

Other than a good knowledge of the presence of pollutants in the atmosphere, their concentration, pathway of deposit on the surface and the velocity of the wind are also important to define exposure. Atmospheric pollution can have an effect on the light spectrum, and vice versa.

XXI. Methods for weatherability assessment

Direct assessment of coating performance

The advantage of direct assessment of the coating performance is that mistakes due to erroneous assumptions in the extrapolation process which is needed for the evaluation of indirect assessment methods are avoided. Therefore, results from such tests are generally treated with more faith, and a good performance is a necessary criterion for coating to be brought to the market.

Examples of direct tests to evaluate the mechanical properties of a coating are the impact test, the Erichsen slow indentation test and the T-bend test, which are described in detail in the experimental section. These tests are used to evaluate if the coatings adhesion, flexibility and hardness are adequate, and can be performed on weathered samples. However, the pass/fail nature of the test results, even if it can be graded to some extent, doesn't facilitate detailed conclusions about the nature or quantity of degradation that has taken place.

Gloss retention and colour change are a more useful means to quantify degradation. The gloss retention test measures the amount of light reflected at a specific angle, generally 60°. As the coating surface develops cracks, the incident light gets more scattered and less is reflected back at the original angle. The advantage of this technique is therefore that it correlates both to loss in quality, i.e. matting, that could be observed by the consumer, and to the microstructure of the coating surface.

Colour change test measures the colour along the black and white, green and red and blue and yellow axes, and gives an estimate of the total change which has occurred. This test is also highly relevant to the perception of the coating quality by the customer, but its results are a little harder to interpret than the gloss retention. Furthermore, the test is mostly relevant to pigmented coatings. As the evaluation of resins often takes place in clearcoats to avoid catalytic acceleration of degradation reactions or shielding from UV light, the colour change is not as common as a weatherability parameter.

The elongation at break can also be a direct measure of the brittleness developing in the film. However, it can only be measured on a free film. Therefore, it is directly consumer relevant solely for polymer products which are used separate from a support.

Lastly, the loss of film matter, also referred to as the difference in film thickness (DFT), is a straightforward way to evaluate the degradation. It can be assumed that it is relevant to the consumer, and the test is fast and easy. However, the evaluation of the results can be less straightforward, as several mechanisms such as the erosion of degraded material but also the loss of free volume may be responsible for the result.

Indirect assessment of coating performance

The indirect assessment of coating performance often allows a much finer differentiation between samples, and is also more closely linked to the molecular structure of the coatings. Unfortunately, it also adds a step of interpretation between the results and the actual performance. The outcome has to be therefore treated with caution, and correlation between good performance and certain parameters have to be established for each type of coatings. Depending on the technique, indirect assessment of coating stability can be performed either on the bulk or on individual molecular species.

Bulk properties

The advantage of measuring bulk properties of the sample is that the result represents an average of the entire film over the property that is measured. This adds to the validity of the result.

Examples of techniques used to evaluate bulk properties are differential scanning calorimetry (DSC) and thermogravimetric analysis (TGA) which can be used to define thermal properties such as the glass transition temperature (T_g), and dynamic mechanical analysis (DMA), which can be used to determine the T_g but also the crosslinking density.

Another example are μ-hardness tests, which use a pyramid-shaped indenter to determine the force necessary to penetrate the sample, but also the viscoelastic response when the force is maintained and relieved again.

A similar method is to measure the chemical relaxation, which is the change of the response to an applied strain that occurs by rearrangement of bonds.

The responses to DSC, DMA, μ-hardness and chemical relaxation tests all largely depend on the polymer network structure, and the physical and chemical interaction of the chains and individual monomer units. While the results can change depending on exterior factors such as temperature and humidity, it is possible to standardise the techniques if care is taken to keep parameters such as the heating rate, force applied and frequency constant.

Surface characterisation

A popular method to assess the quality of the surface is by microscopy. Mostly, four different techniques are used. Optical microscopy is the least expensive, and can be used to observed rough changes and heterogeneities. In order to evaluate the surface on a molecular level, atomic force microscopy (AFM) or scanning electron microscopy (SEM) can be used. The former can be quantified by measuring the surface roughness root mean square, and plotting a curve of the depth of irregularities. Other than that, there is no standard for the optical evaluation of scans. Chemical force microscopy (CFM) is less common, and can be used for example to evaluate the response of a surface to specific functional groups, and thus to derive its polarity.

Where direct assessment of coating performance is concerned, surface characterisation will probably correlate best with gloss retention measurements, since both derive from the surface structure.

Another possible approach is X-ray photoelectron spectroscopy (XPS), which can be used to determine the relative amount of different elements on the surface. Generally, upon degradation an increase of nitrogen, due to the migration of melamine to the surface, can be observed. Furthermore, oxidation reactions can cause a relative increase in oxygen and decrease in carbon. However, the possibility of picking up signals from dirt accumulated on the surface has to be taken into account when results are evaluated.

Individual molecular species

Assessment of individual molecular species is easiest to relate back to changes made in the structure or the formulation. However, additional care has to be taken as to the method that was used. One of the most popular techniques used is Fourier transform infrared spectroscopy (FTIR), which can pick up signals from different depths of the film depending on the thermal conductivity of the sample and the parameters used. Experiments with step scan photoacoustic infrared spectroscopy have shown that degradation varies in different depths of the film.[88] Similarly, attenuated total reflection (ATR) IR depends largely on the contact of the probe with the surface, and intensity can decrease when surface roughness increases. Therefore, the results assessments of individual molecular species always have to be evaluated carefully, keeping in mind that the observations might be specific to a certain region of the sample.

FTIR analysis has been used to qualitatively and quantitatively examine the chemical changes in weathered coatings in many studies. The following peak changes are generally monitored where melamine crosslinked polyester films are concerned and can be found reported for example by Delorme *et al.*[89]: A broad band between δ3000 cm^{-1} and δ3800 cm^{-1} is attributed to N-H and O-H stretching vibrations. More specifically, the maximum for the O-H stretching vibration υ(O-H) can be found at δ3500 cm^{-1}, and the vibration from unreacted or newly formed N-H bonds υ(N-H) has a maximum at δ3360 cm^{-1}. These are generally expected to increase with ageing.

The carbonyl stretching vibration υ(C=O) can be found at δ1735 cm^{-1}. With ageing, broadening or the growth of additional maxima at δ1850 cm^{-1} to δ1750 cm^{-1}, δ1710 cm^{-1} and at δ1620 cm^{-1} is observed.

The triazine ring of the melamine crosslinker υ(C=N) absorbs at δ1550 cm^{-1} in an in plane and at δ815 cm^{-1} in an out of plane deformation. While the out of plane deformation is not expected to change and can therefore be used as a reference, the in plane deformation is highly dependent on the nature of substituents, and is expected to decrease during degradation.

Lastly, a vibration from the C-O ester bond of residual methoxy groups on the melamine ring absorbs at 913 cm^{-1} and can be used to determine the completeness of the crosslinking process.

Other spectroscopic techniques that can be used include Raman spectroscopy, which is less common, and electron resonance spectroscopy (ESR), which can be used to identify and quantify radicals. This is particularly important for the examination of photolytic degradation, but can be difficult due to the short lifetime of radicals. Two techniques are possible to circumvent this problem: Either the spectrum can be measured at very low temperatures, where the radicals are trapped in the glassy matrix, or the film can be doped with nitroxide species prior to curing. The degradation of the nitroxide species, which are used up as they trap the radicals formed, can then be observed to indirectly quantify the radical formation rate.

Ultraviolet/visible spectroscopy (UV/Vis) can be a useful means to determine the presence and formation of chromophores in a coating. However, in pigmented coatings the signal of the pigment is likely to be so strong that it obscures all signals from the resin.

The measuring of chemiluminescence, i.e. the emission of excess energy from a chemical reaction in the form of luminescence, can also be used to understand the processes involved in polymer degradation. Lastly, slow positron beam technique (SPBT) has also been used to determine the free volume in a sample of polymer film.

Characterisation on film components prior to curing

Some characterisation techniques, such as size exclusion chromatography (SEC), gas chromatography-mass spectrometry or matrix assisted laser desorption/ionisation – time of flight mass spectrometry (MALDI-ToF), which can reveal the exact size of molecules and therefore help identify for example degradation fragments, require solubilisation of the sample that is to be analysed. As this is not possible for most thermosetting coatings, analysis of this type on the realistic weathered coating is not possible.

Several studies have been conducted on the degradation of thermoplastic polyesters which can be solubilised, or on single components of the coating formulation prior to curing. While this enables a much more precise identification of the products formed than the techniques described above, many differences exist between a thermoplastic polyester and its equivalent in a thermosetting coating. These include the bonds to the crosslinker, the presence of the other ingredients of the formulation, but also of course the structural elements which limit for example chain mobility.

In a best case scenario, it would be possible to study the weatherability of a coating and relate any improvements or problems to single components, and then accordingly improve the design. In reality however, a compromise generally has to be made between the ease at which the assessment can be related to the molecular composition of the coating, and the relevancy of the assessment to the final properties the coating will display, as shown in the figure above. As a result, properties whose relevance is questionable are often measured and related to structural aspects of the coatings which are secondary effects of the formulation, and cannot easily be adjusted.

XXII. Details of literature studies on the degradation of thermoplastic polyesters of interest

An interesting study was published by Carroccio *et al.*, who found direct evidence of α-hydrogen abstraction and the Norrish type I degradation mechanism, and of an increase of chromophore concentration with weathering.[90] They studied the photodegradation of polybutyl succinate pressed into a 100 µm film in a QUVa chamber, i.e. a weathering chamber with UVa radiation, at 60 °C during 8 days using MALDI-Tof spectrometry and UV/Vis spectroscopy. While originally, only four different type of compounds, distinguished by their end groups being either two hydroxy groups, two carboxylic acid groups, one of each, or by the absence of end groups due to cyclic nature, evidence of degradation products was found after short periods of exposure. The amount of cyclic oligomers was found to decline, while a slight increase of the amount of carboxylic end groups was observed at the expense of a slight decrease in hydroxy end groups. This was interpreted as evidence for an oxidation reaction of the former to the latter.

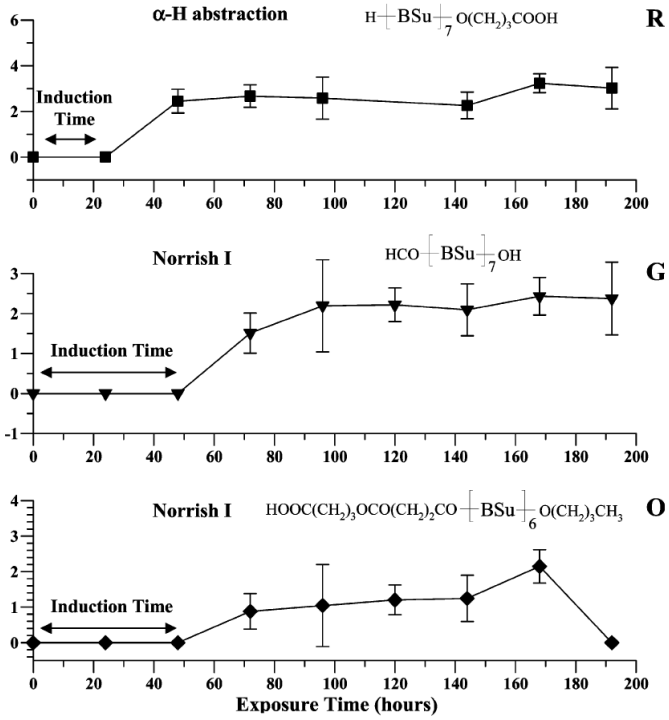

Figure 6: Evidence of α-hydrogen abstraction, Norrish I and Norrish II type degradation products (Carrocio 2004)

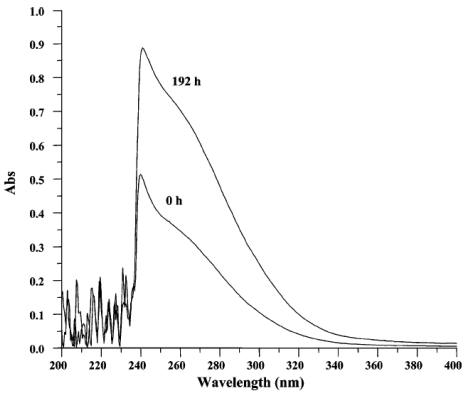

Figure 7: Broadening of UV spectrum after degradation (Carroccio 2004)

Furthermore, evidence of α-hydrogen abstraction and Norrish type I degradation products such as butyl formate, ethyl ester, butyl ester and malonic acid was detected. Both mechanisms occurred after an induction period as shown above. This was explained with the increase of chromophores detected from an increase in intensity and a broadening of the UV absorption spectrum, shown above. Since a β-hydrogen abstraction would lead to products with the same mass as cyclic oligomers, this mechanism could not be confirmed. However, it was assumed not to be dominant due to the decrease in concentration of products of such mass mentioned above.

Shigemoto *et al.* used computational chemistry to shed some light on the β-hydrogen abstraction mechanism.[91] They evaluated its contribution to thermal degradation of polyterephthalates in a quantum chemical study using B3LYP level of theory. Ethylene-, 1,3-propylene- and 1,4-butylene dibenzoates were used as model compounds in the simulation. The optimised structures of the starting material, transition state and product are shown on the left.

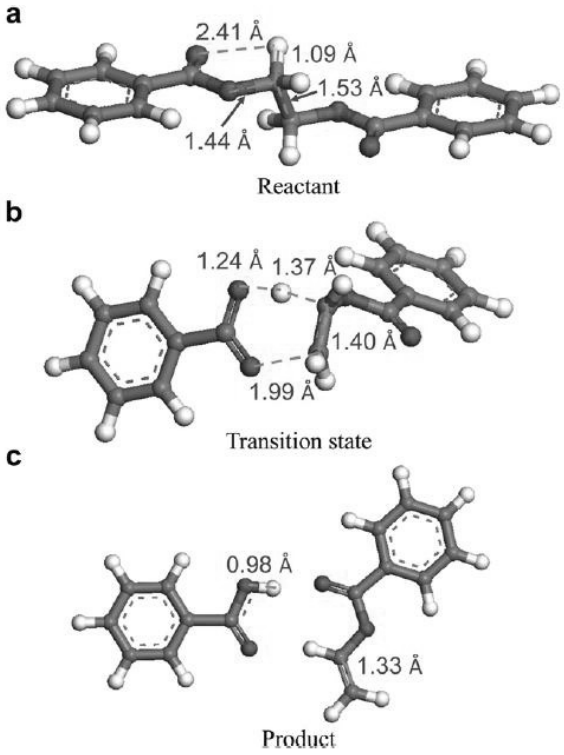

Figure 8: States of aromatic-aliphatic β-hydrogen abstraction (Shigemoto 2012)

The activation energy for the uncatalysed reaction under vacuum was calculated as 51,1 kcal/mol, which matches the experimental activation energy of 53,4 kcal/mol well. The effect of various metal acetate and alkoxy catalysts were evaluated, but no decrease in the activation energy due to the presence of the metal and therefore no catalytic effect on the reaction were observed.

Nagai *et al.* studied both the relative importance of different degradation mechanisms, and the wavelength regions responsible for photolytic degradation. In a first publication, they compared the importance of different degradation causes for a polybutylene terephthalate-polytetramethylene glycol polyester-polyether thermoplastic film.[92] Samples were irradiated with a 1500 W xenon lamp equipped with a filter for wavelength below 290 nm, thermally degraded at 100 °C, and exposed to different corrosive solutions including potassium hydroxide, sulphuric acid, nitric acid and hydrochloric acid. Analysis was performed using FTIR, NMR and molecular weight measurements.

Photolytic degradation was found to mainly occur in the ether part of the chains in both accelerated and natural weathering. In analysing the effect of different wavelength, it was found that main chain scission was mostly caused by wavelengths below 310 nm. The photolytic degradation process was found to be accelerated by temperature, but little evidence of degradation caused by temperature alone was detected. Similarly, the structural changes observed in natural weathering were not observed in the hydrolysis experiments. It was therefore concluded that UV light is the most important factor causing the degradation.

Later on, Nagai *et al.* also investigated the importance of different wavelengths in photolytic degradation for poly (2,6-butylenenaphthalate-co-tetramethyleneglycol).[93] In this study, it was found that wavelengths below 380 nm can cause chain scission. Furthermore, the wavelengths in the area of 370 – 380 nm were identified to be particularly influential in forming the degradation products of aldehydes, esters and formates.

The effect that single monomers can have on weatherability was also investigated by several groups. One example is the work of Malanowski *et al.*, who investigated the difference in degradation mechanisms between isophthalic acid and terephthalic acid, but also between different accelerated

weathering tests.[94-96] The photolytic degradation of polyneopentyl isophthalate and polyneopentyl terephthalate was studied using MALDI-Tof, size exclusion chromatography and ATR FTIR spectroscopy. It was found to proceed in a Norrish type I mechanism via the three different radical intermediates shown below.

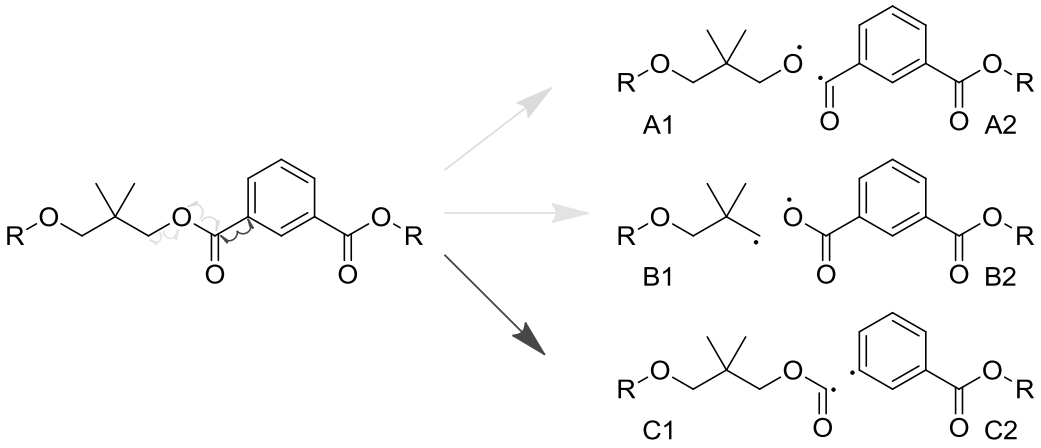

Scheme 31: Radical intermediates in Norrish type I degradation (Malanowski 2011)

Radicals A2 and B2 are thought to convert to C2 by loss of carbon monoxide or decarboxylation. The nature of crosslinks formed from these radicals was determined by breaking ester bonds through methanolysis and thus producing soluble degraded fragments. Two different types of crosslinks, formed between two aromatic rings or between the neopentyl glycol chain parts, were observed and are presented below.

In comparing the degradation of isophthalate and terephthalate polyester, the same mechanism was observed. The rate was considerably higher for the terephthalate containing polyester than for the isophthalate containing polyester according to FTIR and SEC. This was attributed to the greater overlap of the absorption spectrum of terephthalate with the UV light emitted in the weathering test. Generally, the authors observed a correlation between the photon absorption and the degree of degradation.

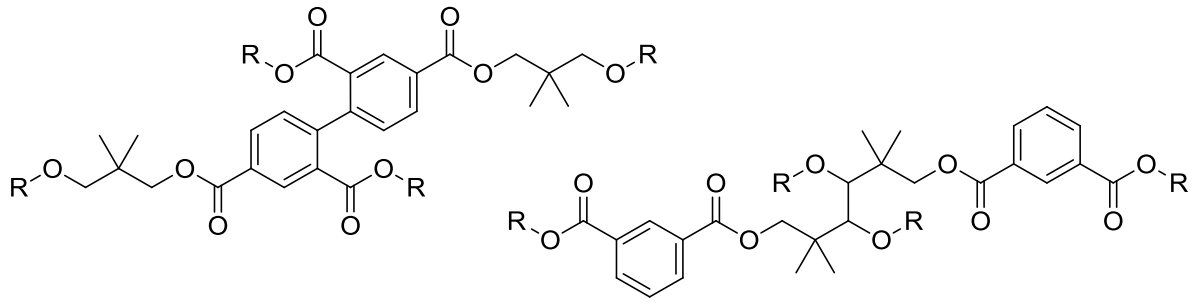

Scheme 32: Types of crosslinks formed after radical degradation (Malanowski 2011)

The authors also compared the different effects of weathering in a QUVa chamber, a xenon arc suntest and natural exposure. Generally, MALDI-Tof and FTIR analysis revealed the same products and degradation mechanisms, validating accelerated weathering as a prediction method. SEC however revealed a difference in the crosslinking to chain scission ratio between the polyester aged in a QUVa chamber, with a peak at 240 nm, and a polyester aged with a filtered xenon arc, with a peak at 300 nm. This is explained by the fact that in a QUVa test, most radicals are absorbed in the

surface, creating a large concentration in a small space, while the light from the xenon arc suntest penetrates also the deeper layers. Since radical recombination reactions are second order rate dependent on the radical concentration, while Norrish type I reactions, leading to chain scissions, are only first order dependent on the radical concentration, a higher concentration will lead to a higher rate of recombination reactions compared to chain scissions.

A lot of attention has also been dedicated to the impact of renewable monomers. For example, Commereuc *et al.* studied the impact of aliphatic and aromatic monomers on the balance between chain scission and crosslinking reactions during the degradation process.[97] The dominance of either process was examined in five different polyesters upon exposure to UV light through the melt viscosity which was used to estimate the molecular weight over time. Two aliphatic polyesters, polylactic acid and polybutyldodecanoate, a cycloaliphatic polyester made from 1,4-butanediol and cyclohexanedicarboxylic acid, and two aliphatic/aromatic polyesters, poly(butylenes terephthalate-co-butylene adipate), commercially available as Ecoflex, and secondly polybutylene terephthalate, were evaluated. A mix of polybutyldodecanoate and the cycloaliphatic polyester was also evaluated.

Chain scission was observed to be the predominant mechanisms for the polylactic acid and polybutyldodecanoate. Contrarily, the Ecoflex and polybutylterephthalate polyesters were observed to undergo crosslinking reactions. Interestingly, a decrease in molecular weight was observed for the polyesters containing a cycloaliphatic monomer in the first half of the weathering, followed by an increase in the second half, indicating a strong competition between crosslinking and chain scission.

This led the authors to conclude that aliphatic monomers cause degradation by chain scission, while aromatic monomers cause degradation by recombination reactions. The degradation of the different polyesters was not compared quantitatively.

These conclusions are confirmed and materials are examined in a later paper by Commereuc *et al.*, in which some thought is also given to the crystallinity and stereochemistry of the monomers.[98]

Celli *et al.*, part of the same group, also studied the impact of glycerol on the photodegradation.[99] The properties of polybutyl dodecanoate containing 0,5%, 1% and 2% of glycerol incorporated into the structure were evaluated. The glass transition temperature and melting temperature of the polyesters was analysed, but no significant difference was observed. Crosslinking density as determined by DMA was found to increase with increasing glycerol content. Upon weathering, it was observed that due to the introduction of glycerol, chain scission dominated the photodegradation behaviour.

Hydrolysis is highly relevant to the degradability of polymers in the nature. In order to develop polymers both biosourced and biodegradable, many authors have therefore studied the impact on hydrolytic stability of different biosourced monomers.

One example is the work of Zamora *et al.*, who synthesised copolymers based on isophthalic acid, terephthalic acid and hexitols or pentitols with different configurations shown below and examined their resistance to hydrolysis through the decrease in molecular weight.[100] Copolyesters also containing 50% ethylene glycol were also prepared. They found that the degradation proceeds via an initially steep rate gradient and then slows down for the rest of the process. Only a small increase in rate was observed when the pH was lowered from 7 to 4. However, a negative dependence of hydrolysis rate on crystallinity was found.

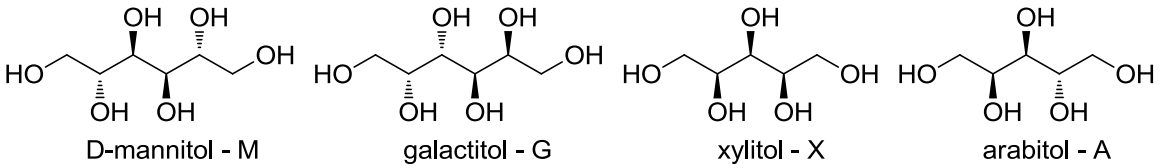

Scheme 33: Structures of hexitols and pentitols

In both terephthalic and isophthalic polyesters, the best stability was observed for the galacto-monomer, and the worst for the manno-monomer. For the terephthalic acid samples, arabino stability was slightly higher than xylo stability. The reverse was true for isophthalic samples, but the difference between the two pentitols was small.

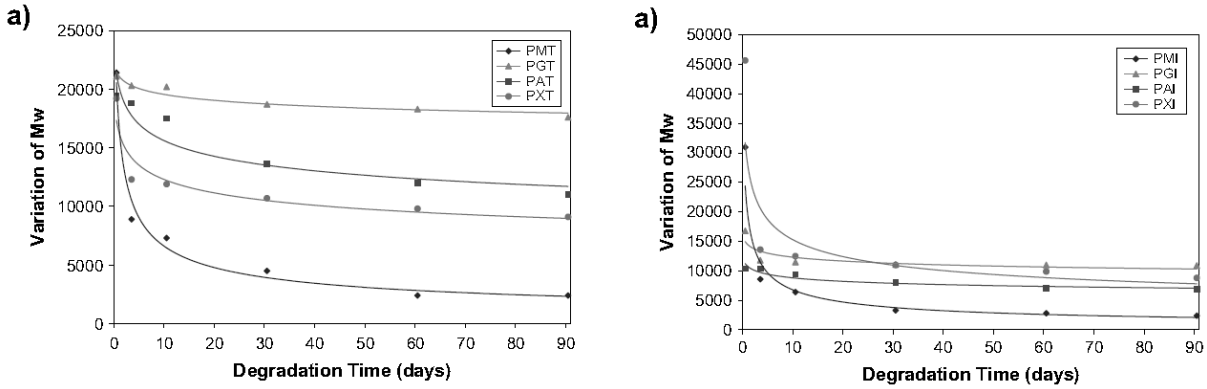

Figure 9: Degradation time of poly (P) hexitol- and pentitol- (M, G, A or X) isophthaltes (I) and terephthalates (T) (Zamora 2006)

Very similar hydrolysis properties were observed for the copolyesters containing also ethylene glycol, implying that 50% of the carbohydrate monomer is enough to cause hydrolytic liability. NMR analysis of the products revealed that chain scission in those samples took place primarily at ester groups adjacent to the carbohydrate monomer units.

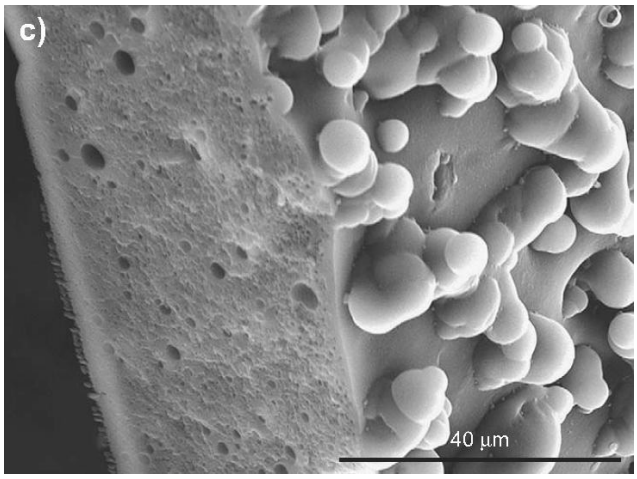

Figure 10: SEM image of hydrolytically degraded sample (Zamora 2006)

No weight loss was observed upon hydrolysis. This was explained by SEM analysis of the samples, which revealed that the small degraded parts were not water soluble, and stuck to the surface of the film, as shown on the right.

A less unambiguous result was obtained by Okada *et al.*, who studied the hydrolytic degradation of polyesters synthesised from isosorbide and isomannide with C_4 to C_6 chain length alkyl dichlorides.[101] A thin polymer film was immersed in a phosphate buffer solution at 27 °C and 50 °C, and the amount of dissolved polymer was weighed. Only small amounts were solubilised at 27 °C, but nearly everything was lost at 50 °C. For the isosorbide polyesters, the best stability at 27 °C was displayed by the adipate sample, while the best stability at 50 °C with about 20% remaining insoluble film after 20 days was shown by the succinate. The isomannide polyesters displayed a similar behaviour. Hydrolysis at 27 °C was very

slow, and no real difference between the samples could be established. At 50 °C, the poorest stability was observed for the adipate sample, followed by the glutarate sample. The succinate displayed much better stability than all others, the sample was recovered to 60% after 40 days. This was explained by the fact that partial crystallinity was observed in this polyester only.

Degradation of the polyesters in microorganism activated sludge, leading to the recovery of monomer units and the emission of CO_2 was also studied. In the case of isosorbide samples, more sample was recovered the longer the aliphatic chain. For the isomannide sample, the glutarate sample performed slightly better than the adipate sample. No significant change was observed in either molecular weight or polydispersity.

Lastly, the degradation when buried in soil was tested. No difference could be discerned between isosorbide succinate and glutarate. Isomannide succinate performed best of all samples tested, and isomannide glutarate performed worst. The authors concluded that polyesters of dianhydro glucitol – aliphatic acid type are biodegradable.

A different type of biosourced monomer, originating from lignin and not sugar based biomass, was studied by Jin *et al.* in the context of liquid crystalline polymers.[102] The synthesis of a polyester from glycolic acid, *p*-hydroxycinnamic acid and *p*-hydroxybenzoic acid was reported and its hydrolytic degradation properties were investigated. The water uptake in neutral (7) and basic (10) pH and at 37 °C or 60 °C was measured to estimate the susceptibility to degradation. Significantly higher water uptake compared to a terephthalic acid based polymer was observed, and the rate of water uptake was found to increase with lower molecular weight, as shown below on the right. No change in degradation rate was observed upon changing the pH from 10 to 7. A small mass loss and a large decrease in viscosity accompanied the degradation.

FTIR analysis revealed that the hydrolysis was taking place at the glycolic acid ester bonds. It was further concluded that it took place in the amorphous regions causing an increase of crystallinity, observable through a narrower melting transition in DSC. In scanning electron microscopy, surface cracks were observed as shown in an example above.

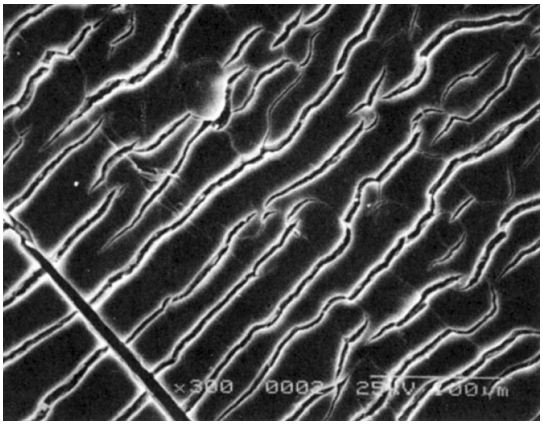

Figure 12: Cracks on the polymer surface following hydrolysis (Jin 1995)

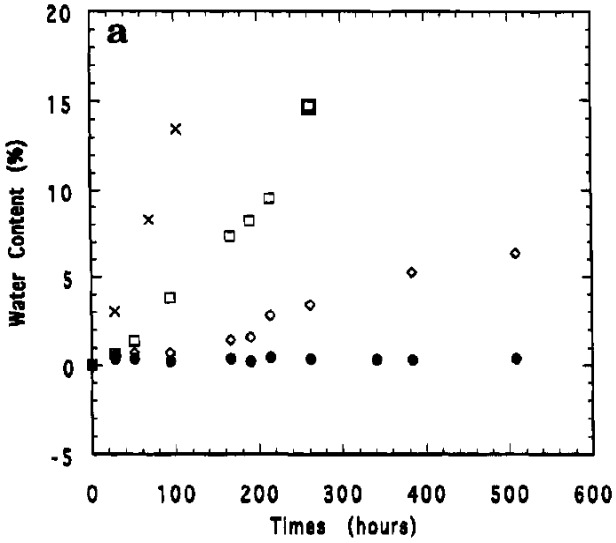

Figure 11: Water uptake dependency on M_w (Jin 1995)

XXIII. ESR spectra of different HMMM contents by Gamage *et al.*

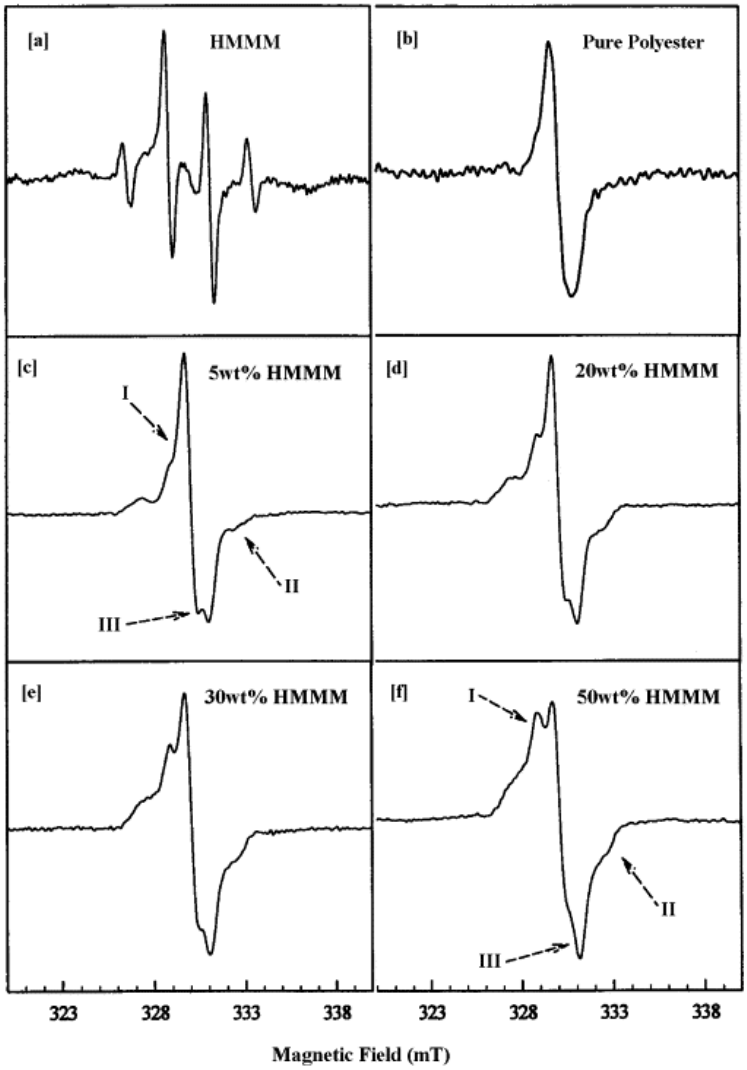

Figure 13: ESR spectra of HMMM cured polyesters (Gamage 2003)

XXIV. Coatings and weathering conditions used by Zhang *et al.*

The top clear coat used by Zhang *et al.* was applied on a 20 µm layer with TiO_2 and a base 3 µm layer phthalate base coat.[103] It was cured to a peak metal temperature of 232 °C for 30 s and a thickness of 20 µm. Weathering was performed for 3000 h in 12 h cycles, with 8 h irradiation with a QUV-A340 nm fluorescent tube (295 – 400 nm) at 60 °C and decreasing relative humidity (100% - 30%), followed by 4 h in darkness at 50 °C with relative humidity at 100%. Samples were analysed every 500 h.

XXV. Weathering conditions used by Biggs *et al.*

Biggs *et al.* exposed samples for up to 10 weeks of accelerated ageing in a QUVb cabinet using an 8 h cycle consisting of 4 h radiation with a maximum intensity at 313 nm at 60 °C and 4 h of condensation at 50 °C.

XXVI. Composition of resins used in the weathering tests by Sullivan *et al.*

According to the authors assertion, the polyester binders were formulated with only 24 – 32 mol% in diol content as detailed in the table below and separately described in a patent by the same author.[104] This makes the acid numbers of 5 – 6,8 mg KOH/g, the hydroxyl number of 23 – 40 mg KOH/g and the success in crosslinking the resin with a melamine resin (9:1 weight ratio) reported in the article somewhat surprising.

Table 3: Composition of different polyester films (Sullivan 1995)

Resins	**M**	**PE-100**		**PE-200**		**PE-500**		**PE-2186**	
monomers	**g/mol**	**weight/ 1000[a]**	**mol%[b]**	**weight/ 1000[a]**	**mol%[b]**	**weight/ 1000[a]**	**mol%[b]**	**weight/ 1000[a]**	**mol%[b]**
NPG	104,1	411,4	**31,7**	-	**-**	-	**-**	-	**-**
MPD	90,1	-	-	376,8	**25,8**	-	**-**	366,7	**24,2**
1,2 PD	76,1	-	-	-	**-**	349,9	**20,7**	-	**-**
IPA	166,1	308,3	**37,9**	325,9	**41,1**	340,5	**44,0**	554,2	**67,4**
PAN	148,1	126,6	**13,9**	133,8	**15,1**	139,8	**16,1**	-	**-**
ADI	146,1	153,7	**16,6**	162,5	**18,0**	169,8	**19,3**	79,1	**8,5**

a: as reported by the authors; b: calculated

XXVII. Degradation of different melamine compounds studied by Lukey *et al.*

The study by Lukey *et al.* examines the mechanism of radical degradation of two types of melamine crosslinkers by trapping the radicals at low temperature and observing the changes in an ESR spectrum during gradual heating.[105] Samples of hexamethoxymethylmelamine (HMMM) and trimethoxymethylmelamine (TMMM) shown below are cooled under vacuum to -196 °C and irradiated with a 1000 W mercury/xenon lamp, filtered to have a cut of at 250 nm. They were then heated to -163 °C, -103 °C and -53 °C after waiting for 30 min and taking and ESR spectrum after each stage.

Firstly, it was found that both molecules have a single UV absorption maximum at 238 nm, which is attributed to the triazine ring. It is also found that the radical intensity in TMMM after 30 min of irradiation was nine times lower than that observed in HMMM, indicating that the later is less susceptible to photodegradation.

Both spectra are initially dominated by a methyl radical, though a formyl radical in 5% intensity is also present. The latter is attributed to formaldehyde present in low quantities, or rearrangement reactions.

For HMMM, a methoxy radical was also observed, which decayed away at higher temperatures, where terminal methylene radicals and methane radicals appeared in the spectrum. A mechanism initiated by the absorption of UV light resulting in homolytic bond scission to give a methyl and an alkoxy radical, followed by a hydrogen abstraction from the end of the molecule and a cyclic hydrogen abstraction was proposed, and is shown below.

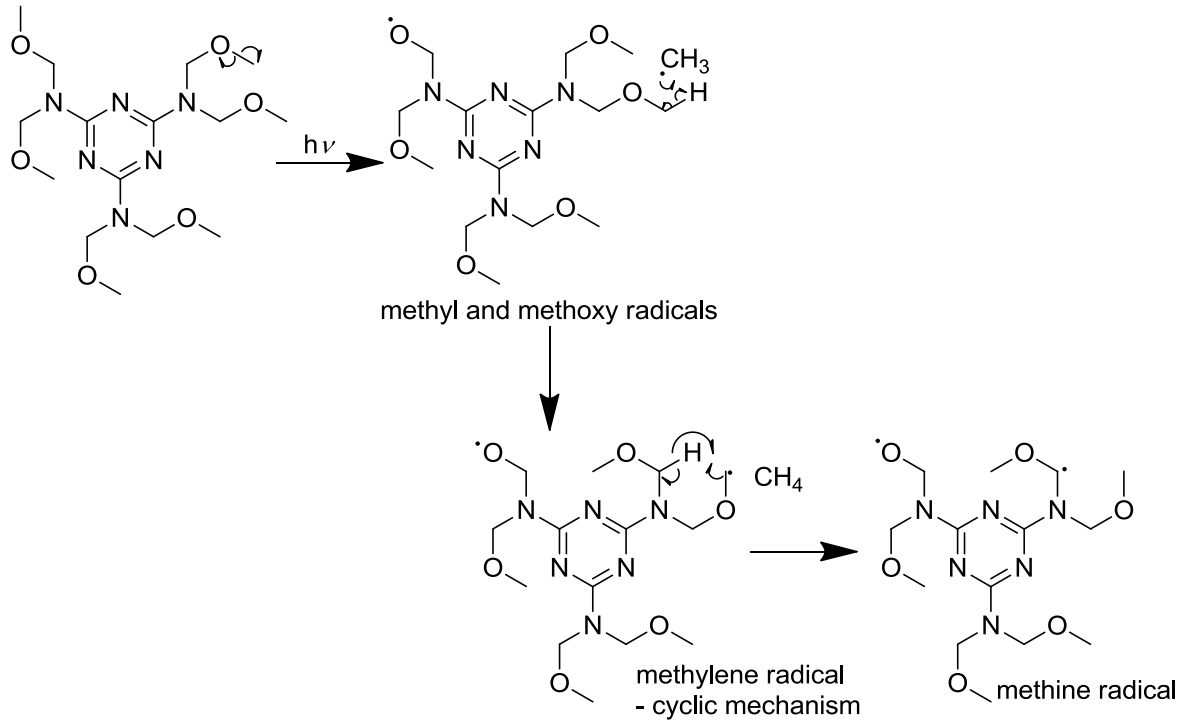

Scheme 34: Degradation mechanism of HMMM (Lukey 2002)

The same mechanism is proposed for TMMM degradation, except that the cyclic mechanism to transform the methylene radical into a methine radical is not available. The reaction therefore stops at the less stable methylene radical, which is quenched directly.

XXVIII. Methodology for the study of the influence of different pigments on coating weatherability by Zhang *et al.*

The work of Zhang *et al.* is interesting due to the differences it reveals about the different methodologies used to study the degradation.[106] In this paper, the group investigated the effect of lead chromate- , iron oxide- and copper phthalocyanine- titanium dioxide pigment mixes on the weatherability of a melamine crosslinked cycloaliphatic polyester coating after outdoor exposure in Hainan, China, at 300 m from the ocean for two years at an average humidity of 81% and an average temperature between 11 and 37 °C. The change in surface morphology was examined by scanning electron microscopy, tapping mode atomic force microscopy, X-ray photoelectron spectroscopy and gloss retention as well as colour change measurements. Photoacoustic FTIR spectroscopy was used to examine the bulk chemistry at different depths in the spectrum. A study of panels containing only lead chromate or titanium dioxide pigment weathered using a QUVa weathering chamber in a 12 h cycle consisting of 8 h UV radiation at 60 °C followed by 4 h of humidity at 50 °C was also characterised by FTIR spectroscopy.

The smoothest surface before weathering was observed for the copper-phthalocyanine paint, because the pigment size was below the detection limit of the SEM technique. After weathering, all surfaces increased in roughness, and traces of each pigment as well as an increase in nitrogen and oxygen and a decrease in carbon were detected in elemental analysis. This was attributed to the erosion of the surface layer, accumulation of dirt and the photooxidation of the material.

The copper phthalocyanine paint, which contained 12% of titanium dioxide compared to 1% and 3% in the other paints, was found to display larger levels of chalking, i.e. migration of titanium dioxide to the surface, which caused lower overall gloss retention, and a larger difference between the surface before and after washing. The AFM measurement also confirmed a smaller average particle size for the copper phthalocyanine paint than for the other two paints.

While the surface roughness and particle size were similar for the lead chromate and the iron oxide paints, the lead chromate paint was found to both exhibit the highest colour change and the highest gloss retention. The iron oxide paint exhibited the lowest colour change, and gloss retention in between the other two paints.

The study of the QUVa weathered paints showed higher melamine degradation and lower gloss retention for the titanium dioxide based paint compared to the lead chromate based paint. Contrarily, in the naturally weathered samples, the lead chromate based paint showed the highest increase of hydroxyl groups and the highest degradation of melamine. This was attributed to the increased acidity, causing increased solubility of the lead chromate and allowing it to catalyse oxidation reaction, which was present thanks to acid rain in the natural weathering, but not in the QUVa chamber. The increase in hydroxyl groups in the iron oxide and copper phthalocyanine paint was identical. However, the iron oxide paint showed the lowest melamine degradation. A large difference of melamine degradation depending on the sampling depths was observed for the copper phthalocyanine paint, which was attributed to the high levels of titanium dioxide shielding the deeper layers from UV radiation.

XXIX. Photoacoustic infrared spectroscopy

See chapter *6.3.2.2.2*

XXX. Nitroxide monitoring of free radicals

In this technique, developed earlier also by Mielewski *et al.*, a solution of nitroxide is absorbed into the coating prior to curing.[107] The nitroxide concentration is determined by ESR prior to ageing. It is then followed during the weathering process. The nitroxides are scavenging free radicals produced in the photooxidation of the coating, and their disappearance can therefore be related to the free radical initiation rate.

XXXI. Creep recovery study by Mitra *et al.*

The aim of the study was to investigate the correlation between dynamical mechanical analysis and gloss retention after exposure to UVB radiation of four different types of topcoats, including an economic aliphatic polyurethane coat (A), an alkyd modified polyurethane coat (B), a high performance aliphatic polyurethane coat (C) and an epoxy modified polysiloxane coat (D).[108]

Mitra *et al.* detected an increase of T_g in all films, and an increase of crosslinking density in all films except for film C. FTIR spectroscopy was qualitatively used to confirm chemical changes, but no quantification was reported. Interestingly, a correlation between the creep recovery and the gloss retention was observed as shown in the figures below. Both classed the films in the order D>C>A>B. This was not observed for the creep deformation resistance.

XXXII. Peak fitting study of different polyurethanes by Zhang *et al.*

Cycloaliphatic polyester resins crosslinked with three different blocked isocyanates as well as artificial weathering and three different natural exposure sites were compared in the study. The IR spectra were normalised and a peak fitting function was used to interpret the amide / NH-CO peak between 1573 cm^{-1} and 1535 cm^{-1} and the carbonyl peak between 1832 cm^{-1} and 1770 cm^{-1}.

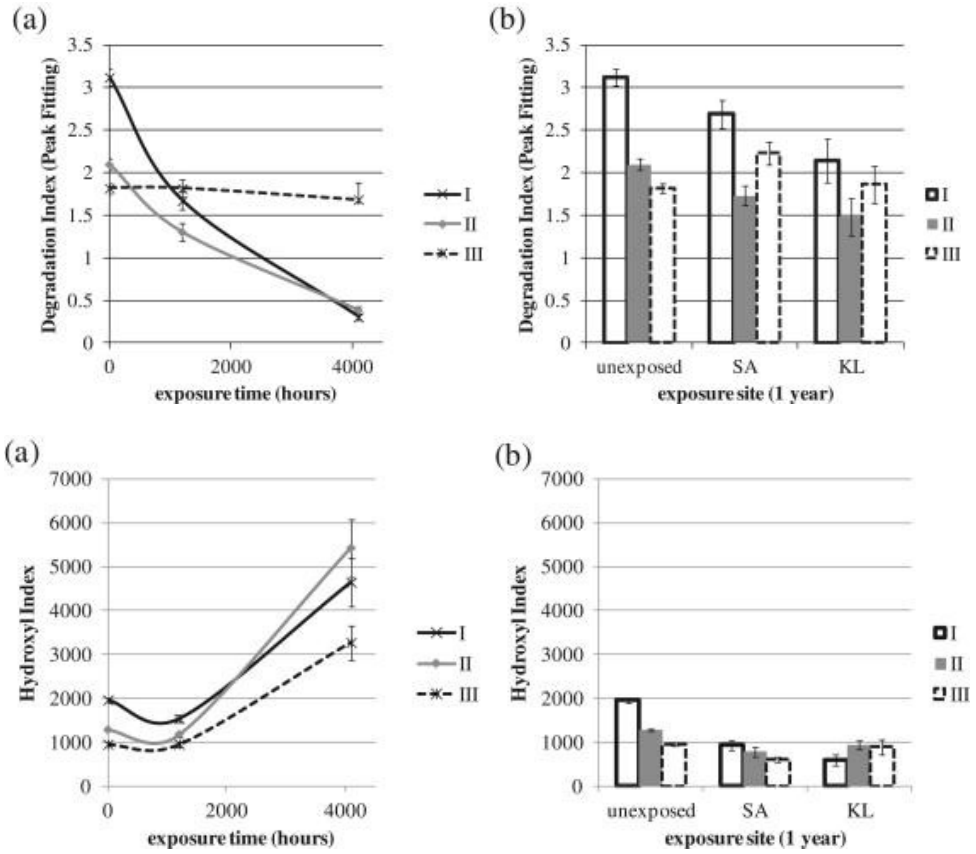

Figure 14: Results of degradation evaluation at different sites using the peak fitting method (Zhang 2013)

XXXIII. DSC measurements by Larché *et al.*

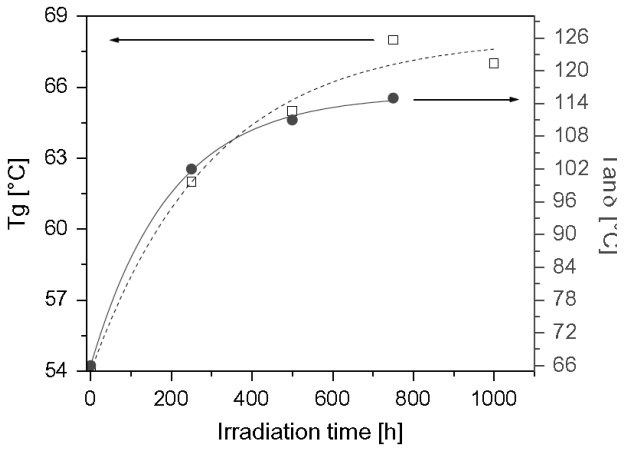

Figure 15: Glass transition temperature increase upon degradation by DSC and DMA (Larché 2012)

XXXIV. Study on the influence of aromatic monomers on melamine crosslinked polyols

Osterhold *et al.* studied three resins with no, medium and high aromatic content in the polyol.[109] Other monomers used and percentages were not specified. The films were cured for 20 min at 140 – 145 °C to give a thickness of 35 – 45 µm, and exposed to 1000 h of three hour cycles consisting of 40 min irradiation from a xenon high pressure burner with quartz inner and borosilicate outer filters at 340 nm (0,55 W/m^2) at 70 °C panel temperature and 50 % humidity, followed by 20 min at 95% humidity and 1 h at 50 % humidity, and ended with 1 h at 38 °C panel temperature and 95% humidity in darkness.

A growth in surface tension with ageing attributed to the formation of polar groups after chain scission was observed, which was more pronounced for the aromatics containing samples. This was confirmed by the decrease of ester groups and the increase of carbonyl groups in the 400 – 2000 cm^{-1} region of the FTIR spectrum. From 400 h of exposure on, a larger increase in NH/OH peak intensity was observed for larger aromatic contents. In comparing the surface topography of the film without aromatics to that with a high aromatic content, a much more developed microstructure was observed in the aromatic sample. He authors attribute this to the higher degradation and consequent washing out of low molecular weight products. Concurrently, lower gloss retention was observed with higher aromatic content.

The development of the glass transition temperature was followed during weathering with DMA and DSC analysis, and a much more pronounced increase (x 1,5) was observed in the first 150 h for the two films containing aromatics compared to the aromatic free film. After 150 h, a small slope is observed, and differentiation between the two medium and high aromatics containing films is not possible. Crosslinking density was found to rise in the first 100 h, and then decrease below original levels, but was not found to be affected by the aromatic content. This is attributed to the self-condensation of the melamine resin and crosslinking reactions dominating at the start of the degradation, and chain cleavage dominating in the later stages, when mobility is reduced by the higher glass transition temperature.

XXXV. Weatherability of polyester powder coating film by Maetens *et al.*

Maetens *et al.* studied the weatherability of triglycidyl isocyanurate crosslinked polyester powder coating films formulated from neopentyl glycol, trimethylol propane and terephthalic acid or isophthalic acid under accelerated and natural weathering by photoacoustic FTIR.[110] The polyesters before crosslinking were acid functionalised with an acid value of 28 – 35 mgKOH/g, a molecular weight of 5000 Da and a T_g around 65 °C, and were cured at 200 °C for 20 min to give film of 60 – 80 µm thickness. Degradation was assessed after irradiation with a mercury bulb equipped with a borosilicate filter to block out wavelength below 320 nm at 60 °C with and without humidity, and after natural exposure in Florida. Degraded films aged without humidity were placed in water after ageing.

After accelerated weathering, an increase in carboxylic acid groups and anhydride carbonyls was observed in the IR spectra of both types of films, but significantly stronger degradation was observed for the terephthalic acid containing film. Yellowing was also observed more clearly in the terephthalic acid film.

Immersion in water after ageing caused a decrease in both the carboxylic acid and anhydride absorption, which was attributed to leaching of low molecular weight compounds and hydrolysis of anhydride groups, respectively. Where humidity was present during the weathering process, only formation of carboxylic acid groups but no formation of anhydride groups were observed. Both the weathering in the presence of humidity and the natural weathering in Florida confirmed the superiority of the isophthalic acid containing film.

Chapter 4

XXXVI. Literature NMR spectra of trans-aconitic acid and trans-aconitic anhydride[111, 112]

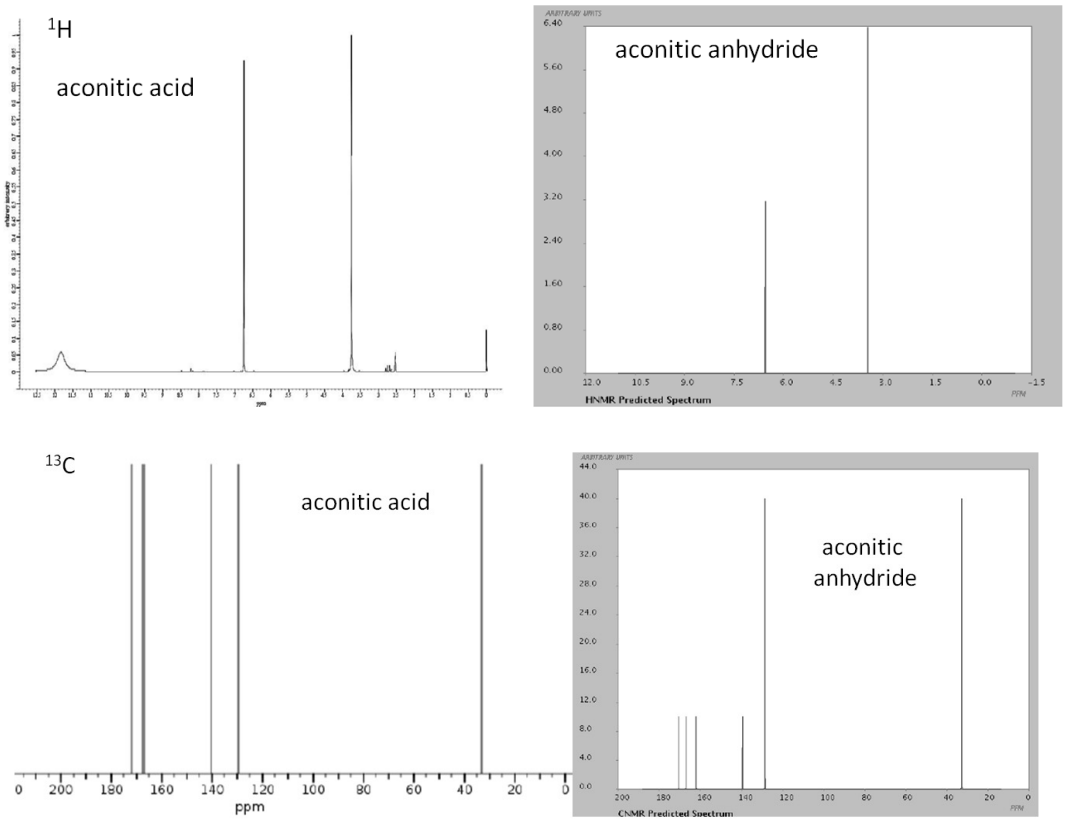

XXXVII. Solubility issues with ferulic acid based products

One of the main challenges that had to be solved is demonstrated below for the product LH246 obtained from ferulic acid, sebacic acid and 1,3-propanediol. The majority of the ferulic acid based products were not soluble in acetone, chloroform, methanol, acetonitrile, DMF or THF.

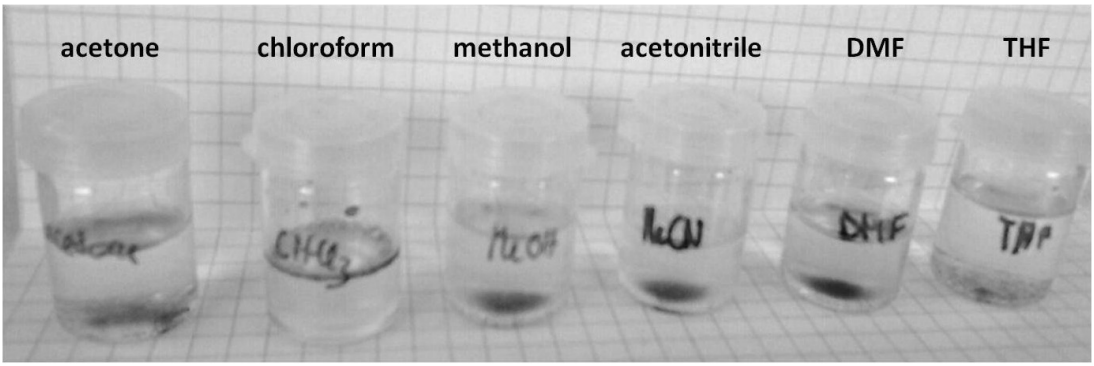

Figure 16: Lack of solubility of ferulic acid based product LH246 in common organic solvents

Therefore, only very good solvents could be used for the purification and analysis of the products. One example is the work-up procedure taken from Mialon *et al.* for the purification of the polymer based on dihydroacetylferulic acid. In order to dissolve the polymer, a mixture of dichloromethane and trifluoroacetic acid was used.

This was used as an inspiration for the analysis, and mixtures of trifluoroacetic acid and chloroform or deuterated trifluoracetic acid and $CDCl_3$ were used to dissolve the products for mass spectrometry and NMR analysis respectively. As trifluoracetic acid cannot be used in a GPC, the products were instead dissolved in *N*-methyl pyrrolidone at high temperatures.

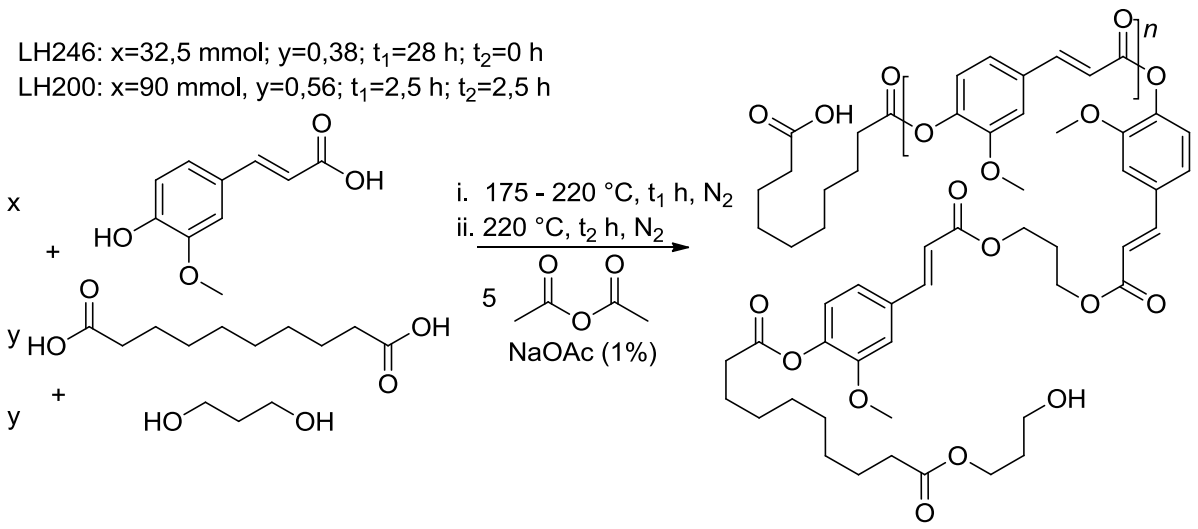

Scheme 35: Reaction leading to the products LH246 and LH200 used for the solubility tests

Unfortunately, the use of the highly acidic trifluoracetic acid, as well as the high temperatures necessary to dissolve the products in NMP, carry the risk of breaking formed ester bonds and thus changing the product composition and decreasing the accuracy of the analysis results. As shown in the table below, a range of fluorinated solvents available in the laboratory with lower acidities were therefore tested for their potential.

Table 4: Solubility tests of LH200 in different fluorinated solvents

solvent	concentration	observation
	g/L	
perfluorohexane	45	phase separation – not soluble
hexafluoroisopropanol	100	dissolved - soluble
trifluoroethanol	28	suspension – not soluble
tridecafluorooctanol	125	suspension – not soluble
trifluoroacetic acetate	38	phase separation – not soluble
trifluorotoluene	29	phase separation – not soluble
pentafluorobenzaldehyde	38	partially dissolved
pentafluorophenol*	25	dissolved (1 min) - soluble

* at 80 °C

In order to determine possible suitable solvents, 50 mg of LH200, the reaction product of ferulic acid, sebacic acid and 1,3-propanediol, were tested in eight different solvents at room temperature. It was

first stirred at a high concentration of 167 g/L for 45 min. As none of the solvents tested dissolved the product, the concentration was then gradually decreased to the concentrations shown in the table and the mixture was left to stir overnight for a total of 22 h.

The only solvents in which LH200 was finally dissolved were hexafluoroisosopropanol after 22 h of agitation at room temperature, and pentafluorophenol. As pentafluorophenol is a solid at room temperature, the mixture was heated to 80 °C in this case.

Due to the need for high temperatures in the case of pentafluorophenol and the high price of both pentafluorophenol and hexafluoroisopropanol, it was decided to continue using trifluoroacetic acid for the NMR and mass spectrometry analysis in order to be able to compare a large number of products. Hexafluoroisopropanol (HFIP) was only used for the GPC analysis of LH200.

XXXVIII. Details of the GPC peaks observed in the ferulic acid copolymerisation reactions

In the GPC, two different peaks, one between 9,4 min and 9,5 min and one between 13,4 min and 13,8 min, were observed. The former corresponded to products with number average molecular weights of 29 739 g/mol to 33 114 g/mol and weight average molecular weights of 31 311 g/mol to 34 737 g/mol, while the latter was calculated to belong to products with number average molecular weights of 2454 g/mol to 3718 g/mol and weight average molecular weights of 3264 g/mol to 4153 g/mol. The relative area of each peak is also listed together with the overall yield in weight %.

Chapter 5

XXXIX. Increased isosorbide content with constant hydroxy value

Because the melamine crosslinker reacts with free hydroxy groups to create the thermosetting coating, the hydroxy value is an important parameter for the curing behaviour. Therefore, options to keep the hydroxy value constant while increasing the isosorbide content were explored. For this, three different strategies were tested.

Firstly, the amount of succinic acid and sebacic acid was adjusted to compensate for the difference in weight between isosorbide and 1,2-propanediol. Instead of 35,24mol% of succinic acid and 13,49 mol% of sebacic acid, 39,41 mol% and 9,32 mol% were used respectively. This kept the ratio of acid and alcohols at the same level while also resulting in a hydroxy value of 56,24 mg_{KOH}/g.

Table 5: Formulation of LH038 with an increased amount of isosorbide and a constant r_0

LH038	**n (mol)**	**mol %**
ISO	1,8594	34,37
SUC	2,1321	39,41
SEB	0,5042	9,32
1,2 PD	0,5821	10,76
GLY	0,3322	6,14

F_n		1,9492
r_0		1,115
hydroxyl $_{theor.}$	*mg_{KOH}/g*	56,24
viscosity	*mPa*s*	41 768
solvents	*70:30*	Solvarex 9, DBE
concentration	*%*	69,96

However, the combined increase in polarity and rigidity caused by the increase of succinic acid and isosorbide resulted in a viscosity of 41 786 mPa*s at a concentration of 70% in a mixture of DBE and Solvarex 9 (S9) solvents. Solvarex 9 is an aromatic solvent mixture which is discussed in detail in

section *5.3.2.1*. As this is considerably above the target viscosity, which is between 1000 mPa*s and 6000 mPa*s, this strategy was not pursued further.

Instead, the ratio of alcohols to acid groups r_0 was increased to 1,119, while the hydroxy value was kept constant at 56,24 mg_{KOH}/g. This was achieved by increasing the amount of 1,2-propanediol in the formulation from 10,76 mol% to 10,92 mol%, or by decreasing the amount of glycerol in the formulation and replacing it by 1,2-propanediol.

Table 6: Resins synthesised with higher r_0 values but constant hydroxy values

resin reference	isosorbide content	1,2-propanediol content	glycerol content
	mol%	mol%	mol%
LH168	34,31	10,92	6,13
LH067	33,96	13,80	4,09
LH079	38,44	11,88	2,09

Glycerol has a lower molecular weight per hydroxy group than 1,2-propanediol and its decrease also counteracts the increase in viscosity observed from the addition of isosorbide. Therefore, the last strategy was expanded to a resin in which the isosorbide content was increased to 38,44 mol%. The glycerol content of the resin LH079 was lowered to 2,09%, and resulted in a r_0 ratio of 1,124.

All resins with the exception of LH243 and LH040 were cured with melamine to evaluate their properties as films. Due to promising early results, the resin LH168 was used instead of LH040 to evaluate the properties of a resin containing 34 mol% of isosorbide.

XL. Calculation of monomer ratios for a phthalic anhydride resin equivalent to the isosorbide resin

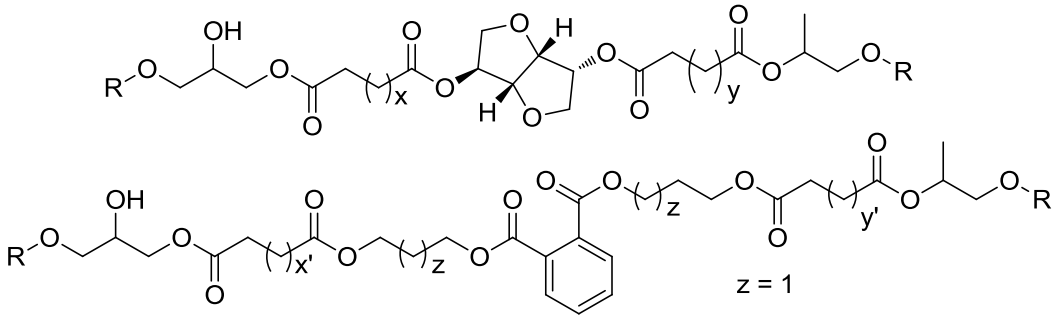

Scheme 36: Segments of isosorbide and phthalic anhydride resins illustrating the replacement of monomers

First, the quantity of isosorbide present in the formulation was replaced entirely by phthalic anhydride. The additional quantity of acid groups introduced thus was then subtracted from the amount of sebacic acid and succinic acid present in the formulation. Lastly, 1,3-propanediol was added to the new formulation to make up both for the decrease in alcohol groups from the replacement of isosorbide and for the decrease of linear chains from sebacic acid and succinic acid.

The number of carbon atoms present in the aliphatic chains in the new formula, derived from succinic acid (x'), sebacic acid (y') and 1,3-propanediol (z) was then adjusted to equal the amount present from succinic acid (x) and sebacic acid (y) in the new formulation. This was achieved by changing the ratio of succinic acid and sebacic acid from 72,3% and 27,7% to 55,7% and 44,3%.

Table 7: Calculations for the design of a phthalic anhydride resin close to the isosorbide resin

		ISO			PAN		
monomer	**chainlength**	**mol%**	**%**	**x,y**	**mol%**	**%**	**x', y', z**
ISO		29,4					
PAN					29,4		
SUC	2	35,2	72,3	1,45	10,8	22,1	0,44
SEB	8	13,5	27,7	2,21	8,6	17,6	1,41
1,3PD	3				29,4	60,3	1,80
1,2 PD		15,8			15,8		
GLY		6,1			6,1		
Σ	x+y+z			3,66			3,66

The ratio of alcohol to acid groups was kept a 1,115 this way, as well as the resin functionality. The theoretical hydroxy value changed to 62,11 mg_{KOH}/g.

XLI. The effect of changing the reaction order by order of monomer additions

The effect of changing the reaction order in the isosorbide synthesis

The possibility of accessing new resin compositions by deviating from the procedure was tested. In one case, 1,2-propanediol and glycerol were added to the synthesis before the esterification of the hydroxy groups was complete. At the point of addition, around 13% of the total amount of isosorbide hydroxy groups, or 26% of the endo hydroxy groups remained free according to the acid and hydroxy value titrations performed.

The synthesis was repeated to test the reproducibility of the result, and the two alternatively synthesised resins were compared in terms of molecular weight, viscosity and glass transition temperature to two resins with identical formulations synthesised the usual way.

Table 8: Effect of early addition on resin properties

resins		**normal synthesis**		**early addition synthesis**	
		LH059	**LH075**	**LH072**	**LH123**
viscosity	**mPa*s**	5193	4977	7667	3738
conc. in MPA	**%**	67	65	67	65
M_w	**g/mol**	5264	5290	6413	11092
M_w/M_n		3,678	3,757	4,399	6,984
T_g	**°C**	7	10	12	7

The first resin synthesised by adding 1,2-propanediol and glycerol to the synthesis before the isosorbide hydroxy groups had completely reacted showed a higher glass transition temperature and viscosity than its equivalents. However, the repetition of the synthesis did not confirm this observation. Overall, both the viscosity and the glass transition temperature are within the normal variation between syntheses.

On the other hand, the molecular weight of the resins increased when the early addition synthesis pathway was followed. This is possibly due to the unavailability of the isosorbide groups, decreasing the excess of hydroxy groups and therefore leading to larger chains.

Unfortunately, the polydispersity also increased in both resins, which can have a negative effect on the mechanical properties once the resin is crosslinked to a film. Furthermore, the availability of the free isosorbide groups for crosslinking is not certain. Therefore, the changed reaction procedure was not further employed.

The effect of changing the reaction order in the phthalic anhydride resin synthesis

A similar experiment was also conducted for the partially biosourced resins based on phthalic anhydride. As all monomers are usually added at the same time in this synthesis, it was changed by reacting the non-rigid diols and diacids together first before adding phthalic anhydride and glycerol when an acid value below 10 mg_{KOH}/g was reached.

Three new resins, LH198, LH210 an LH201, were synthesised using the new method. They each contain a different amount of phthalic anhydride, and were compared with an equivalent resin containing the same amount but synthesised with the normal method.

Table 9: Comparison of phthalic anhydride resins synthesised with and without late addition

PAN content		T_g	M_w	M_w/M_n
mol%	resin	°C	g/mol	
24,37	LH162	-15	17250	5,1
	LH198	-17	11250	3,7
29,37	LH189	-6	15200	4,6
	LH210	-7	12850	4,2
34,37	LH163	1	9150	3,5
	LH201	1	11350	3,9

For the two resins containing 24,37 mol% and 29,37 mol% of phthalic anhydride, a lower molecular weight and polydispersity as well as a slightly higher glass transition temperature can be observed. This trend is not reflected in the resin containing 34,37 mol% phthalic anhydride, which is very similar to its equivalent synthesised with a different method in every respect.

Two different conclusions can be drawn. It is possible that the esterification of the less reactive succinic acid and sebacic acid with propanediol is increased to a degree that does not usually occur, leading to a higher conversion when the more reactive phthalic anhydride is added only in the end. This effect is more pronounced when more succinic acid and sebacic acid are present in the reaction, and therefore strongest in the case of the resin with the least amount of phthalic anhydride.

However, the differences between the glass transition temperature and molecular weight measurements are quite small and in the case of the T_g within the error margin. Therefore, the trend observed could also be coincidental. Further experiments are necessary to confirm or refute either hypothesis, but were not prioritised due to the small difference in properties that can be achieved this way.

XLII. Loss of hydroxy functional monomers

One of the main challenges in the beginning of the project was the fact that the hydroxy values measured after the resin synthesis was completed did not match the theoretical values calculated. The hydroxy values are expressed in mg_{KOH}/g, which is a unit used to match their practical measurement.

In order to determine the amount of free hydroxy groups present in a resin, a pre-weighed sample is acetylated with a known amount of acetic anhydride. The leftover acetic acid is then titrated with a potassium hydroxide solution. The precision of the test is limited and requires at least two replicas to confirm its validity. A standard of acetic anhydride not containing any resin is also tested each time. Therefore, the entire procedure takes about an hour to complete.

Table 10: Examples of resins for which the final hydroxy value deviated from the theoretically calculated one

		OH theoretical	OH final	difference
	resin	mg_{KOH}/g	mg_{KOH}/g	mg_{KOH}/g
isosorbide based	LH037	56,2	135,6	-79,4
	LH043	56,2	81,1	-24,8
	LH045	56,2	49,3	6,9
	LH188	58,1	45,5	12,6
	LH057	56,2	41,9	14,4
phthalic anhydride based	LH167	66,9	51,2	15,7
	LH202	62,1	45,8	16,3
	LH128	62,3	41,5	20,8
	LH127	62,1	40,0	22,1
	LH119	53,7	14,3	39,4

Since the titration also takes into account the unreacted acid groups in the resin, the hydroxy value is a measure of the difference between the free acid and hydroxy groups present in the synthesis and should remain constant once all monomers are added to the reaction.

$$\text{Theoretical hydroxy value} = 56100\ mg/mol * (e_{OH} - e_A) / m_{final}$$

The theoretical hydroxy value can thus be calculated by multiplying the difference in mol of hydroxy (e_{OH}) and acid (e_A) groups by the molecular weight of potassium hydroxide, which is 56 100 mg/mol, and then dividing the result by the theoretical final mass of the resin (m_{final}) in g. The quoted theoretical hydroxy value is therefore the value that would be reached at an acid value of 0 mg_{KOH}/g, but also the difference between the acid value and the hydroxy value that should be observed throughout the reaction.

Table 11: Boiling and melting points of the different monomers

	melting point	boiling point
monomer	°C	°C
1,2-propanediol	-59	188
1,3-propanediol	-27	214
succinic acid	184	235

	melting point	boiling point
monomer	**°C**	**°C**
glycerol	18	290
sebacic acid	131	294
phthalic anhydride	132	295
cyclohexanedicarboxylic acid	164	339
isosorbide	63	372

A deviation from the theoretical hydroxy value can occur when the monomer composition changes for example due to the loss of volatile compounds in the reactor. While the temperature is generally kept below the boiling point of all alcohol monomers until it is reasonable to assume that they have reacted at least once, the constant flow of water and azeotropic solvent as well as nitrogen gas out of the reaction can entrain small amounts of monomer.

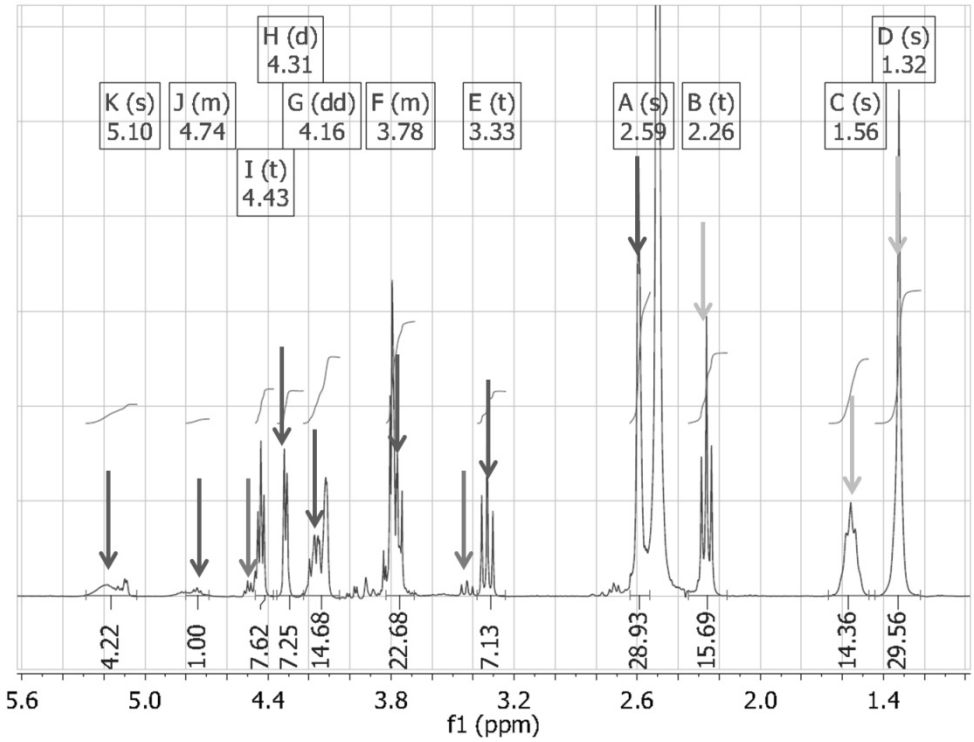

Figure 17: NMR of a sample of sublimated material containing isosorbide, succinic acid and sebacic acid

In the case of monomers with high melting points, the outflow can be observed from the sublimation of material on the reactor walls. While the sublimated material can easily be reintroduced into the reaction mixture by the addition of more azeotropic solvent, other monomers can escape in gaseous form or gather in the Dean-Stark trap. The NMR spectrum of a sample of sublimated material showed that it consists of a mixture of all solid monomers, including some 1,2-propanediol.

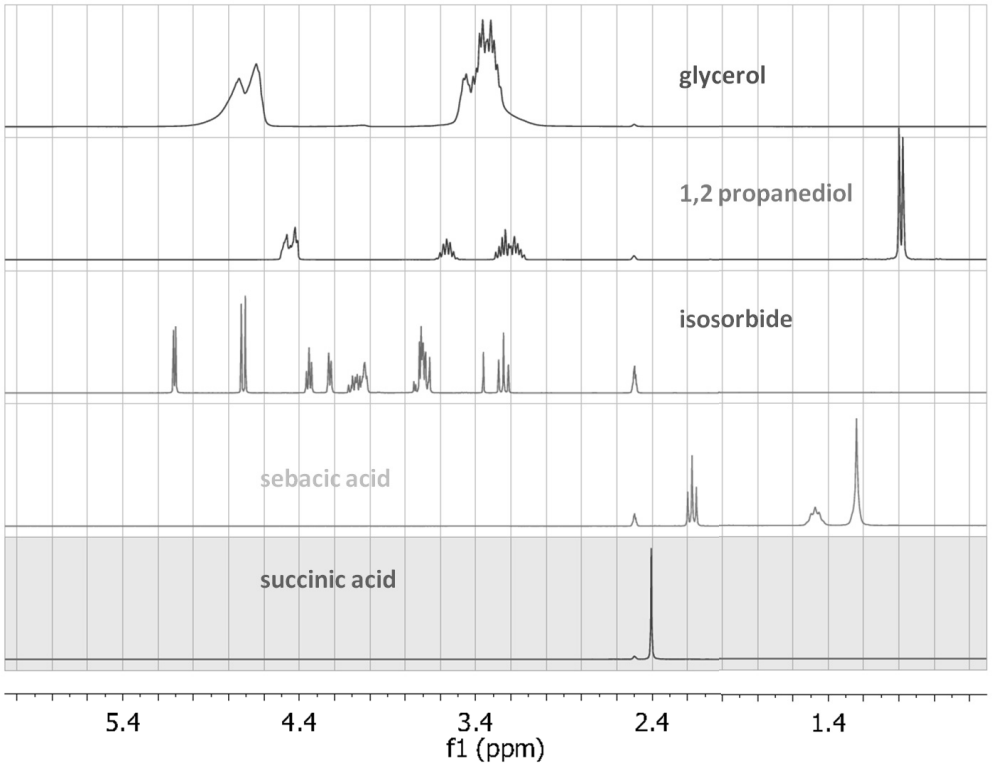

Figure 18: NMR spectra of monomers used in isosorbide resin synthesis

Even though it is possible to determine the composition of the sublimed material, it would necessitate opening the reactor, risking an increase in leakage and breaking the inert atmosphere. Furthermore, the composition of the sublimated material is unlikely to represent the actual composition of leaked monomers, but instead a much higher amount of those monomers with high melting points that are actually less likely to escape.

Therefore, it is difficult to exactly compensate for the loss of monomers. Due to a lack of other options, the nitrogen flow was adjusted and the reactor was sealed as much as possible as described in the section below in more detail. Furthermore, it is assumed that the loss of monomers is relative to their presence in the resin, and that only minor changes in the formulation are caused.

However, the hydroxy value is an important parameter for the crosslinking of the resins, and had to be adjusted, also to ensure that the films resulting from the curing of the resins are comparable and do not differ significantly in term of crosslinking. In order to adjust the final hydroxy value to its theoretical level, it was therefore tested shortly before the end of the reaction.

Generally, the test was done when the acid value reached around 30 mg_{KOH}/g. The purpose was to ensure that the final amount of lost hydroxy groups was correctly estimated but also to leave enough time in the reaction to incorporate a new diol. The difference between the hydroxy value two hours before the end of the reaction and the desired final value was calculated, taking into account the actual mass of resin left, and an equivalent amount of the most volatile hydroxy functionalised monomer was added. Due to the duration of the test, the addition was generally done when the acid value had reached 15 – 20 mgK_{OH}/g. The reaction was never stopped less than an hour after the addition.

Table 12: Improvement of hydroxy value deviation achieved for phthalic anhydride and cyclohexanedicarboxylic acid resins

		ΔOH test	ΔOH end	ΔCOOH (test-end)
main monomer	**reference**	**mg_{KOH}/g**	**mg_{KOH}/g**	**mg_{KOH}/g**
phthalic anhydride	LH163	6,7	-3,3	21,7
	LH189	3,7	1,2	12,1
	LH242	11,1	-2,3	22,8
	LH228	16,4	5,1	20,0
	LH231	17,3	10,2	17,8
	LH238	14,7	1,9	26,3
	LH234	14,2	1,4	21,9
	LH192	24,5	8,1	7,4
	LH193	12,8	1,2	6,6
	LH199	18,6	0,5	3,7
cyclohexane dicarboxylic acid	LH265	3,0	2,4	12,6
	LH272	-0,3	4,7	30,2

The tables above and below show the deviation from the theoretical hydroxy value and the difference in acid values between the moment when the hydroxy value was tested and the end of the reaction for a selection of resins. The final deviation of the hydroxy value is also shown. Firstly, it can be seen that the method consistently improved the agreement between theoretical and experimental hydroxy value. In the case of phthalic anhydride resins, the average deviation was decreased from 12,6 mg_{KOH}/g to 4,05 mg_{KOH}/g, and for isosorbide resins, it was decreased from 5,77 mg_{KOH}/g to 2,65 mg_{KOH}/g.

Table 13: Improvement of hydroxy value deviation achieved for isosorbide based resins

		ΔOH test	ΔOH end	ΔCOOH (test-end)
main monomer	**reference**	**mg_{KOH}/g**	**mg_{KOH}/g**	**mg_{KOH}/g**
isosorbide	LH059	13,2	-0,3	30,9
	LH075	3,0	-1,6	14,7
	LH184	-2,9	-6,3	15,8
	LH067	6,6	-1,7	19,1
	LH070	11,8	-0,6	24,8
	LH079	7,2	-3,4	28,3
	LH168	-1,7	-5,3	22,6
	LH190	10,9	-1,7	20,2
	LH249	5,1	-0,5	9,2
	LH267	-1,0	-6,4	27,3
	LH248	-	1,4	-
isosorbide and phthalic anhydride	LH269	-2,0	-1,7	16,8
	LH266	-3,8	-0,5	29,9

Overall, it can be observed that the deviation observed for isosorbide is smaller than that for phthalic anhydride contents. Furthermore, the tests shortly before the reaction seem to slightly overestimate the deviation for isosorbide resins, resulting in overall too high hydroxy values. This can be explained by two factors. Firstly, some of the isosorbide missing in the first determination of the hydroxy value is still present in the reactor, for example as sublimation in the Vigreux columns, and is reintroduced into the reaction mix when the solvent is added.

Secondly, the quantity of volatile 1,2-propanediol present in the phthalic anhydride resins is considerably larger than that present in the isosorbide resins. In the phthalic anhydride reaction, the 1,2-propanediol is also present during the entire reaction, but slowly heated from 150 °C, while it was only added towards the end in the isosorbide containing reactions, and heated to 220 °C more quickly. This suggests that the duration of the heating is more important for the evaporation than the temperature with respect to the boiling point in this case.

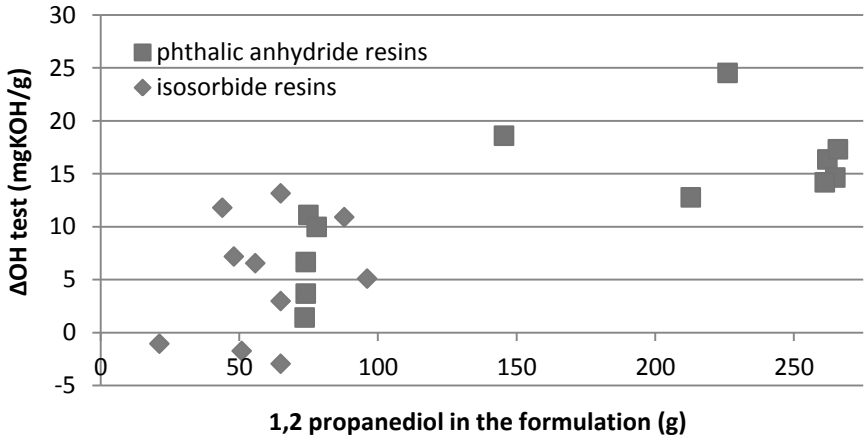

Figure 19: Deviation of hydroxy value in test *vs.* total quantity of 1,2-propanediol in the resin

In plotting the dependence of the hydroxy value end deviation on the quantity of 1,2-propanediol present in the resins, a vague dependence can be observed especially for larger quantities in phthalic anhydride resins. This dependence is not present for isosorbide resins, which only contain smaller quantities. However, the fact that no addition of new diol was necessary in four resins not containing any 1,2-propanediol supports the hypothesis that it is the main evaporating monomer. In LH248, all the 1,2-propanediol was replaced with isosorbide, and a deviation of only 1,4 mg_{KOH}/g was obtained in the end. In the resins LH267, LH266 and LH269, 1,2-propanediol was replaced by 1,3-propanediol, and no addition of new diol was found necessary.

No dependence of the deviation on the time of addition and therefore the time the added monomer was given to react, i.e. the difference between acid values, was observed. This suggests that neither the evaporation of the new diol nor the reactivity was a deciding factor, or that they cancelled each other out.

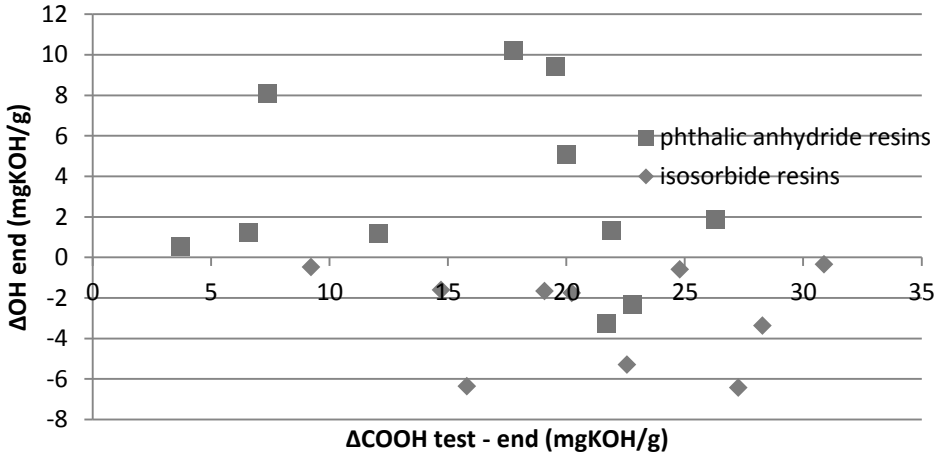

Figure 20: Non-dependence of end hydroxy value deviation on the difference in acid values (test - end)

Nevertheless, a significant number of resins still had to be discarded, due to leaks in the reactor, low reactivity after the addition of the diol which permitted it to evaporate rather than be incorporated into the resin or false results of the hydroxy value determining test.

Some cases were also observed in which the hydroxy value was too high, presumably due to loss of acidic monomers. While acid monomers can be added to the reaction, this can lead to erroneous reading of the reaction progress. The acid value is used to determine how close to completion the reaction is, and adding free acid monomers invalidates the test. Fortunately, after the reactor was adjusted, few incidents of larger than designed excess of hydroxy groups were observed.

The total amount of diol added at the end of the reaction was generally very small, especially relative to the total mass of the resin, as shown below. For phthalic anhydride based resins, the quantity of 1,2-propanediol added was on average 4,5% of the total amount of 1,2-propanediol present in the formulation, and never more than 2% of the total mass of the resin. For isosorbide based resins, it was 3,5% of the total mass of 1,2-propanediol on average, and never more than 1% of the total resin mass.

Still, the probability of the presence of unreacted or partially reacted monomer was considerably increased. This has to be kept in mind when evaluating the properties of the final resin, even though no link between the properties and the point of addition could be identified so far.

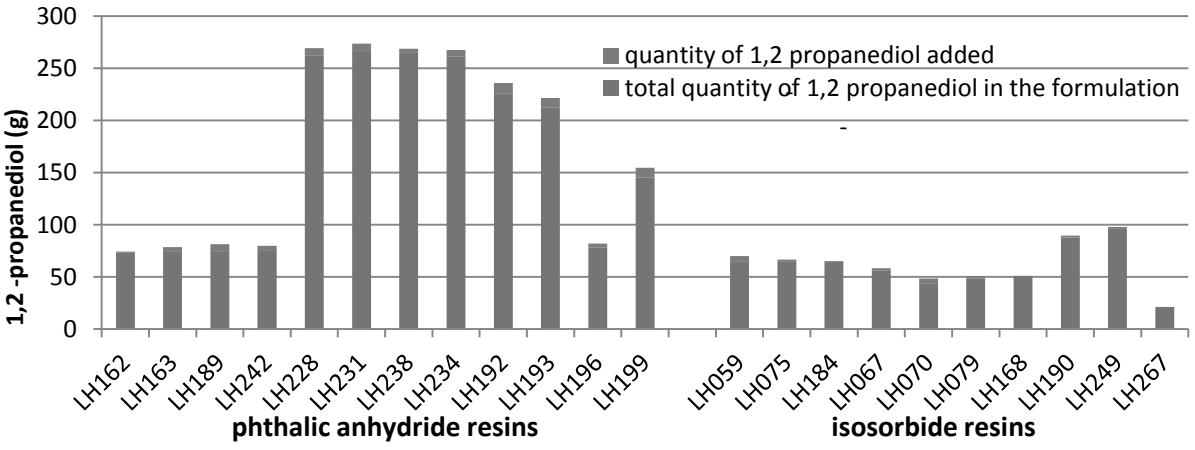

Figure 21: Amount of 1,2-propanediol added compared to the total amount in the formulation

XLIII. Resin colouration

Ideally, the resins should be transparent and colourless. However, yellow products were sometimes obtained instead. Different possible causes will be discussed here.

The yellowness of transparent liquids can be evaluated using the Gardner scale, which grades the darkness of their colour from 1 – 18. In the Gardner method, the liquid is filled into test tube, compared to a standard and assigned the number corresponding to the closest match. Due to the lack of a standard, the resins were instead only roughly classed in terms of their colour in this work.

Figure 22: Colourless and transparent resins based on phthalic anhydride (LH174 – LH182)

Several of the prototypes synthesised were yellow or dark yellow when observed in a 500 mL glass. Two factors have to be taken into account: Firstly, the colour is more visible the thicker the layer of paint that is examined. This effect is already obvious when the resin is transferred form a 500 mL glass to a 5 mL glass. Even less colour is visible in the final application, which results in a resin layer only 15 -20 µm thick. Secondly, the intensity of the colour is also decreased during the application by the addition of colourless solvents, melamine resins and other additives.

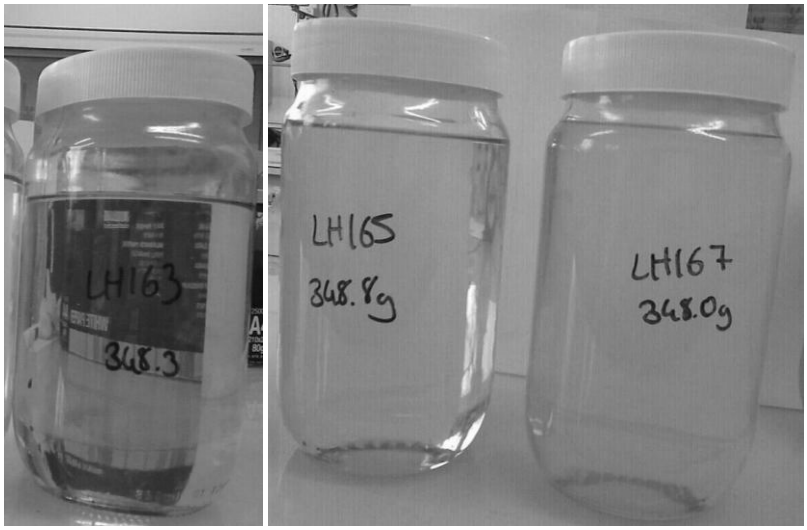

Figure 23: Selection of phthalic anhydride resins including yellow LH163

The two factors governing the colour of the resins are the vulnerability of the monomers towards degradation and the reaction procedure. Concerning the monomers, isosorbide based resins were found to be more prone to colouration than phthalic anhydride based resins. However, coloured samples of phthalic anhydride resins, for example LH163, and relatively colourless isosorbide resins, for example LH077 and LH168, were also obtained.

It was observed that long storage of the isosorbide monomers could have a negative impact on the colour of the resin, possibly due to degradation prior to the reaction. No further correlation between the colour and the formulation could however be established, since identical formulations sometimes yielded differently coloured products.

Both the duration of the reaction and its temperature impacted upon the colouration. A compromise was necessary, since colouration is risked both when the reaction takes too much time and when the temperature is too high. Obviously, high temperatures can accelerate the reaction, so the exact right temperature necessary to achieve reaction progress has to be found at each point to ensure minimum colouration. This is also part of the reason why no precise reaction protocol can be followed, as it has to be adjusted to the reactivity of each formulation.

The resin LH266 is evidence of the fact that a long reaction time can induce colouration. The low reactivity of the monomers caused the reaction to last for 5 days instead of 2 or 3 before an acid value below 10 mg_{KOH}/g could be obtained, and the resulting resin had a dark green colour. A similar problem was encountered with the resin LH166, which was synthesised using isosorbide diluted to 80% in water. The time needed for the distillation of the water prolonged the reaction, which lasted for 4 days. The product had a reddish colour which was much darker than LH077, a resin with an equivalent formulation synthesised using dry isosorbide.

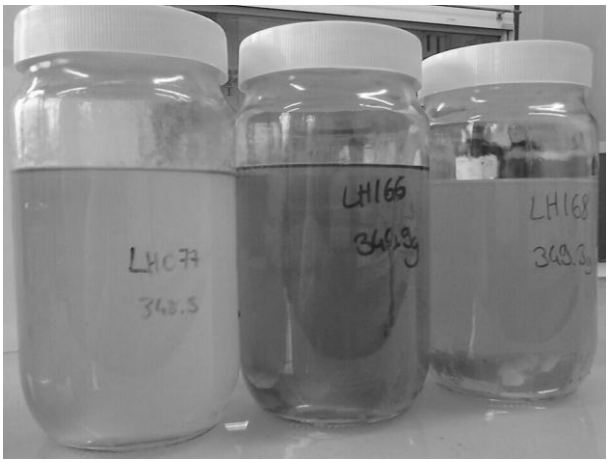

Figure 24: Resins synthesised with dry and diluted isosorbide

The problem was finally solved by accelerating the distillation through higher temperatures and additional azeotropic solvent, and a much lighter product, LH168, could be obtained after three days when the synthesis was repeated.

Another important factor is the inertness of the reaction atmosphere. Nitrogen or argon gas was always bubbled through the resin during the reaction. The colouration of the products could therefore be improved by increasing the gas flow and ensuring air tightness of the reactor. As described above, high nitrogen flow could also lead to an increased loss of volatile 1,2-propanediol, so a compromise between the colour and the accuracy of the formulation had to be found.

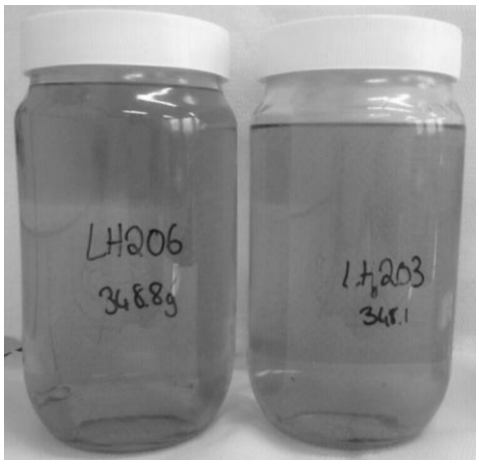

Figure 25: Highly coloured isosorbide resins synthesised from isosorbide stored for several months

It should further be noted that the resin synthesis took around 18 h for phthalic anhydride resins and around 21 h for isosorbide based resins. Therefore, the reaction had to be stopped at night during which time the reactor was closed but no nitrogen flow was possible. Furthermore, the hard resin had to be heated up again in the morning, during which time homogeneous stirring was not possible so that the outer layers of the resin were subjected to high localised heating.

In an industrial application, where a continued reaction is possible, neither the reheating nor the interruption of the nitrogen flow would occur.

Overall, it was assumed that the yellowness was induced by minor oxidation and degradation processes which have little impact on the overall resin properties. Furthermore, it was in a large part not due to the resin formulation but to the reaction procedure, reactor design and monomer storage which would not be a problem in an actual industrial application. Therefore, it was decided to keep and test prototypes within an acceptable degree of yellowness. After curing, no problematic colouration of the films was observed even with the darkest prototypes.

XLIV. Modifications on the polyesterification reactor

The reactor was modified continually during the project to address problems of colouration and hydroxy functionality loss. As these were associated with the gas flow, the presence of oxygen and the tightness of the reactor, weaknesses in these areas were investigated. Steps taken to improve the reactor are discussed in this section.

First, in order to improve the nitrogen flow, the inlet tube was changed from a 3 mm diameter to 5 mm diameter. This successfully increased the gas flow. Furthermore, the joints between the tube and rubber tubing connecting to the gas bottle or a Schlenk line were sealed with parafilm, and simultaneous use of the Schlenk line for other purposes was avoided where possible.

Secondly, several sources of leaks were identified in the reactor. The primary sources of weakness were the joints between the different parts of the reactor. The joint connecting the reactor top to the Vigreux column is vulnerable because it connects two parts which are resting on different clamping systems, and can be loosened when the clamps are not perfectly aligned. It was therefore exchanged with a screw fitted version. Furthermore, teflon film was also wrapped around several joints.

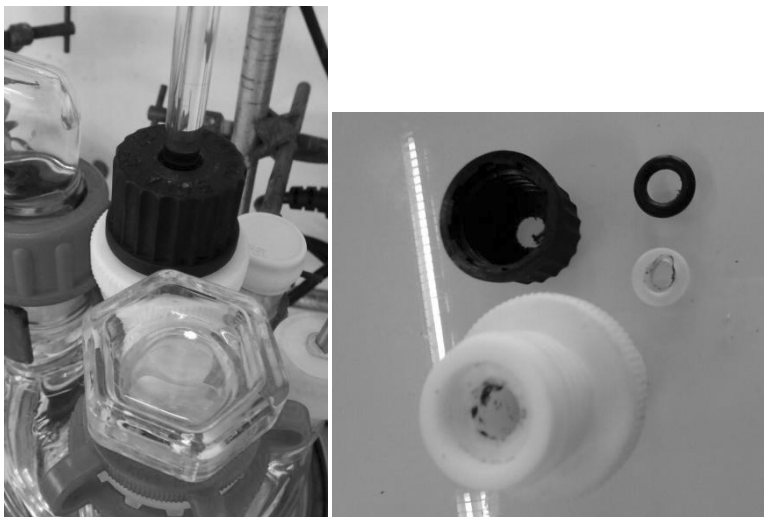

Figure 26: Old joint with glass mechanical stirrer and screw fit as well as disintegration of the different part of the old joint

The inlet joints for the nitrogen tube and the temperature probe are moved up and down often, the former to avoid clogging of the tube with hardened resin, the latter to allow better stirring when

temperature control is not necessary. Therefore, the septa originally used were replaced by customised teflon joints.

Figure 27: Leak in reactor with new joint

The most vulnerable joint was the connection between the rotating mechanical stirrer and the reactor top. The alignment of the stirrer with the reactor is crucial to avoid unnecessary vibration. Due to the usage induced decrease of accuracy of the motor rotations, a short plastic tube connection was inserted between motor and reactor. At first, a simple joint was used as connection as shown in the picture below. However, the continuous rotation caused the inner lining to disintegrate and fall into the reaction mixture, so it was replaced with a self-rotating joint.

As demonstrated by the picture on the left, even the self-rotating joint still required a careful alignment of stirrer and reactor to avoid leakage. In the end, the glass top was replaced with a teflon top to eliminate any leak in the direct joints.

Two sources of metal are present in the reactor which could potentially catalyse the thermal degradation of monomers during the reaction. One is the temperature probe, which is unavoidable, but the other, which is the stainless steel mechanical stirrer, was replaced by a glass version.

Due to the lower mechanical stability of glass, the radius of the glass stirrer had to be smaller than that of its steel equivalent, possibly leading to lower mixing rates during the reaction.

Figure 28: Teflon reactor top

The quality of the stirring is also essential for the coloration and for the hydroxy loss in the reaction as it determines both the heat distribution within the reaction mixture as well as the surface of the reaction, and therefore the possible contact with oxygen.

The heat distribution is particularly important at the start of the reaction, and it is one of the reasons why isosorbide resins colour more easily than phthalic anhydride resins. While phthalic anhydride resins contain enough liquid for it to be possible to stir the mixture from the start of the reaction, isosorbide, succinic acid and sebacic acid are all solids and have to be warmed up to around 60 °C to start.

In order to address this problem, Arkema started using liquid isosorbide diluted in water. However, the benefits of being able to stir the reaction during the entire heating phase were offset by the longer overall reaction time on the lab scale, as described above.

The form of the reagents can also have an influence on the stirring at the start of the reaction. It was observed for example that coarser sebacic acid is easier to stir than fine powder, which can form clumps as soon as it is in contact with any liquid.

XLV. Hazy aspect due to grease

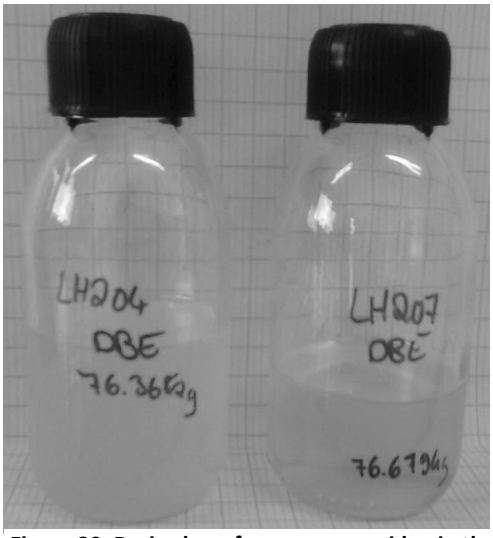

Figure 29: Resins hazy from grease residue in the reactor

One cause identified for a hazy aspect for some resins, such as LH204 and LH207, was that grease had been added to the joints connecting the Vigreux column to the reactor top in the intention to improve the sealing. Even after several reactions, small parts of the grease were still washed out into the resin and caused incompatibility with the solvent. This problem was solved after cleaning the reactor joints thoroughly.

XLVI. Isosorbide NMR

135 DEPT and HSQC techniques were used to differentiate between the CH and the CH_2 signals.

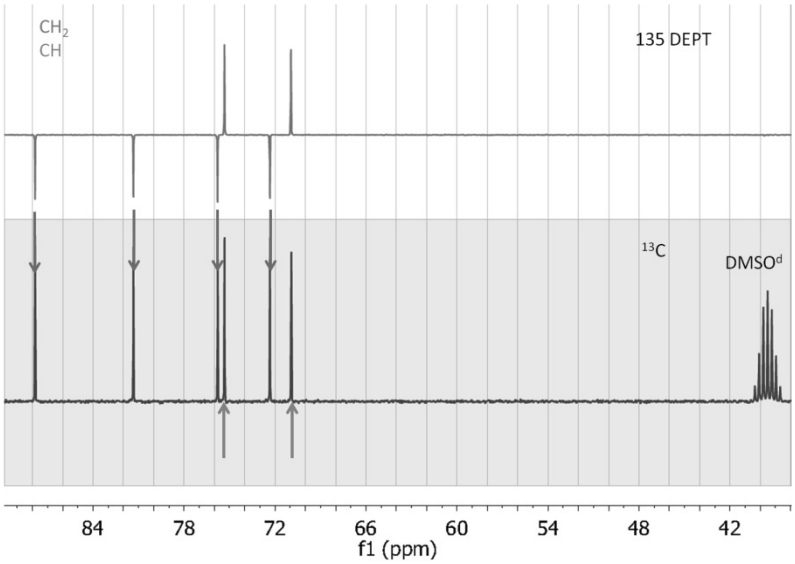

Figure 30: Assignment of isosorbide ^{13}C peaks using 135 DEPT

The protons corresponding to the hydroxy groups can be found furthest downfield, followed by the CH protons and furthest upfield the CH_2 protons.

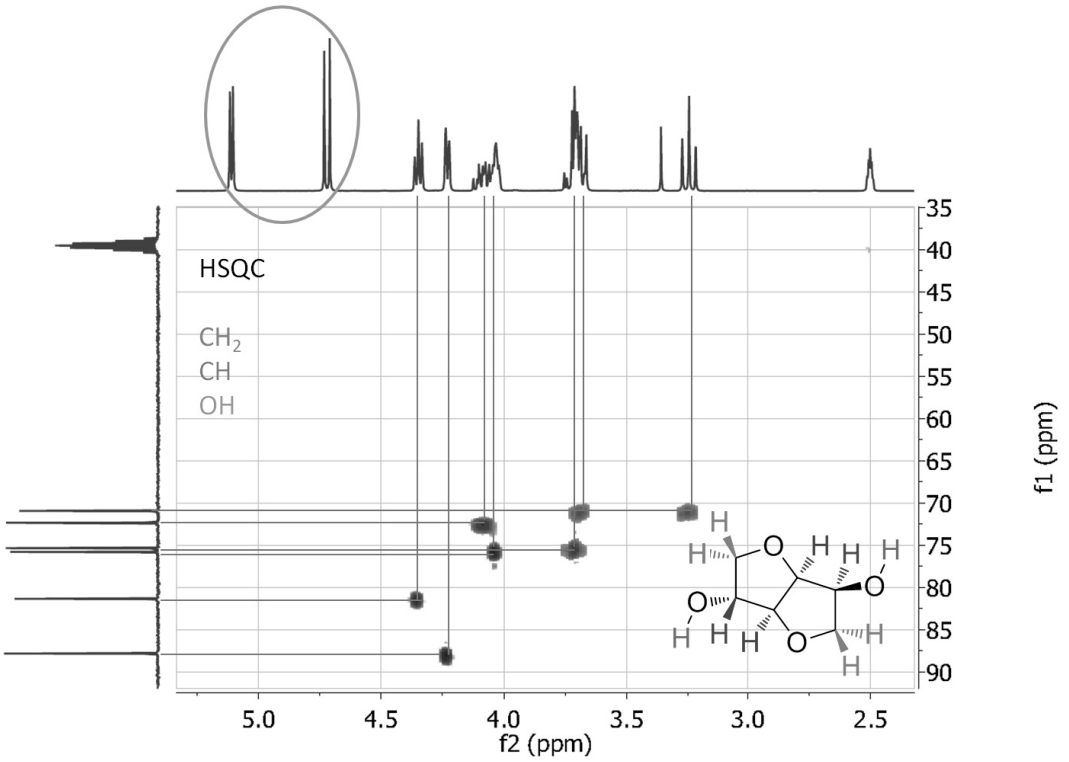

Figure 31: HSQC of isosorbide

COSY was used to distinguish between the CH protons β to the hydroxy groups, which form two distinct signals, and the protons α to the hydroxy group which form an overlapping signal further upfield and couple to the hydroxy protons.

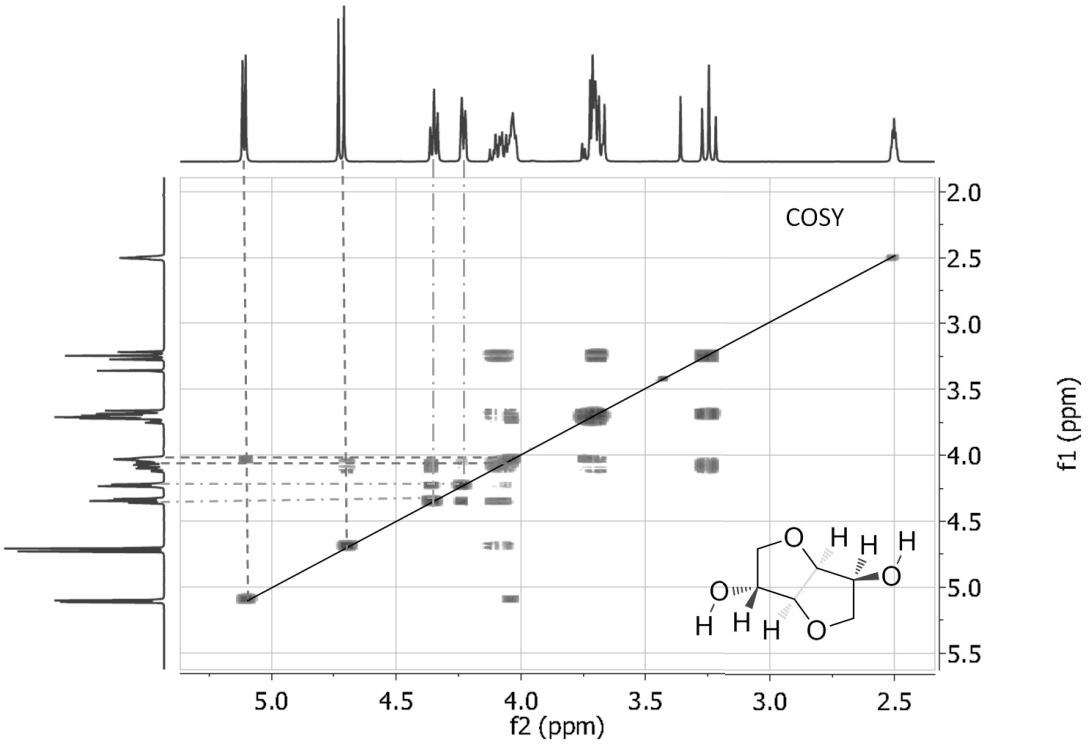

Figure 32: COSY NMR of isosorbide

The two CH protons β to the hydroxy group were distinguished using nuclear Overhauser effect (NOESY) spectroscopy. As can be seen in the 3D image of one of the isosorbide conformers retrieved from the PubChem 3D database, only the proton adjacent to the endo-orientated hydroxy group is in spatial proximity with one of the hydroxy protons.[113]

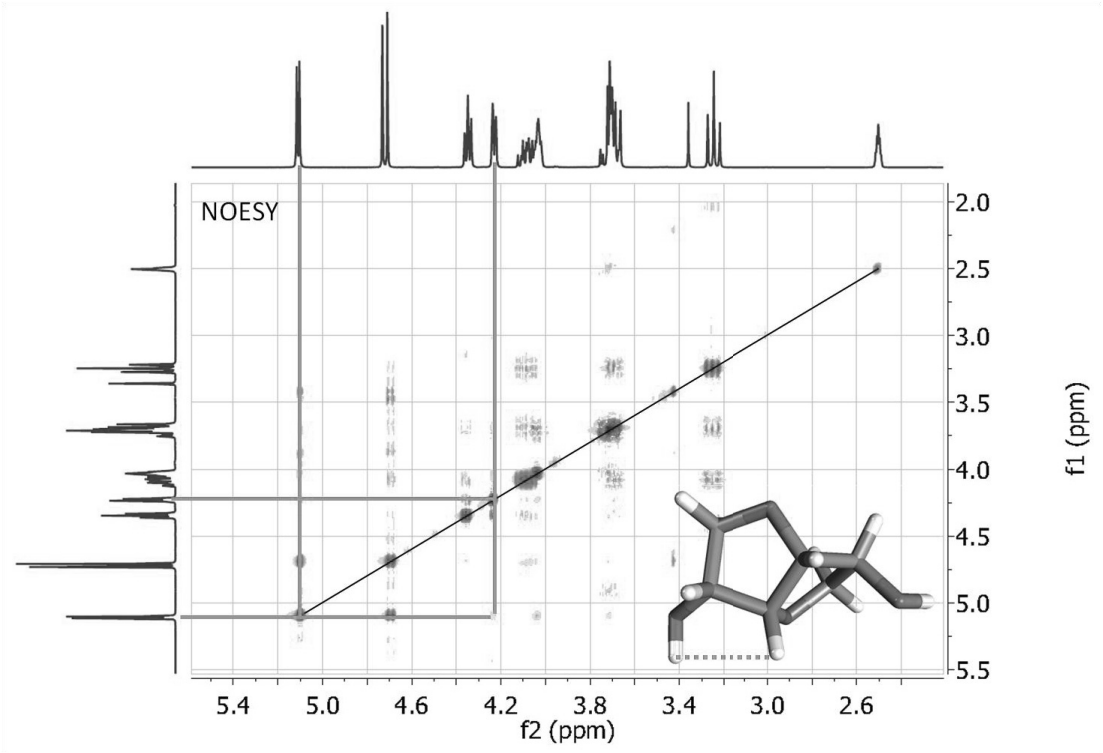

Figure 33: NOESY NMR of isosorbide

Lastly, the closer proximity of three of the CH_2 protons to one of the hydroxy oxygens shown visible in the 3D structure permitted to distinguish the signal corresponding to the fourth CH_2 proton which is oriented exo with respect to the cavity and located β to the endo hydroxy groups.

XLVII. M_w *vs.* polydispersity

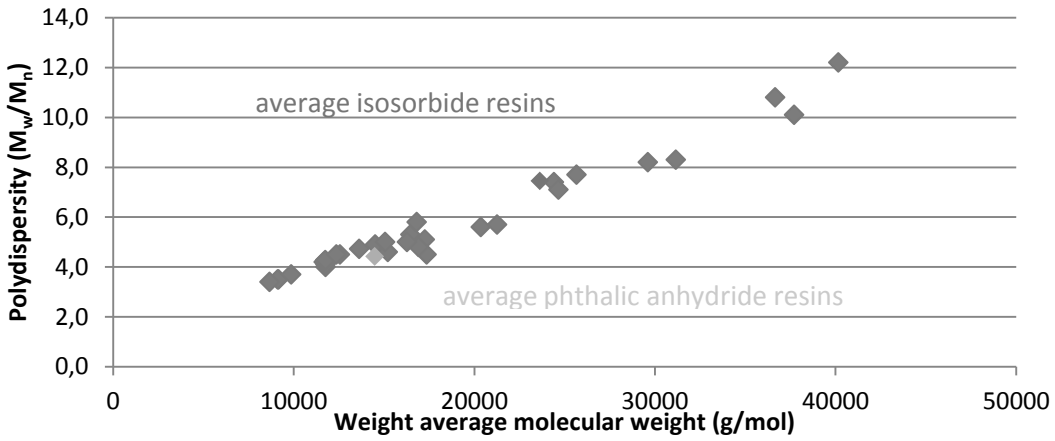

Figure 34: M_w *vs.* polydispersity

XLVIII. Prototypes discarded due to their molecular weight

Isosorbide resins with elevated viscosities

The viscosity of a paint is one of the most important factors to determine its applicability on a coil coating line and the quality of the resulting film. When diluted to about 65% with a suitable solvent, the resin viscosity should be below 1000 mPa*s to fulfil the criteria. While a minimum viscosity above 1000 mPa*s is also desirable, it can easily be increased by limiting the amount of solvent added. Viscosities significantly above 6000 mPa*s are problematic because they necessitate the addition of large amounts of solvent for application, increasing the cost and waste produced in the curing process.

Because the viscosity could also be adjusted by changing the solvent used, only resins with viscosities twice as high as the maximum, i.e. above 12 000 mPa*s, were considered problematic in this case. All the resin products displaying problematically elevated viscosities were based on isosorbide, and their characterisations are shown below.

Table 14: Characterisation of isosorbide resins with elevated viscosities

Resin	ISO	end AV	viscosity	concentration	solvent	$M_{n\ theoretical}$	M_n	M_w
	mol%	mg_{KOH}/g	mPa*s	%		g/mol	g/mol	g/mol
LH184	29,37	6,3	8 553	65,5	MPA	2 956	3600	29600
LH034	29,37	16,6	60 000	67,4	S9	1 913	-	-
LH037	29,37	7,9	188 133	64,7	S9, DBE	2 719	-	-
LH044	29,37	8,3	23 840	66,8	S9, DBE	2 667	-	-
LH038	34,37	7,8	41 786	70,0	S9, DBE	2 739	-	-
LH040	34,37	6,3	16 400	67,2	S9, DBE	3 004	-	-
LH186	24,37	2,1	40 793	66,1	MPA	3 673	3 650	39 900
LH188	24,37	10,0	21 410	64,7	MPA	2 428	-	-
LH190	24,37	8,5	18 934	66,0	MPA	2 590	3 300	40 150
LH263	34,31	7,6	14 278	63,6	MPA	2 695	-	-
LH243	39,37	7,2	20 839	64,3	MPA	2 928	3 400	36 650
LH267	39,37	9,4	25 806	65,6	MPA	2 962	-	-

The reason for the elevated viscosities of the different resins is not obvious. Neither a correlation with the isosorbide content nor with the theoretical molecular weight or the acid value at which the reaction was stopped is apparent. Because few of the resins were used as prototypes, their molecular weights were not determined experimentally for the most part. However, for the LH186, LH190 and LH243, higher than average M_w were observed.

The resins LH034 – LH040 were synthesised without compensation for the loss of 1,2-propanediol during the synthesis. Therefore, the changed ratio of alcohol and acid groups could have caused an increased chain length and therefore high viscosities.

On the other hand, the quality of the isosorbide used was identified as a possible reason for the high viscosities of the resins LH186 – LH190. The monomer had been in storage for several months and

the synthesis yielded only resins with high viscosities even after being repeated carefully three times. Because new isosorbide was not available, LH190 was used as a prototype despite its high viscosity.

Gel formation

Theoretically, gel formation occurs when the polymer chain length approaches infinity, so that all chains are connected with each other. Practically, solubilisation or processing of the polymer is then no longer possible, and problems with the reaction equipment arise. Firstly, a gel cannot be properly stirred even at high temperatures, and its formation risks to break the stirring equipment. Secondly, because the gel cannot be solubilised, it is difficult to remove it and to clean the reactor.

Figure 35: LH195 gel hanging upside down in its glass

Therefore, gel formation should be avoided at all cost. Generally, the resin is formulated so that gel formation should not occur even when the acid value reaches zero. For this, the functionality, or amount of reactable groups per molecule, is calculated. As the acid groups are in the minority, they constitute the limiting quantity, and the functionality can be obtained by dividing the amount of acid groups by the total amount of molecules in the reaction. In general, when the amount of acid groups per molecule is smaller than 1 or twice the ratio of acid groups per molecule is smaller than 2, gel formation should not occur.

While all resins were formulated respecting this principle, gel formation still happened in four cases for resins based on phthalic anhydride and in two cases for resins based on cyclohexanedicarboxylic acid. They are described below. No gel formation was observed for resins synthesised on the basis of isosorbide.

Table 15: Description of resin syntheses which resulted in gel formation

	resin	description	AV last measurement	F_n	r_0
			mg_{KOH}/g		
phthalic anhydride	LH195	high T_g	13,67	1,9492	1,115
	LH233	low petro content	22,89	1,9492	1,115
	LH259	GLY 9,28 mol%	12,32	1,9789	1,115
	LH261	GLY 9,28 mol%	14,63	1,9789	1,115
cyclohexane dicarboxylic acid	LH270	SEB 4,00 mol%	16,3	1,9492	1,115
	LH273	GLY 7,71 mol%	10,51	1,9663	1,113

In some of the cases, the formation of the gel can be attributed to the higher functionality. In the case of LH259 and LH261, it was raised to permit the incorporation of 9,28 mol% glycerol while keeping the ratio of alcohol to acid groups at 1,115. In the case of LH273, it was raised to permit the incorporation of 7,71 mol% glycerol and 31,04 mol% of succinic acid in the hope of increasing the glass transition temperature. It can be concluded that the functionality cannot be raised above 1,95 without risking the formation of a gel.

In the case of LH195, LH233 and LH270, the functionality of the resin was not changed, but gel formation still occurred. The exact compositions of all three can be found in section 5.1.5. They were all formulated to maximise the glass transition temperature of the product, and contained only 1,2-propanediol as a diol and no or only small quantities of sebacic acid. It can be concluded that the flexibility of the chains which is normally provided by long, linear aliphatic chains was very limited.

It is possible that the limited flexibility of the chains, or the relative reactivity of the monomers led to the preferential reaction with certain groups, or prevented the reaction of others, thus changing the real ratio of available acid and alcohol groups and therefore the functionality. However, this is could not be verified as processing and therefore analysis of the gel is very difficult.

XLIX. Hansen solubility parameters evaluation

The Hansen solubility parameters are a way to evaluate the dispersion forces, polarity and hydrogen bonding ability of products. The similarity of these parameters for two substances can be a good indication of their compatibility and are therefore used to predict solubility.

For small molecules, the three parameters can be derived from thermodynamic measurements such as the enthalpy of vaporisation, from their refractive index and their dipole moment. However, this is not possible for polymer molecules due to their size, and the parameters have to be determined from comparison with other molecules whose parameters are known.

The group of prototypes based on phthalic anhydride that contained increased amounts of rigid monomers was the first group available during the project, and the two most promising resins in terms of their glass transition temperature were selected for solubility testing. The resins LH196, which contains an 34,37 mol% of phthalic anhydride and in which the sebacic acid was entirely replaced by succinic acid, and LH199, which contains an increased amount of 1,2-propanediol in addition to the changes made in LH196, were sent to Activation for evaluation.

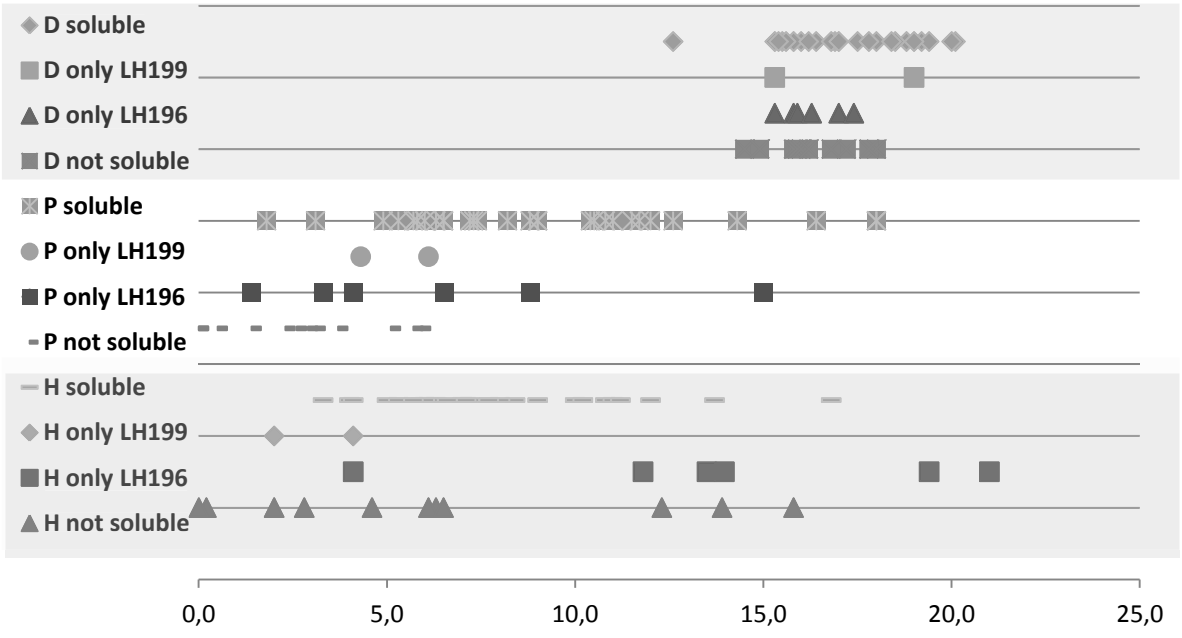

Figure 36: Hansen solubility parameters of solvents tested with LH196 and LH199

Activation diluted each resin to a concentration of 0,7 g/mL in 48 different solvents by agitation at room temperature for two days and divided the results into soluble, which corresponds to dissolution, swelling and stable dispersions, or not soluble, which corresponds to precipitation, phase separation or a hazy aspect. Overall, LH196 was soluble in 34 of the solvents tested, while LH199 was soluble in 31.

Above, the Hansen solubility parameters dispersion of the solvents tested are visualised classed by their compatibility with the two resins. The dispersion forces (D) are shown on the top, followed by the polarity (P) in the middle and the hydrogen bonding ability (H) at the bottom. The solubility parameters for the solvents which were compatible with both resins are shown on top in green, while those of the solvents not compatible with either resin are shown in red on the bottom. The parameters of solvents only compatible with LH196 are shown in purple and those only compatible with LH199 are shown in blue.

It is clear from the graph that no fast conclusions can be drawn about the region in either of the parameters which is compatible with the resins. Slightly higher dispersion forces, high polarity and medium hydrogen bonding ability seem to be advantageous, but many of the parameters for compatible and non-compatible solvents overlap. A selection of solvents not compatible with either resins are shown below with their Hansen parameters.

Table 16: Hansen parameters of solvents not compatible with either resin

	δD	**δP**	**δH**
butyl acetate	15,8	3,7	6,3
diethylamine	14,9	2,3	6,1
toluene	18,0	1,4	2,0
m-xylene	17,8	2,6	2,8
1-pentanol	15,9	5,9	13,9
1-butanol	16,0	5,7	15,8
diethyl ether	14,5	2,9	4,6
butylglycol	16,0	5,1	12,3
1-chlorobutane	16,2	0,5	2,0
cyclohexane	16,8	0,0	0,2
hexane	14,9	0,0	0,0

Instead of trying to determine average values for each parameter, a software called HSPiP, which stands for Hansen solubility parameters in practice, is used to construct a solubility sphere for each resin.[114] This sphere represents the area in the three dimensional Hansen space which includes all solvents that are compatible but excludes all that are not.

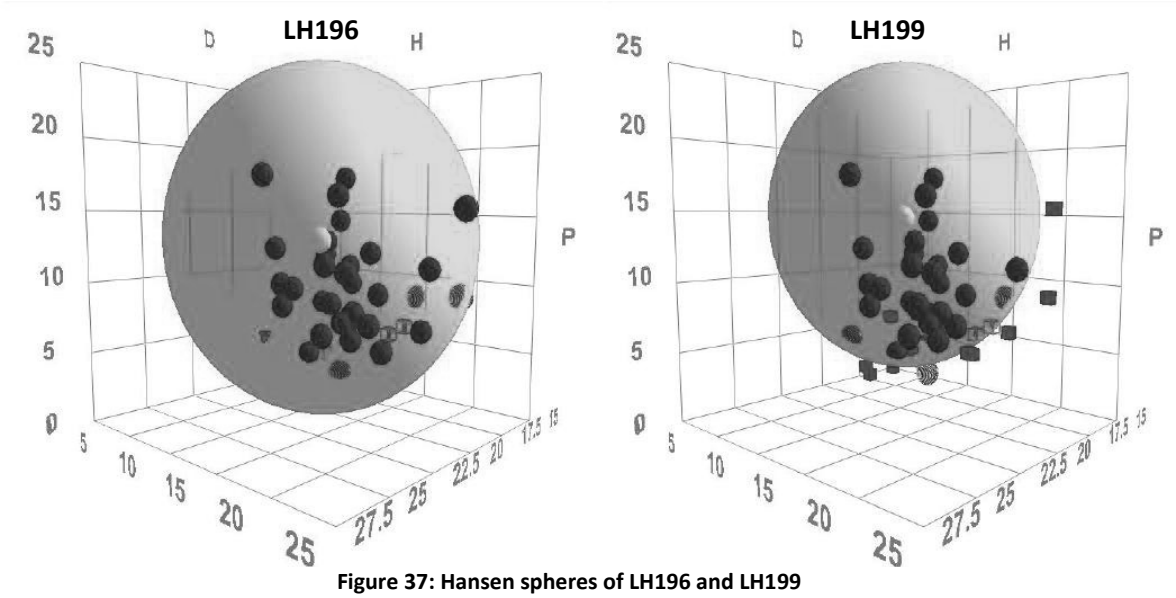

Figure 37: Hansen spheres of LH196 and LH199

The solubility spheres are shown above, including the compatible solvents represented in blue and the non-compatible solvents represented in red. The Hansen solubility parameters specific to the resins are assumed to correspond to the centre of the sphere. The calculated parameters as well as the diameter of the sphere of both resins are compared below to the parameters of a petrosourced resin and the biosourced Arkema resin based on isosorbide proposed for interior use.

Compared to the isosorbide resin, both LH196 and LH199 have larger spheres. A selection of relevant solvents which were compatible with both or only one of the resins is shown below.

Table 17: Hansen parameters of solvents compatible with only one of the resins

		δD	δP	δH
LH196	**dipropyl amine**	15,3	1,4	4,1
	ethanol amine	17,0	15,0	21,0
	ethanol	15,8	8,8	19,4
	2-ethylhexanol	15,9	3,3	11,8
	cyclohexanol	17,4	4,1	13,5
LH199	**MIBK**	15,3	6,1	4,1
	chlorobenzene	19,0	4,3	2,0

Only LH199 is compatible with MIBK, and neither of the two is compatible with *m*-xylene. It is possible that the presence of a small quantity of the non-compatible xylenes solvent, which is introduced for the azeotropic synthesis, contributes to the lower viscosity of phthalic anhydride based resins compared to the isosorbide resins tested.

Table 18: Hansen parameters of solvents compatible with both resins

	δD	δP	δH
acetone	15,5	10,4	7,0
DBE	12,6	6,5	8,4
ethyl acetate	15,8	5,3	7,2
γ-valerolactone	16,9	11,5	6,3

	δD	δP	δH
β-butyrolactone	17,0	12,6	6,6
acetonitrile	15,3	18,0	6,1
morpholine	18,0	4,9	11,0
acetophenone	18,8	9,0	4,0
THF	16,8	5,7	8,0
MPA	15,6	6,3	7,7
dichloromethane	17,0	7,3	7,1
DMSO	18,4	16,4	10,2
propylene carbonate	20,0	18,0	4,1
chloroform	17,8	3,1	5,7

Generally, both resins are compatible with a large number of organic solvents including THF, acetone, ethyl acetate and acetonitrile.

Compatibility of LH196 and LH199 with biobased solvent systems

In parallel to the efforts to design and synthesise resins based on renewable resources, alternatives for petroleum based solvent systems were also evaluated by Activation. After determining the Hansen parameters of the two resin prototypes, their compatibility with these solvent systems was evaluated.

The components of the solvent system were selected by Activation based on three criteria. Their similarity to current solvent systems and to the resins was judged using the Hansen parameters. Their composition in terms of functional groups, and their boiling point range was also adjusted to suit the coil coating process.

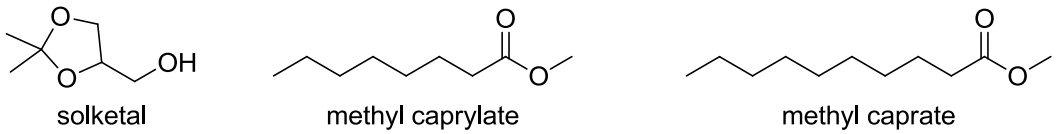

Scheme 37: Biosourced solvent system components

The main components used to make up new solvents were two methyl esters of saturated fatty acids, methyl caprate and methyl caprylate, an acetal based on glycerol called solketal and methyl, ethyl and isobutyl succinates. Five different formulations were created and targeted to resemble a mixture of 92% MPA and 8% MIBK, which is the petroleum based solvent mixture used for the dilution of the resins so far.

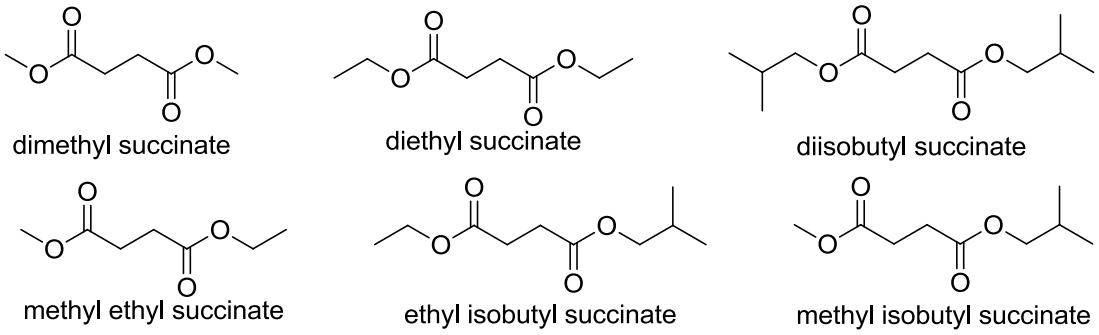

Scheme 38: Succinates used in biosourced solvent systems

The composition of each formulation is shown in the table below. The abbreviations used correspond to different combinations of the products shown above. Radia 7983 refers to a 50:50 mixture of methyl caprate and methyl caprylate. Succinate 1 refers to a mixture of all succinate esters shown above, while succinate 2 contains only methyl and ethyl succinates, with a majority of ethyl ester groups. Succinate 3 equally contains only methyl and ethyl succinates, but the majority of the compounds are mixed methyl ethyl succinates.

Table 19: Composition of biosourced solvent mixtures

	MPA	Succinates	%	Other	%	RED LH196	RED LH199	bio content (%)
Mélange 3	92	-	-	MIBK	8	0,955	0,92	0
M3A	70	3	30	-	-	0,919	0,881	33
M3B	60	2	20	Radia 7983	20	0,964	0,916	49
M3C	60	3	30	Radia 7983	10	0,937	0,889	46
M3D	-	3	60	Solketal	40	0,778	0,746	82
M3E	-	1	60	Solketal	40	0,813		83

The compatibility of a resin with a solvent can be evaluated with the relative energy difference (RED) parameter, which is the ratio of the distance of the compounds in the Hansen space and the diameter of the resin sphere. If the RED parameter is below 1, the solvent mixture falls within the sphere and the two components are theoretically compatible.

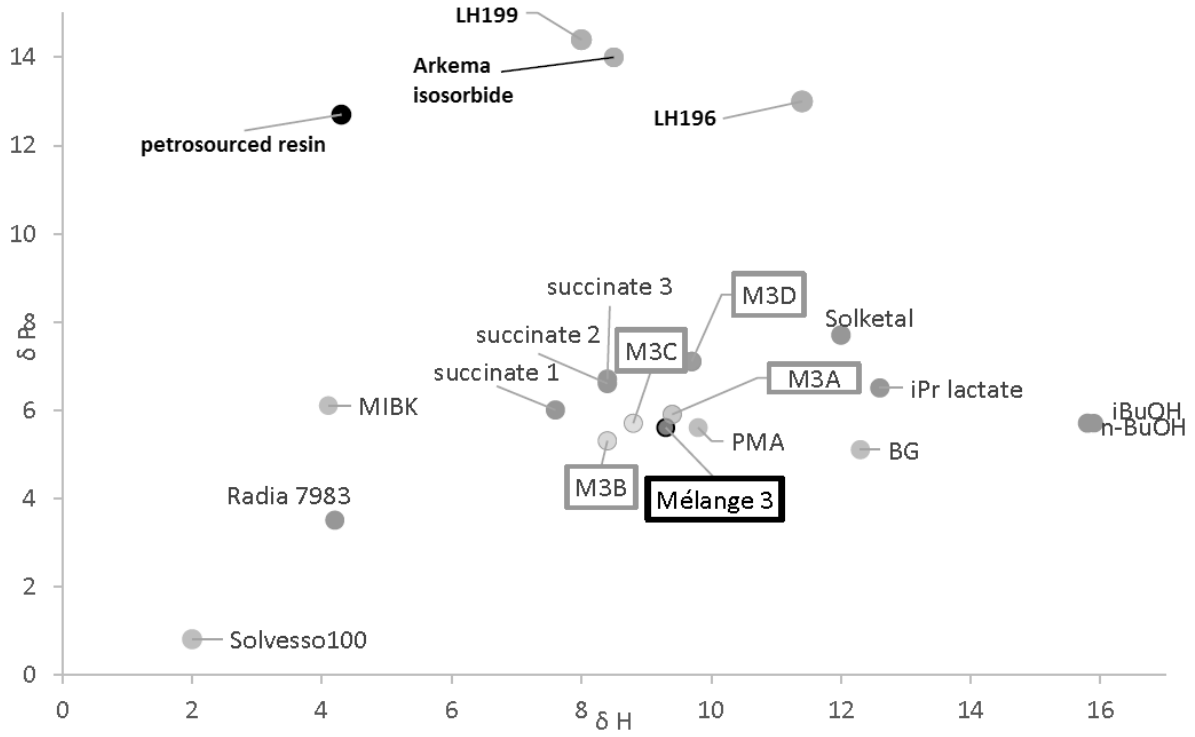

Figure 38: Position of solvent mixtures and resins in the Hansen space

The relative position of LH196, LH199 and the different solvent mixtures in the two dimensional space of hydrogen bonding ability and polarity are shown below. The petrosourced standard resin as well as the isosorbide resin proposed by Arkema for interior use are also shown. Both phthalic anhydride resins are closer to the isosorbide resin than to the petrosourced resin. The close

proximity to the Arkema isosorbide resin is very convenient as the solvent systems developed for it are likely to be suitable for LH199 and LH196 as well.

As predicted by the RED parameters, the solvent formulations were compatible with LH196 and LH199. The resulting viscosities were evaluated and are shown in the table below. Only very low viscosities below 2000 mPa*s were obtained for the mixtures with LH196 studied. The viscosity of LH199 was on the other hand increased by each biosourced solvent compared to that in MPA. The highest viscosity was unsurprisingly obtained for both resins when they were combined with solvent mixtures M3D and M3E which contain 60% of succinate esters, which is 2 and 3 times the succinate content of the other solvent mixtures.

Table 20: Viscosities of LH196 and LH199 in biosourced solvent mixtures

		Melange 3	M3A	M3B	M3C	M3D	M3E
LH196	**mPa*s**	1713		1850			1920
LH199	**mPa*s**	1533	2272	2844	2433	5436	

The highest and lowest viscosities vaguely correlate to the lowest and highest RED parameters. Overall, it can be concluded that phthalic anhydride based resins are compatible with a variety of biosourced solvent systems proposed by Activation. The possibility to combine them with a solvent made up to 82% from renewable sources validates the presence of phthalic anhydride in the resin by increasing the probability of meeting the target of an 65% biosourced content overall.

From the relative position of the two resins as well as from their proximity to the isosorbide based resin, it can be concluded that the monomers other than succinic acid and phthalic anhydride have a major influence on the solubility of the resins. Furthermore, the presence of phthalic anhydride was shown to increase the diameter of the Hansen sphere, which probably corresponds to a better compatibility with traditionally used aromatic solvents compared to the isosorbide resins.

L. Development of the viscosity upon addition of DBE

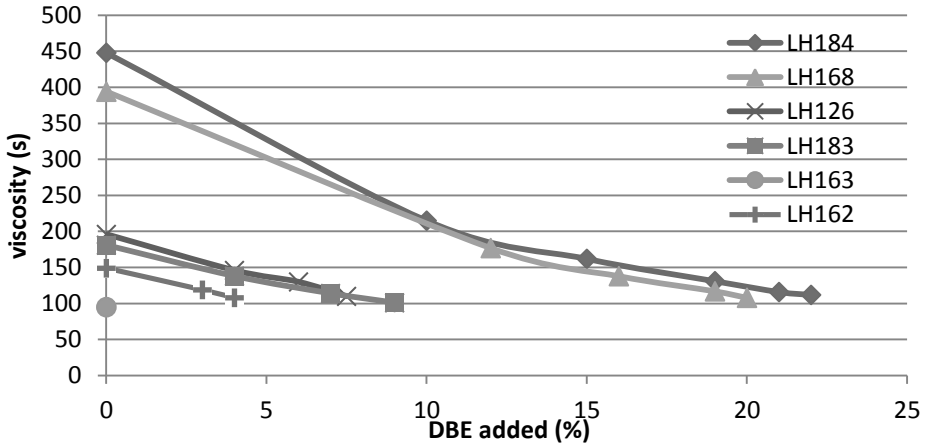

Figure 39: Viscosity adjustment before curing using DBE

The relative amount added to each resin is shown above together with the resulting viscosities after each addition. The viscosity was in this case measured using a funnel according to specifications for an Arcelor Mittal coil coating plant and is reported in terms of the seconds necessary for the resin to flow out of the funnel.

LI. Reproducibility of glass transition temperature measurements

Several factors can introduce uncertainty into the DSC results. Since the glass transition temperature was used as one of the most important parameters for the evaluation of the resin, several steps were taken to eliminate errors.

The heating rate can influence the position of the transition, since the rearrangement of the chains with respect to each other is slow. The advantage of a high heating rate is not only to save time but also often results in more marked transitions. Therefore, the heating rate was fixed to 20 °C/min for all experiments.

The sample size is another factor which can impact on the measurement. The machine specifications dictate the use of samples between 5 mg and 20 mg. While smaller sample sizes can give more precise transitions, larger amounts are generally used where transitions are hard to spot. Since the transitions were generally very clear for the polyester resins examined, the sample size was fixed to 5 – 10 mg. However, due to the small volume of these samples and their high viscosity, a higher precision was not possible.

Lastly, the presence of solvent in the resin can significantly broaden the transition, introducing uncertainty into the determination of the midpoint. The figure on the right shows the heat flow curves for the resin LH072 with and without solvent. In the bottom, the resin containing 35% solvent displays a broad transition with a distance of 25,1 °C between the onset and the midpoint. At the top, the heat flow curve of the resin containing no solvent other than the 1% of azeotropic solvent residue displays a much narrower transition with a distance of 3,4 °C between onset and midpoint. The midpoints of the curves also differ by 11,5 °C.

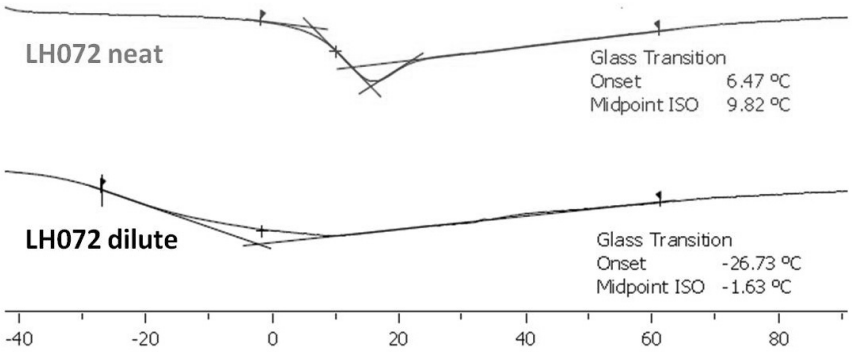

Figure 40: The effect of solvent on the glass transition

While resins were generally examined in neat form, the quantity of azeotropic solvent present can differ from synthesis to synthesis. In order to avoid any deviation due to the presence of solvent, each resin was dried at 125 °C under vacuum for 1 h before the glass transition temperature was analysed.

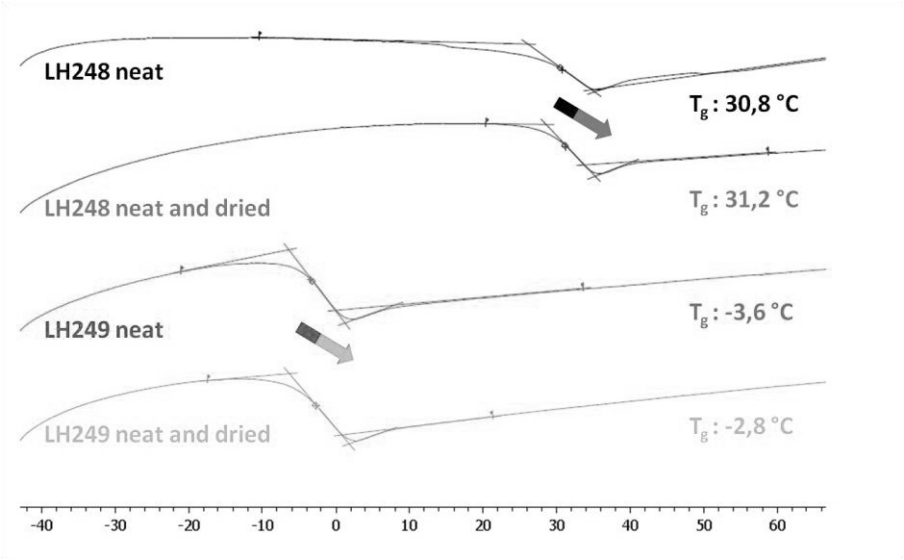

Figure 41: Glass transition temperature shift after drying of the resin

As shown above for the resins LH248 and LH249, a small shift of the glass transition towards higher temperatures was observed after the resin was dried each time. The average difference between the glass transition temperature midpoints of 25 dried and not dried resins was 1,3 °C.

The uncertainty of the established protocol was tested by repeating the same glass transition temperature measurement for the isosorbide resin LH075 ten times. The resulting curves as well as the midpoints determined are shown below.

Table 21: T_g uncertainty

	sample weight	T_g midpoint
no.	mg	°C
1	6,33	6,32
2	9,73	5,30
3	8,29	5,32
4	9,77	5,25
5	8,17	5,37
6	6,88	5,67
7	9,03	4,34
8	7,11	4,55
9	9,54	5,47
10	5,06	4,99

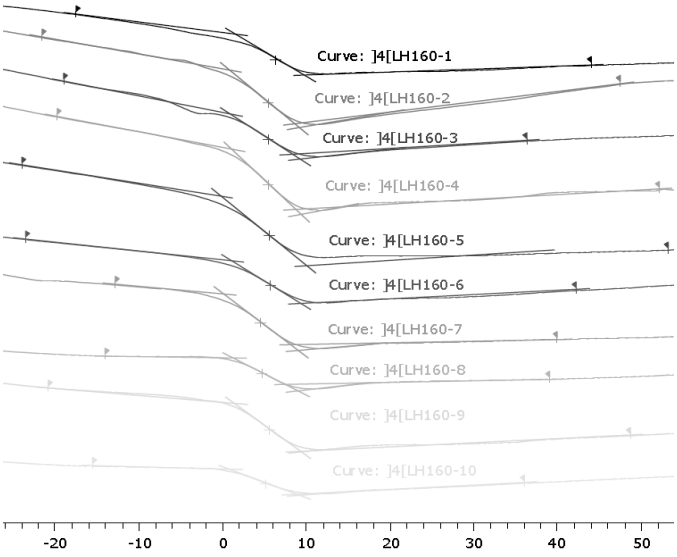

Figure 42: T_g uncertainty test

A standard deviation of 0,56 °C from the average was observed. For this reason, the glass transition temperatures are reported rounded to the full °C.

LII. Glass transition temperatures of resins with an increased isosorbide content but a constant hydroxy value

Different strategies were evaluated to increase the glass transition temperature of the isosorbide resins without changing their hydroxy value. The relative amount of succinic acid and sebacic acid

was adjusted in the resin LH038, the overall quantity of 1,2-propanediol was increased in the resin LH168 and the amount of glycerol was decreased in the resins LH067 and LH079.

Table 22: T_g's of isosorbide resins with higher isosorbide constant but constant hydroxy value

	isosorbide content	1,2-propanediol content	glycerol content	T_g
resin	**mol%**	**mol%**	**mol%**	**°C**
LH075	29,37	15,76	6,14	7
LH168	34,31	10,92	6,13	8
LH067	33,96	13,8	4,09	12
LH079	38,44	11,88	2,09	12
LH038	34,37	10,76	6,14	15

The resulting glass transition temperatures are shown above. In general, the glass transition temperature was successfully increased with respect to the basic isosorbide formulation in LH075. In accordance with the results obtained for phthalic anhydride based resins, the increase in succinic acid and decrease in sebacic acid in LH038 led to the highest T_g. The smallest increase was observed for LH168, followed by the resins LCH067 and LH079. The latter two displayed the same glass transition temperatures, indicating that the decrease in glycerol compensated for the increase in isosorbide.

Chapter 6

LIII. Unedited optical microscopy images

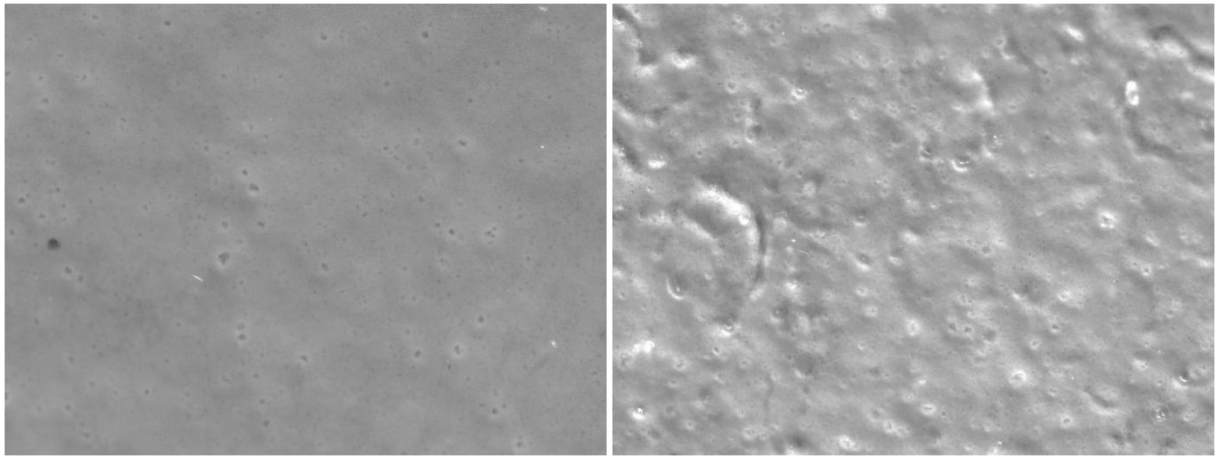

Figure 43: LH184 t0 and t2000 unedited

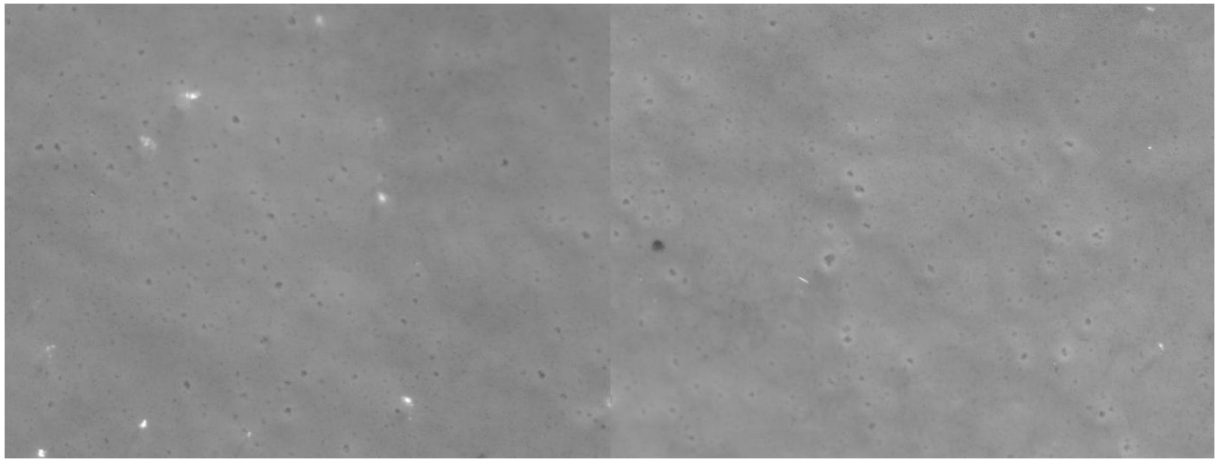

Figure 44: LH189 t0 and t2000 unedited

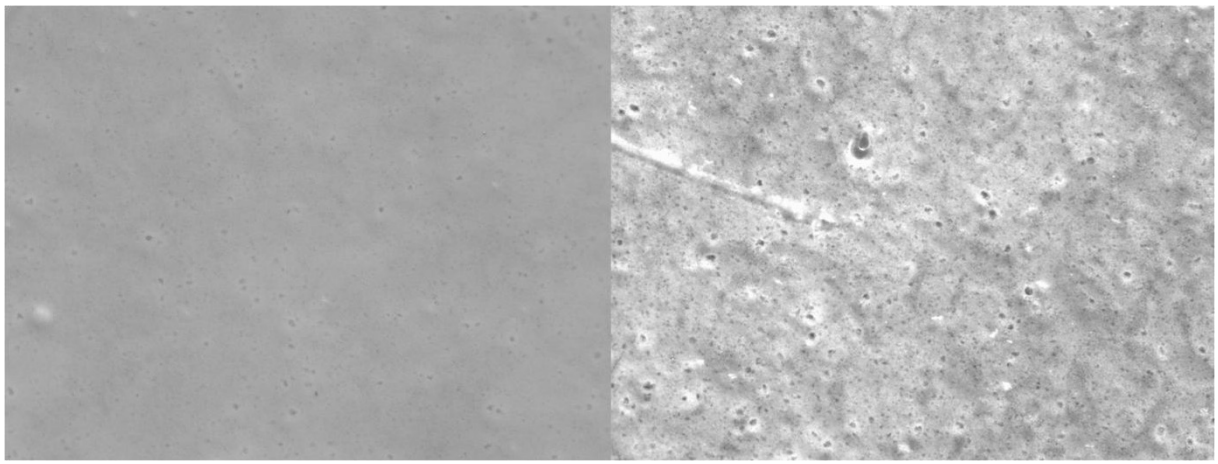

Figure 45: standard t0 and t2000 unedited

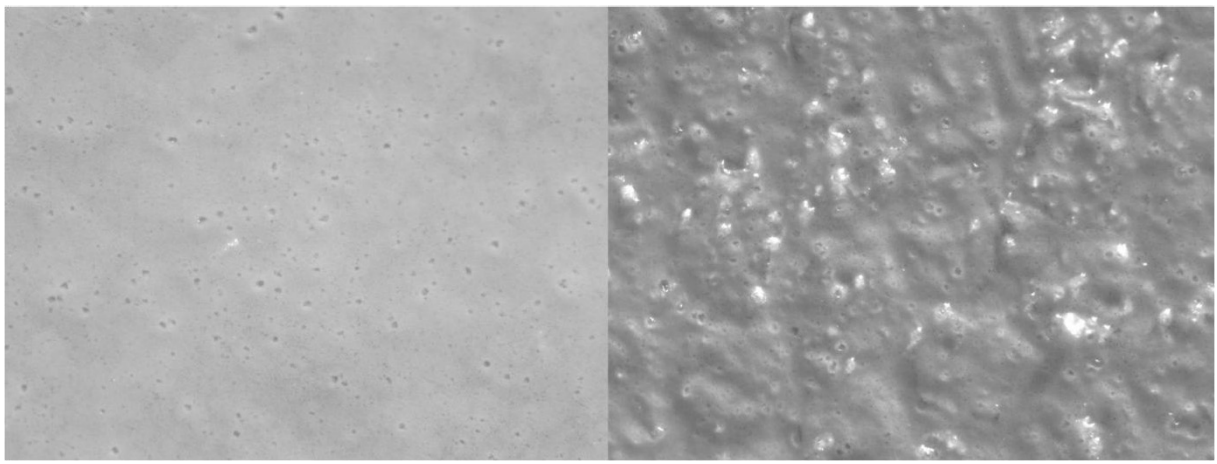

Figure 46: LH174 t0 and t1920 unedited

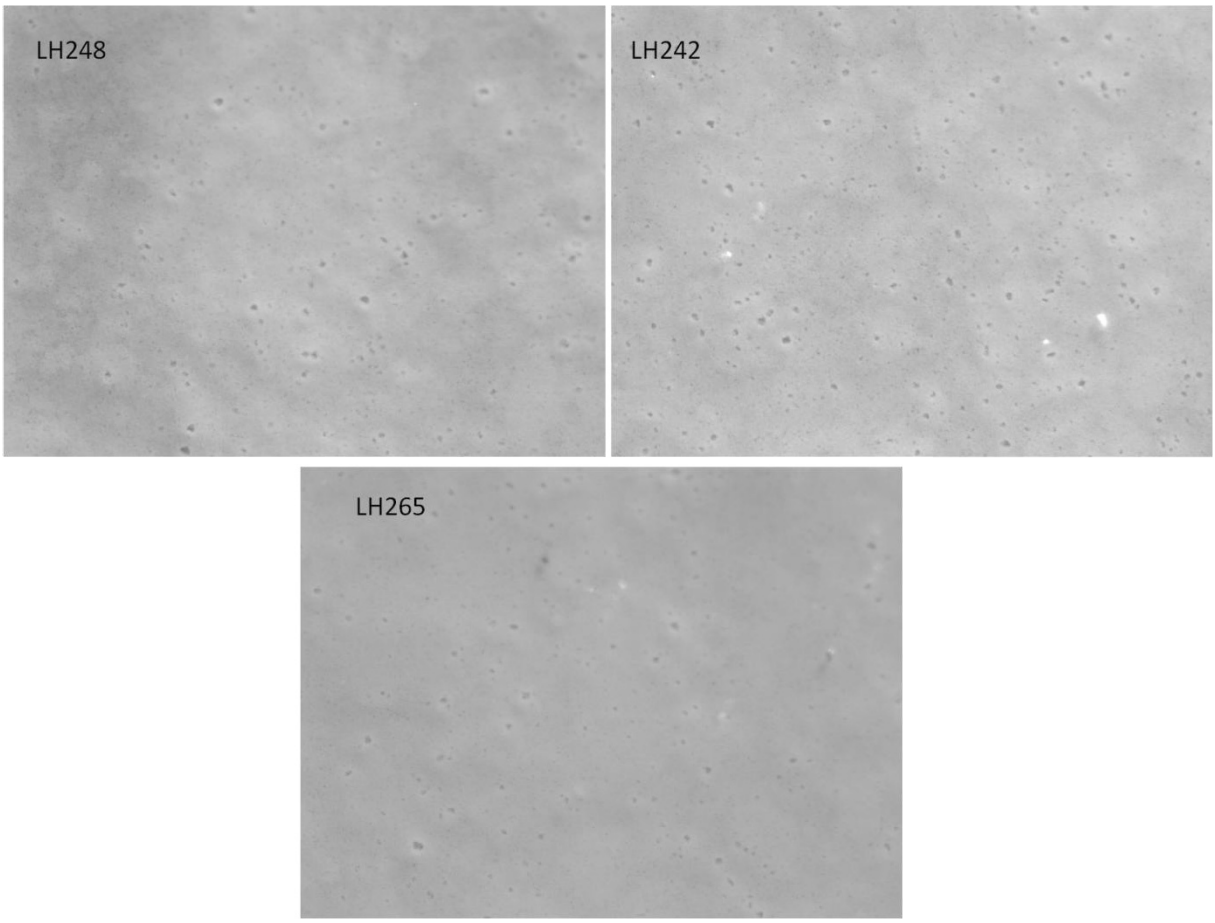

Figure 47: LH248, LH242 and LH265 t0 unedited

LIV. Assessment of the UV absorption of the resins

UV absorption of the isosorbide based coating containing the resin LH184

Below, the UV region of the absorption spectrum of an isosorbide based coating is shown before and after exposure to Hot QUVa conditions. The absorption measured was only very weak compared to the absorption in the other regions of the spectrum, and only small differences can be observed between the two spectra.

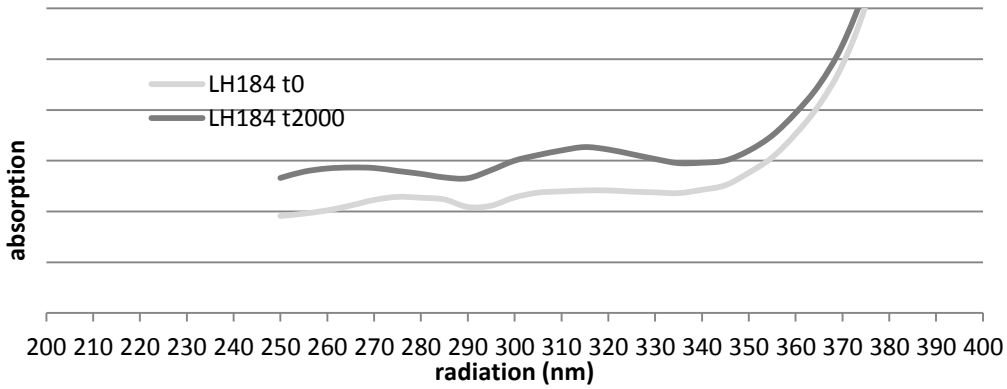

Figure 48: UV absorption of an isosorbide coating before and after weathering

The unexposed coating has two absorption peaks at 275 nm and 320 nm. These were slightly shifted to lower wavelengths after exposure, where they appeared at 265 nm and 315 nm respectively. The

exposed coating absorbs more strongly than the unexposed coating, which could be due to the increased amount of chromophores formed during the weathering. Since the exposed coating was considerably thinner than the unexposed one, as shown in the film thickness analysis, the difference could also be due to stronger influence of the primer.

Overall, the differences between the unexposed and exposed coating are only small. The absorption was only assessed in 5 nm steps, so the shift of the peaks may be within experimental error. More precise evaluation and a non-absorbent substrate would be necessary to draw any definitive conclusions.

Choice of solvent and concentrations used in the UV/Vis study

UV/Vis spectra are sometimes recorded in water, which does not absorb any UV light, but since the polyester resins are not soluble in water, several organic solvents were tested instead. Solvents already present in some of the resins, including methyl isobutyl ketone (MIBK), xylenes and methoxypropyl acetate (MPA), were evaluated for their suitability to minimise the presence of non-resin compounds in the spectra.

Below, the absorptions of several solvents recorded against an air background are shown. In addition to the solvents inherently present in small quantities in the resins, acetonitrile (MeCN) and acetone were also evaluated.

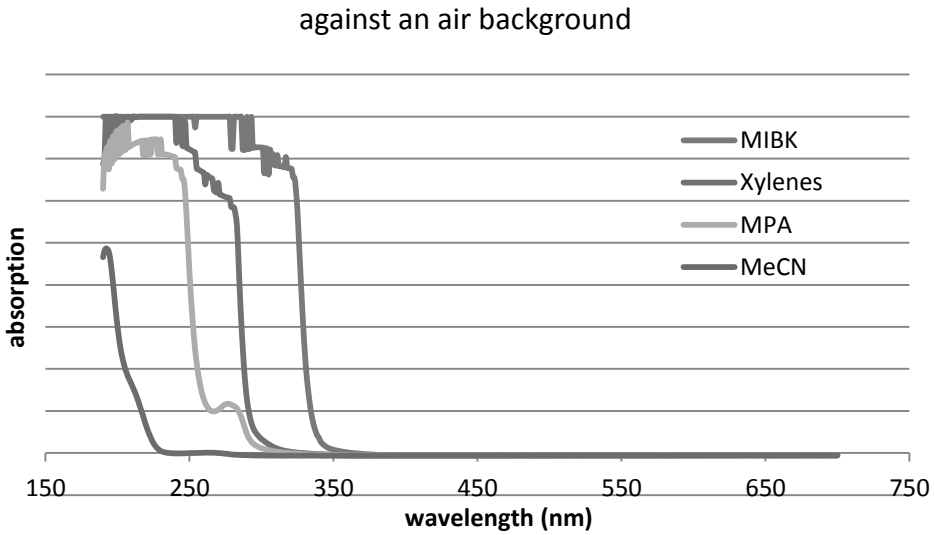

Figure 49: UV absorption of different solvents

The largest UV absorption was detected in MIBK, with a cutoff near 330 nm, followed by xylenes, which had a cutoff near 290 nm and MPA, with a peak at 303 nm and a cutoff near 250 nm. All three were judged not suitable for the evaluation of UV absorption of the resins. Instead, acetonitrile, which not only displayed considerably less absorption but also a cutoff only near 200 nm, was selected.

In order to be able to compare the different UV/Vis spectra, acetonitrile was used as a solvent in all following measurements. A background with pure acetonitrile was recorded before each series of measurements, but a peak near 200 nm was nevertheless detected in all the spectra. The absorption of this peak changed with the concentration of the dissolved product, so it could possibly be due to an interaction between acetonitrile and the products.

In order to be able to identify resident solvent absorption from MIBK or xylenes used for the azeotropic synthesis of the resins, their absorption as well as that of residual acetone from glassware washing was tested when diluted in acetonitrile.

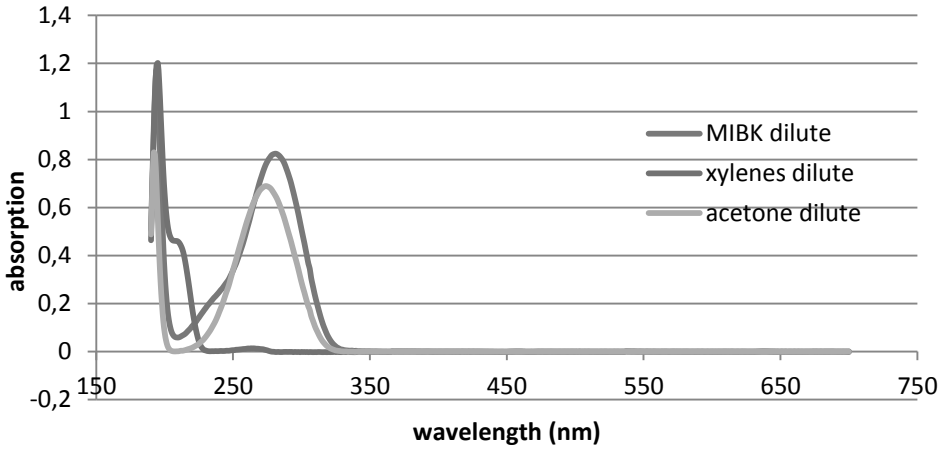

Figure 50: Residual solvent UV absorption in acetonitrile

The MIBK showed a peak at 281 nm, while the xylenes showed a peak at 241 nm and a much smaller one at 263 nm. The absorption of acetone was very similar to that of MIBK, with a peak at 274 nm. The absorptions observed in MIBK and acetone are probably due to n-π* transitions in the ketone group, while the absorption of the xylenes is most likely a π-π*transition in the aromatic ring.

UV absorption of the monomers used for resin synthesis

In order to detect possible differences in UV absorption induced by the individual monomers, each was diluted in acetonitrile and the spectrum was recorded. The monomers were diluted to a level at which their absorption was below 2. This was achieved between 0,24 mol/L and 0,34 mol/L for 1,2-propanediol, 1,3-propanediol and glycerol, at 0,06 mol/L for isosorbide and unsurprisingly only at the much lower 0,02 mmol/L for phthalic anhydride. The diacids succinic acid and sebacic acid did not show any absorption at concentrations low enough to be soluble, so they are not shown here.

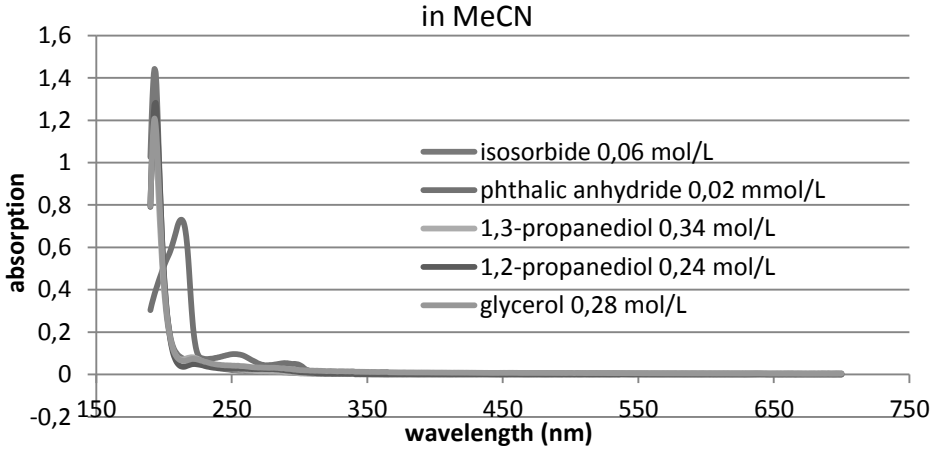

Figure 51: UV absorption of monomers used in the resin synthesis

The strongest absorption was observed for phthalic anhydride. Three peaks can be found at 213 nm, 276 nm and 289 nm in decreasing intensity with higher wavelengths. They first two probably

correspond to $^{1}(\pi\text{-}\pi^*)$ and $^{3}(\pi\text{-}\pi^*)$ transitions within the aromatic ring, while the latter can be attributed to the n-π* transition of the anhydride group.

The absorptions of the diol and triol monomers are negligible in intensity compared to that of phthalic anhydride, and are shown in more detail in the zoomed graph below.

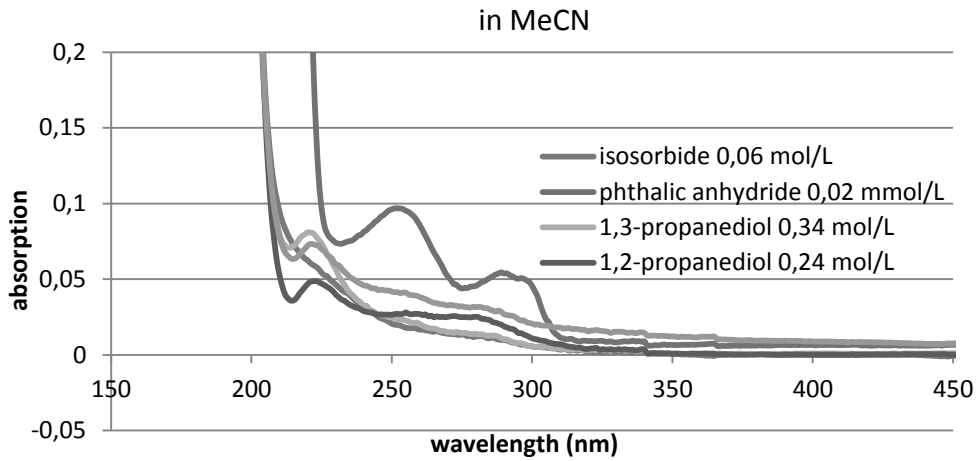

Figure 52: UV absorption of monomers used in resin synthesis - zoom

Taking a closer look, we can see that the isosorbide displays no visible peaks at the concentration in question. The other hydroxy group containing monomers each display a small peak between 220 and 223 nm. The absorption coefficients calculated according to the Beer-Lambert law for the peaks are tabulated below. The Beer-Lambert law states that the absorption coefficient can be calculated according to ε=A/l*c, where A is the absorption at the maximum of the peak, l is the length of the cuvette in cm and c is the concentration of the product in mol/L.

Table 23: Absorption coefficients of monomers used in the resin synthesis

	1,2-propanediol	**1,3-propanediol**	**glycerol**	**phthalic anhydride**		
λ	223 nm	220 nm	221 nm	213 nm	289 nm	276 nm
ε	0,20	0,24	0,26	48096	35939	2923

UV absorption of resins containing different amounts of isosorbide and phthalic anhydride

The UV absorption spectra of the resins containing different amounts of isosorbide (used in 1A) are shown below. The resins were diluted until their highest peak was below 1. The first three resins examined, containing 24,37 mol% to 34,31 mol% isosorbide, behaved very differently from the resins LH249, containing a minimum of isosorbide and LH248, containing a maximum of isosorbide.

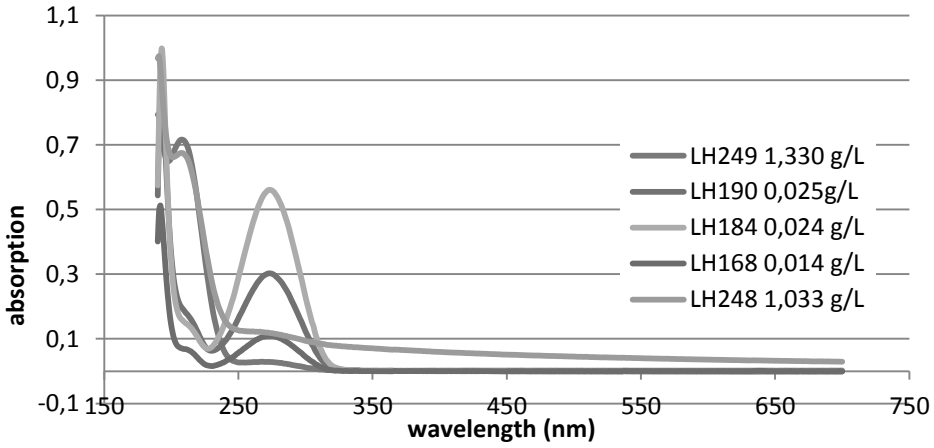

Figure 53: UV/Vis spectra of isosorbide resins (used in 1A) in MeCN

The former displayed the strongest peak around 266 – 275 nm, which presumably corresponds to the ester groups. While the latter also displayed this peak, a much stronger, unidentified peak at 208 nm was also observed.

The absorption coefficients for the two peaks can be calculated using either the number average molecular weight (M_n) or the weight average molecular weight (M_w). The results of both calculations for the different peaks are tabulated below.

Table 24: Absorption coefficients of isosorbide resins

	LH249	**LH190**	**LH184**	**LH168**	**LH248**
λ	*208*	-	-	-	*208*
ε_{Mw}	0,016777	-	-	-	0,010747
ε_{Mn}	0,002020	-	-	-	0,002025
λ	*268*	*273*	*274*	*275*	*266*
ε_{Mw}	0,000682	0,486457	0,696478	0,187666	0,001948
ε_{Mn}	0,000082	0,039983	0,084707	0,025381	0,000367

As the weight average molecular weights were generally significantly higher for the isosorbide containing resins, the absorption coefficients calculated using the concentration derived from them are naturally also higher.

Contrary to the isosorbide resins, the phthalic anhydride resins (used in 1B) all behaved in a similar manner, showing three peaks that mirror the peaks of the phthalic anhydride monomer.

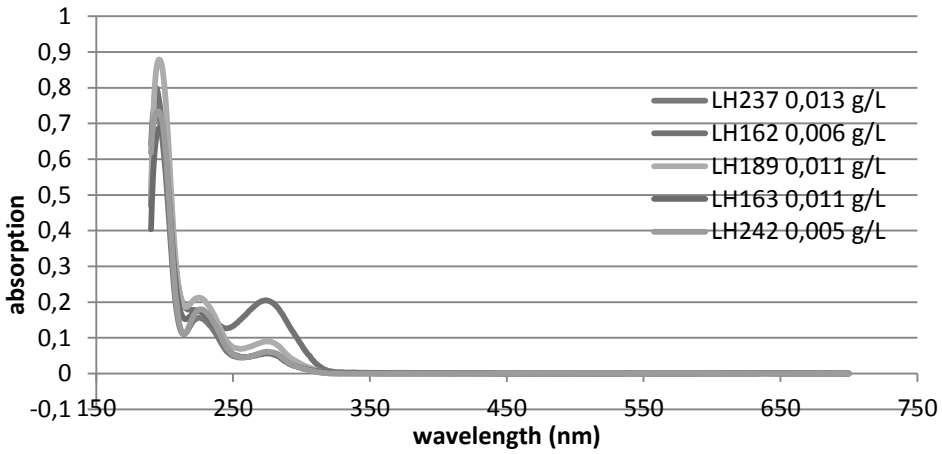

Figure 54: UV/Vis spectra of phthalic anhydride resins in MeCN

Two peaks probably corresponding to the $^{1}(\pi\text{-}\pi^*)$ and $^{3}(\pi\text{-}\pi^*)$ transitions of the aromatic ring were observed between 193 nm and 196 nm and 273 nm and 275 nm, and a peak corresponding to the ester group was observed in between them at 219 nm to 226 nm. The absorption coefficients calculated using M_w and M_n are shown below. As observed in the phthalic anhydride monomer, the strongest peak corresponds to the lowest wavelength. With the exception of the resin LH162, the peak with the highest wavelength also corresponds to the lowest absorption coefficient.

Table 25: Absorption coefficients of phthalic anhydride resins

	LH237	LH162	LH189	LH163	LH242
λ	*193*	*194*	*196*	*196*	*195*
ε_{Mw}	1,1911	2,4290	1,1879	0,5999	0,8426
ε_{Mn}	0,2102	0,4788	0,2579	0,1705	0,2854
λ	*225*	*219*	*225*	*224,5*	*226*
ε_{Mw}	0,2486	0,5435	0,2871	0,1518	0,2071
ε_{Mn}	0,0439	0,1071	0,0623	0,0431	0,0702
λ	*275*	*274*	*274*	*273*	*275*
ε_{Mw}	0,0941	0,6237	0,1225	0,0492	0,0705
ε_{Mn}	0,0166	0,1229	0,0266	0,0140	0,0239

The absorption coefficients of the peak corresponding to the ester group are on a similar scale for the resins containing isosorbide and for those containing phthalic anhydride. As shown below, no dependence on the quantity of either monomer present in the formulation could be determined.

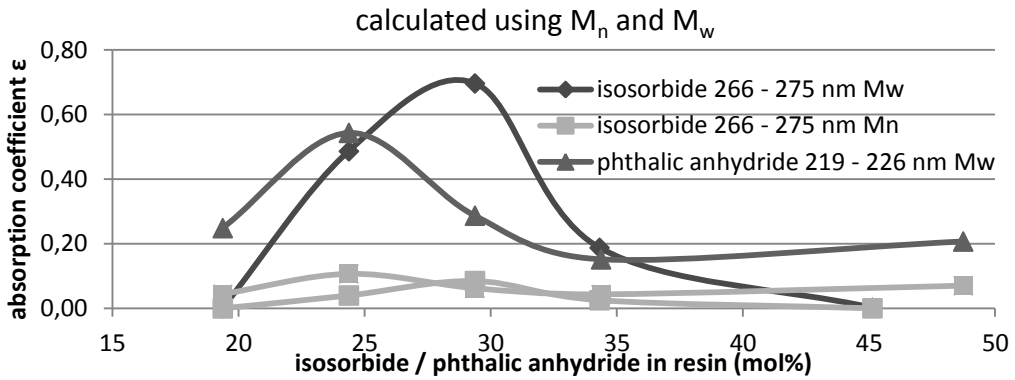

Figure 55: Absorption coefficients *vs.* isosorbide and phthalic anhydride contents

Therefore, the main factor differentiating phthalic anhydride resins from isosorbide resins in terms of UV absorption are the additional peaks, particularly that around 195 nm, which absorbs considerably stronger than that all other peaks.

The lack of dependence of the absorption of the ester group on the quantity of phthalic anhydride or isosorbide is not very surprising, since the overall quantity of ester links was not changed from one resin to another. However, no dependence of the absorption coefficients that correspond specifically to the aromatic ring was detected either.

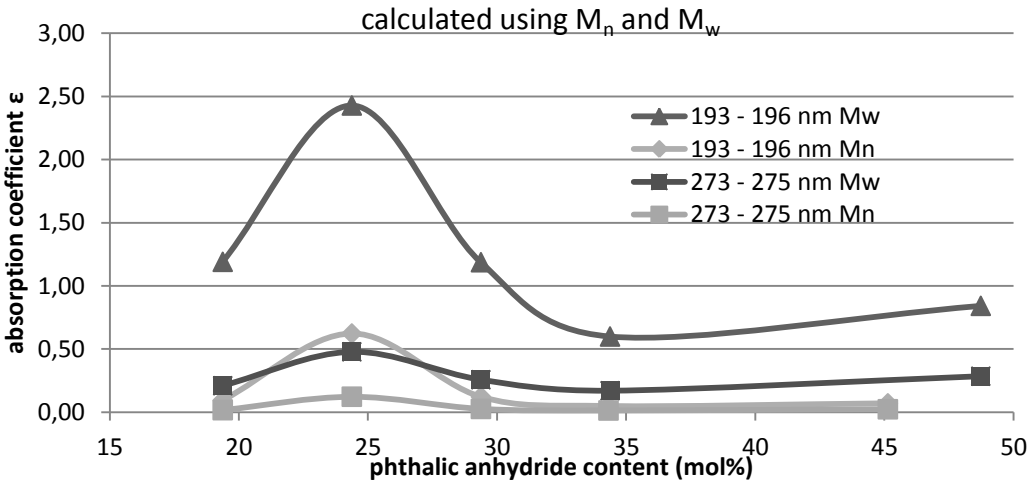

Figure 56: Aromatic UV absorption *vs.* phthalic anhydride content

It is possible that the UV absorption of the resins will differ fundamentally in the coatings. Reasons could include the absence of acetonitrile, the loss of mobility and of course the crosslinking with melamine, which, notably, is also likely to absorb UV light to an extent due to the presence of nitrogen and its aromaticity.

However, from the spectrum of absorption shown in acetonitrile, it seems that only small differences exist between the isosorbide and the phthalic anhydride resins. The amount of phthalic anhydride does not seem to impact significantly on the absorption coefficient, and the aromatic peak which absorbs considerably stronger than any present in isosorbide is located below 200 nm. Sunlight of that wavelength will most likely be absorbed in the atmosphere before reaching the coating, and is therefore unlikely to affect the coating weatherability.

It seems on the other hand more likely that the ester group is the most important source of UV absorption in the relevant region. Since it is equally present in both resins, the result of the investigation suggests that UV light is not a factor that negatively affects phthalic anhydride resins compared to isosorbide resins.

Effect of other monomers on the UV spectrum

The spectra taken of the phthalic anhydride based resins LH174, LH177, LH181, LH182 and LH219 (used in 1C), in which the effects of succinic acid, sebacic acid, 1,2-propanediol, 1,3-propanediol and glycerol on the resin properties were testes respectively, unsurprisingly resembled the spectrum of the phthalic anhydride resins described above.

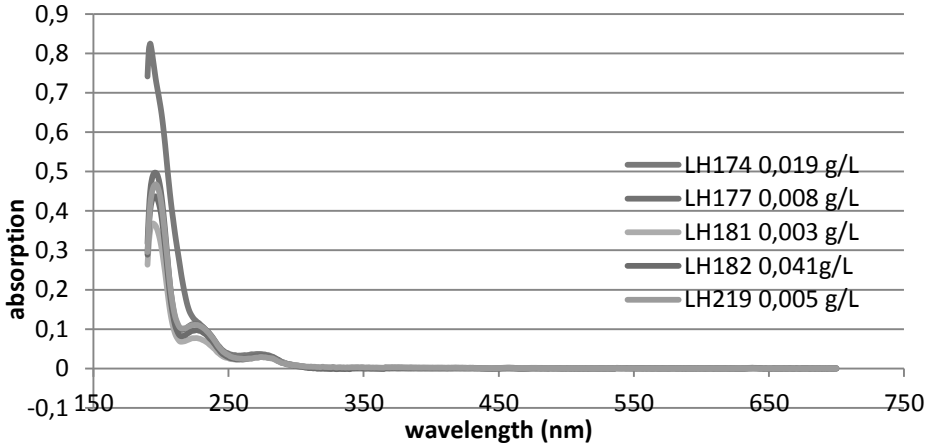

Figure 57: UV/Vis spectrum of resins in which the quantities of other monomers were varied in MeCN

The same three peaks can be observed in each resin. Their absorption coefficients are presented below. The highest absorption in all three peaks was observed in the resin LH181 containing an increased amount of 1,3-propanediol. The lowest absorption was observed in the resin LH182, containing increased amounts of 1,2-propanediol. Compared to the phthalic anhydride series described above, the absorption coefficients for each peak were small, particularly when calculated using the number average molecular weights.

Table 26: UV absorption coefficients of resins in which the effect of other monomers were tested

	LH174	**LH177**	**LH181**	**LH182**
λ	192	196	194	196
ε_{Mw}	0,5209	1,0630	1,4421	0,2627
ε_{Mn}	0,000329	0,002274	0,005648	0,000158
λ	-	226	226	226,5
ε_{Mw}	-	0,2413	0,3028	0,0584
ε_{Mn}	-	0,0005162	0,0011858	0,0000351
λ	272	275	277	274
ε_{Mw}	0,02350	0,07316	0,11202	0,01858
ε_{Mn}	0,0000148	0,0001565	0,0004387	0,0000112

Comparison of the UV spectrum of the resin before and after curing

Not many similarities are obvious when comparing the spectra obtained in solution and that the coating. The ester group peak is present in both spectra, but the spectrum in solution is much more detailed, and most of the peaks observed lie outside of the range that was measured for the coating.

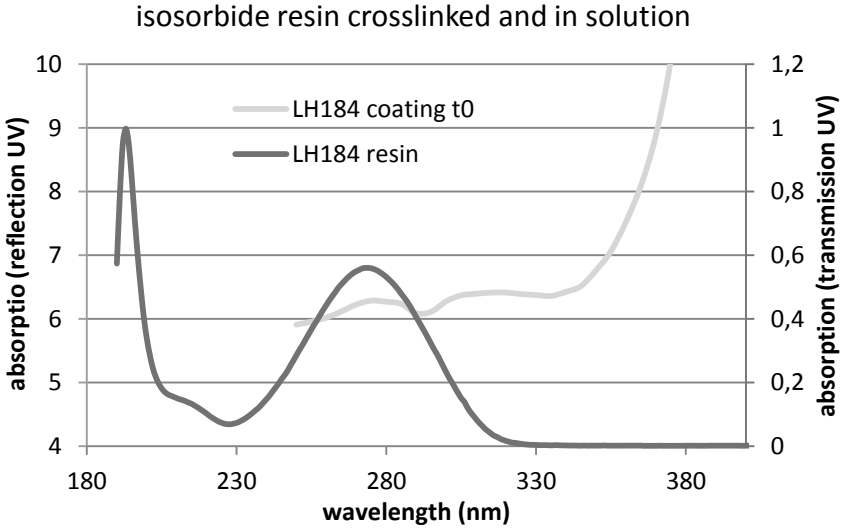

Figure 58: UV spectrum comparison before and after crosslinking

LV. Normalisation of IR spectra

Normalisation methods between different spectra

In order to quantitatively compare the intensity of absorption of each functional group between separate spectra, normalisation of the amount of coating examined is necessary. Since the measurement is done on coating which is fixed to a steel panel, weighing of the substrate is not possible. Instead, a peak which is assumed to be constant between different types of coatings and despite the exposure can be used as a reference.

While there is no peak which can be assumed not to change with certainty, there are two different ways in which the problem has been handled in the literature. Both were evaluated in this work.

The first possibility is to use the carbonyl peak as a point of normalisation. It can be assumed to stay constant even when ester bonds are broken, and it is in the same position for all coatings. The quantity of carbonyls would however change if small molecules such as formaldehyde are formed and escape as gas, or if larger molecules are eroded with humidity such as it was observed in the case of isosorbide containing coatings.

The main issue with the carbonyl peak is however the relatively large distance to the other peaks examined. As the penetration depth of the infrared radiation changes depends on the wavelength, so does the amount of coating examined. Therefore, we can assume that the similarity between the regions in the coating examined decreases with larger distances between two peaks.

This issue is addressed in the second normalisation method, in which the C-H bond is used as a reference. The stretching vibration around 2900 cm^{-1} is used to normalise the NHOH peak, while the bending vibration in the fingerprint region is used to normalise the melamine and methoxy group

peaks. Thus, the distance between the peaks in question and the reference used for normalisation is considerably reduced.

However, the constant presence of the CH related absorptions is more doubtful than that of the carbonyl group, as several degradation mechanisms involving the abstraction of hydrogen and the formation of new carbon-carbon bond crosslinks could potentially change the size of this peak.

The shape of the peaks upon exposure as well as the relative absorption of the CH bond compared to the carbonyl bonds were used to assess the suitability of each normalisation method.

Development of the carbonyl and CH-peak shapes upon exposure
Comparing the spectra of the standard resin taken after 500 – 2000 h of exposure with that taken before weathering, the shape of the CH peak stayed exactly the same, as shown below.

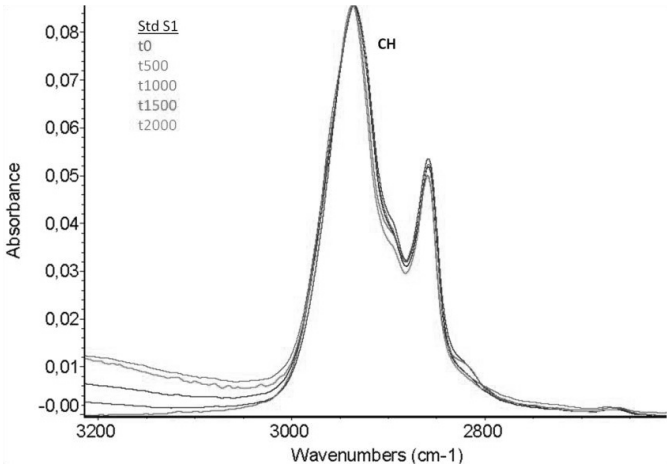

Figure 59: CH peak shape of the standard coating over time

This observation was however not confirmed in the spectra of the coatings containing isosorbide. The shape change for the coating containing the resin LH184 upon exposure are presented below, and clearly show the appearance of a new peak to the left of the original peak after 1500 h and 2000 h of exposure. Furthermore, what starts out as two separate peaks in the beginning becomes increasingly blurred. The same trend was also observed in the coatings containing the other isosorbide resins, LH190 and LH168.

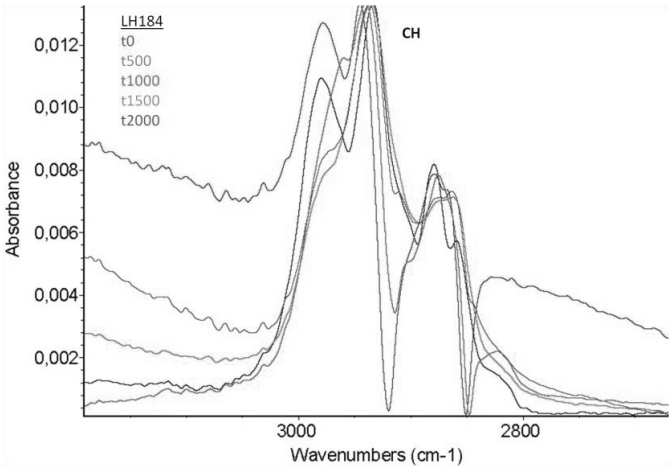

Figure 60: CH peak shape over time in an isosorbide coating

The CH peaks of the coatings containing phthalic anhydride, here exemplified by the coatings containing the resins LH189 and LH174, were less stable than those of the standard coating, but more consistent than those of the coatings containing isosorbide resins. While the CH peak of the coating containing LH189 seems to change its composition slightly over time, that of the coating containing LH174 remains largely the same.

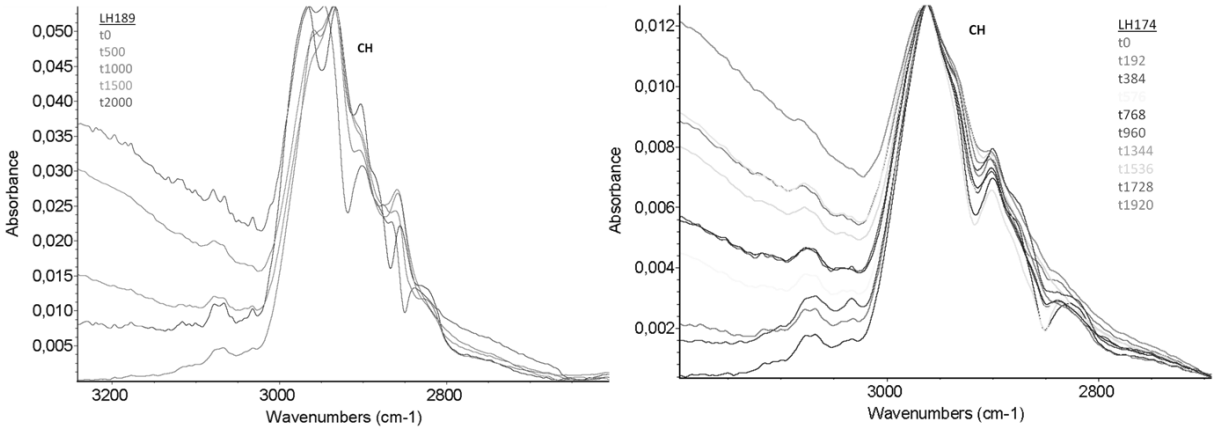

Figure 61: CH peak shapes over time of the coatings containing the resins LH189 (left) and LH174 (right)

Overall, the CH stretching vibration can be influenced by weathering, but this mostly occurs in coatings containing isosorbide. On the other hand, the peak in the fingerprint region corresponding to the CH bending vibration was not stable in any of the coatings examined.

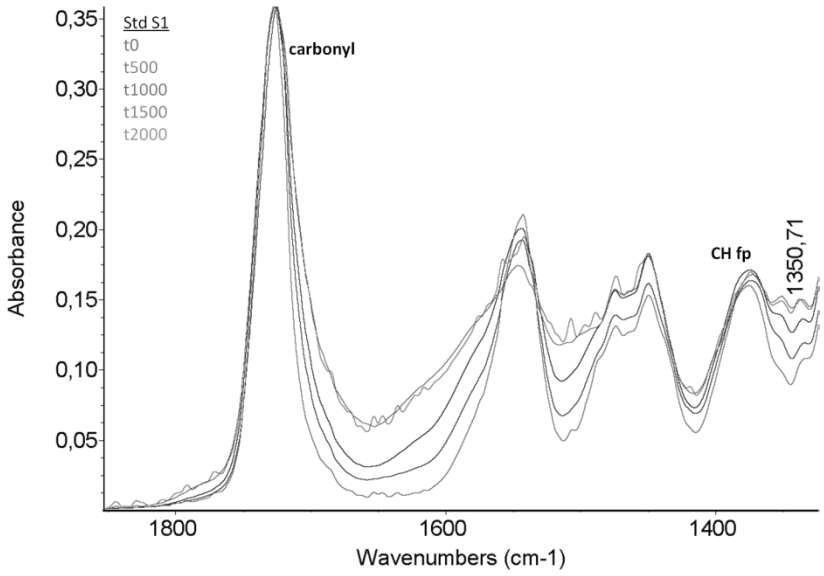

Figure 62: Fingerprint region of the standard coating over time

A new peak around 1350 cm^{-1} was observed to emerge with increasing exposure in all of the coatings examined. As this peak overlaps strongly with the CH fingerprint region peak, it is not possible to separately integrate both, making the CHfp peak unsuitable as a reference.

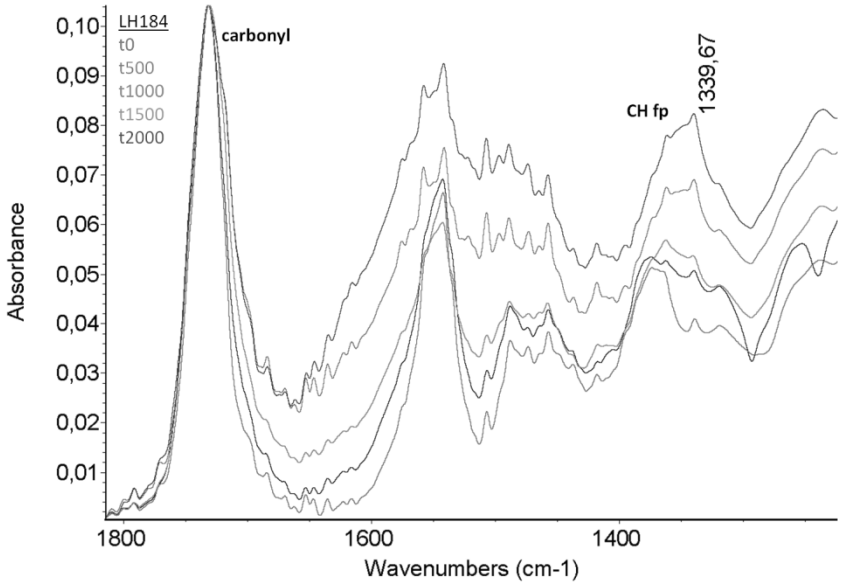

Figure 63: Fingerprint region of the isosorbide coating containing LH184 over time

The carbonyl peak can be observed to broaden to the lower wavenumber region upon ageing. Other than that, its shape and position remains constant in the different spectra measured. This and the fact that the carbonyl peak, contrary to the CH fingerprint peak, is common in position to all coatings containing different monomers, suggests that it is a better reference at least for the assessment of the fingerprint region absorptions.

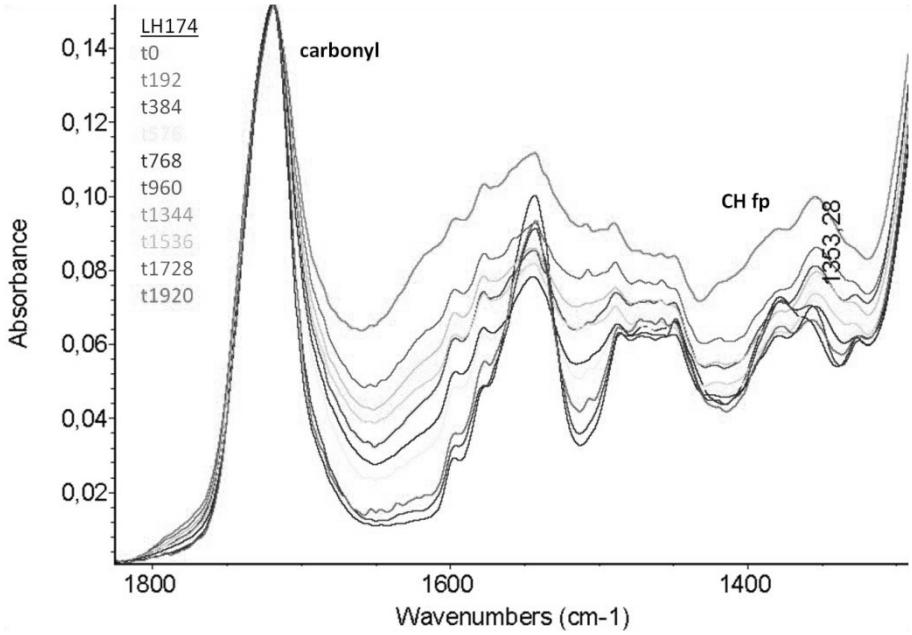

Figure 64: Fingerprint region of the coating based on the phthalic anhydride resin LH174

CH and CHfp peak size with respect to carbonyl

The observations concerning the shape of the CH related peaks are confirmed when the size of the CH peaks is compared over time. The graphs below show the development of the area of the CH fingerprint peak of coatings containing isosorbide (1A) and coatings with different alcohols based on phthalic anhydride (1C) over time when normalised using the carbonyl peak.

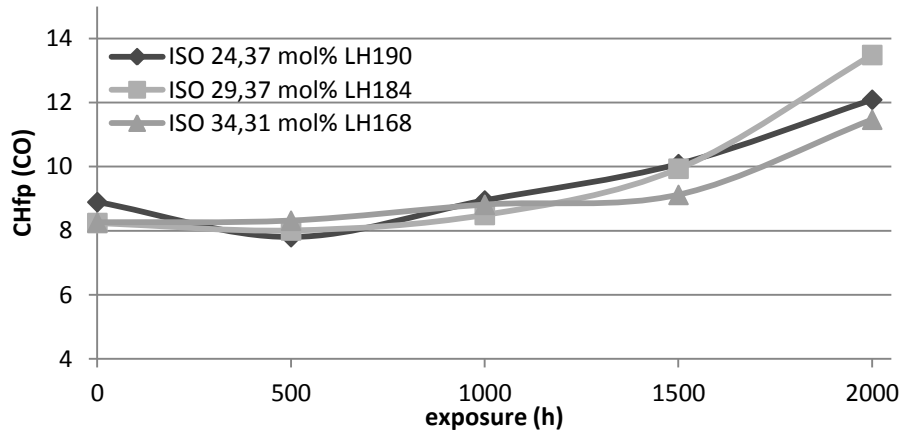

Figure 65: CH fingerprint peak size of isosorbide coatings over time normalised with the carbonyl peak

A clear increase of the peak size with respect to the carbonyl peak size can be observed upon exposure. The same observation was made for other coatings based on phthalic anhydride, and for the Arkema resin based coatings.

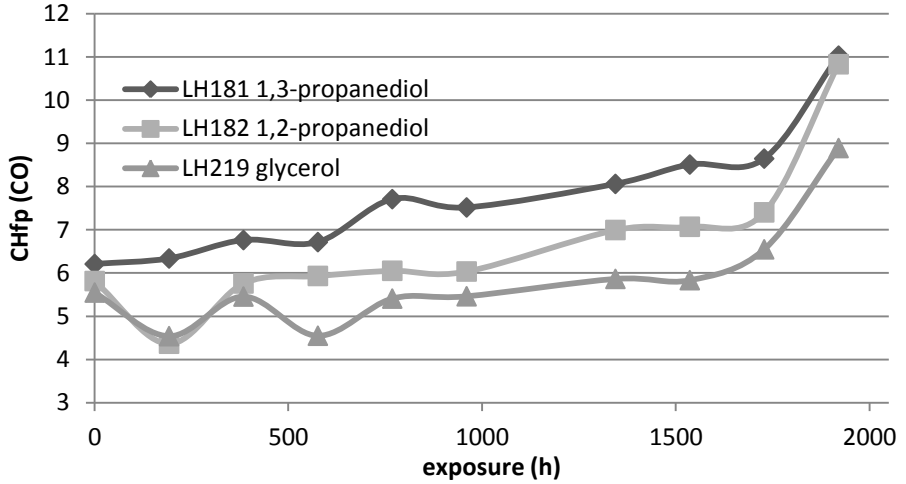

Figure 66: CHfp peak size normalised with the carbonyl peak for coatings containing different alcohols over time

Due to the observations made concerning the peak shape, it seems more likely that the increase in CH fingerprint peak area is due to the extra peak appearing beside it rather than to a decrease of the area of the carbonyl peak.

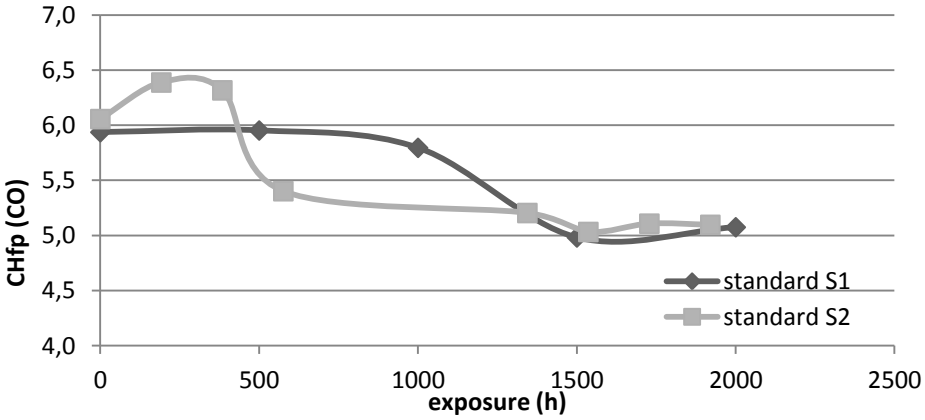

Figure 67: CH fingerprint normalised with carbonyl of the standard coatings over time

Interestingly, a decrease in peak size was observed for the corresponding peak in the standard coating, even though the additional peak around 1350 cm^{-1} was also observed. This could indicate that the broadening of the carbonyl peak leads to a slight decrease in peak size, which is compensated for in the other cases by the larger increase in CHfp peak size.

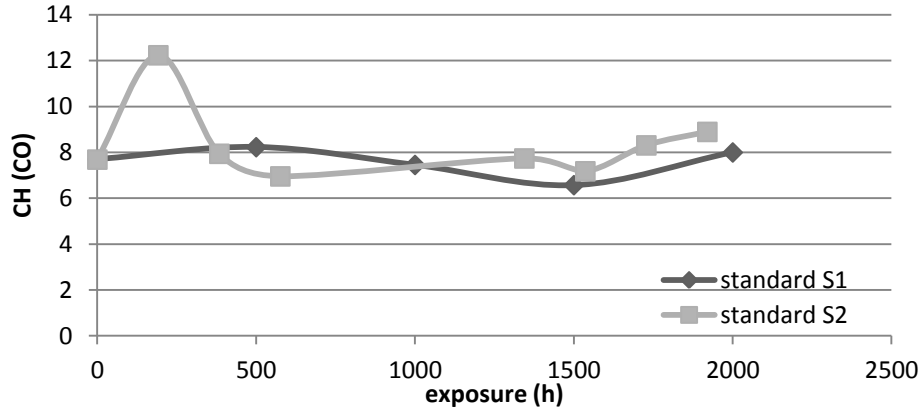

Figure 68: CH peak of the standard coatings normalised with the carbonyl peak over time

The development of the area of the other CH peak was a little less clear. While it stays constant with respect to the carbonyl peak for the standard coating in agreement with the lack in change of its shape, relatively large change is observed for the isosorbide and phthalic anhydride containing coatings in the first series.

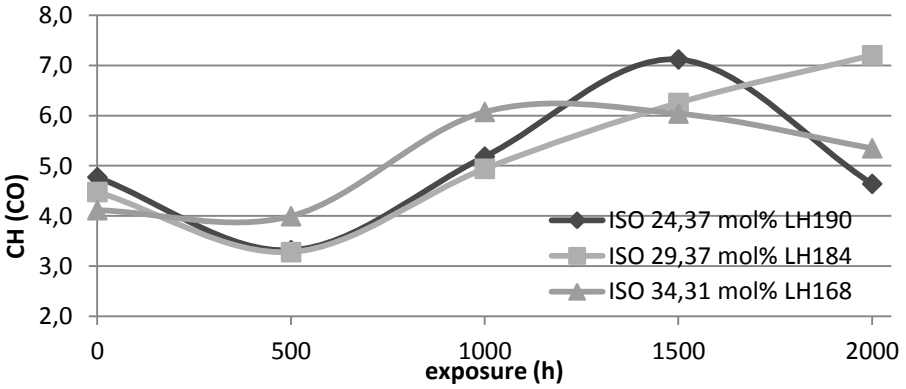

Figure 69: CH peak normalised with carbonyl over time for isosorbide containing coatings (1A)

The up and down shown by the curves may be due to the poor quality of the spectra, especially towards the longer exposure times. Overall, an increase in CH area is observed in most resins after 2000 h of exposure, but no clear trend can be distinguished from the curves.

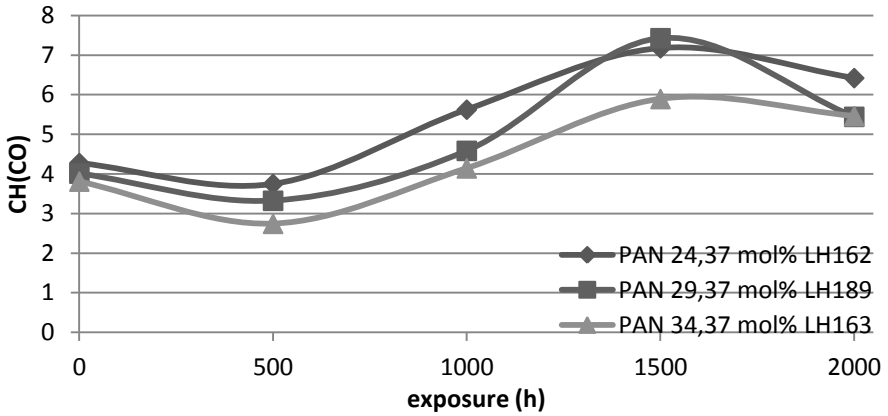

Figure 70: CH peak normalised with carbonyl over time for phthalic anhydride containing coatings of series 1 (1B)

Nevertheless, the change in area suggests that the use of the peak as a reference may obscure the development in the size of other absorptions.

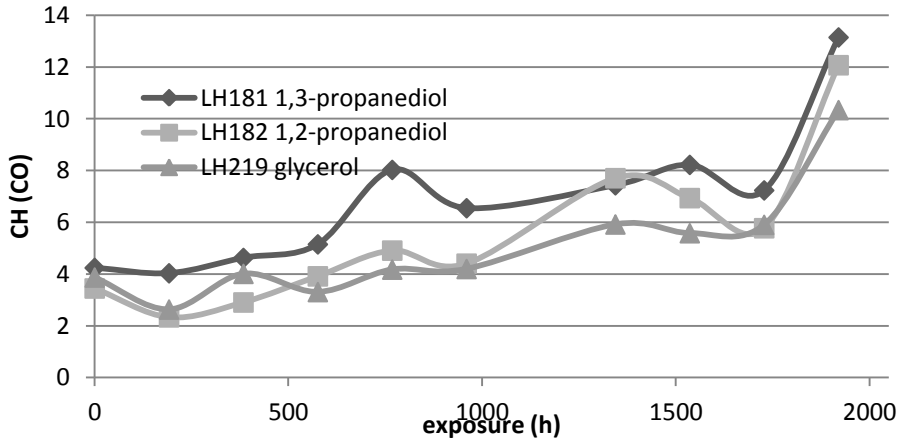

Figure 71: CH peak normalised with carbonyl for coatings containing different alcohol monomers over time (1C)

The development of the CH peak for phthalic anhydride containing coatings observed in the second series displayed a more obvious trend. As for the CH peak in the fingerprint region, a steady increase was measured with longer exposure times. Above, the development is shown for the coatings containing different alcohol monomers, but the same trend was observed for the coatings containing different diacids and for the high T_g prototypes.

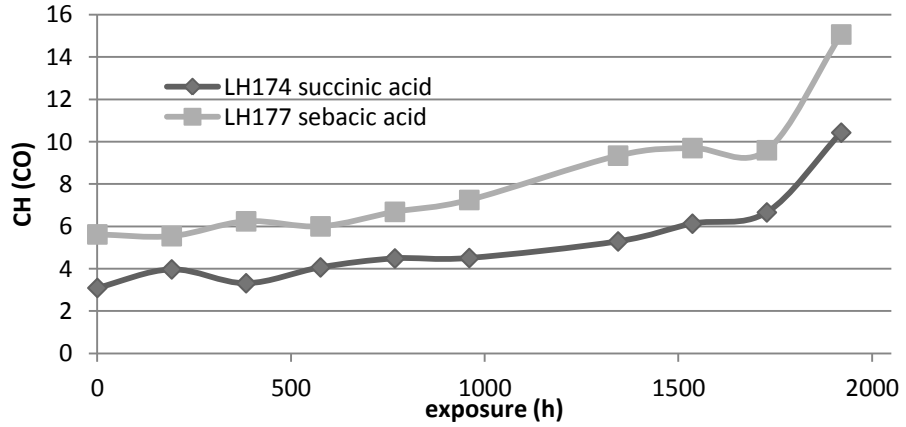

Figure 72: CH peak normalised with carbonyl for coatings containing different linear diacids over time (1C)

This suggests that even in cases such as that of the coating containing the resin LH174, where the shape of the CH peak stayed constant upon exposure, it might not be a suitable reference for the normalisation of other peaks.

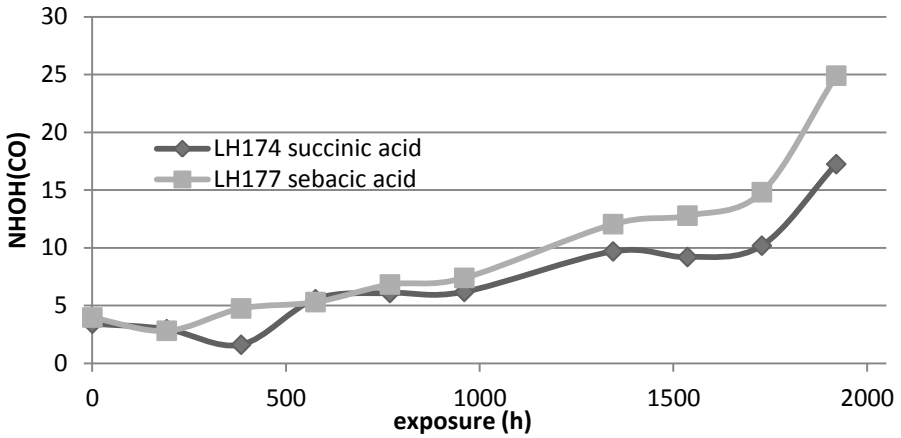

Figure 73: NHOH peak development normalised by the carbonyl peak for coatings containing different diacids (1C)

Therefore, it was decided to use the carbonyl peak as a standard for the normalisation of the coating IR spectra. In all cases, the carbonyl peak was set to an absorption of 10, and all other peaks were adjusted accordingly. This decision was validated for example by the absorptions calculated for the NHOH absorption of the coatings containing the resins LH174 and LH177 with succinic and sebacic acid respectively.

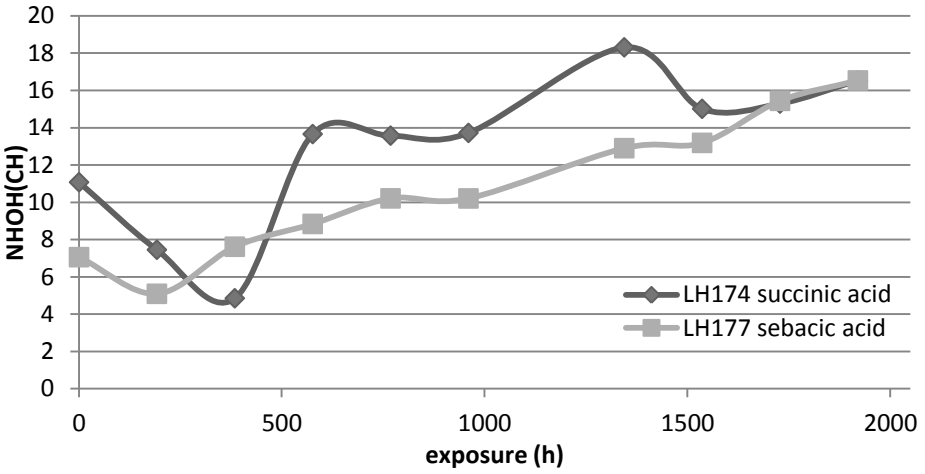

Figure 74: NHOH absorption of coatings containing different diacids normalised using the CH peak (1C)

The data normalised using the carbonyl peak not only showed a more consistent trend than that normalised using the CH peak, but also showed more degradation in the coating containing sebacic acid. In contrast to the result obtained with CH normalisation, this is in agreement with the result of the gloss retention measurements.

LVI. Details of IR treatments

The exact wavenumbers used for the analysis and interpretation of the IR spectra are detailed below for each type of coating.

Table 27: Baseline and integration limits used for the different types of coatings

	coating type	baseline		integration	
		start	end	start	end
Absorption		**cm^{-1}**	**cm^{-1}**	**cm^{-1}**	**cm^{-1}**
CH + NHOH	all	2400	3950	2400	3730
CH	all	2400	3950	2680	3130
carbonyl	all	1660	1800	1680	1780
melamine	all	825	1800	1510	1625
CH fingerprint	isosorbide	825	1800	1290	1425
CH fingerprint	phthalic anhydride	825	1800	1315	1415
CH fingerprint	standard	825	1800	1345	1415
OMe	isosorbide	825	1800	895	930
OMe	standard and phthalic anhydride	825	1800	890	930

LVII. Representation of the IR data

Presentation of the IR data

Several different approaches to the presentation of the data obtained from the analysis of the infrared spectra are reported in the literature. In some cases, for example by Zhang *et al.*, the normalised absorption value is simply reported as its absolute value.[115] In other cases, such as presented by Batista *et al.*, the absorption value is reported relative to the value obtained before weathering.[116] Another possibility, exemplified by Zhang *et al.*, is to plot the absolute difference measured in absorption values before and after weathering as a percentage of the original absorption.[103]

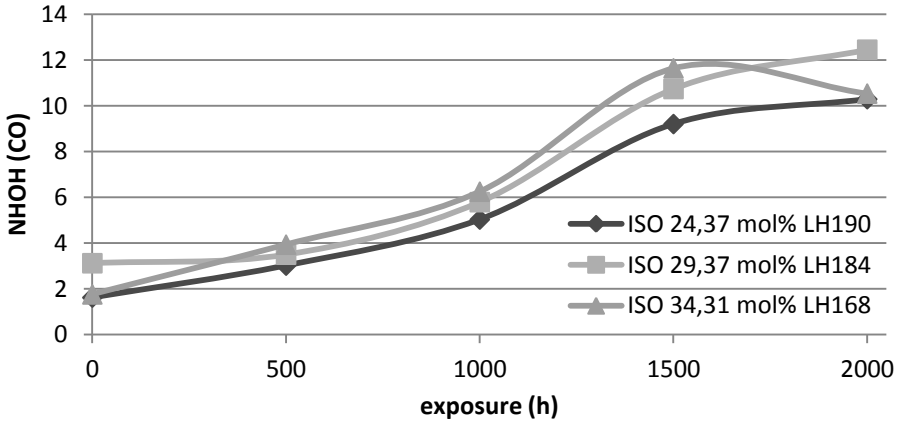

Figure 75: NHOH peak of isosorbide coatings absolute values (1A)

The different options for presentation are shown below on the example of the NHOH absorption of the three isosorbide containing coatings. The absolute values after normalisation using the carbonyl peak are shown above for comparison.

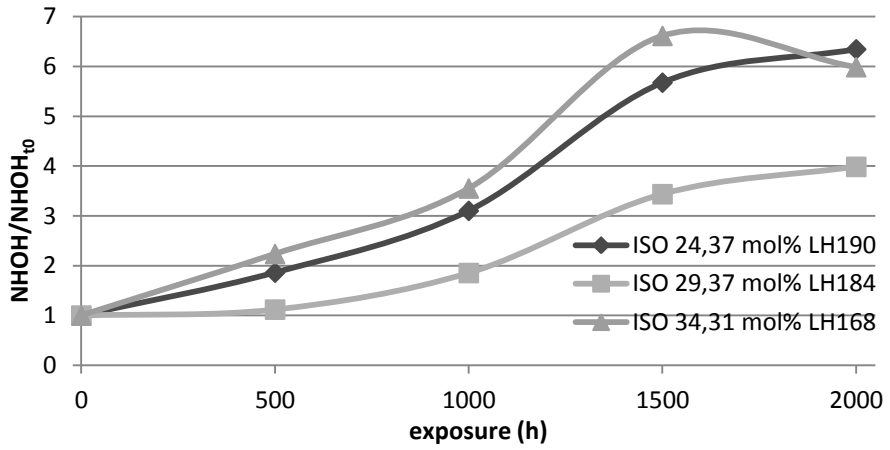

Figure 76: NHOH/NHOHt_0 peak divided by the value at t_0 of isosorbide coatings (1A)

The first example shows the absorption as a percentage of the absorption recorded before weathering. This treatment considerably changes the ranking of the three coatings. While their absolute values are quite close, suggesting similar degradation behaviour, the relative degradation of the coating containing the resin LH184 is much lower than that of the two others. This is due to the fact that the absorption of 3,1 measured before weathering was almost twice as high as those measured for the coatings LH190 and LH168, which were 1,6 and 1,8 respectively, as shown in the first figure in this section above.

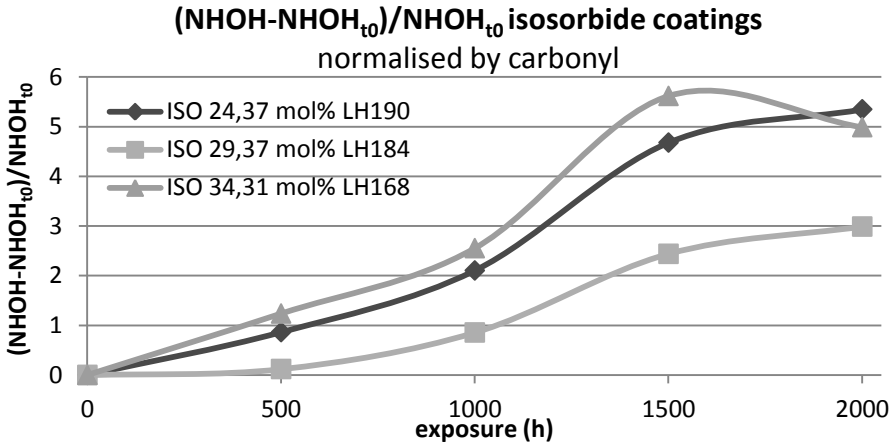

Figure 77: NHOH peak percentage increase of isosorbide coatings (1A)

The same effect is observed when the percentage increase, i.e. the difference in absorption compared to the measurement before weathering relative to the measurement before weathering, is plotted. While it is important to reflect the difference in absorption before the exposure was started, it was decided that this presentation of the data does not accurately reflect the performance of each coating. A further concern was the possible error in the value measured for t0, which could vastly impact the display of the entire progress if each value is divided by it.

LVIII. Original IR data

Below, the absorptions measured for the different peaks before any calculation or normalisation are tabulated.

Series 1 – ATR – no HALS

Standard S1						
time	**total**	**CH**	**carbonyl**	**CH fingerprint**	**melamine**	**OMe**
0	9,4084	8,2931	10,7670	6,3930	8,0700	3,2200
500	7,3435	5,5301	6,7190	4,0000	5,3250	2,0110
1000	6,6904	4,4302	5,9420	3,4440	5,3190	1,6030
1500	7,4253	3,9192	5,9610	2,9700	5,5030	1,2150
2000	6,2998	3,7286	4,6600	2,3650	4,2800	0,9430

Arkema						
time	**total**	**CH**	**carbonyl**	**CH fingerprint**	**melamine**	**OMe**
0	4,6218	3,4356	6,5450	5,8620	3,5600	1,4580
500	3,7203	2,4472	4,3970	3,8320	2,6070	0,8550
1000	6,0716	3,2118	5,5360	5,1330	3,9790	0,9490
1500	11,8307	5,0679	7,9640	8,4440	8,1160	1,0670
2000	3,1286	1,2231	2,0958	2,5704	2,8556	0,3050

LH190						
time	**total**	**CH**	**carbonyl**	**CH fingerprint**	**melamine**	**OMe**
0	5,5610	4,1512	8,6960	7,7360	4,5810	1,8090
500	3,5896	1,8805	5,6630	4,4190	3,3880	1,0210
1000	6,6347	3,3672	6,4960	5,8120	4,5040	0,9570
1500	3,3776	1,4730	2,0693	2,0865	2,1830	0,2141
2000	3,4599	1,0753	2,3173	2,8022	3,3666	0,2313

LH184						
time	**total**	**CH**	**carbonyl**	**CH fingerprint**	**melamine**	**OMe**
0	2,6843	1,5815	3,5310	2,9110	1,8090	0,7020
500	1,9035	0,9215	2,8086	2,2504	1,7578	0,5136
1000	2,6895	1,2381	2,5060	2,1293	1,8274	0,3495
1500	6,7389	2,4800	3,9670	3,9430	4,4260	0,4200
2000	2,3486	0,8606	1,1950	1,6120	1,9361	0,1335

LH168						
time	**total**	**CH**	**carbonyl**	**CH fingerprint**	**melamine**	**OMe**
0	3,6138	2,5317	6,1510	5,0820	3,2560	1,3210
500	4,7371	2,3874	5,9730	4,9670	3,8810	1,1830
1000	6,0858	2,9996	4,9390	4,3530	3,8000	0,7610
1500	5,4870	1,8749	3,1033	2,8310	3,3860	0,3410
2000	2,7627	0,9304	1,7393	1,9949	2,4808	0,2367

LH162						
time	**total**	**CH**	**carbonyl**	**CH fingerprint**	**melamine**	**OMe**
0	7,8662	6,2414	14,5930	9,0730	9,0090	3,4420
500	8,3415	4,5315	12,0880	7,8390	9,1060	2,6680
1000	9,8474	4,7849	8,5080	5,8370	7,5470	1,5780
1500	18,8563	7,9028	11,0140	8,8010	13,4880	1,4240
2000	5,8647	2,0702	3,2237	2,7494	4,9928	0,3183

LH189						
time	**total**	**CH**	**carbonyl**	**CH fingerprint**	**melamine**	**OMe**
0	8,3207	6,6551	16,5940	9,4600	9,7940	3,8480
500	5,1530	2,6535	7,9810	4,9430	6,3050	2,0560
1000	6,9209	3,3684	7,3470	4,4600	6,0400	1,4580
1500	11,5590	4,8960	6,5900	4,8320	7,9180	0,9500
2000	5,8943	2,1666	3,9800	2,7480	5,0820	0,4810

LH163						
time	**total**	**CH**	**carbonyl**	**CH fingerprint**	**melamine**	**OMe**
0	7,3342	5,6038	14,7150	8,2040	9,0960	3,6910
500	4,8524	2,2402	8,1680	4,6740	6,4900	2,0810
1000	5,0998	2,2862	5,5200	3,1890	4,8960	1,1250
1500	6,6490	2,4953	4,2340	2,8170	5,1670	0,6830
2000	3,7220	1,3190	2,4154	1,5187	3,1802	0,3680

Series 2 – ATR – no HALS

Standard S2						
time	**total**	**CH**	**carbonyl**	**CH fingerprint**	**melamine**	**OMe**
0	8,5581	6,7454	8,7720	5,3130	7,4570	2,5470
192	4,5533	3,2261	2,6362	1,6842	2,3103	0,8615
384	7,0537	6,0847	7,6610	4,8400	6,3390	2,5040
576	3,0734	2,0986	3,0162	1,6295	2,5170	0,9066
1344	9,1946	5,2464	6,7790	3,5280	6,1020	1,3910
1536	7,7741	4,5495	6,3370	3,1890	5,6380	1,2470
1728	10,3251	5,6061	6,7470	3,4460	6,2430	1,2650
1920	6,6842	3,2627	3,6670	1,8690	3,4750	0,7120

Arkema S2						
time	**total**	**CH**	**carbonyl**	**CH fingerprint**	**melamine**	**OMe**
0	12,8821	7,3904	13,2290	12,9410	9,4960	1,8940
192	4,0299	2,6161	2,8439	2,5810	1,7760	0,5560
384	9,8007	5,3666	9,3490	9,0650	6,8820	1,4330
576	11,5482	6,2877	10,6200	10,4040	8,0770	1,6000
960	5,8804	2,7288	3,0294	3,5750	3,4900	0,4340
1344	6,9814	2,9700	4,5580	5,1030	4,8160	0,6400
1536	5,7425	2,5298	3,2727	4,0830	4,1450	0,4710
1728	5,3729	2,2879	2,6959	3,6660	3,9380	0,3860
1920	6,5827	2,4807	2,1918	3,8730	4,3550	0,3680

LH174						
time	**total**	**CH**	**carbonyl**	**CH fingerprint**	**melamine**	**OMe**
0	3,7060	1,7586	5,6840	3,4280	4,3290	1,2740
192	3,3971	1,9468	4,9050	2,8860	3,2810	1,4700
384	2,4322	1,6380	4,9410	3,2620	3,5370	1,2650
576	7,9642	3,3667	8,2840	5,2080	6,9990	1,6510
768	10,8775	4,6148	10,2860	6,6530	9,4600	1,7130
960	3,1931	1,3463	2,9872	1,8074	2,8232	0,5177
1344	11,5872	4,0934	7,7370	5,3440	8,6020	1,0530
1536	7,6891	3,0744	5,0170	3,4590	5,7830	0,6750
1728	7,0845	2,8012	4,2060	2,9890	5,2470	0,5070
1920	6,9887	2,6338	2,5254	2,5486	4,4628	0,2589

LH177						
time	**total**	**CH**	**carbonyl**	**CH fingerprint**	**melamine**	**OMe**
0	14,6256	8,5766	15,2540	9,8410	13,1450	2,4860
192	6,7907	4,5011	8,1260	5,4990	6,6160	2,1950
384	16,7548	9,5130	15,2410	10,3810	13,4680	2,8330
576	17,0062	9,0293	15,0430	9,9560	13,7370	2,4310
768	14,5399	7,1956	10,7580	7,6220	11,1120	1,7190
960	12,4110	6,1433	8,4750	6,2080	9,5480	1,3250
1344	12,6434	5,5216	5,9100	5,0980	8,3800	0,8570
1536	7,2498	3,1274	3,2239	2,9282	4,9718	0,3955
1728	6,0309	2,3708	2,4700	2,3486	4,1864	0,2452
1920	7,9563	2,9989	1,9903	2,5767	4,6428	0,0927

LH181						
time	**total**	**CH**	**carbonyl**	**CH fingerprint**	**melamine**	**OMe**
0	11,9850	7,1194	16,7890	10,4230	12,7130	3,4900
192	6,6387	4,1795	10,3670	6,5690	7,5440	2,8630
384	7,9400	4,4898	9,7070	6,5640	8,0460	2,2930
576	14,5948	7,3053	14,1860	9,5260	12,6810	2,7840
768	7,7957	3,8993	4,8580	3,7450	5,3720	1,0280
960	15,5203	7,0600	10,7850	8,1070	12,0340	1,9230
1344	13,4290	5,5633	7,4850	6,0340	9,4660	1,2760
1536	10,7248	4,4858	5,4570	4,6440	7,5930	0,8650
1728	5,8564	2,1638	2,9911	2,5863	4,5476	0,3809
1920	18,5836	6,1564	4,6830	5,1650	9,1120	0,4220

LH182						
time	**total**	**CH**	**carbonyl**	**CH fingerprint**	**melamine**	**OMe**
0	4,5371	2,6557	7,7080	4,4820	5,4290	1,5270
192	1,2436	0,5724	2,4570	1,0724	1,0889	0,9774
384	3,2285	1,7967	6,1870	3,5630	4,2980	1,3340
576	7,5890	3,8018	9,7130	5,7620	7,5670	1,6180
768	7,1114	3,5518	7,2370	4,3800	6,1190	1,0940
960	4,5487	2,0220	4,5930	2,7720	4,2480	0,6450
1344	6,0202	2,5103	3,2573	2,2785	3,7777	0,3840
1536	4,6119	1,9148	2,7605	1,9517	3,4257	0,2983
1728	3,4674	1,1664	2,0201	1,4956	2,8751	0,1836
1920	6,6159	2,3849	1,9754	2,1395	3,8483	0,1605

LH219						
time	**total**	**CH**	**carbonyl**	**CH fingerprint**	**melamine**	**OMe**
0	6,7783	4,2995	11,1140	6,1670	6,9470	2,2810
192	3,0741	1,6579	6,3000	2,8600	3,1350	2,0150
384	6,8014	4,0783	10,1700	5,5490	6,4740	2,0300
576	1,8528	0,7033	2,1270	0,9676	1,5039	0,4487
768	5,9548	2,9953	7,1760	3,8810	5,1860	1,2640
960	5,1852	2,4099	5,7410	3,1360	4,4950	1,0110
1344	6,8094	2,9912	5,0540	2,9640	4,4700	0,7810
1536	4,6968	2,0795	3,7260	2,1740	3,5120	0,5720
1728	4,7318	1,8140	3,0724	2,0119	3,4366	0,4538
1920	6,1237	2,3932	2,3150	2,0585	3,5174	0,3236

LH192						
time	**total**	**CH**	**carbonyl**	**CH fingerprint**	**melamine**	**OMe**
0	3,0555	1,5453	5,3350	2,9410	3,5270	1,0150
192	2,4684	0,9758	3,7868	1,4755	1,5640	1,4018
384	4,3602	2,2877	7,9960	4,5020	5,2630	1,5200
576	3,2897	1,3404	2,6322	1,2193	1,8909	0,4339
768	2,9739	1,1897	4,0350	2,1010	3,0980	0,5370
960	2,0382	0,7856	2,5617	1,1323	1,9197	0,2980
1344	2,9734	1,1420	2,4898	1,2634	2,1315	0,2178
1536	3,1431	1,2934	2,4272	1,3574	2,3046	0,1925
1728	3,1977	1,0936	2,8113	1,4611	2,7038	0,1957
1920	4,6935	1,7740	2,2042	1,6281	2,8848	0,1378

LH193						
time	**total**	**CH**	**carbonyl**	**CH fingerprint**	**melamine**	**OMe**
0	3,6444	1,7052	4,6980	2,5920	3,7140	0,9680
192	2,9965	1,0497	3,5540	1,1130	1,2290	1,6480
384	2,3653	1,4603	4,7760	2,5580	3,2400	1,1610
768	3,4565	1,4354	4,0150	2,1420	3,3400	0,7000
960	3,6022	1,5216	4,3190	2,2970	3,7650	0,7110
1152	4,7586	2,0788	4,3240	2,5290	4,1070	0,6590
1344	6,9383	2,8697	4,8870	3,0340	5,1630	0,6530
1536	5,6615	2,4024	3,7440	2,3800	4,2910	0,4850
1728	6,2666	2,6025	2,6406	2,0585	3,7660	0,3434
1920	7,2314	2,7180	2,2709	2,1754	4,1406	0,2665

LH196						
time	**total**	**CH**	**carbonyl**	**CH fingerprint**	**melamine**	**OMe**
0	2,9762	1,4814	5,4440	2,9190	3,8440	1,3440
192	3,8761	1,4245	3,2518	1,0525	1,2216	1,4971
384	2,5401	1,3889	4,7640	2,5420	3,2240	1,2470
768	3,2824	1,3202	4,6610	2,4570	3,7250	0,9600
960	2,3662	0,8927	3,2543	1,6269	2,6954	0,6595
1344	5,2693	2,1591	4,6240	2,5780	4,3360	0,7720
1536	6,7654	2,8659	5,2330	3,0020	5,2630	0,8020
1728	3,6885	1,5399	2,4525	1,3578	2,5542	0,3584
1920	5,9454	2,5286	2,6240	1,7714	3,3793	0,3507

LH199						
time	**total**	**CH**	**carbonyl**	**CH fingerprint**	**melamine**	**OMe**
0	3,2349	1,5751	5,5940	3,0140	4,0610	1,2060
192	1,8432	0,7846	4,2040	1,7560	2,1860	1,5600
384	2,7728	1,5111	5,0430	2,6880	3,5020	1,1920
576	4,1583	1,6864	5,7380	2,9690	4,5740	1,1730
768	3,0978	1,3765	4,1780	2,1240	3,3660	0,7680
960	3,4220	1,3623	3,8330	1,9300	3,3550	0,6400
1344	4,5216	1,8247	3,5723	2,0001	3,5908	0,4525
1536	3,8544	1,5696	2,8122	1,5639	3,0782	0,3577
1728	4,4386	1,5806	2,9916	1,7823	3,6707	0,3438
1920	5,9835	2,2575	2,3927	1,9604	3,7944	0,2628

Series 1 – ATR – with HALS

t0	**total**	**CH**	**carbonyl**	**CH fingerprint**	**melamine**	**OMe**
Std S1	11,535	10,444	13,026	7,744	9,635	3,955
Arkema S1	8,3481	7,1162	13,38	11,929	6,629	2,963
LH190	7,4428	6,0599	11,873	10,335	5,705	2,311
LH184	7,3139	6,1215	11,499	10,676	6,38	2,258
LH168	2,05648	1,24971	2,3599	1,8593	1,1578	0,4511
LH162	8,3932	7,0232	15,865	9,868	9,604	3,701
LH189	7,6034	6,195	14,321	8,2	8,23	3,337
LH163	8,0837	6,4341	17	9,313	10,3	3,972

t2000	**total**	**CH**	**carbonyl**	**CH fingerprint**	**melamine**	**OMe**
Std S1	6,0516	4,3851	6,052	3,456	5,104	1,842
Arkema S1	8,7909	4,9597	9,186	8,189	6,212	1,376
LH190	6,9981	3,4049	7,188	6,161	4,759	1,011
LH184	5,2283	2,8339	5,912	5,428	4,214	0,939
LH168	1,47114	0,61248	1,8006	1,3498	1,2731	0,2628
LH162	8,751	3,588	5,899	4,675	7,005	0,957
LH189	5,9631	2,2975	5,148	3,373	5,43	0,933
LH163	7,4629	3,0285	5,942	3,972	6,763	1,039

Series 2 - ATR – with HALS

t0	total	CH	carbonyl	CH fingerprint	melamine	OMe
Std S2	8,1723	6,8765	9,396	5,348	6,989	2,776
Arkema S2	6,2196	4,5701	8,942	7,816	4,543	1,691
LH174	6,5929	3,7282	13,326	7,872	9,085	2,86
LH177	12,8492	8,3558	15,09	9,476	11,86	2,852
LH181	10,9261	6,3097	13,783	8,903	11,2	2,797
LH182	2,8003	1,638	4,837	2,762	3,426	1,04
LH219	6,7482	4,0504	9,93	5,514	6,462	1,933
LH192	3,4284	2,0499	7,113	3,907	4,307	1,622
LH193	3,0378	1,4679	3,2564	1,8603	2,6006	0,7692
LH196	3,4543	1,7033	5,22	2,866	3,918	1,256
LH199	3,2903	1,5882	6,04	3,139	4,266	1,358

t1920	total	CH	carbonyl	CH fingerprint	melamine	OMe
Std S2	5,1563	3,3617	5,38	2,988	4,458	1,546
Arkema S2	4,2593	2,0993	3,6053	3,4644	2,7182	0,5249
LH174	2,67753	0,95773	1,9202	1,5284	2,2558	0,2592
LH177	14,2127	6,4148	8,533	6,872	10,233	1,52
LH181	17,3289	7,3826	12,114	9,523	13,925	2,158
LH182	5,7684	2,3467	4,038	2,983	4,82	0,551
LH219	13,9969	6,0285	10,009	6,765	9,618	1,579
LH192	4,01457	1,55932	3,3394	2,0659	3,505	0,3789
LH193	3,76598	1,47607	2,5959	1,7507	3,1146	0,3414
LH196	4,4984	1,7373	3,809	2,467	4,092	0,717
LH199	3,38353	1,29269	2,2374	1,64	2,698	0,2564

Series 1 and 2 – photoacoustic – no HALS

t0	area CH	area total	carbonyl	CH fingerprint	melamine	OMe
Std	516,3800	584,586	312,4370	300,7480	335,4070	142,6990
LH190	516,0510	618,515	409,2210	682,2060	348,4060	128,7780
LH184	1742,4080	2395,038	1350,7060	2242,0330	1283,1200	373,4540
LH168	395,0130	531,875	283,2800	482,6540	271,2840	85,8270
LH162	316,2140	407,622	268,4840	317,1490	266,6560	68,3120
LH189	292,4540	344,72	262,9010	310,0940	252,2470	78,1090
LH163	808,0980	1009,277	749,8860	901,1860	751,7550	239,2500
LH174	229,2750	314,529	170,0170	180,9690	155,6410	43,2630
LH177	596,0900	698,599	536,4140	601,2050	533,8490	141,6890
LH181	214,0310	263,322	203,0410	236,3260	203,0360	58,2290
LH182	257,5600	335,208	223,9700	253,6670	217,8100	51,2350
LH219	1161,1160	1453,175	809,6960	854,5100	723,8330	206,8720

t2000	area CH	area total	carbonyl	CH fingerprint	melamine	OMe
Std	495,2870	970,398	252,1970	199,6910	298,1390	2,3400
LH190	508,9450	1261,729	188,4940	318,6510	326,8200	12,8640
LH184	571,2820	1545,302	152,9530	281,7150	354,9180	9,1760
LH168	638,3250	1683,553	193,2410	314,6650	378,3580	11,2590
LH162	437,1810	1144,45	172,4490	220,9990	319,8370	9,5620
LH189	496,6470	1317,943	187,9060	230,5960	327,8740	14,3610
LH163	516,7230	1408,13	199,0910	249,4050	355,1400	11,9130
LH174	1000,4480	2712,859	212,8680	257,3520	409,0950	5,1970
LH177	415,2050	1197,628	62,9780	74,0000	141,4570	1,5950
LH181	687,3550	1833,708	247,9260	308,7600	479,0180	8,2570
LH182	425,1380	1140,764	125,9830	147,1280	223,6780	5,7840
LH219	1513,1580	4044,264	357,6130	367,2140	1039,7820	14,1930

LIX. Agreement between different IR methods

The agreement between the results obtained using ATR and PAS techniques is discussed here. It was found to depend largely on the normalisation method and the distance between the peaks and the reference used in each case.

Below, the total differences in NHOH peak areas between the spectrum taken before and after 2000 h of exposure for the different coatings examined in the first series are presented. In the first graph, the carbonyl peak was used as a reference, while in the second graph, the values were normalised using the CH peak. The result of the photoacoustic measurement is shown directly to the right of the result of each ATR measurement.

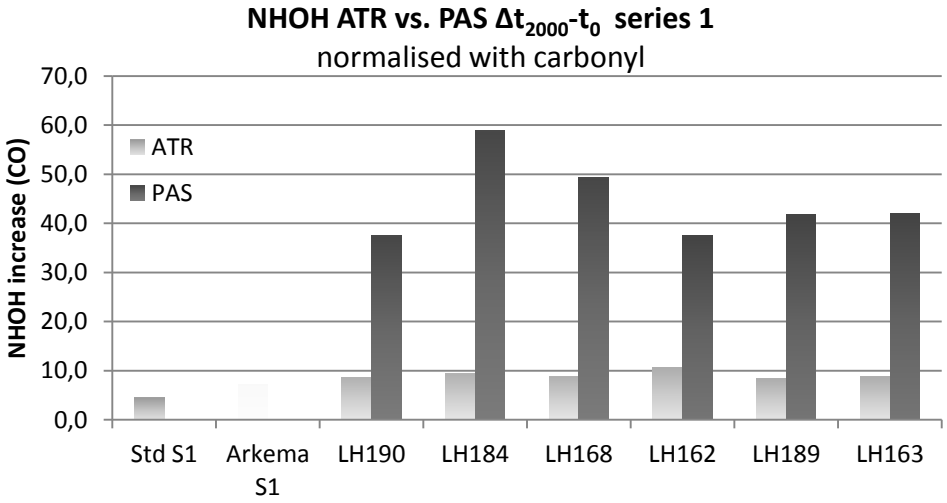

Figure 78: NHOH peak increase ATR *vs.* PAS normalised with carbonyl series 1

Not all spectra were examined twice due to time and availability constraints. It can however clearly be seen that the agreement between the two techniques is much better for the results normalised using the close by CH peak than for those normalised using the carbonyl.

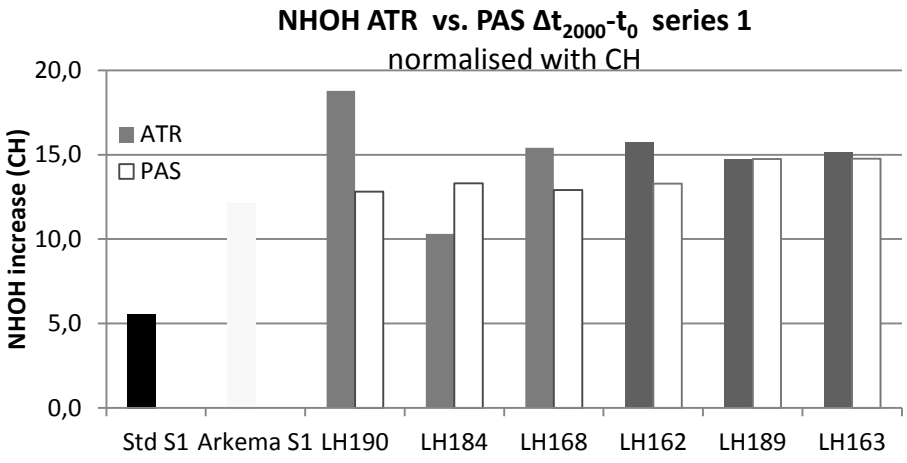

Figure 79: NHOH peak increase ATR *vs.* PAS normalised with CH series 1

Similar observations were made for the second series, as shown below. As for the first series, significantly larger growth in the NHOH peak was observed when the PAS technique was used, including in the standard coating, when values were normalised with carbonyl.

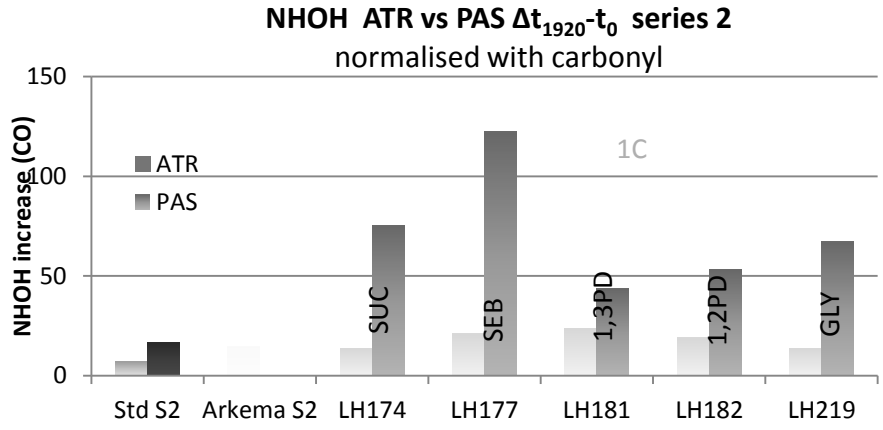

Figure 80: NHOH peak increase ATR *vs.* PAS normalised with carbonyl series 2

When the values were however normalised using the CH peak, better agreement was obtained, even though the PAS results were still slightly larger.

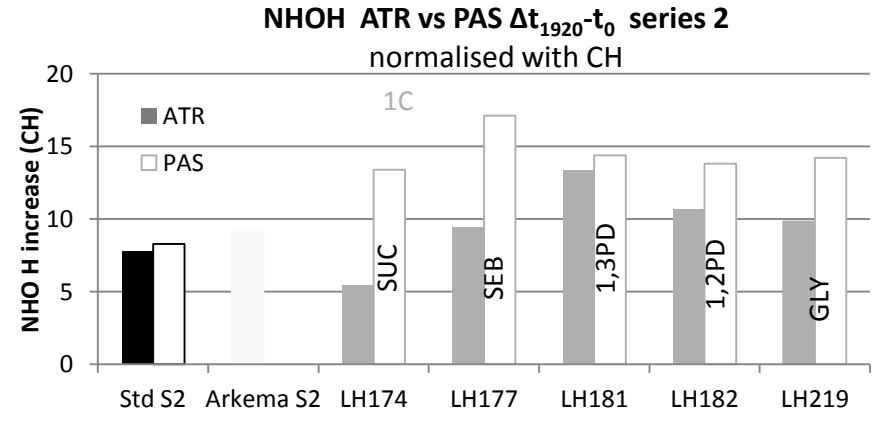

Figure 81: NHOH peak increase ATR *vs.* PAS normalised with CH series 2

On the other hand, good agreement between the two methods was obtained for the melamine peak, no matter whether it was normalised using the carbonyl peak or the CH fingerprint peak (not shown here).

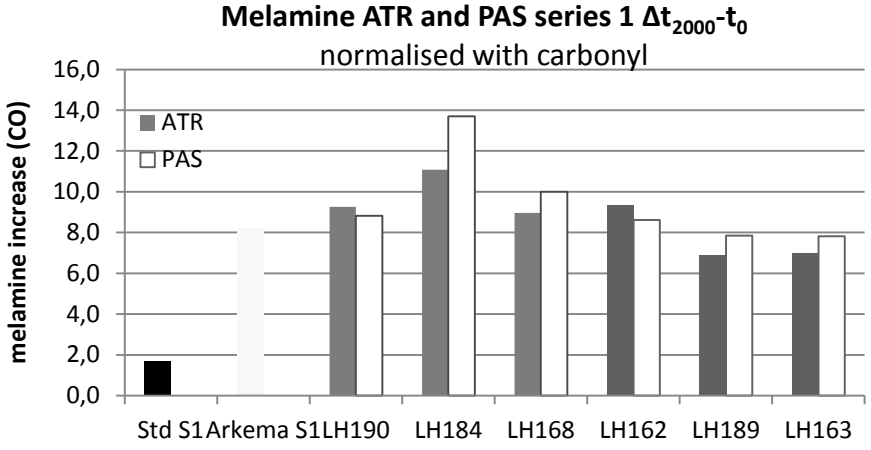

Figure 82: Melamine peak increase ATR *vs.* PAS series 1 normalised by carbonyl

For the methoxy peak corresponding to unreacted melamine side groups, very different values were again obtained when the measurements were normalised using the carbonyl peak. Contrary to the other peaks examined, the area actually decreased upon weathering. As for the NHOH peak discussed above, the change was significantly larger for the results of the photoacoustic measurement.

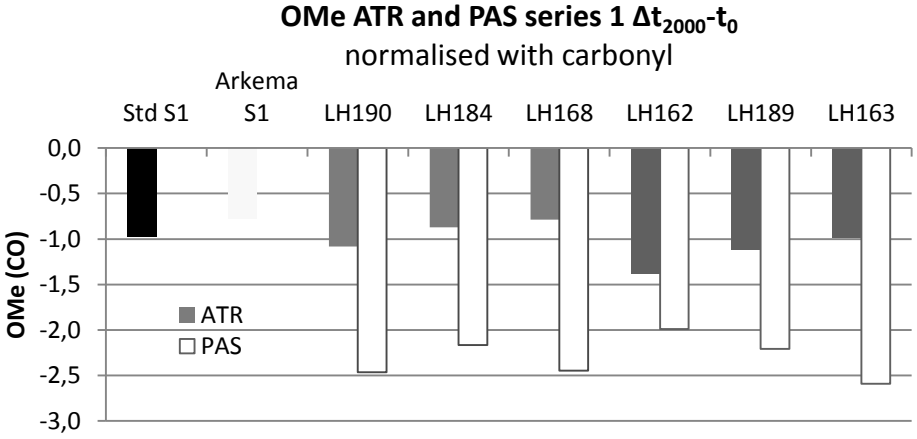

Figure 83: OMe peak decrease ATR *vs.* PAS series 1 normalised with carbonyl

The agreement between the two measurements was considerably improved when the peaks were instead normalised using the CH fingerprint peak. It was therefore concluded that the proximity of the peak used for normalisation is crucial to the accuracy of the photoacoustic measurements.

This phenomenon is probably due to the different penetration depths of each technique. Since the photoacoustic measurement can penetrate almost the entire coating, especially after some of it has been eroded, the differences between the depths corresponding to each peak are more relevant. Therefore, the normalisation with the carbonyl peak yields false results for those peaks that are far away in the spectrum, i.e. the NHOH and OMe peaks.

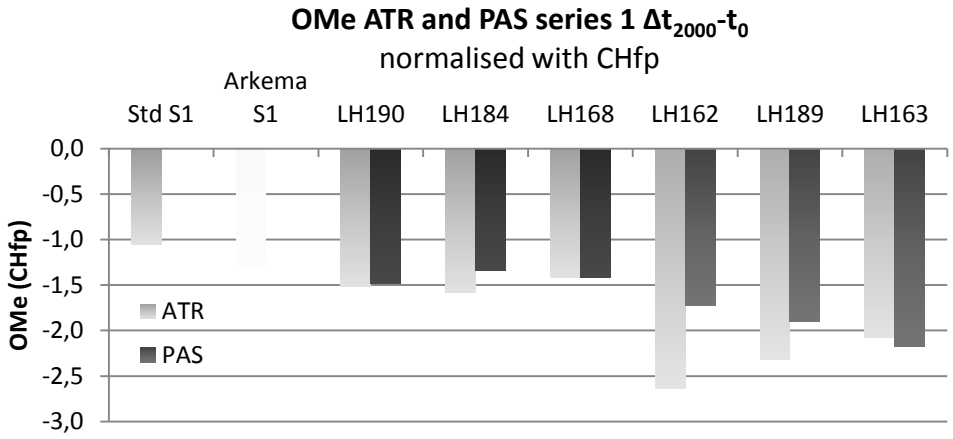

Figure 84: OMe peak decrease ATR *vs.* PAS series 1 normalised with carbonyl

For this reason, the results of the photoacoustic measurements discussed below were normalised with different peaks. In order to keep the measurements as comparable as possible, only the melamine peak will be normalised using the carbonyl peak. The NHOH and OMe peaks will be normalised with the CH peak closest to them.

LX. IR spectra before exposure

No correlation between the quantity of either isosorbide or phthalic anhydride in the coating and any of the peak areas examined before weathering was observed, as shown for the photoacoustic results below. Overall, the differences between the coatings were small. Since the paint formulations as well as the amount of free hydroxy groups in the resins were kept constant, the differences can probably be attributed to measurement uncertainty.

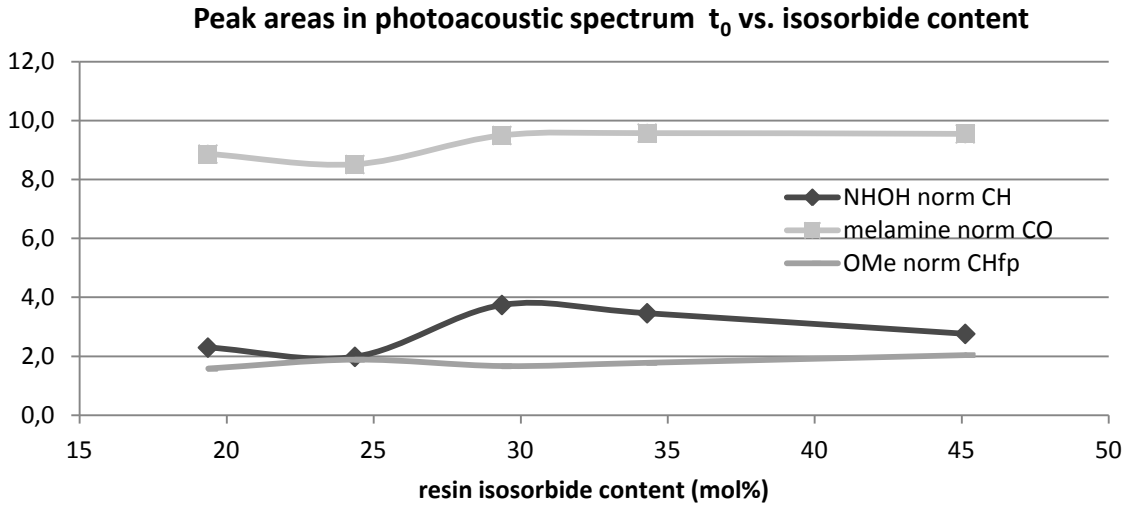

Figure 85: Peak areas in PAS t0 *vs.* isosorbide content

In both isosorbide and phthalic anhydride containing coatings, the largest absorption corresponds to the melamine peak, while the methoxy and NHOH peaks are comparatively small before the exposure was started.

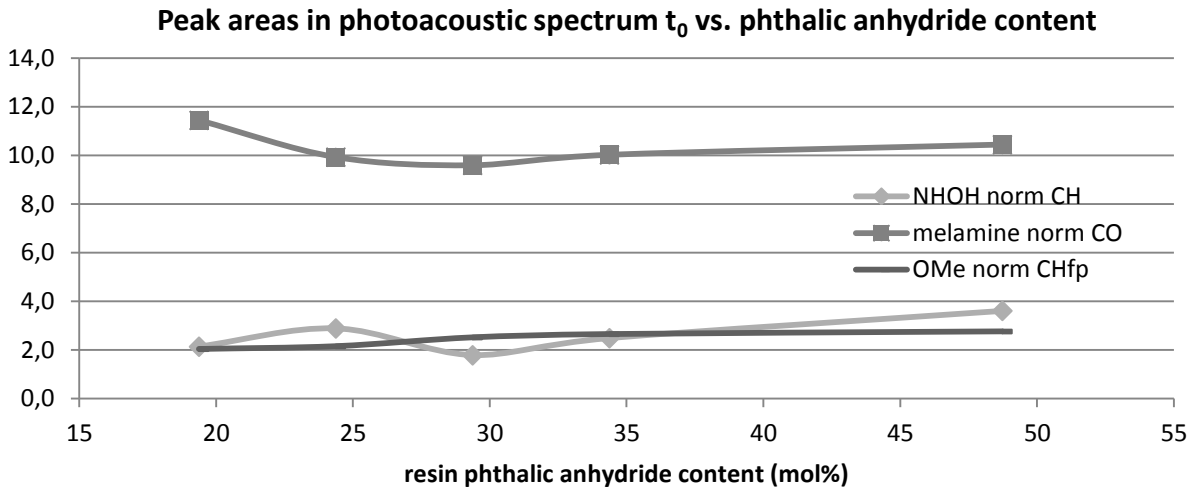

Figure 86: Peak areas in PAS t0 vs phthalic anhydride content

Compared to the standard, the isosorbide containing resins showed larger NHOH peaks, while the phthalic anhydride resins had similar absorptions. The trends observed between the different isosorbide coatings were the same for ATR and PAS methods.

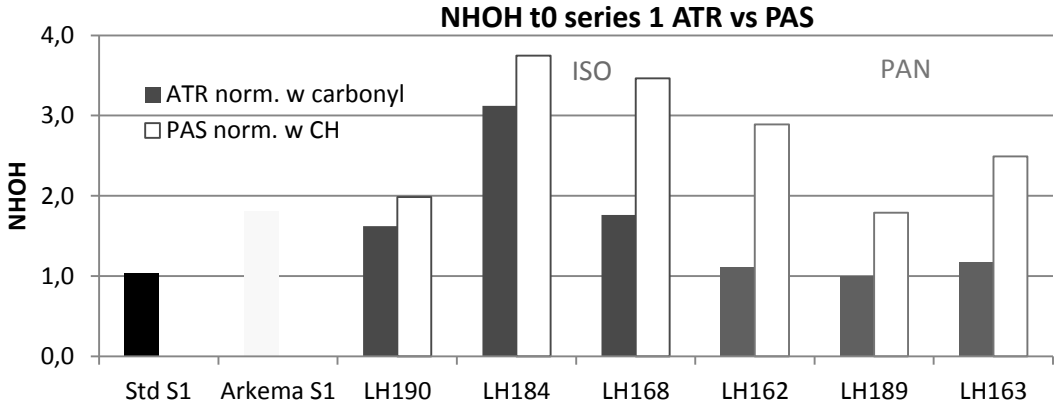

Figure 87: NHOH peaks at t0 series 1

The phthalic anhydride containing coatings examined in the second series, on the other hand, all showed larger NHOH peaks compared to the standard in both ATR and PAS methods. While the trends between different coatings observed in ATR and PAS were not identical, it should be kept in mind that the absolute differences were very small.

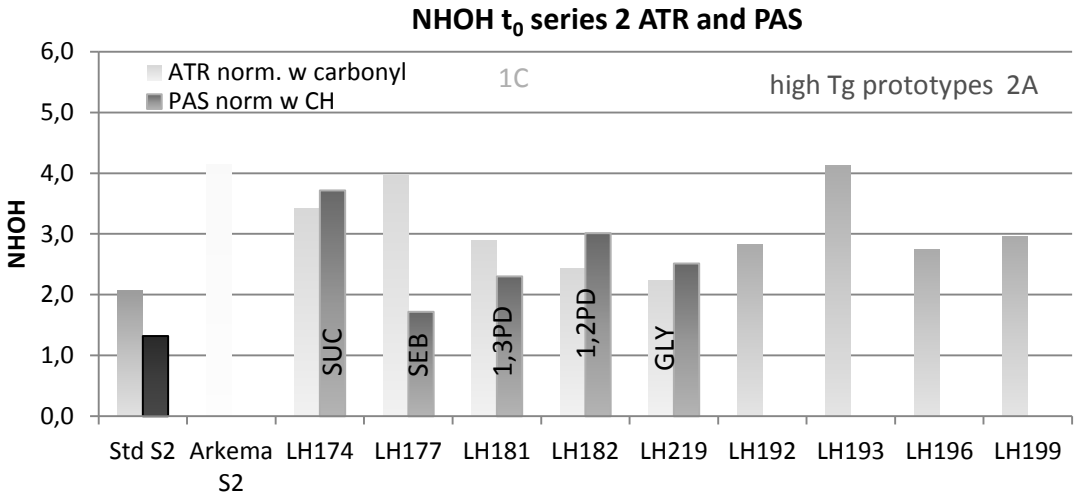

Figure 88: NHOH peaks at t0 series 2

Interestingly, the absorption of the CH fingerprint peak was larger than that of the CH peak with respect to the carbonyl peak for all biobased coatings, but smaller for the standard coating. This could be due to the different integration areas used for the different types of coatings, which was smaller for the standard coating due to an additional neighbouring peak in the spectrum.

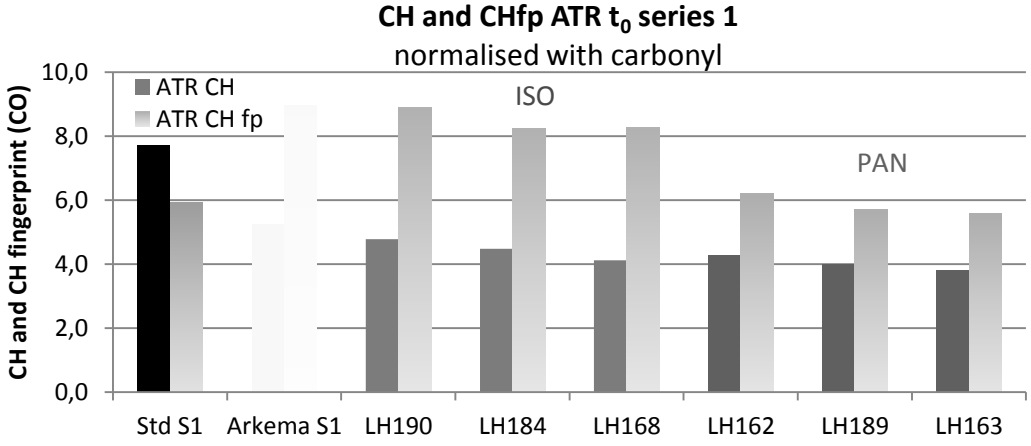

Figure 89: CH and CHfp peaks at t0 series 1

Overall, the areas of both peaks were smaller for increasing amounts of isosorbide and phthalic anhydride incorporated in the corresponding resins, as shown above. The CH peak for all biobased coatings was smaller than that of the standard coating. The CH fingerprint peak was larger than that of the standard for isosorbide containing coatings, and similar for phthalic anhydride containing coatings, which is probably again related to the area of integration used for the different coatings, which was biggest for isosorbide containing coatings.

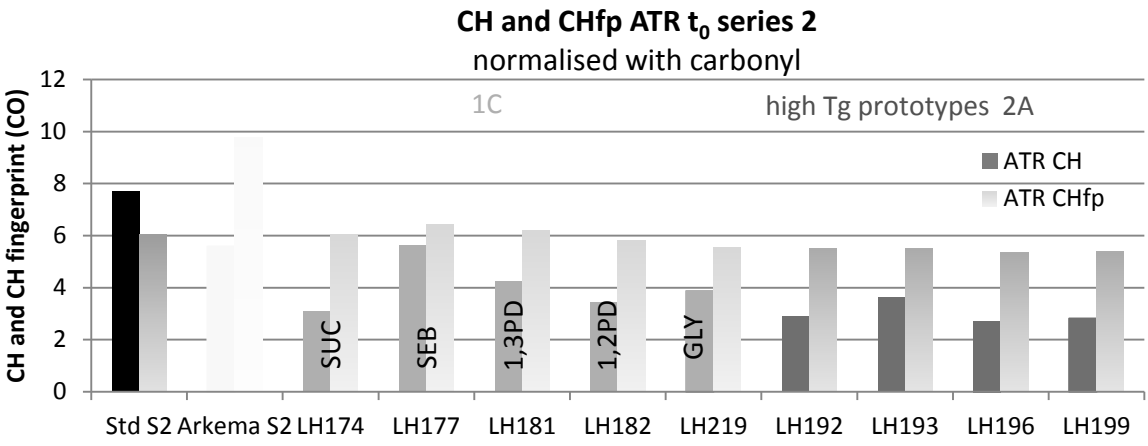

Figure 90: CH and CHfp peaks at t0 series 2

While the area for the CH fingerprint peak shown above was very similar across all coatings, some differences could be observed in the CH peak. The CH peak was largest for the coating containing the resin LH177. It contains increased amounts of sebacic acid and therefore the largest linear carbon chain, which could be responsible for the additional C-H bonds.

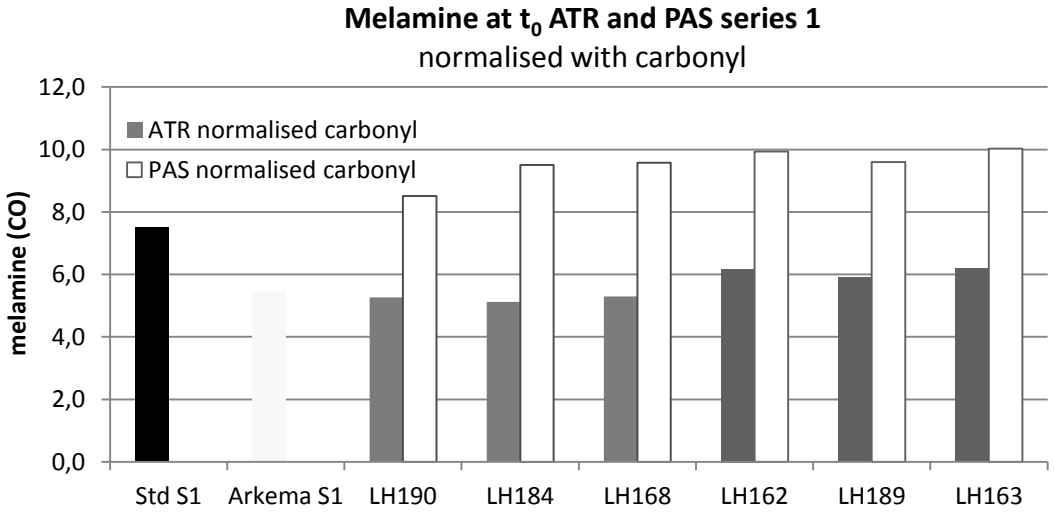

Figure 91: Melamine peak areas at t0 series 1

The peak corresponding to the C=N bond in the melamine ring was constant across all coatings in both ATR and PAS methods, as shown above and below. This reflects the equal amount of melamine used for the crosslinking of all coatings and validates the comparison between different formulations.

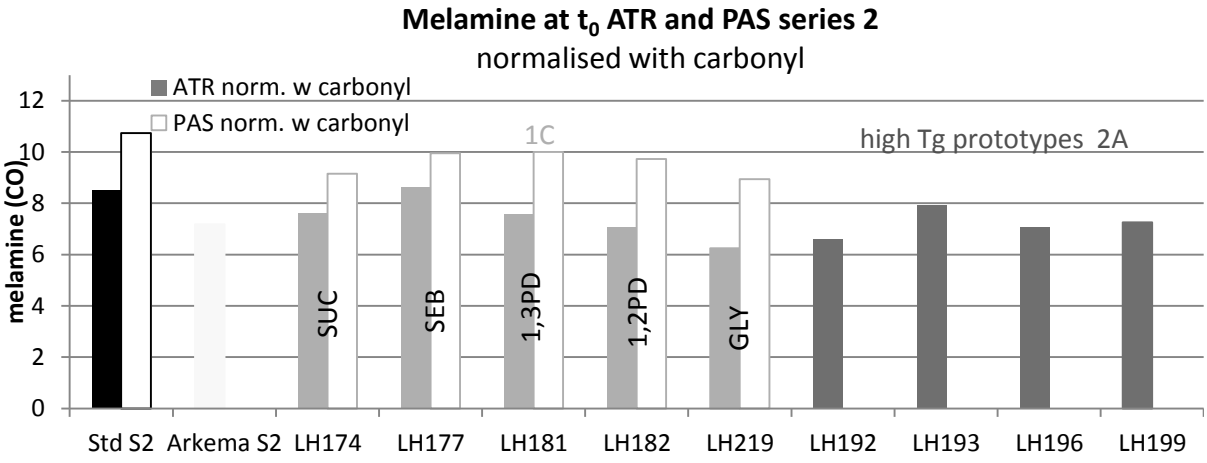

Figure 92: Melamine peak areas at t0 series 2

Lastly, the link between the absorption of the methoxy peak, corresponding to unreacted melamine groups, and the crosslinking density was investigated. In both ATR and PAS measurements, the standard resin displayed a considerably higher absorption of the methoxy group corresponding to a significantly lower crosslinking density measured in DMA. However, no similar trend could be detected in the other resins.

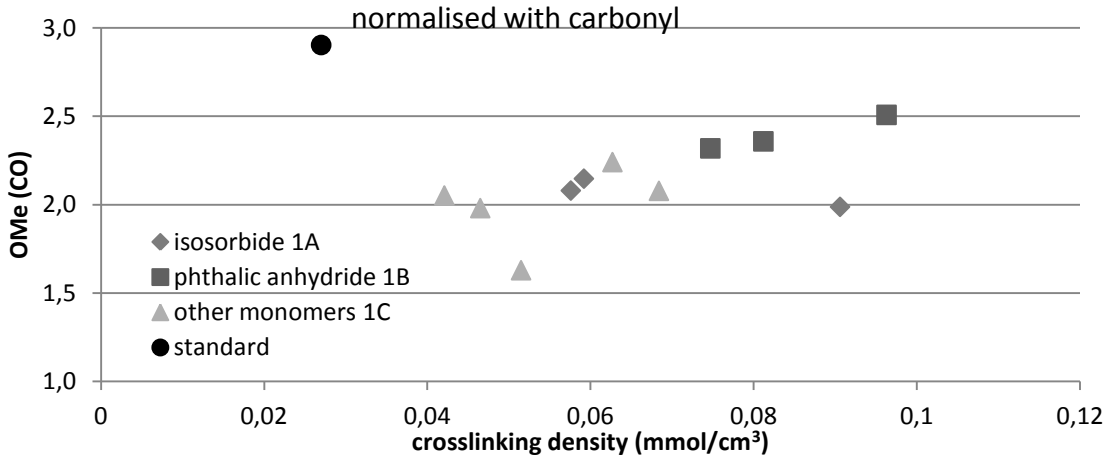

Figure 93: OMe peak at t_0 *vs.* crosslinking density ATR

A larger amount of free methoxy groups would be expected to correspond to a lower crosslinking density, but the opposite was observed in the ATR measurements. The trend was however not very clear and not reflected in the PAS measurements, so it is probable that no correlation between the crosslinking density and the amount of free methoxy group is observable in these IR spectra.

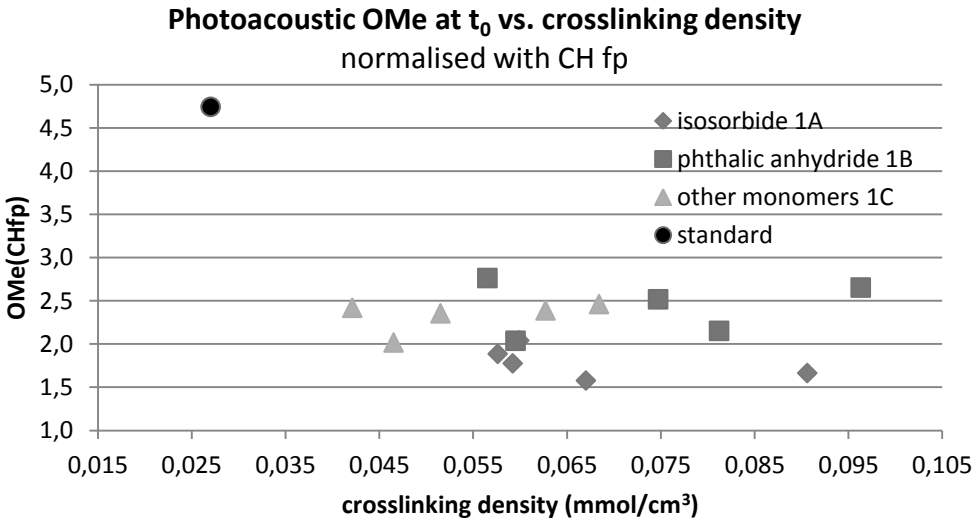

Figure 94: OMe peak *vs.* crosslinking density PAS

LXI. IR spectra of coatings formulated with HALS before exposure

One exception where a peak in the coating spectrum with HALS was not identical to the peak in the coating without HALS was the NHOH absorption of isosorbide containing coatings. In the case of the Arkema coating and of the coatings containing the resin LH190 and LH184, the NHOH peaks measured with HALS were smaller than those measured without it.

On the other hand, the peak of the coating containing the resin LH168 increased to almost twice the size after the addition of HALS. In absolute terms, however, the differences were small and it is possible that they are due to the poor quality of the spectrum.

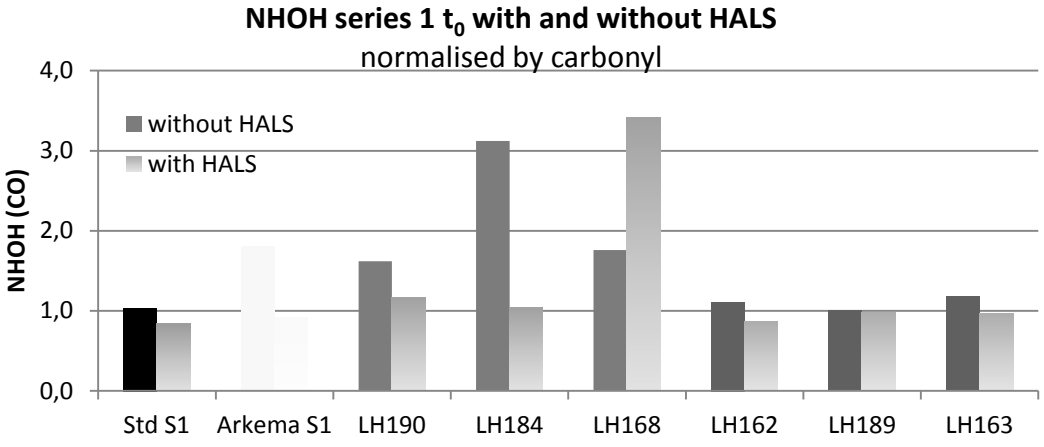

Figure 95: NHOH series 1 t0 with and without HALS

LXII. Development of the CHfp, melamine and OMe peaks in coatings with HALS

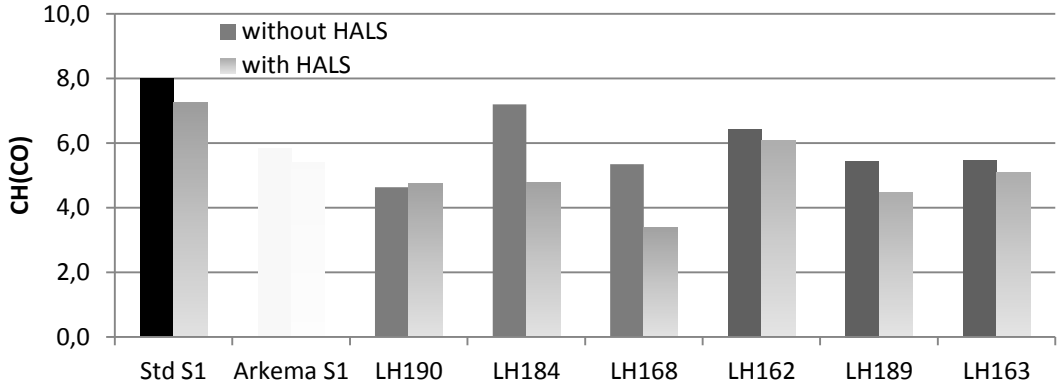

Figure 96: CH peak t2000 with and without HALS series 1

By examining the development of the other peaks, further differences between the coatings and the two series can be observed. The size of the CH peaks in the first series was affected only a little by the addition of HALS.

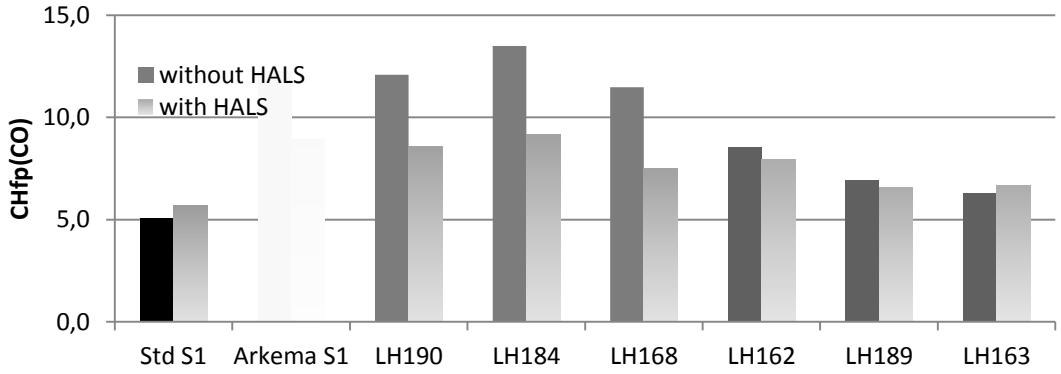

Figure 97: CHfp peak with and without HALS t2000 series 1

On the other hand, we can see that the size of the CH fingerprint peak was decreased through the addition of HALS in all coatings containing isosorbide, but not in the phthalic anhydride containing coatings or the standard coating.

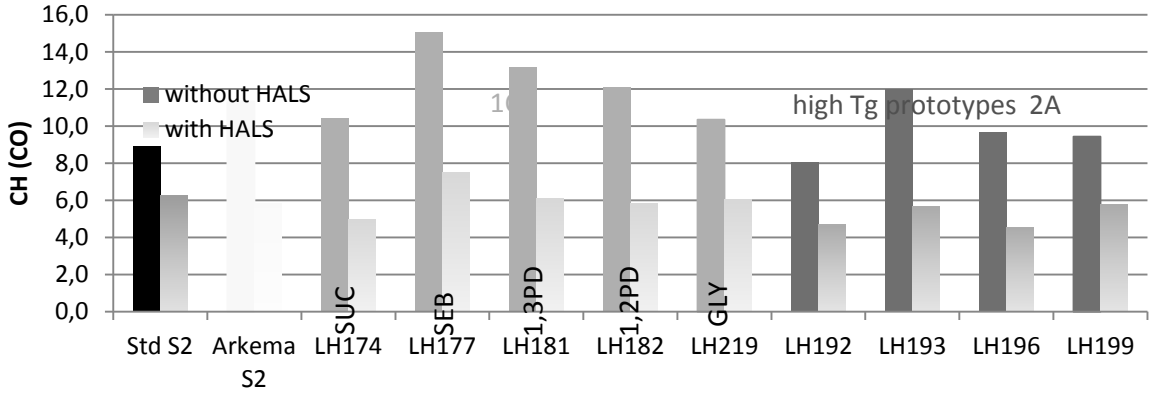

Figure 98: CH peak t1920 with and without HALS series 2

Contrarily, in the second series, the size of all CH peaks was decreased through the addition of HALS, while the size of the CH fingerprint peak was changed to a smaller amount. The isosorbide containing Arkema coating was an exception, with a much larger improvement in CH fingerprint peak as observed in the first series.

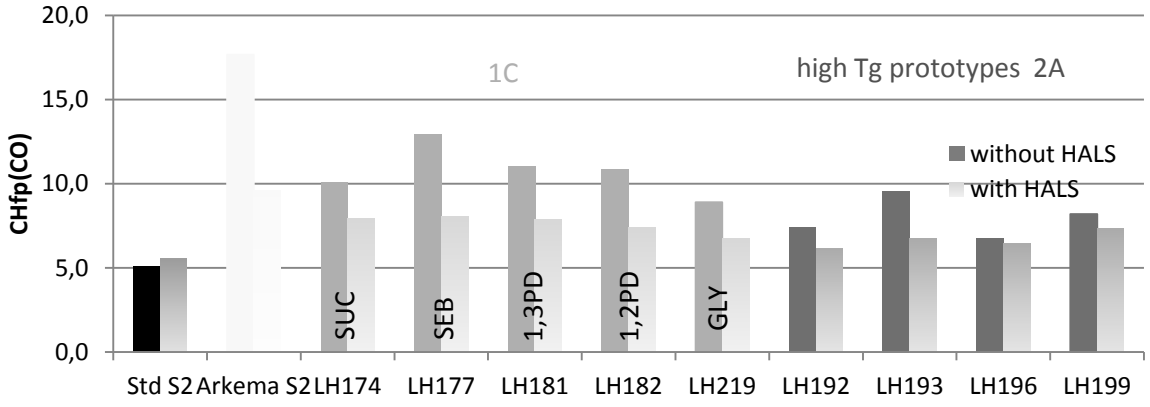

Figure 99: CHfp t1920 series 2 with and without HALS

This indicates that the difference made by the addition of HALS is affecting the CH peak more in isosorbide coatings, but the CH fingerprint peak more where the degradation caused by more frequent sampling in the second series is concerned. Since both peaks originate from different vibrations of the same functional group, it is possible that this observation is due to the proximity to the surface of the peaks examined or to the proximity to the carbonyl peak used for normalisation.

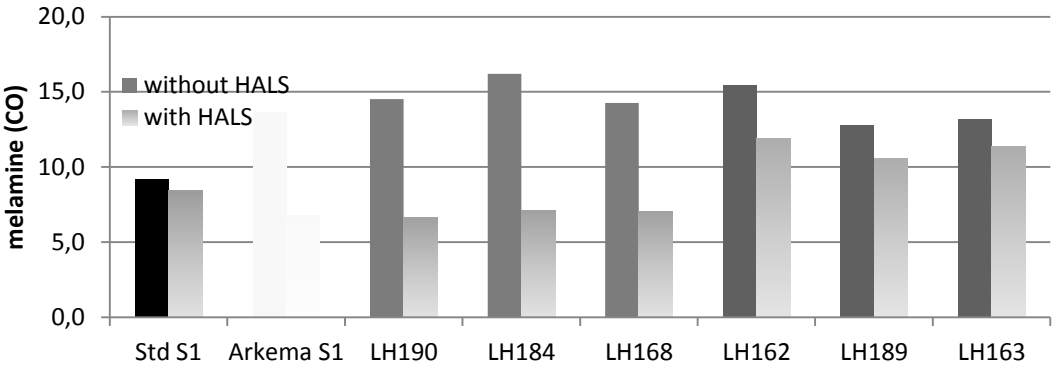

Figure 100: Melamine t2000 series 1 with and without HALS

The behaviour of the melamine peak was analogous to that of the NHOH peak. It was significantly decreased for isosorbide containing coatings, and for phthalic anhydride containing coatings of the second series but not the first series.

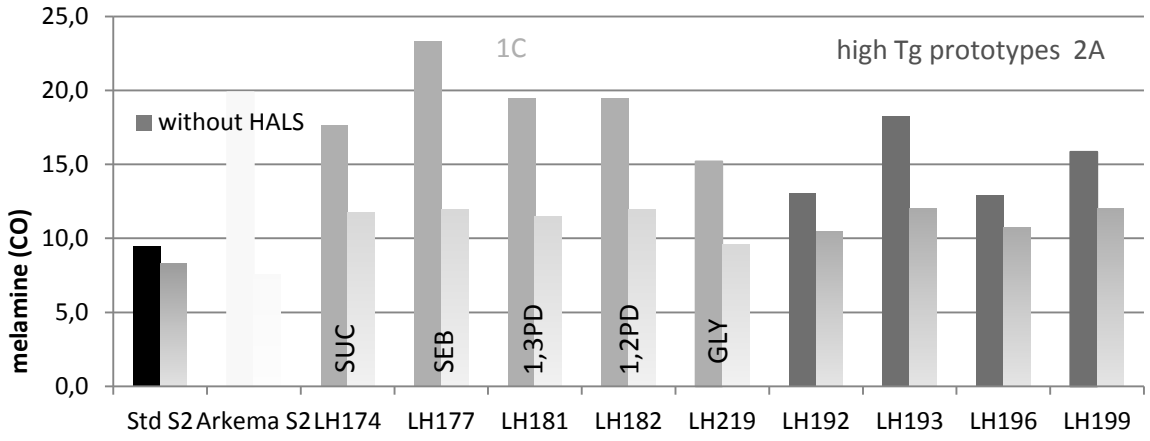

Figure 101: Melamine t1920 with and without HALS series 2

The absorption of the standard coating was barely changed. On the other hand, the degradation of the methoxy group was completely reversed in the standard coating in the first series through the addition of HALS, and approximately halved for the biobased coatings, as shown below.

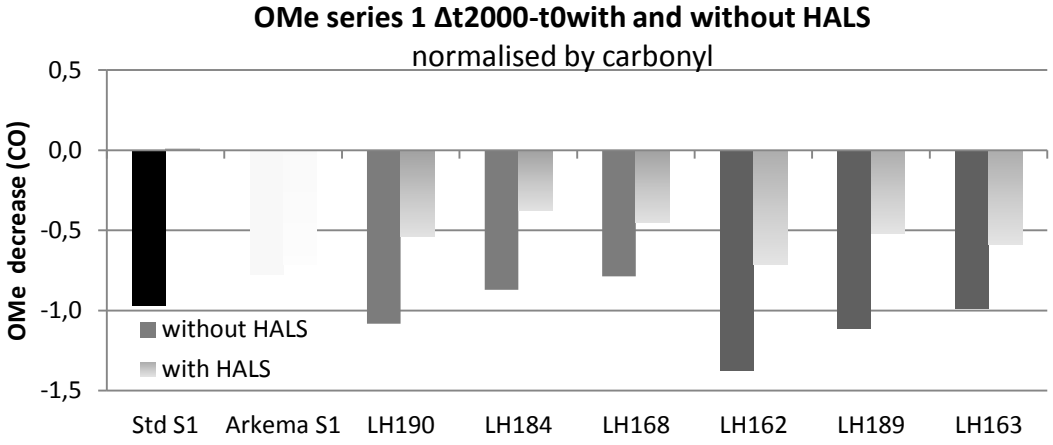

Figure 102: OMe decrease series 1 with and without HALS

In the second series, the standard and the Arkema coating's OMe absorption was affected most by the addition of HALS, followed by the coatings containing the resin LH177 and LH181, which also showed the highest degradations in terms of an increase in NHOH groups without HALS. Contrarily, the change in methoxy absorption of the high T_g prototypes was barely changed by the addition of HALS.

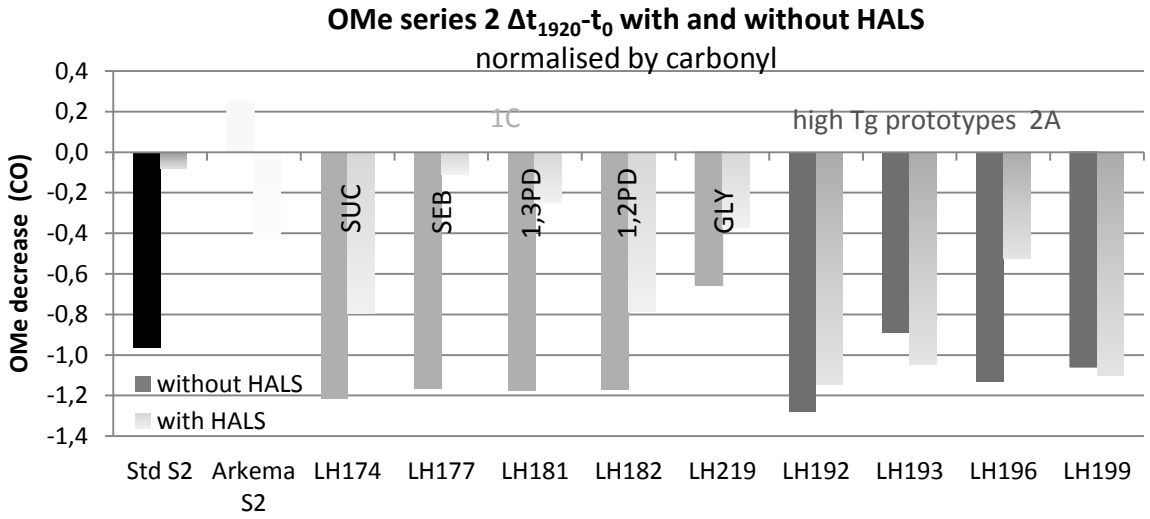

Figure 103: OMe decrease series 2 with and without HALS

LXIII. Example of NMR spectrum used for the calculation of incorporation of different monomers

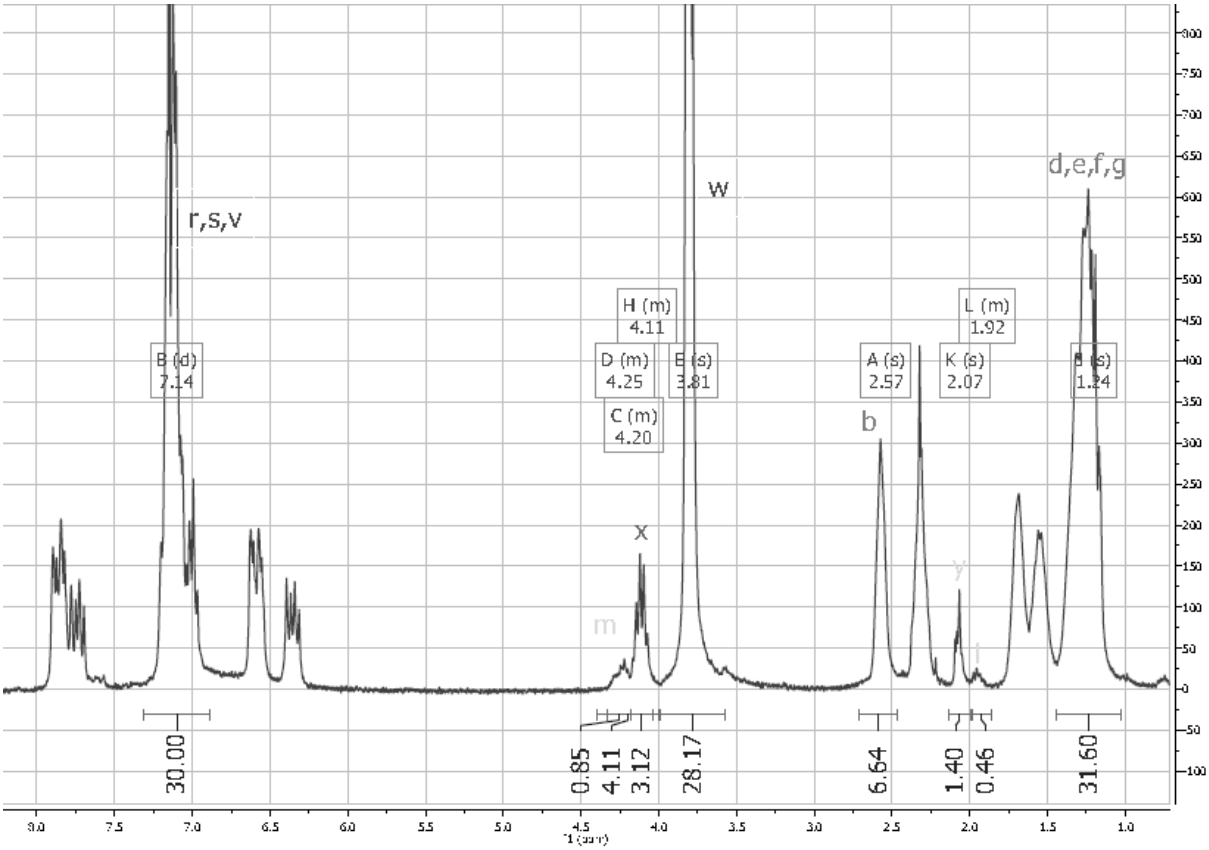

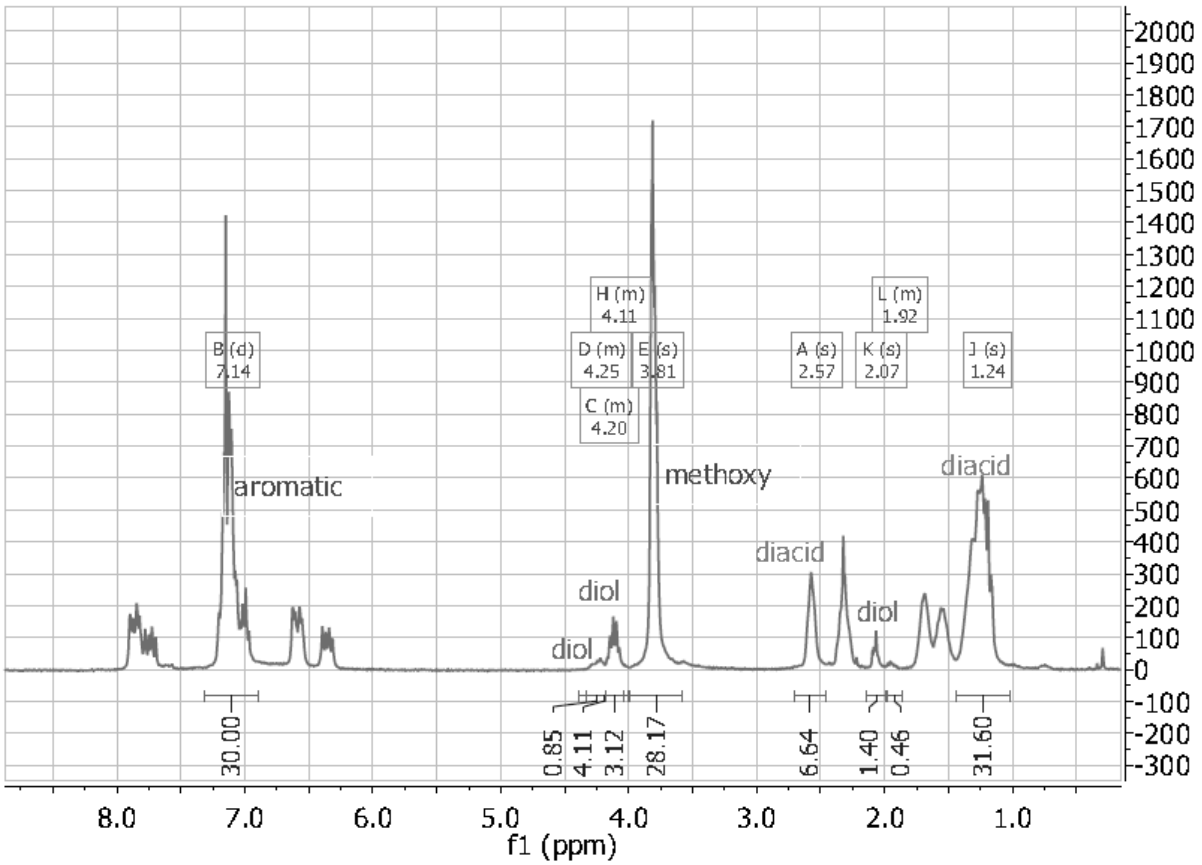

LXIV. Resin formulation details

Prototypes with different quantities of isosorbide used in weathering tests

The first five resins were synthesised to explore the effect of different quantities of isosorbide on the mechanical properties and weathering resistance of the resins. The isosorbide content was varied from 19,37% to 45,13%, replacing an equimolar amount of 1,2-propanediol. The quantity of all other monomers as well as the functionality and ratio of acid to hydroxy equivalents r_0 were kept constant.

The yield quoted in the following tables refers to the weight of diluted polymer obtained in the end of the reaction and serves as an indication of the scale at which the reaction was conducted, not as a measure of conversion, as no purification was employed and solvent was added.

LH249

Monomer	**n (mol)**	**mol %**
ISO	0,9490	19,37
SUC	1,7265	35,24
SEB	0,6609	13,49
1,2PD	1,2621	25,76
GLY	0,3008	6,14

F_n		1,9492
r_0		1,115
hydroxyl $_{theor.}$	mg_{KOH}/g	59,99
acid $_{end}$	mg_{KOH}/g	4,88
hydroxyl $_{end}$	mg_{KOH}/g	60,46
yield	*g*	632,8

LH190

Monomer	n (mol)	mol %
ISO	1,3542	24,37
SUC	1,9583	35,24
SEB	0,7496	13,49
1,2PD	1,1536	20,76
GLY	0,3412	6,14

F_n		1,9492
r_0		1,115
hydroxyl $_{theor.}$	mg_{KOH}/g	58,05
acid $_{end}$	mg_{KOH}/g	8,52
hydroxyl $_{end}$	mg_{KOH}/g	59,80
yield	*g*	667,7

LH184

Monomer	n (mol)	mol %
ISO	1,5880	29,37
SUC	1,9054	35,24
SEB	0,7294	13,49
1,2PD	0,8521	15,76
GLY	0,3320	6,14

F_n		1,9492
r_0		1,115
hydroxyl $_{theor.}$	mg_{KOH}/g	56,24
acid $_{end}$	mg_{KOH}/g	6,25
hydroxyl $_{end}$	mg_{KOH}/g	62,59
yield	*g*	642,2

LH168

Monomer	n (mol)	mol %
ISO	2,0965	34,31
SUC	2,1496	35,18
SEB	0,8229	13,47
1,2PD	0,6675	10,92
GLY	0,3745	6,13

F_n		1,9456
r_0		1,119
hydroxyl $_{theor.}$	mg_{KOH}/g	56,24
acid $_{end}$	mg_{KOH}/g	5,94
hydroxyl $_{end}$	mg_{KOH}/g	61,52
yield	*g*	669,8

LH248

Monomer	n (mol)	mol %
ISO	2,2485	45,13
SUC	1,7557	35,24
SEB	0,6721	13,49
GLY	0,3059	6,14

F_n		1,9492
r_0		1,115
hydroxyl $_{theor.}$	mg_{KOH}/g	51,19
acid $_{end}$	mg_{KOH}/g	11,84
hydroxyl $_{end}$	mg_{KOH}/g	49,83
yield	*g*	723,3

Prototypes with different quantities of phthalic anhydride used in weathering tests

The second five resins were synthesised both to determine the effect of phthalic anhydride content on the mechanical properties and weathering resistance of the resin, and to compare the difference between phthalic anhydride and isosorbide. The phthalic anhydride content was varied from 19,37% - 48,73%, and in the first four resins, the mol % of phthalic anhydride is the same as the mol % of isosorbide in a corresponding resin.

The phthalic anhydride replaced an equimolar amount of succinic acid and sebacic acid, while keeping the amount of sebacic acid at around 80% of that of succinic acid. The last resin contains no other diacids than phthalic anhydride, just as the last isosorbide resin contains no other diols than isosorbide. Due to the presence of glycerol and the non-stochiometry of the acid and hydroxy

equivalents in the reaction, the mol% of isosorbide and phthalic anhydride is no longer the same in the last two resins.

LH237

Monomer	**n (mol)**	**mol %**
PAN	1,0151	19,37
SUC	0,8455	16,13
SEB	0,6931	13,23
1,2PD	0,8259	15,76
GLY	0,3218	6,14
1,3PD	1,5391	29,37

F_n		1,9492
r_0		1,115
hydroxyl $_{theor.}$	mg_{KOH}/g	62,67
acid $_{end}$	mg_{KOH}/g	6,63
hydroxyl $_{end}$	mg_{KOH}/g	60,11
yield	*g*	668,6

LH162

Monomer	**n (mol)**	**mol %**
PAN	1,4938	24,37
SUC	0,8131	13,27
SEB	0,6801	11,10
1,2PD	0,9660	15,76
GLY	0,3764	6,14
1,3PD	1,8002	29,37

F_n		1,9492
r_0		1,115
hydroxyl $_{theor.}$	mg_{KOH}/g	62,29
acid $_{end}$	mg_{KOH}/g	5,36
hydroxyl $_{end}$	mg_{KOH}/g	52,84
yield	*g*	741,3

LH189

Monomer	**n (mol)**	**mol %**
PAN	1,8098	29,37
SUC	0,6634	10,77
SEB	0,5296	8,60
1,2PD	0,9711	15,76
GLY	0,3784	6,14
1,3PD	1,8098	29,37

F_n		1,9492
r_0		1,115
hydroxyl $_{theor.}$	mg_{KOH}/g	62,11
acid $_{end}$	mg_{KOH}/g	4,96
hydroxyl $_{end}$	mg_{KOH}/g	60,93
yield	*g*	622,3

LH163

Monomer	**n (mol)**	**mol %**
PAN	2,1179	34,37
SUC	0,5093	8,27
SEB	0,3756	6,10
1,2PD	0,9711	15,76
GLY	0,3784	6,14
1,3PD	1,8098	29,37

F_n		1,9492
r_0		1,115
hydroxyl $_{theor.}$	mg_{KOH}/g	61,93
acid $_{end}$	mg_{KOH}/g	7,68
hydroxyl $_{end}$	mg_{KOH}/g	65,19
yield	*g*	699,7

LH242

Monomer	**n (mol)**	**mol %**
PAN	3,0410	48,73
1,2PD	0,9835	15,76
GLY	0,3832	6,14
1,3PD	1,8329	29,37

F_n		1,9492
r_0		1,115
hydroxyl $_{theor.}$	mg_{KOH}/g	60,88
acid $_{end}$	mg_{KOH}/g	8,54
hydroxyl $_{end}$	mg_{KOH}/g	63,19
yield	*g*	654,3

Prototypes designed to test the effect of other monomers used in weathering tests

In the third group of five resins, the effect of each of the other monomers was explored. Based on the phthalic anhydride resin LH189, sebacic acid was completely replaced with succinic acid and vice versa, and 1,2-propanediol was completely replaced with 1,3-propanediol and vice versa. Lastly, the quantity of glycerol was raised by 3%, replacing both 1,2-propanediol and 1,3-propanediol, while keeping their ratio at around 55:100.

LH174

Monomer	**n (mol)**	**mol %**
PAN	2,2091	29,37
SUC	1,4562	19,36
1,2PD	1,1854	15,76
GLY	0,4618	6,14
1,3PD	2,2091	29,37

F_n		1,9492
r_0		1,115
hydroxyl $_{theor.}$	mg_{KOH}/g	66,89
acid $_{end}$	mg_{KOH}/g	4,52
hydroxyl $_{end}$	mg_{KOH}/g	62,34
yield	*g*	861,5

LH177

Monomer	**n (mol)**	**mol %**
PAN	1,9155	29,37
SEB	1,2627	19,36
1,2PD	1,0279	15,76
GLY	0,4005	6,14
1,3PD	1,9155	29,37

F_n		1,9492
r_0		1,115
hydroxyl $_{theor.}$	mg_{KOH}/g	57,01
acid $_{end}$	mg_{KOH}/g	5,43
hydroxyl $_{end}$	mg_{KOH}/g	56,47
yield	*g*	930,26

LH181

Monomer	**n (mol)**	**mol %**
PAN	1,8098	29,37
SUC	0,6634	10,77
SEB	0,5296	8,60
GLY	0,3784	6,14
1,3PD	2,7810	45,13

F_n		1,9492
r_0		1,115
hydroxyl $_{theor.}$	mg_{KOH}/g	62,11
acid $_{end}$	mg_{KOH}/g	5,22
hydroxyl $_{end}$	mg_{KOH}/g	60,75
yield	*g*	800,6

LH182

Monomer	**n (mol)**	**mol %**
PAN	1,8098	29,37
SUC	0,6634	10,77
SEB	0,5296	8,60
1,2PD	2,7810	45,13
GLY	0,3784	6,14

F_n		1,9492
r_0		1,115
hydroxyl $_{theor.}$	mg_{KOH}/g	62,11
acid $_{end}$	mg_{KOH}/g	6,36
hydroxyl $_{end}$	mg_{KOH}/g	63,15
yield	*g*	795,8

LH219

Monomer	**n (mol)**	**mol %**
PAN	1,8190	29,79
SUC	0,6667	10,92
SEB	0,5323	8,72
1,2PD	0,8832	14,47
GLY	0,5661	9,27
1,3PD	1,6379	26,83

F_n		1,9492
r_0		1,115
hydroxyl $_{theor.}$	mg_{KOH}/g	63,32
acid $_{end}$	mg_{KOH}/g	6,88
hydroxyl $_{end}$	mg_{KOH}/g	62,21
yield	*g*	784,2

Resins synthesised a second time for further testing at Beckers

After the first round of tests was conducted on the above resins, some were synthesised a second time to enable tests on a larger scale, for example with formulations including pigments. The nine resins below are therefore repetitions identical in formulation to a resin above.

LH206 – identical to LH190

Monomer	**n (mol)**	**mol %**
ISO	1,5477	24,37
SUC	2,2381	35,24
SEB	0,8567	13,49
1,2PD	1,3184	20,76
GLY	0,3899	6,14

F_n		1,9492
r_0		1,115
hydroxyl $_{theor.}$	mg_{KOH}/g	58,05
acid $_{end}$	mg_{KOH}/g	8,49
hydroxyl $_{end}$	mg_{KOH}/g	57,74
yield	*g*	866,1

LH262 – identical to LH184

Monomer	**n (mol)**	**mol %**
ISO	1,5880	29,37
SUC	1,9054	35,24
SEB	0,7294	13,49
1,2PD	0,8521	15,76
GLY	0,3320	6,14

F_n		1,9492
r_0		1,115
hydroxyl $_{theor.}$	mg_{KOH}/g	56,24
acid $_{end}$	mg_{KOH}/g	7,41
hydroxyl $_{end}$	mg_{KOH}/g	52,9
yield	*g*	728,9

LH203 – identical to LH168

Monomer	n (mol)	mol %
ISO	2,0657	34,31
SUC	2,1180	35,18
SEB	0,8108	13,47
1,2PD	0,6577	10,92
GLY	0,3690	6,13

F_n		1,9492
r_0		1,115
hydroxyl $_{theor.}$	mg_{KOH}/g	56,24
acid $_{end}$	mg_{KOH}/g	8,17
hydroxyl $_{end}$	mg_{KOH}/g	58,93
yield	*g*	805,7

LH263 – identical to LH168

Monomer	n (mol)	mol %
ISO	2,0657	34,31
SUC	2,1180	35,18
SEB	0,8108	13,47
1,2PD	0,6577	10,92
GLY	0,3690	6,13

F_n		1,9492
r_0		1,115
hydroxyl $_{theor.}$	mg_{KOH}/g	56,24
acid $_{end}$	mg_{KOH}/g	7,60
hydroxyl $_{end}$	mg_{KOH}/g	52,16
yield	*g*	707,1

LH198 – identical to LH162

Monomer	n (mol)	mol %
PAN	1,4938	24,37
SUC	0,8131	13,27
SEB	0,6801	11,10
1,2PD	0,9660	15,76
GLY	0,3764	6,14
1,3PD	1,8002	29,37

F_n		1,9492
r_0		1,115
hydroxyl $_{theor.}$	mg_{KOH}/g	62,29
acid $_{end}$	mg_{KOH}/g	4,76
hydroxyl $_{end}$	mg_{KOH}/g	66,50
yield	*g*	634,6

LH210 – identical to LH189

Monomer	n (mol)	mol %
PAN	1,8098	29,37
SUC	0,6634	10,77
SEB	0,5296	8,60
1,2PD	0,9711	15,76
GLY	0,3784	6,14
1,3PD	1,8098	29,37

F_n		1,9492
r_0		1,115
hydroxyl $_{theor.}$	mg_{KOH}/g	62,11
acid $_{end}$	mg_{KOH}/g	4,9
hydroxyl $_{end}$	mg_{KOH}/g	56,65
yield	*g*	626,7

LH201 – identical to LH163

Monomer	n (mol)	mol %
PAN	2,1293	34,37
SUC	0,5120	8,27
SEB	0,3776	6,10
1,2PD	0,9763	15,76
GLY	0,3804	6,14
1,3PD	1,8195	29,37

F_n		1,9492
r_0		1,115
hydroxyl $_{theor.}$	mg_{KOH}/g	61,93
acid $_{end}$	mg_{KOH}/g	5,09
hydroxyl $_{end}$	mg_{KOH}/g	59,06
yield	*g*	634,9

LH260 – identical to LH182

Monomer	**n (mol)**	**mol %**
PAN	1,8098	29,37
SUC	0,6634	10,77
SEB	0,5296	8,60
1,2PD	2,7810	45,13
GLY	0,3784	6,14

F_n		1,9492
r_0		1,115
hydroxyl $_{theor.}$	mg_{KOH}/g	62,11
acid $_{end}$	mg_{KOH}/g	5,6
hydroxyl $_{end}$	mg_{KOH}/g	52,96
yield	*g*	770,0

LH264 – identical to LH219

Monomer	**n (mol)**	**mol %**
PAN	1,5596	29,79
SUC	0,5716	10,92
SEB	0,4564	8,72
1,2PD	0,7572	14,47
GLY	0,4853	9,27
1,3PD	1,4042	26,83

F_n		1,9774
r_0		1,117
hydroxyl $_{theor.}$	mg_{KOH}/g	63,32
acid $_{end}$	mg_{KOH}/g	11,94
hydroxyl $_{end}$	mg_{KOH}/g	56,74
yield	*g*	721,1

Resins with higher isosorbide content to raise the T_g while keeping the OH value constant

The following seven resins were made to explore different possibilities of raising the glass transition temperature by increasing the isosorbide content while keeping the theoretical hydroxy value constant. This was done by modifying the ration of succinic and sebacic acid, modifying the ratio of hydroxy equivalents to acid equivalents and decreasing the amount of glycerol in the formulation.

LH038

Monomer	**n (mol)**	**mol %**
ISO	1,8594	34,37
SUC	2,1321	39,41
SEB	0,5042	9,32
1,2PD	0,5821	10,76
GLY	0,3322	6,14

F_n		1,9492
r_0		1,115
hydroxyl $_{theor.}$	mg_{KOH}/g	56,24
acid $_{end}$	mg_{KOH}/g	7,75
hydroxyl $_{end}$	mg_{KOH}/g	82,78
yield	*g*	/

LH039

Monomer	**n (mol)**	**mol %**
ISO	1,8080	34,31
SUC	1,8538	35,18
SEB	0,7096	13,47
1,2PD	0,5756	10,92
GLY	0,3230	6,13

F_n		1,9456
r_0		1,119
hydroxyl $_{theor.}$	mg_{KOH}/g	56,24
acid $_{end}$	mg_{KOH}/g	6,69
hydroxyl $_{end}$	mg_{KOH}/g	125,82
yield	*g*	/

LH043

Monomer	**n (mol)**	**mol %**
ISO	1,8013	33,96
SUC	1,8469	34,82
SEB	0,7070	13,33
1,2PD	0,7319	13,80
GLY	0,2170	4,09

F_n		1,9260
r_0		1,119
hydroxyl $_{theor.}$	mg_{KOH}/g	56,24
acid $_{end}$	mg_{KOH}/g	5,82
hydroxyl $_{end}$	mg_{KOH}/g	81,07
yield	*g*	/

LH067 – delivered to Beckers for tests

Monomer	**n (mol)**	**mol %**
ISO	1,8013	33,96
SUC	1,8469	34,82
SEB	0,7070	13,33
1,2PD	0,7319	13,80
GLY	0,2170	4,09

F_n		1,9260
r_0		1,119
hydroxyl $_{theor.}$	mg_{KOH}/g	56,24
acid $_{end}$	mg_{KOH}/g	7,09
hydroxyl $_{end}$	mg_{KOH}/g	57,89
yield	*g*	638,3

LH070

Monomer	**n (mol)**	**mol %**
ISO	1,8080	34,31
SUC	1,8538	35,18
SEB	0,7096	13,47
1,2PD	0,5756	10,92
GLY	0,3230	6,13

F_n		1,9456
r_0		1,119
hydroxyl $_{theor.}$	mg_{KOH}/g	56,24
acid $_{end}$	mg_{KOH}/g	8,09
hydroxyl $_{end}$	mg_{KOH}/g	56,82
yield	*g*	/

LH077

Monomer	**n (mol)**	**mol %**
ISO	1,8013	33,96
SUC	1,8469	34,82
SEB	0,7070	13,33
1,2PD	0,7319	13,80
GLY	0,2170	4,09

F_n		1,9260
r_0		1,119
hydroxyl $_{theor.}$	mg_{KOH}/g	56,24
acid $_{end}$	mg_{KOH}/g	7,78
hydroxyl $_{end}$	mg_{KOH}/g	53,64
yield	*g*	662,1

LH079 – delivered to Beckers for tests

Monomer	**n (mol)**	**mol %**
ISO	2,0391	38,44
SUC	1,8252	34,41
SEB	0,6987	13,17
1,2PD	0,6304	11,88
GLY	0,1108	2,09

F_n		1,9033
r_0		1,124
hydroxyl $_{theor.}$	mg_{KOH}/g	56,24
acid $_{end}$	mg_{KOH}/g	5,68
hydroxyl $_{end}$	mg_{KOH}/g	59,60
yield	*g*	723,8

The last resins, LH040, was made as a reference for the above seven resins to see how the resin properties changed when the amount of 1,2-propanediol is decreased by the same amount as the isosorbide is increased, without adjustments to keep the hydroxy value constant.

LH040

Monomer	**n (mol)**	**mol %**
ISO	1,8094	34,37
SUC	1,8552	35,24
SEB	0,7102	13,49
1,2PD	0,5665	10,76
GLY	0,3232	6,14

F_n		1,9492
r_0		1,115
hydroxyl $_{theor.}$	mg_{KOH}/g	54,53
acid $_{end}$	mg_{KOH}/g	6,33
hydroxyl $_{end}$	mg_{KOH}/g	54,65
yield	*g*	/

The following resin was used as a reference for the above resins, also delivered to Beckers.

LH075 – used as a reference in Tg tests

Monomer	**n (mol)**	**mol %**
ISO	1,5880	29,37
SUC	1,9054	35,24
SEB	0,7294	13,49
1,2PD	0,8521	15,76
GLY	0,3320	6,14

F_n		1,9492
r_0		1,115
hydroxyl $_{theor.}$	mg_{KOH}/g	56,24
acid $_{end}$	mg_{KOH}/g	7,82
hydroxyl $_{end}$	mg_{KOH}/g	57,85
yield	*g*	678,8

High glass transition temperature prototypes based on phthalic anhydride

The following four resins are prototypes based on the phthalic anhydride containing resin LH189, which was modified to increase the glass transition temperature. In order to achieve this, the amounts of phthalic anhydride, succinic acid and 1,2-propanediol were increased.

LH192

Monomer	**n (mol)**	**mol %**
PAN	1,9330	29,37
SUC	1,2742	19,36
1,2PD	2,9702	45,13
GLY	0,4041	6,14

F_n		1,9492
r_0		1,115
hydroxyl $_{theor.}$	mg_{KOH}/g	66,89
acid $_{end}$	mg_{KOH}/g	5,35
hydroxyl $_{end}$	mg_{KOH}/g	58,79
yield	*g*	426,2

LH193

Monomer	**n (mol)**	**mol %**
PAN	2,1293	34,37
SUC	0,5120	8,27
SEB	0,3776	6,10
1,2PD	2,7958	45,13
GLY	0,3804	6,14

F_n		1,9492
r_0		1,115
hydroxyl $_{theor.}$	mg_{KOH}/g	61,93
acid $_{end}$	mg_{KOH}/g	5,38
hydroxyl $_{end}$	mg_{KOH}/g	60,72
yield	*g*	538,4

LH196

Monomer	n (mol)	mol %
PAN	2,2306	34,37
SUC	0,9319	14,36
1,2PD	1,0228	15,76
GLY	0,3985	6,14
1,3PD	1,9061	29,37

F_n		1,9492
r_0		1,115
hydroxyl $_{theor.}$	mg_{KOH}/g	65,22
acid $_{end}$	mg_{KOH}/g	6,84
hydroxyl $_{end}$	mg_{KOH}/g	61,24
yield	*g*	570,1

LH199

Monomer	n (mol)	mol %
PAN	2,5492	34,37
SUC	1,0651	14,36
1,2PD	1,9106	25,76
GLY	0,4554	6,14
1,3PD	1,4367	19,37

F_n		1,9492
r_0		1,115
hydroxyl $_{theor.}$	mg_{KOH}/g	65,22
acid $_{end}$	mg_{KOH}/g	6,79
hydroxyl $_{end}$	mg_{KOH}/g	64,69
yield	*g*	644,3

New prototypes for exterior use 2B

The following four resins are prototypes formulated according to the results of the weathering tests performed on the above resins, which are proposed as partially bio based alternatives for outdoor use.

Prototype containing isosorbide and phthalic anhydride, with a minimised amount of succinic acid and 1,2-propanediol:

LH269

Monomer	n (mol)	mol %
ISO	1,9485	38,98
PAN	0,4949	9,90
SEB	1,9169	38,35
1,3PD	0,2851	5,70
GLY	0,3534	7,07

F_n		1,9299
r_0		1,146
hydroxyl $_{theor.}$	mg_{KOH}/g	54,68
acid $_{end}$	mg_{KOH}/g	9,29
hydroxyl $_{end}$	mg_{KOH}/g	56,41
yield	*g*	761,2

Prototypes based on phthalic anhydride, but with an increased quantity of succinic acid and 1,2-propanediol permitting to limit the quantity of the former:

LH231

Monomer	n (mol)	mol %
PAN	1,4992	19,37
SUC	2,2724	29,36
1,2PD	3,4930	45,13
GLY	0,4752	6,14

F_n		1,9492
r_0		1,115
hydroxyl $_{theor.}$	mg_{KOH}/g	70,48
acid $_{end}$	mg_{KOH}/g	7,21
hydroxyl $_{end}$	mg_{KOH}/g	60,25
yield	*g*	663,7

LH238

Monomer	n (mol)	mol %
PAN	0,7227	9,37
SUC	2,7271	35,36
SEB	0,3085	4,00
1,2PD	3,4807	45,13
GLY	0,4735	6,14

F_n		1,9492
r_0		1,115
hydroxyl $_{theor.}$	mg_{KOH}/g	71,63
acid $_{end}$	mg_{KOH}/g	8,9
hydroxyl $_{end}$	mg_{KOH}/g	69,73
yield	*g*	630,3

Prototype based on cyclohexanedicarboxylic acid:

LH265

Monomer	n (mol)	mol %
CHDC	0,7073	9,37
SUC	2,6691	35,36
SEB	0,3019	4,00
1,2PD	3,4065	45,13
GLY	0,4635	6,14

F_n		1,9492
r_0		1,115
hydroxyl $_{theor.}$	mg_{KOH}/g	71,17
acid $_{end}$	mg_{KOH}/g	6,11
hydroxyl $_{end}$	mg_{KOH}/g	68,79
yield	*g*	822,09

Details of prototypes not used in weathering tests

Solvent test:

LH042

Monomer	n (mol)	mol %
ISO	1,5880	29,37
SUC	1,9054	35,24
SEB	0,7294	13,49
1,2PD	0,8521	15,76
GLY	0,3320	6,14

F_n		1,9492
r_0		1,115
hydroxyl $_{theor.}$	mg_{KOH}/g	56,24
acid $_{end}$	mg_{KOH}/g	9,57
hydroxyl $_{end}$	mg_{KOH}/g	57,66
yield	*g*	/

Early addition tests

The following two resins were made to check if adding the 1,2-propanediol and glycerol earlier would have an effect on the resin properties, according to synthesis procedure IV.

LH072

Monomer	n (mol)	mol %
ISO	1,5880	29,37
SUC	1,9054	35,24
SEB	0,7294	13,49
1,2PD	0,8521	15,76
GLY	0,3320	6,14

F_n		1,9492
r_0		1,115
hydroxyl $_{theor.}$	mg_{KOH}/g	56,24
acid $_{end}$	mg_{KOH}/g	7,72
hydroxyl $_{end}$	mg_{KOH}/g	58,10
yield	*g*	709,6

LH123

Monomer	n (mol)	mol %
ISO	1,5880	29,37
SUC	1,9054	35,24
SEB	0,7294	13,49
1,2PD	0,8521	15,76
GLY	0,3320	6,14

F_n		1,9492
r_0		1,115
hydroxyl $_{theor.}$	mg_{KOH}/g	56,24
acid $_{end}$	mg_{KOH}/g	9,02
hydroxyl $_{end}$	mg_{KOH}/g	62,37
yield	*g*	698,5

Additional resins with different quantities of isosorbide and phthalic anhydride

The following three resins were synthesised to explore the effect of phthalic anhydride and isosorbide content on the resin, but not used in any application or weathering test due to limited space.

LH243 Iso 39,37%

Monomer	n (mol)	mol %
ISO	2,0195	39,37
SUC	1,8076	35,24
SEB	0,6920	13,49
1,2PD	0,2955	5,76
GLY	0,3149	6,14

F_n		1,9492
r_0		1,115
hydroxyl $_{theor.}$	mg_{KOH}/g	52,93
acid $_{end}$	mg_{KOH}/g	7,18
hydroxyl $_{end}$	mg_{KOH}/g	51,38
yield	*g*	629,2

LH239 PAN 9,37 mol%

Monomer	n (mol)	mol %
PAN	0,4872	9,37
SUC	1,1181	21,50
SEB	0,9284	17,86
1,2PD	0,8195	15,76
GLY	0,3193	6,14
1,3PD	1,5271	29,37

F_n		1,9492
r_0		1,115
hydroxyl $_{theor.}$	mg_{KOH}/g	63,24
acid $_{end}$	mg_{KOH}/g	5,44
hydroxyl $_{end}$	mg_{KOH}/g	60,60
yield	*g*	544,2

LH228 PAN 24,37 mol%, no sebacic acid or 1,3-propanediol

Monomer	n (mol)	mol %
PAN	1,8592	24,37
SUC	1,8585	24,36
1,2PD	3,4431	45,13
GLY	0,4684	6,14

F_n		1,9492
r_0		1,115
hydroxyl $_{theor.}$	mg_{KOH}/g	68,64
acid $_{end}$	mg_{KOH}/g	5,69
hydroxyl $_{end}$	mg_{KOH}/g	62,09
yield	*g*	693,6

LH165 PAN 39,37 mol%

Monomer	n (mol)	mol %
PAN	2,4522	39,37
SUC	0,3591	5,77
SEB	0,2239	3,60
1,2PD	0,9816	15,76
GLY	0,3824	6,14
1,3PD	1,8293	29,37

F_n		1,9492
r_0		1,115
hydroxyl $_{theor.}$	mg_{KOH}/g	61,75
acid $_{end}$	mg_{KOH}/g	6,76
hydroxyl $_{end}$	mg_{KOH}/g	58,68
yield	*g*	825,5

Discarded resin details

Lastly, the following resins were discarded because their properties (T_g or viscosity) did not correspond to the specifications, because they were too coloured, because their hydroxy or acid value were not as predicted or because they turned into gels.

Prototypes for outdoors not used in any tests

LH194

Monomer	n (mol)	mol %
PAN	2,2306	34,37
SUC	0,9319	14,36
1,2PD	1,0228	15,76
GLY	0,3985	6,14
1,3PD	1,9061	29,37

F_n		1,9492
r_0		1,115
hydroxyl $_{theor.}$	mg_{KOH}/g	65,22
acid $_{end}$	mg_{KOH}/g	4,18
hydroxyl $_{end}$	mg_{KOH}/g	52,11
yield	*g*	491,6

LH197

Monomer	n (mol)	mol %
PAN	2,2306	34,37
SUC	0,9319	14,36
1,2PD	1,6718	25,76
GLY	0,3985	6,14
1,3PD	1,2571	19,37

F_n		1,9492
r_0		1,115
hydroxyl $_{theor.}$	mg_{KOH}/g	65,22
acid $_{end}$	mg_{KOH}/g	5,18
hydroxyl $_{end}$	mg_{KOH}/g	47,07
yield	*g*	461,3

LH234

Monomer	n (mol)	mol %
PAN	1,0925	14,37
SUC	2,3081	30,36
SEB	0,3041	4,00
1,2PD	3,4310	45,13
GLY	0,4668	6,14

F_n		1,9492
r_0		1,115
hydroxyl $_{theor.}$	mg_{KOH}/g	69,73
acid $_{end}$	mg_{KOH}/g	5,57
hydroxyl $_{end}$	mg_{KOH}/g	68,37
yield	*g*	662,8

Viscosity, T_g or colour – isosorbide containing resins

LH186 – not used because of dark colour and high viscosity

Monomer	**n (mol)**	**mol %**
ISO	1,5477	24,37
SUC	2,2381	35,24
SEB	0,8567	13,49
1,2PD	1,3184	20,76
GLY	0,3899	6,14

F_n		1,9492
r_0		1,115
hydroxyl $_{theor.}$	mg_{KOH}/g	58,05
acid $_{end}$	mg_{KOH}/g	2,13
hydroxyl $_{end}$	mg_{KOH}/g	55,70
yield	*g*	884,2

LH166 – not used because of dark colour

Monomer	**n (mol)**	**mol %**
ISO	1,5880	29,37
SUC	1,9054	35,24
SEB	0,7294	13,49
1,2PD	0,8521	15,76
GLY	0,3320	6,14

F_n		1,9492
r_0		1,115
hydroxyl $_{theor.}$	mg_{KOH}/g	56,24
acid $_{end}$	mg_{KOH}/g	8,65
hydroxyl $_{end}$	mg_{KOH}/g	55,37
yield	*g*	703,7

LH267 – not used because of low T_g

Monomer	**n (mol)**	**mol %**
ISO	1,8958	39,37
SEB	2,3465	48,73
1,3PD	0,2774	5,76
GLY	0,2957	6,14

F_n		1,9492
r_0		1,115
hydroxyl $_{theor.}$	mg_{KOH}/g	42,36
acid $_{end}$	mg_{KOH}/g	9,35
hydroxyl $_{end}$	mg_{KOH}/g	48,78
yield	*g*	739,9

Colour - Isosorbide and phthalic anhydride containing resins

LH266 – not used because of dark colour

Monomer	**n (mol)**	**mol %**
PAN	0,9258	19,37
SUC	0,7712	16,13
SEB	0,6321	13,23
ISO	0,7533	15,76
GLY	0,2935	6,14
1,3PD	1,4038	29,37

F_n		1,9492
r_0		1,115
hydroxyl $_{theor.}$	mg_{KOH}/g	56,47
acid $_{end}$	mg_{KOH}/g	9,48
hydroxyl $_{end}$	mg_{KOH}/g	57,00
yield	*g*	564,7

T_g - Cyclohexanedicarboxylic acid prototypes

LH272 – not used due to low T_g

Monomer	**n (mol)**	**mol %**
CHDC	0,6850	14,26
SUC	0,5131	10,68
SEB	1,1247	23,42
1,2PD	2,1511	44,79
GLY	0,3284	6,84

F_n		1,9347
r_0		1,138
hydroxyl $_{theor.}$	mg_{KOH}/g	69,75
acid $_{end}$	mg_{KOH}/g	5,37
hydroxyl $_{end}$	mg_{KOH}/g	65,07
yield	*g*	524,0

Hazy aspect – isosorbide resins

Some resins displayed a hazy aspect, due either to too rapid addition of the solvent in the end, or to grease which was present in the reactor joints and got into the batch. If there was an alternative to these resins with clear aspect, they were not used, and are listed below.

LH126 – not used because of hazy aspect

Monomer	**n (mol)**	**mol %**
ISO	1,6444	24,37
SUC	2,3779	35,24
SEB	0,9103	13,49
1,2PD	1,4008	20,76
GLY	0,4143	6,14

F_n		1,9492
r_0		1,115
hydroxyl $_{theor.}$	mg_{KOH}/g	58,05
acid $_{end}$	mg_{KOH}/g	6,65
hydroxyl $_{end}$	mg_{KOH}/g	54,71
yield	*g*	850,2

LH059 – not used because of hazy aspect

Monomer	**n (mol)**	**mol %**
ISO	1,5880	29,37
SUC	1,9054	35,24
SEB	0,7294	13,49
1,2PD	0,8521	15,76
GLY	0,3320	6,14

F_n		1,9492
r_0		1,115
hydroxyl $_{theor.}$	mg_{KOH}/g	56,24
acid $_{end}$	mg_{KOH}/g	9,01
hydroxyl $_{end}$	mg_{KOH}/g	56,57
yield	*g*	715,0

Hazy aspect - Phthalic anhydride resins

LH152 – not used due to hazy aspect

Monomer	**n (mol)**	**mol %**
PAN	1,8098	29,37
SUC	0,6634	10,77
SEB	0,5296	8,60
1,2PD	0,9711	15,76
GLY	0,3784	6,14
1,3PD	1,8098	29,37

F_n		1,9492
r_0		1,115
hydroxyl $_{theor.}$	mg_{KOH}/g	62,11
acid $_{end}$	mg_{KOH}/g	5,16
hydroxyl $_{end}$	mg_{KOH}/g	58,35
yield	*g*	756,3

LH161 – not used due to hazy aspect

Monomer	n (mol)	mol %
PAN	1,8098	29,37
SUC	0,6634	10,77
SEB	0,5296	8,60
1,2PD	0,9711	15,76
GLY	0,3784	6,14
1,3PD	1,8098	29,37

F_n		1,9492
r_0		1,115
hydroxyl $_{theor.}$	mg_{KOH}/g	62,11
acid $_{end}$	mg_{KOH}/g	6,18
hydroxyl $_{end}$	mg_{KOH}/g	56,97
yield	*g*	818,6

LH183 – not used due to hazy aspect

Monomer	n (mol)	mol %
PAN	1,8098	29,37
SUC	0,6634	10,77
SEB	0,5296	8,60
1,2PD	0,9711	15,76
GLY	0,3784	6,14
1,3PD	1,8098	29,37

F_n		1,9492
r_0		1,115
hydroxyl $_{theor.}$	mg_{KOH}/g	62,11
acid $_{end}$	mg_{KOH}/g	2,71
hydroxyl $_{end}$	mg_{KOH}/g	62,57
yield	*g*	808,6

LH204 – not used due to hazy aspect (grease in the reactor)

Monomer	n (mol)	mol %
PAN	1,5573	29,67
SUC	0,5708	10,87
SEB	0,4557	8,68
1,2PD	0,7801	14,86
GLY	0,4316	8,22
1,3PD	1,4538	27,69

F_n		1,9689
r_0		1,115
hydroxyl $_{theor.}$	mg_{KOH}/g	62,38
acid $_{end}$	mg_{KOH}/g	5,58
hydroxyl $_{end}$	mg_{KOH}/g	61,48
yield	*g*	545,3

LH207 – not used due to hazy aspect (grease in the reactor)

Monomer	n (mol)	mol %
PAN	1,5543	29,52
SUC	0,5697	10,82
SEB	0,4549	8,64
1,2PD	0,8063	15,31
GLY	0,3779	7,18
1,3PD	1,5026	28,54

F_n		1,9590
r_0		1,115
hydroxyl $_{theor.}$	mg_{KOH}/g	62,25
acid $_{end}$	mg_{KOH}/g	5,34
hydroxyl $_{end}$	mg_{KOH}/g	51,00
yield	*g*	532,0

Hydroxy value problems – isosorbide resins

Due to leaks in the reactor, some of the unreacted diols were lost during the reaction. Whenever this could not be corrected by the addition of compensating diols, the final hydroxy value didn't correspond to the theoretical value, and the resins were not used.

LH188

Monomer	**n (mol)**	**mol %**
ISO	1,3542	24,37
SUC	1,9583	35,24
SEB	0,7496	13,49
1,2PD	1,1536	20,76
GLY	0,3412	6,14

F_n		1,9492
r_0		1,115
hydroxyl $_{theor.}$	mg_{KOH}/g	58,05
acid $_{end}$	mg_{KOH}/g	9,96
hydroxyl $_{end}$	mg_{KOH}/g	45,45
yield	*g*	608,5

LH034

Monomer	**n (mol)**	**mol %**
ISO	1,5880	29,37
SUC	1,9054	35,24
SEB	0,7294	13,49
1,2PD	0,8521	15,76
GLY	0,3320	6,14

F_n		1,9492
r_0		1,115
hydroxyl $_{theor.}$	mg_{KOH}/g	56,24
acid $_{end}$	mg_{KOH}/g	16,59
hydroxyl $_{end}$	mg_{KOH}/g	76,19
yield	*g*	/

LH037

Monomer	**n (mol)**	**mol %**
ISO	1,5880	29,37
SUC	1,9054	35,24
SEB	0,7294	13,49
1,2PD	0,8521	15,76
GLY	0,3320	6,14

F_n		1,9492
r_0		1,115
hydroxyl $_{theor.}$	mg_{KOH}/g	56,24
acid $_{end}$	mg_{KOH}/g	7,9
hydroxyl $_{end}$	mg_{KOH}/g	135,6
yield	*g*	/

LH044

Monomer	**n (mol)**	**mol %**
ISO	1,5880	29,37
SUC	1,9054	35,24
SEB	0,7294	13,49
1,2PD	0,8521	15,76
GLY	0,3320	6,14

F_n		1,9492
r_0		1,115
hydroxyl $_{theor.}$	mg_{KOH}/g	56,24
acid $_{end}$	mg_{KOH}/g	8,3
hydroxyl $_{end}$	mg_{KOH}/g	45,74
yield	*g*	/

LH045

Monomer	**n (mol)**	**mol %**
ISO	1,5880	29,37
SUC	1,9054	35,24
SEB	0,7294	13,49
1,2PD	0,8521	15,76
GLY	0,3320	6,14

F_n		1,9492
r_0		1,115
hydroxyl $_{theor.}$	mg_{KOH}/g	56,24
acid $_{end}$	mg_{KOH}/g	9,75
hydroxyl $_{end}$	mg_{KOH}/g	49,33
yield	*g*	/

LH057

Monomer	n (mol)	mol %
ISO	1,5880	29,37
SUC	1,9054	35,24
SEB	0,7294	13,49
1,2PD	0,8521	15,76
GLY	0,3320	6,14

F_n		1,9492
r_0		1,115
hydroxyl $_{theor.}$	mg_{KOH}/g	56,24
acid $_{end}$	mg_{KOH}/g	9,36
hydroxyl $_{end}$	mg_{KOH}/g	41,87
yield	*g*	/

Hydroxy value problem - resins containing isosorbide and phthalic anhydride:

LH268 – not used due to high acid value

Monomer	n (mol)	mol %
ISO	1,4698	39,37
PAN	0,3733	10,00
SEB	1,4459	38,73
1,3PD	0,2150	5,76
GLY	0,2292	6,14

F_n		1,9492
r_0		1,115
hydroxyl $_{theor.}$	mg_{KOH}/g	43,42
acid $_{end}$	mg_{KOH}/g	19,87
hydroxyl $_{end}$	mg_{KOH}/g	39,20
yield	*g*	616,8

Hydroxy value problem - phthalic anhydride resins:

LH128

Monomer	n (mol)	mol %
PAN	1,4938	24,37
SUC	0,8131	13,27
SEB	0,6801	11,10
1,2PD	0,9660	15,76
GLY	0,3764	6,14
1,3PD	1,8002	29,37

F_n		1,9492
r_0		1,115
hydroxyl $_{theor.}$	mg_{KOH}/g	62,29
acid $_{end}$	mg_{KOH}/g	6,16
hydroxyl $_{end}$	mg_{KOH}/g	41,52
yield	*g*	805,9

LH127

Monomer	n (mol)	mol %
PAN	1,8098	29,37
SUC	0,6634	10,77
SEB	0,5296	8,60
1,2PD	0,9711	15,76
GLY	0,3784	6,14
1,3PD	1,8098	29,37

F_n		1,9492
r_0		1,115
hydroxyl $_{theor.}$	mg_{KOH}/g	62,11
acid $_{end}$	mg_{KOH}/g	7,3
hydroxyl $_{end}$	mg_{KOH}/g	40,04
yield	*g*	713,3

LH202

Monomer	n (mol)	mol %
PAN	1,5513	29,37
SUC	0,5686	10,77
SEB	0,4540	8,60
1,2PD	0,8324	15,76
GLY	0,3243	6,14
1,3PD	1,5513	29,37

F_n		1,9492
r_0		1,115
hydroxyl $_{theor.}$	mg_{KOH}/g	62,11
acid $_{end}$	mg_{KOH}/g	8,99
hydroxyl $_{end}$	mg_{KOH}/g	45,77
yield	*g*	510,5

LH119

Monomer	n (mol)	mol %
PAN	2,2030	35,37
SUC	0,5563	8,93
SEB	0,2782	4,47
1,2PD	2,9006	46,56
GLY	0,2911	4,67

F_n		1,9505
r_0		1,099
hydroxyl $_{theor.}$	mg_{KOH}/g	53,72
acid $_{end}$	mg_{KOH}/g	13,77
hydroxyl $_{end}$	mg_{KOH}/g	14,32
yield	*g*	742,2

LH167

Monomer	n (mol)	mol %
PAN	2,2091	29,37
SUC	1,4562	19,36
1,2PD	1,1854	15,76
GLY	0,4618	6,14
1,3PD	2,2091	29,37

F_n		1,9492
r_0		1,115
hydroxyl $_{theor.}$	mg_{KOH}/g	66,89
acid $_{end}$	mg_{KOH}/g	4,21
hydroxyl $_{end}$	mg_{KOH}/g	51,19
yield	*g*	939,5

Lastly, the following six resins turned into a gel before the reaction was finished.

Phthalic anhydride gels:

LH195

Monomer	n (mol)	mol %
PAN	2,2306	34,37
SUC	0,9319	14,36
1,2PD	2,9289	45,13
GLY	0,3985	6,14

F_n		1,9492
r_0		1,115
hydroxyl $_{theor.}$	mg_{KOH}/g	65,22
acid$_{last\ measurement}$	mg_{KOH}/g	13,67
yield	*g*	194,1

LH233

Monomer	n (mol)	mol %
PAN	0,8465	14,37
SUC	2,0239	34,36
1,2PD	2,6583	45,13
GLY	0,3617	6,14

F_n		1,9492
r_0		1,115
hydroxyl $_{theor.}$	mg_{KOH}/g	72,43
acid$_{last\ measurement}$	mg_{KOH}/g	22,89
yield	*g*	/

LH259

Monomer	**n (mol)**	**mol %**
PAN	2,0805	29,82
SUC	0,7626	10,93
SEB	0,6088	8,73
1,2PD	1,0048	14,40
GLY	0,6474	9,28
1,3PD	1,8733	26,85

F_n		1,9789
r_0		1,115
hydroxyl $_{theor.}$	mg_{KOH}/g	62,52
acid$_{last\ measurement}$	mg_{KOH}/g	12,32
hydroxyl $_{end}$	mg_{KOH}/g	/
yield	*g*	/

LH261

Monomer	**n (mol)**	**mol %**
PAN	2,0805	29,82
SUC	0,7626	10,93
SEB	0,6088	8,73
1,2PD	1,0048	14,40
GLY	0,6474	9,28
1,3PD	1,8733	26,85

F_n		1,9789
r_0		1,115
hydroxyl $_{theor.}$	mg_{KOH}/g	62,52
acid$_{last\ measurement}$	mg_{KOH}/g	14,63
hydroxyl $_{end}$	mg_{KOH}/g	/
yield	*g*	583,2

CHDC based gels

LH270

Monomer	**n (mol)**	**mol %**
CHDC	0,6611	14,37
SUC	1,3967	30,36
SEB	0,1840	4,00
1,2PD	2,0761	45,13
GLY	0,2825	6,14

F_n		1,9492
r_0		1,115
hydroxyl $_{theor.}$	mg_{KOH}/g	69,06
acid$_{last\ measurement}$	mg_{KOH}/g	16,3
yield	*g*	375,1

LH273

Monomer	**n (mol)**	**mol %**
CHDC	0,6850	9,45
SUC	2,2491	31,04
SEB	0,6283	8,67
1,2PD	3,1260	43,14
GLY	0,5585	7,71

F_n		1,9663
r_0		1,113
hydroxyl $_{theor.}$	mg_{KOH}/g	67,04
acid$_{last\ measurement}$	mg_{KOH}/g	10,51
yield	*g*	518,1

References Annexe:

1. Banach, T. E.; Berti, C.; Colonna, M.; Fiorini, M.; Marianucci, E.; Messori, M.; Pilati, F.; Toselli, M., New catalysts for poly(butylene terephthalate) synthesis 1. Titanium-lanthanides and titanium-hafnium systems. *Polymer* **2001,** *42* (18), 7511-7516.
2. Banach, T. E.; Colonna, M., New catalysts for poly(butylene terephthalate) synthesis. 2. Kinetic comparison using model compounds. *Polymer* **2001,** *42* (18), 7517-7522.
3. Colonna, M.; Banach, T. E.; Berti, C.; Fiorini, M.; Marianucci, E.; Messori, M.; Pilati, F.; Toselli, M., New catalysts for poly(butylene terephthalate) synthesis. Part 3: Effect of phosphate co-catalysts. *Polymer* **2003,** *44* (17), 4773-4779.
4. Kricheldorf, H. R.; Al Masri, M.; Lomadze, N.; Schwarz, G., Telechelic poly(butylene terephthalate)s by means of bismuth catalysts. *Macromolecules* **2005,** *38* (22), 9085-9090.
5. Yoda, K., Catalytic action of metal compounds in trans-esterification. *Kog Kagaku Zasshi* **1971,** *74* (7), 1476-&.
6. Rafler, G.; Tesch, F.; Kunath, D., Metalalkoxide catalysis in the Formation of polyesters. *Acta Polymerica* **1988,** *39* (6), 315-320.
7. Tomita, K.; Ida, H., Studies on Formation of poly(ethylene terephthalate) -.3.Catalytic activity of metal-compounds in transesterification of dimethyl terephthalate with ethylene-glycol. *Polymer* **1975,** *16* (3), 185-190.
8. Lasarova, R.; Dimov, K., Polycondensation kinetics of low-molecular weight polyethyleneterephthalate. *Angewandte Makromolekulare Chemie* **1976,** *55* (OCT), 1-9.
9. Borges da Silva, E. A.; Zabkova, M.; Araujo, J. D.; Cateto, C. A.; Barreiro, M. F.; Belgacem, M. N.; Rodriques, A. E., An integrated process to produce vanillin and lignin-based polyurethanes from Kraft lignin. *Chemical Engineering Research & Design* **2009,** *87* (9A), 1276-1292.
10. Otera, J.; Danoh, N.; Nozaki, H., Novel template effects of distannoxane catalysts in highly efficient transesterification and esterification. *Journal of Organic Chemistry* **1991,** *56* (18), 5307-5311.
11. Otera, J.; Kawada, K.; Yano, T., Direct condensation polymerization of L-lactic acid catalyzed by distannoxane. *Chemistry Letters* **1996,** (3), 225-226.
12. Takahashi, H.; Hayakawa, T.; Ueda, M., Convenient synthesis of poly(butylene succinate) catalyzed by distannoxane. *Chemistry Letters* **2000,** (6), 684-685.
13. Ishihara, K.; Ohara, S.; Yamamoto, H., Direct condensation of carboxylic acids with alcohols catalyzed by hafnium(IV) salts. *Science* **2000,** *290* (5494), 1140-1142.
14. Takasu, A.; Iio, Y.; Oishi, Y.; Narukawa, Y.; Hirabayashi, T., Environmentally benign polyester synthesis by room temperature direct polycondensation of dicarboxylic acid and diol. *Macromolecules* **2005,** *38* (4), 1048-1050.
15. Takasu, A.; Shibata, Y.; Narukawa, Y.; Hirabayashi, T., Chemoselective dehydration polycondensations of dicarboxylic acids and diols having pendant hydroxyl groups using the room temperature polycondensation technique. *Macromolecules* **2007,** *40* (2), 151-153.
16. Evstatiev, M.; Fakirov, S.; Krasteva, B.; Friedrich, K.; Covas, J. A.; Cunha, A. M., Recycling of poly(ethylene terephthalate) as polymer-polymer composites. *Polymer Engineering & Science* **2002,** *42* (4), 826-835.
17. Paszun, D.; Spychaj, T., Chemical recycling of poly(ethylene terephthalate). *Industrial & Engineering Chemistry Research* **1997,** *36* (4), 1373-1383.
18. Al-Sabagh, A. M.; Yehia, F. Z.; Eshaq, G.; Rabie, A. M.; ElMetwally, A. E., Greener routes for recycling of polyethylene terephthalate. *Egyptian Journal of Petroleum* **2016,** *25* (1), 53-64.
19. Spliman, G. E.; Emerson, A. W.; Beatty, M.; Brown, M.; Christy, M.; Kovsky, J.; Rogers, K.; Vrabel, E.; Tabor, R., Creating multifunctional coatings using recycled raw material streams. *Jct Coatingstech* **2015,** *12* (6), 40-49.
20. Park, S. H.; Kim, S. H., Poly (ethylene terephthalate) recycling for high value added textiles. *Fashion and Textiles* **2014,** *1* (1), 1-17.
21. Lu, M.; Kim, S., Unsaturated polyester resins based on recycled PET: Preparation and curing behavior. *Journal of Applied Polymer Science* **2001,** *80* (7), 1052-1057.

22. Ristic, I.; Cakic, S.; Ilic, O.; Budinski-Simendic, J.; Marinovic-Cincovic, M., Investigation of potentional use of recycled poly(ethylene terephthalate) in Polyurethane Synthesis. In *Contemporary Materials*, 2012; Vol. III, pp 86 - 92.
23. Nikles, D. E.; Farahat, M. S., New Motivation for the Depolymerization Products Derived from Poly(Ethylene Terephthalate) (PET) Waste: a Review. *Macromolecular Materials and Engineering* **2005,** *290* (1), 13-30.
24. Mueller, R.-J., Biological degradation of synthetic polyesters—Enzymes as potential catalysts for polyester recycling. *Process Biochemistry* **2006,** *41* (10), 2124-2128.
25. Tran, T. N.; Paul, U.; Heredia-Guerrero, J. A.; Liakos, I.; Marras, S.; Scarpellini, A.; Ayadi, F.; Athanassiou, A.; Bayer, I. S., Transparent and flexible amorphous cellulose-acrylic hybrids. *Chemical Engineering Journal* **2016,** *287*, 196-204.
26. Chauhan, G. S.; Dhiman, S. K.; Guleria, L. K.; Misra, B. N.; Kaur, I., Polymers from renewable resources: kinetics of 4-vinyl pyridine radiochemical grafting onto cellulose extracted from pine needles. *Radiation Physics and Chemistry* **2000,** *58* (2), 181-190.
27. Kengkhetkit, N.; Amornsakchai, T., A new approach to "Greening" plastic composites using pineapple leaf waste for performance and cost effectiveness. *Materials & Design* **2014,** *55*, 292-299.
28. Audo, M.; Paraschiv, M.; Queffelec, C.; Louvet, I.; Hemez, J.; Fayon, F.; Lepine, O.; Legrand, J.; Tazerout, M.; Chailleux, E.; Bujoli, B., Subcritical Hydrothermal Liquefaction of Microalgae Residues as a Green Route to Alternative Road Binders. *Acs Sustainable Chemistry & Engineering* **2015,** *3* (4), 583-590.
29. Bao, Y.; He, J.; Li, Y., Facile and efficient synthesis of hyperbranched polyesters based on renewable castor oil. *Polymer International* **2013,** *62* (10), 1457-1464.
30. Türünc, O.; Meier, M. A. R., Fatty Acid Derived Monomers and Related Polymers Via Thiol-ene (Click) Additions. *Macromolecular Rapid Communications* **2010,** *31* (20), 1822-1826.
31. Vilela, C.; Silvestre, A. J. D.; Meier, M. A. R., Plant Oil-Based Long-Chain C26 Monomers and Their Polymers. *Macromolecular Chemistry and Physics* **2012,** *213* (21), 2220-2227.
32. Quinzler, D.; Mecking, S., Linear Semicrystalline Polyesters from Fatty Acids by Complete Feedstock Molecule Utilization. *Angewandte Chemie-International Edition* **2010,** *49* (25), 4306-4308.
33. Warwel, S.; Bruse, F.; Demes, C.; Kunz, M.; Klaas, M. R. G., Polymers and surfactants on the basis of renewable resources. *Chemosphere* **2001,** *43* (1), 39-48.
34. Warwel, S.; Brüse, F.; Demes, C.; Kunz, M., Polymers and polymer building blocks from meadowfoam oil. *Industrial Crops and Products* **2004,** *20* (3), 301-309.
35. Corma, A.; Iborra, S.; Velty, A., Chemical routes for the transformation of biomass into chemicals. *Chemical Reviews* **2007,** *107* (6), 2411-2502.
36. Dhamaniya, S.; Jacob, J., Synthesis and characterization of polyesters based on tartaric acid derivatives. *Polymer* **2010,** *51* (23), 5392-5399.
37. Japu, C.; Martinez de Ilarduya, A.; Alla, A.; Munoz-Guerra, S., Bio-based poly(ethylene terephthalate) copolyesters made from cyclic monomers derived from tartaric acid. *Polymer* **2014,** *55* (10), 2294-2304.
38. Dworakowska, S.; Kasprzyk, W.; Bednarz, S.; Bogdal, D., Polyesters from renewable sources. In *15th International Electronic Conference on Organic Synthetic Chemistry (ECSOC-15)*, 2011; Vol. D.
39. Barroso-Bujans, F.; Martinez, R.; Ortiz, P., Structural characterization of oligomers from the polycondensation of citric acid with ethylene glycol and long-chain aliphatic alcohols. *Journal of Applied Polymer Science* **2003,** *88* (2), 302-306.
40. Tsutsumi, N.; Oya, M.; Sakai, W., Biodegradable network polyesters from gluconolactone and citric acid. *Macromolecules* **2004,** *37* (16), 5971-5976.
41. Doll, K. M.; Shogren, R. L.; Willett, J. L.; Swift, G., Solvent-free polymerization of citric acid and D-sorbitol. *Journal of Polymer Science Part a-Polymer Chemistry* **2006,** *44* (14), 4259-4267.
42. Ding, T.; Liu, Q. Y.; Shi, R.; Tian, M.; Yang, H.; Zhang, L. Q., Synthesis, characterization and in vitro degradation study of a novel and rapidly degradable elastomer. *Polymer Degradation and Stability* **2006,** *91* (4), 733-739.
43. Djordjevic, I.; Choudhury, N. R.; Dutta, N. K.; Kumar, S., Synthesis and characterization of novel citric acid-based polyester elastomers. *Polymer* **2009,** *50* (7), 1682-1691.

44. Yang, J.; Webb, A. R.; Pickerill, S. J.; Hageman, G.; Ameer, G. A., Synthesis and evaluation of poly(diol citrate) biodegradable elastomers. *Biomaterials* **2006,** *27* (9), 1889-1898.
45. Yang, J.; Webb, A. R.; Ameer, G. A., Novel citric acid-based biodegradable elastomers for tissue engineering. *Advanced Materials* **2004,** *16* (6), 511-+.
46. Sathiskumar, P. S.; Madras, G., Synthesis, characterization, degradation of biodegradable castor oil based polyesters. *Polymer Degradation and Stability* **2011,** *96* (9), 1695-1704.
47. Gubbels, E.; Jasinska-Walc, L.; Noordover, B. A. J.; Koning, C. E., Linear and branched polyester resins based on dimethyl-2,5-furandicarboxylate for coating applications. *European Polymer Journal* **2013,** *49* (10), 3188-3198.
48. Gustini, L.; Noordover, B. A. J.; Gehrels, C.; Dietz, C.; Koning, C. E., Enzymatic synthesis and preliminary evaluation as coating of sorbitol-based, hydroxy-functional polyesters with controlled molecular weights. *European Polymer Journal* **2015,** *67*, 459-475.
49. Anand, A.; Kulkarni, R. D.; Gite, V. V., Preparation and properties of eco-friendly two pack PU coatings based on renewable source (sorbitol) and its property improvement by nano ZnO. *Progress in Organic Coatings* **2012,** *74* (4), 764-767.
50. Kong, X. H.; Liu, G. G.; Qi, H.; Curtis, J. M., Preparation and characterization of high-solid polyurethane coating systems based on vegetable oil derived polyols. *Progress in Organic Coatings* **2013,** *76* (9), 1151-1160.
51. Gaikwad, M. S.; Gite, V. V.; Mahulikar, P. P.; Hundiwale, D. G.; Yemul, O. S., Eco-friendly polyurethane coatings from cottonseed and karanja oil. *Progress in Organic Coatings* **2015,** *86*, 164-172.
52. Gubbels, E.; Jasinska-Walc, L.; Koning, C. E., Synthesis and Characterization of Novel Renewable Polyesters Based on 2,5-Furandicarboxylic Acid and 2,3-Butanediol. *Journal of Polymer Science Part a-Polymer Chemistry* **2013,** *51* (4), 890-898.
53. Hussain, S.; Fawcett, A. H.; Taylor, P., Use of polymers from biomass in paints. *Progress in Organic Coatings* **2002,** *45* (4), 435-439.
54. Moore, J. A.; Kelly, J. E., Polyesters derived from furan and tetrahydrofuran nuclei. *Macromolecules* **1978,** *11* (3), 568-573.
55. de Jong, E.; Dam, M. A.; Sipos, L.; Gruter, G. J. M., Furandicarboxylic Acid (FDCA), A Versatile Building Block for a Very Interesting Class of Polyesters. In *Biobased Monomers, Polymers, and Materials*, American Chemical Society: 2012; Vol. 1105, pp 1-13.
56. Gandini, A.; Silvestre, A. J. D.; Neto, C. P.; Sousa, A. F.; Gomes, M., The Furan Counterpart of Poly(ethylene terephthalate): An Alternative Material Based on Renewable Resources. *Journal of Polymer Science Part a-Polymer Chemistry* **2009,** *47* (1), 295-298.
57. Ma, J.; Yu, X.; Xu, J.; Pang, Y., Synthesis and crystallinity of poly(butylene 2,5-furandicarboxylate). *Polymer* **2012,** *53* (19), 4145-4151.
58. Sousa, A. F.; Matos, M.; Freire, C. S. R.; Silvestre, A. J. D.; Coelho, J. F. J., New copolyesters derived from terephthalic and 2,5-furandicarboxylic acids: A step forward in the development of biobased polyesters. *Polymer* **2013,** *54* (2), 513-519.
59. Lasseuguette, E.; Gandini, A.; Belgacem, M. N.; Timpe, H. J., Synthesis, characterization and photocross-linking of copolymers of furan and aliphatic hydroxyethylesters prepared by transesterification. *Polymer* **2005,** *46* (15), 5476-5483.
60. Jiang, M.; Liu, Q.; Zhang, Q.; Ye, C.; Zhou, G., A series of furan-aromatic polyesters synthesized via direct esterification method based on renewable resources. *Journal of Polymer Science Part a-Polymer Chemistry* **2012,** *50* (5), 1026-1036.
61. Khrouf, A.; Boufi, S.; El Gharbi, R.; Gandini, A., Polyesters bearing furan moieties. Part 3. A kinetic study of the transesterification of 2-furoates as a model reaction for the corresponding polycondensations. *Polymer International* **1999,** *48* (8), 649-659.
62. Khrouf, A.; Abid, M.; Boufi, S.; El Gharbi, R.; Gandini, A., Polyesters bearing furan moieties. 2. A detailed investigation of the polytransesterification of difuranic diesters with different diols. *Macromolecular Chemistry and Physics* **1998,** *199* (12), 2755-2765.

63. Khrouf, A.; Boufi, S.; ElGharbi, R.; Belgacem, N. M.; Gandini, A., Polyesters bearing furan moieties .1. Polytransesterification involving difuranic diesters and aliphatic diols. *Polymer Bulletin* **1996,** *37* (5), 589-596.
64. Papageorgiou, G. Z.; Guigo, N.; Tsanaktsis, V.; Papageorgiou, D. G.; Exarhopoulos, S.; Sbirrazzuoli, N.; Bikiaris, D. N., On the bio-based furanic polyesters: Synthesis and thermal behavior study of poly(octylene furanoate) using fast and temperature modulated scanning calorimetry. *European Polymer Journal* **2015,** *68*, 115-127.
65. Wu, L.; Mincheva, R.; Xu, Y.; Raquez, J.-M.; Dubois, P., High Molecular Weight Poly(butylene succinate-co-butylene furandicarboxylate) Copolyesters: From Catalyzed Polycondensation Reaction to Thermomechanical Properties. *Biomacromolecules* **2012,** *13* (9), 2973-2981.
66. Goerz, O.; Ritter, H., Polymers with shape memory effect from renewable resources: crosslinking of polyesters based on isosorbide, itaconic acid and succinic acid. *Polymer International* **2013,** *62* (5), 709-712.
67. Fonseca, A. C.; Lopes, I. M.; Coelho, J. F. J.; Serra, A. C., Synthesis of unsaturated polyesters based on renewable monomers: Structure/properties relationship and crosslinking with 2-hydroxyethyl methacrylate. *Reactive and Functional Polymers* **2015,** *97*, 1-11.
68. Jasinska, L.; Koning, C. E., Waterborne Polyesters Partially Based on Renewable Resources. *Journal of Polymer Science Part a-Polymer Chemistry* **2010,** *48* (24), 5907-5915.
69. Jasinska, L.; Koning, C. E., Unsaturated, Biobased Polyesters and Their Cross-Linking via Radical Copolymerization. *Journal of Polymer Science Part a-Polymer Chemistry* **2010,** *48* (13), 2885-2895.
70. Sadler, J. M.; Toulan, F. R.; Nguyen, A.-P. T.; Kayea, R. V., III; Ziaee, S.; Palmese, G. R.; La Scala, J. J., Isosorbide as the structural component of bio-based unsaturated polyesters for use as thermosetting resins. *Carbohydrate Polymers* **2014,** *100*, 97-106.
71. Lukaszczyk, J.; Janicki, B.; Kozuch, J.; Wojdyla, H., Synthesis and Characterization of Low Viscosity Dimethacrylic Resin Based on Isosorbide. *Journal of Applied Polymer Science* **2013,** *130* (4), 2514-2522.
72. Raytchev, P. D.; Besset, C.; Fleury, E.; Pascault, J.-P.; Bernard, J.; Drockenmuller, E., 1,4:3,6-Dianhydrohexitols: Original platform for the design of biobased polymers using robust, efficient, and orthogonal chemistry. *Pure and Applied Chemistry* **2013,** *85* (3), 511-520.
73. Pion, F.; Ducrot, P.-H.; Allais, F., Renewable Alternating Aliphatic-Aromatic Copolyesters Derived from Biobased Ferulic Acid, Diols, and Diacids: Sustainable Polymers with Tunable Thermal Properties. *Macromolecular Chemistry and Physics* **2014,** *215* (5), 431-439.
74. Oulame, M. Z.; Pion, F.; Allauddin, S.; Raju, K. V. S. N.; Ducrot, P.-H.; Allais, F., Renewable alternating aliphatic-aromatic poly(ester-urethane)s prepared from ferulic acid and bio-based diols. *European Polymer Journal* **2015,** *63*, 186-193.
75. Pemba, A. G.; Rostagno, M.; Lee, T. A.; Miller, S. A., Cyclic and spirocyclic polyacetal ethers from lignin-based aromatics. *Polym. Chem.* **2014,** *5* (9), 3214-3221.
76. Chauhan, N. P. S., Preparation and characterization of bio-based terpolymer derived from vanillin oxime, formaldehyde, and p-hydroxyacetophenone. *Designed Monomers and Polymers* **2014,** *17* (2), 176-185.
77. Beristain, M. F.; Nakamura, M.; Nagai, K.; Ogaw, T., Synthesis and Characterization of Poly[propargyl(3-methoxy-4-propargyloxy)cinnamate]: a Polymer from a Natural Product. *Designed Monomers and Polymers* **2009,** *12* (3), 257-263.
78. Barbara, I.; Flourat, A. L.; Allais, F., Renewable polymers derived from ferulic acid and biobased diols via ADMET. *European Polymer Journal* **2015,** *62*, 236-243.
79. Stanzione, J. F., III; Giangiulio, P. A.; Sadler, J. M.; La Scala, J. J.; Wool, R. P., Lignin-Based Bio-Oil Mimic as Biobased Resin for Composite Applications. *American Chemical Society Sustainable Chemistry and Engineering* **2013,** *1* (4), 419-426.
80. Zhang, C. Q.; Madbouly, S. A.; Kessler, M. R., Renewable Polymers Prepared from Vanillin and Its Derivatives. *Macromolecular Chemistry and Physics* **2015,** *216* (17), 1816-1822.

81. Iemma, F.; Puoci, F.; Curcio, M.; Parisi, O. I.; Cirillo, G.; Spizzirri, U. G.; Picci, N., Ferulic Acid as a Comonomer in the Synthesis of a Novel Polymeric Chain with Biological Properties. *Journal of Applied Polymer Science* **2010,** *115* (2), 784-789.
82. Parisi, O. I.; Puoci, F.; Iemma, F.; De Luca, G.; Curcio, M.; Cirillo, G.; Spizzirri, U. G.; Picci, N., Antioxidant and spectroscopic studies of crosslinked polymers synthesized by grafting polymerization of ferulic acid. *Polymers for Advanced Technologies* **2010,** *21* (11), 774-779.
83. Zhang, H. Y.; Yong, X. Y.; Zhou, J. Y.; Deng, J. P.; Wu, Y. P., Biomass Vanillin-Derived Polymeric Microspheres Containing Functional Aldehyde Groups: Preparation, Characterization, and Application as Adsorbent. *Acs Applied Materials & Interfaces* **2016,** *8* (4), 2753-2763.
84. Amarasekara, A. S.; Wiredu, B.; Razzaq, A., Vanillin based polymers: I. An electrochemical route to polyvanillin. *Green Chemistry* **2012,** *14* (9), 2395-2397.
85. Gryn'ova, G.; Ingold, K. U.; Coote, M. L., New Insights into the Mechanism of Amine/Nitroxide Cycling during the Hindered Amine Light Stabilizer Inhibited Oxidative Degradation of Polymers. *Journal of the American Chemical Society* **2012,** *134* (31), 12979-12988.
86. Jensen, R. K.; Korcek, S.; Zinbo, M.; Gerlock, J. L., Regeneration of Amine in Catalytic Inhibition of Oxidation. *The Journal of Organic Chemistry* **1995,** *60* (17), 5396-5400.
87. Paine, M. R. L.; Gryn'ova, G.; Coote, M. L.; Barker, P. J.; Blanksby, S. J., Desorption electrospray ionisation mass spectrometry of stabilised polyesters reveals activation of hindered amine light stabilisers. *Polymer Degradation and Stability* **2014,** *99*, 223-232.
88. Zhang, W. R.; Zhu, T. T.; Smith, R.; Lowe, C., A non-destructive study on the degradation of polymer coating II: Modelling of degradation depth profiles. *Polymer Testing* **2012,** *31* (8), 1100-1104.
89. Delorme, P.; Lemaire, J.; Carrara, F.; Bonnebat, C., Photooxidation mechanism of aliphatic crosslinked polyesters used for flat steel coating. *AIP Conference Proceedings* **1996,** *354* (1), 413.
90. Carroccio, S.; Rizzarelli, P.; Puglisi, C.; Montaudo, G., MALDI investigation of photooxidation in aliphatic polyesters: Poly(butylene succinate). *Macromolecules* **2004,** *37* (17), 6576-6586.
91. Shigemoto, I.; Kawakami, T.; Taiko, H.; Okumura, M., A quantum chemical study on the thermal degradation reaction of polyesters. *Polymer Degradation and Stability* **2012,** *97* (6), 941-947.
92. Nagai, Y.; Ogawa, T.; Nishimoto, Y.; Ohishi, F., Analysis of weathering of a thermoplastic polyester elastomer II. Factors affecting weathering of a polyether-polyester elastomer. *Polymer Degradation and Stability* **1999,** *65* (2), 217-224.
93. Nagai, Y.; Nakamura, D.; Ueno, H.; Matsumoto, N.; Ohishi, F., Photo degradation mechanisms in poly(2,6-butylenenaphthalate-co-tetramethyleneglycol) (PBN-PTMG). II: wavelength sensitivity of the photo degradation. *Polymer Degradation and Stability* **2005,** *88* (2), 256-260.
94. Malanowski, P.; Huijser, S.; van Benthem, R. A. T. M.; van der Ven, L. G. J.; Laven, J.; de With, G., Photodegradation of poly(neopentyl isophthalate) part I: Laboratory and outdoor conditions. *Polymer Degradation and Stability* **2009,** *94* (11), 2086-2094.
95. Malanowski, P.; van Benthem, R. A. T. M.; van der Ven, L. G. J.; Laven, J.; Kisin, S.; de With, G., Photo-degradation of poly(neopentyl isophthalate). Part II: Mechanism of cross-linking. *Polymer Degradation and Stability* **2011,** *96* (6), 1141-1148.
96. Malanowski, P.; Huijser, S.; Scaltro, F.; van Benthem, R. A. T. M.; van der Ven, L. G. J.; Laven, J.; de With, G., Photodegradation of poly(neopentyl terephthalate). *Progress in Organic Coatings* **2012,** *74* (1), 165-172.
97. Commereuc, S.; Askanian, H.; Verney, V.; Celli, A.; Marchese, P., About Durability of Biodegradable Polymers: Structure/Degradability Relationships. In *Modern Trends in Polymer Science-Epf 09*, Stelzer, F.; Wiesbrock, E., Eds. 2010; Vol. 296, pp 378-387.
98. Commereuc, S.; Askanian, H.; Verney, V.; Celli, A.; Marchese, P.; Berti, C., About the end life of novel aliphatic and aliphatic-aromatic (co)polyesters after UV-weathering: Structure/degradability relationships. *Polymer Degradation and Stability* **2013,** *98* (7), 1321-1328.
99. Celli, A.; Marchese, P.; Sullalti, S.; Berti, C.; Commereuc, S.; Verney, V., New polymers from renewable resources: synthesis, characterization, and photodurability of aliphatic polyesters containing glycerol. *Journal of Biotechnology* **2010,** *150*, S206-S206.

100. Zamora, F.; Hakkou, K.; Muñoz-Guerra, S.; Galbis, J. A., Hydrolytic degradation of carbohydrate-based aromatic homo- and co-polyesters analogous to PET and PEI. *Polymer Degradation and Stability* **2006,** *91* (11), 2654-2659.
101. Okada, M.; Okada, Y.; Aoi, K., Synthesis and degradabilities of polyesters from 1,4/3,6-dianhydrohexitols and aliphatic dicarboxylic-acids. *Journal of Polymer Science Part a-Polymer Chemistry* **1995,** *33* (16), 2813-2820.
102. Jin, X. M.; Carfagna, C.; Nicolais, L.; Lanzetta, R., Synthesis, characterization, and in-vitro degradation of a novel thermotropic ternary copolyester based on p-hydroxycinnamic acid. *Macromolecules* **1995,** *28* (14), 4785-4794.
103. Zhang, W. R.; Zhu, T. T.; Smith, R.; Lowe, C., A non-destructive study on the degradation of polymer coating I: Step-scan photoacoustic FTIR and confocal Raman microscopy depth profiling. *Polymer Testing* **2012,** *31* (7), 855-863.
104. Sullivan, C. J., Linear polyester diols based on isophthalic acid and 2-methyl-1,3-propanediol for thermoset coating compositions. Google Patents: 1995.
105. Lukey, C. A.; Hill, D. J. T.; Pomery, P. J., UV photolysis of melamine formaldehyde crosslinkers. *Polymer Degradation and Stability* **2002,** *78* (3), 485-490.
106. Zhang, W. R.; Hinder, S. J.; Smith, R.; Lowe, C.; Watts, J. F., An investigation of the effect of pigment on the degradation of a naturally weathered polyester coating. *Journal of Coatings Technology and Research* **2011,** *8* (3), 329-342.
107. Gerlock, J. L.; Bauer, D. R., Electron-spin-resonance measurements of free-radical photoinitiation rates by nitroxide termination. *Journal of Polymer Science Part C-Polymer Letters* **1984,** *22* (8), 447-455.
108. Mitra, S.; Ahire, A.; Mallik, B. P., Investigation of accelerated aging behaviour of high performance industrial coatings by dynamic mechanical analysis. *Progress in Organic Coatings* **2014,** *77* (11), 1816-1825.
109. Osterhold, M.; Glockner, P., Influence of weathering on physical properties of clearcoats. *Progress in Organic Coatings* **2001,** *41* (1-3), 177-182.
110. Maetens, D., Weathering degradation mechanism in polyester powder coatings. *Progress in Organic Coatings* **2007,** *58* (2-3), 172-179.
111. Biorad Laboratories.
112. Predicted NMR data calculated using Advanced Chemistry Development, Inc. (ACD/Labs) Software V11.01 (1994-2016 ACD/Labs).
113. Bolton, E. E.; Chen, J.; Kim, S.; Han, L. Y.; He, S. Q.; Shi, W. Y.; Simonyan, V.; Sun, Y.; Thiessen, P. A.; Wang, J. Y.; Yu, B.; Zhang, J.; Bryant, S. H., PubChem3D: a new resource for scientists. *Journal of Cheminformatics* **2011,** *3*.
114. Hansen Solubility Parameters in Practice. http://www.hansen-solubility.com/ (accessed 21.09.2016).
115. Zhang, Y.; Maxted, J.; Barber, A.; Lowe, C.; Smith, R., The durability of clear polyurethane coil coatings studied by FTIR peak fitting. *Polymer Degradation and Stability* **2013,** *98* (2), 527-534.
116. Batista, M. A. J.; Moraes, R. P.; Barbosa, J. C. S.; Oliveira, P. C.; Santos, A. M., Effect of the polyester chemical structure on the stability of polyester-melamine coatings when exposed to accelerated weathering. *Progress in Organic Coatings* **2011,** *71* (3), 265-273.